Variational determination of the two-particle density matrix: the case of doubly-occupied space

Variationele bepaling van de tweedeeltjesdichtheidsmatrix in het geval van de dubbel-bezette ruimte

Ward Poelmans

Supervisors: prof. dr. D. Van Neck, prof. dr. P. Bultinck
Dissertation submitted in fulfillment of the requirements for the degree of Doctor (Ph.D.) in Science: Physics

Department of Physics and Astronomy
Faculty of Sciences
Ghent University
Academic year 2014-2015

UNIVERSITEIT GENT

The computational resources (Stevin Supercomputer Infrastructure) and services used in this work were provided by the VSC (Flemish Supercomputer Center), funded by Ghent University, the Hercules Foundation and the Flemish Government - department EWI.

This research was conducted at the Center for Molecular Modeling.

Members of the examination committee

Chair

prof. dr. Natalie Jachowicz (Universiteit Gent)

Reading Committee

prof. dr. Dimitri Van Neck (Universiteit Gent, *promotor*)
prof. dr. Paul W. Ayers (McMaster University)
dr. Brecht Verstichel (Universiteit Gent)

Other members

prof. dr. Patrick Bultinck (Universiteit Gent, *copromotor*)
dr. Stijn De Baerdemacker (Universiteit Gent)
prof. dr. ir. An Ghysels (Universiteit Gent)
prof. dr. ir. Veronique Van Speybroeck (Universiteit Gent)

Dankwoord

In science, one should use all available resources to solve difficult problems. One of our most powerful resources is the insight of our colleagues.

Peter Agre

Het dankwoord heeft een bijzondere plaats in een doctoraat: het is het enige stukje dat iedereen leest (en begrijpt). Het maken en schrijven van een doctoraat is niet altijd een prettig avontuur. Zeker naar het einde toe is het lijdend voorwerp niet altijd te genieten en is zijn tijd voor alles wat niet met het doctoraat te maken heeft nogal beperkt, om niet te zeggen onbestaande. De mensen die dit van dichtbij hebben meegemaakt en kunnen onderschrijven verdienen dan ook een woordje van dank. Velen hebben een klein of groot steentje bijgedragen aan het eindresultaat, soms zonder het zelf te beseffen. Om zeker niemand te vergeten wil ik dan ook beginnen met het volgende: aan iedereen die heeft meegeholpen, bedankt! Aan iedereen die niet heeft meegeholpen, ook bedankt!

Sommigen verdienen het echter met naam en toenaam vermeld te worden voor hun contributie. Vooreerst wil ik mijn promotoren Dimitri en Patrick bedanken om dit avontuur überhaupt van start te laten gaan. De werelden van many-body theory en quantum chemistry hebben een stuk minder geheimen voor mij dankzij jullie.

Mijn collega fundamentalisten waren ook onmisbaar. Brecht, Sebastian, Matthias, Stijn en Pieter, zonder jullie zou het niet gelukt zijn. Dankzij Sebastian is de wereld van DMRG geen mysterie meer voor mij en door Stijn ben ik de kracht van pairing gaan appreciëren. Maar Brecht verdient een extra schouderklopje, zonder hem was ik nooit aan dit onderwerp begonnen. Je hebt mij de wereld van convexe optimalisatie leren kennen en er bestaat geen probleem of je had een goede suggestie om het op te lossen. Ondertussen heb je de veilige haven van de academische wereld verlaten en zullen onze paden waarschijnlijk niet meer vaak kruisen maar ik ben blij dat ze zo lang hebben samengelopen.

Daarnaast zijn er nog de collega's van het CMM die het leven als doctoraatsstudent een stuk aangenamer maken. Zonder Andy, Thierry, Lennart, Kim, Marc, Paul en de vele andere collega's was het leven een stuk saaier geweest. In het bijzonder wil ik nog eens het vrijdagnamiddag patékes team en Wim bedanken. Zonder Wim zou het niet lang duren voor de tandwielen vastlopen.

In het bijzonder wil ik ook de 33320 computer cores bedanken die gedurende in totaal 1035 jaar mij zo ijverig hebben geholpen. Zonder jullie zou het 4de hoofdstuk bijzonder leeg geweest zijn.

I would also like to thank my jury for their work. You are the only ones who are expected to actually read the entire disseration. Thank you for taking the time and effort to do so. I hope you like it.

Het leven is meer dan werk alleen. Bedankt Nele, Gregory, Dieter, Stef, Sven, Willem, Kevin en Delphine om te zorgen voor de nodige ontspanning.

Mama en Papa, jullie zullen niet alles snappen wat in dit boekje staat maar zonder jullie zou het ook niet mogelijk geweest zijn. Bedankt om mijn altijd te steunen. Mijn schoonfamilie wil ik ook bedanken. Het is in de afgelopen jaren een tweede thuis geworden waar verveling een woord is dat niet bestaat.

Als laatste wil ik nog 3 bijzondere dames bedanken. De eerst twee beschikken over de bijzondere gave dat ze alle wereldse en onwereldse problemen doen verdwijnen als sneeuw voor de zon en het hele universum reduceren tot het hier en nu. Het zal wel nog een aantal jaren duren voor ze dit zelf kunnen lezen en nog meer jaren voor ze snappen wat het eigenlijk betekend maar toch bedankt Catharina en Ariadne. Last but not least, mijn lieftallige wederhelft. De weg naar het einde was niet altijd aangenaam. In mei en juni was ons huis eerder als een hotel voor mij. Ik kwam toe op onmogelijk uren en toch was er steeds iets te eten. Catharina en Ariadne kwamen niks te kort en het huis was altijd in orde. Babysits werden voorzien (waarvoor dank Ellen L., Klaas en An), plannen in de weekends werden aangepast. Alles moest wijken zodat het doctoraat kon worden afgewerkt. Als je dit leest, heb je het finale resultaat van al dat bloed, zweet en tranen in handen. En hiermee wordt het hoofdstuk doctoraat ook finaal afgesloten. Bedankt om er van het begin tot het einde te zijn. Op naar het volgende hoofdstuk!

Ward Poelmans
Gent, 9 september 2015

Contents

Samenvatting

Alle materie is opgebouwd uit atomen. Democritus had dit al in de 5de eeuw v.Chr. gepostuleerd, maar hij kon dit natuurlijk niet bewijzen. De wereld van het atoom bleek echter moeilijk te doorgronden. Pas vanaf de 19de eeuw kwam er echt schot in de zaak. Men ontdekte dat atomen niet ondeelbaar waren en vond het deeltje dat wij tegenwoordig kennen als het elektron. In het begin van de 20ste eeuw schakelde de ontdekkingstocht een versnelling hoger. Men kwam tot de conclusie dat een atoom grotendeels leeg is maar wel een harde kern heeft waarrond er elektronen bewegen. Verschillende nieuwe modellen om het atoom te beschrijven werden ingevoerd en verbeterd. Een belangrijk doorbraak kwam toen men de deeltje-golf dualiteit ontdekte: een elektron kan zich zowel als een golf en als een deeltje gedragen. Via het golfkarakter kunnen typische golf fenomenen zoals diffractie en constructieve interferentie verklaard worden, terwijl het deeltjeskarakter de meer intuïtieve beschrijving van het elektron toelaat. Het hoogtepunt kwam met de formulering van de Schrödinger vergelijking: deze beschrijft een systeem van deeltjes die interageren met elkaar. In het geval van elektronen heb je paarsgewijze interactie via de Coulombkracht: elk elektron wordt afgestoten van alle andere elektronen maar aangetrokken door de kern. Via de Schrödinger vergelijking kun je bepalen wat de meest optimale toestand (de toestand met de laagste energie) is van het systeem.

Het Heisenberg onzekerheidprincipe veranderde de interpretatie van de wereld van het atoom fundamenteel: de absolute zekerheden verdwenen en men werkt nu met kansen. Op elke meting die men doet zit er een onbepaalde factor die fundamenteel is en niet veroorzaakt wordt door het meettoestel. Enkel met herhaalde metingen kun je terug een vorm van zekerheid krijgen. Dit alles is wat nu gekend staat onder de naam kwantummechanica. Deze tak van de wetenschap beschrijft de wereld op kleine schaal: de effecten ervan zijn pas belangrijk op de nanoschaal maar kunnen toch macroscopisch gezien worden. De toestand van een systeem wordt beschreven door een golffunctie en de bijhorende energie. De golffunctie met de laagste energie geeft het meest stabiele systeem. De golffunctie bevat alle informatie over

het systeem. De energie kun je bijvoorbeeld gebruiken om te voorspellen of een chemische reactie zal doorgaan of niet (verlaagt de reactie de energie of niet?). Helaas kan enkel voor het meest simpele systeem, een waterstof atoom, de golffunctie en bijhorende energie exact worden neergeschreven. Voor andere systemen nemen we onze toevlucht tot numerieke methoden en benaderingen. Het probleem is dat de golffunctie slecht schaalt met de grootte van het systeem: de hoeveel rekenkracht die nodig is om de golffunctie te bepalen stijgt heel erg sterk met de grootte van het systeem. Dit maakt dat het enkel voor kleine systemen mogelijk is om de volledige oplossing te bepalen binnen een redelijke tijd. Om rond dit euvel te werken zijn vele mogelijke oplossingen bedacht.

In dit werk bespreken we een van de methoden. Indien we werken in een kwantumsysteem waar de deeltjes paarsgewijs interageren, dan bevat de tweede orde dichtheidsmatrix van dit systeem alle belangrijke informatie. Dit is een handiger object om te gebruiken dan de golffunctie, omdat het veel compacter is en een strikte ondergrens geeft voor de energie. Dit laatste is handig omdat de meeste andere methoden een bovengrens geven op de energie. De moeilijkheid is echter dat bij het zoeken naar de optimale dichtheidsmatrix de zoektocht beperkt moet worden tot een bepaalde klasse: de dichtheidsmatrix moet N-representeerbaar zijn. Dit betekent dat er een ensemble van golffuncties moet bestaan waaruit de dichtheidsmatrix afleidbaar is. Het is helaas bewezen dat dit een ontzettend moeilijk probleem is. Er is een theorema dat de criteria voor N-representeerbaarheid bepaalt, maar dit is niet bruikbaar als een praktische test. Wat we wel kunnen doen is dit theorema gebruiken om een set nodige voorwaarden op te stellen: dit betekent dat we een aantal condities opleggen waaraan de dichtheidsmatrix minimaal moet voldoen. In het algemeen zijn deze condities niet voldoende om een N-representeerbaarheid dichtheidsmatrix te vinden maar we kunnen het nu wel benaderen. De meeste simpele voorwaarden leiden tot de zogenaamde tweeindex en drie-index condities. Dit zijn dan ook de condities die we gebruiken in dit werk.

Daarnaast bevatten de meeste kwantum mechanische systemen een vorm van symmetrie: je kunt bepaalde operaties uitvoeren op het systeem zonder dat dit de golffunctie of dichtheidsmatrix verandert. Deze vrijheidsgraden kunnen gebruikt worden om de voorwaarden te vereenvoudigen.

De condities die we hebben afgeleid zijn algemeen: ze gelden voor elke golffunctie. We beperken de condities nu tot een bepaalde klasse van golffuncties. Voor elk atoom zijn er een aantal orbitalen: dit zijn een soort van energie niveau's waarop een elektron kan geplaatst worden. We beperken ons nu tot het geval waarop alle orbitalen ofwel bezet zijn door twee elektronen ofwel leeg zijn. M.a.w. elk elektron is gepaard met een ander elektron, er mogen

geen elektronen zijn die geen partner hebben. Deze restrictie zorgt ervoor dat de twee- en drie-index condities sterk vereenvoudigd worden.

Het vinden van de optimale dichtheidsmatrix en bijhorende energie kan nu worden geschreven als een gekend optimalisatie probleem: een semi-definiet programmeer probleem. Om dit soort problemen op te lossen bestaan er verschillende methoden. In essentie hebben we de keuze tussen twee soorten algoritmes: robuust maar traag, of snel maar onstabiel. Bij de eerste kunnen we de optimalisatie gewoon starten en wachten op het antwoord, bij de tweede moeten we meestal eerst een aantal parameters afstellen voor het antwoord kan gezocht worden.

De beperking tot golffuncties die enkel gepaarde elektronen hebben heeft een belangrijk nadeel. De energie is nu afhankelijk van de vorm van de orbitalen. Naast de optimale dichtheidsmatrix moeten we ook de optimale vorm van de orbitalen zoeken. Dit is een bijzonder lastig probleem: je moet het diepste dal vinden in een ruig energie-gebergte zonder dat er een kaart beschikbaar is. De enige computationele methoden die dit kunnen zijn bijzonder traag. We gebruiken daarom een benaderende methode. We kiezen een startpunt en gaan van daaruit op zoek naar het laagste punt door steeds te dalen. Als we het startpunt goed kiezen, dan kunnen we het diepste punt vinden. Als we een optimale vorm van de orbitalen hebben gevonden moeten we ook nog de huidige oplossingen omzetten naar deze nieuwe vorm. In het algemeen is dit ook een dure zaak om te berekenen. Wij lossen dit op door enkel op een bepaalde manier naar beneden te gaan: ruw gezegd zou je het kunnen vergelijken met de beperking dat je enkel in een van de vier hoofdrichtingen van een kompas mag dalen. Op zich is dit geen beperking, je zult misschien niet altijd de kortste weg kunnen volgen, maar je zult wel altijd op je eindbestemming raken. Door deze beperking is het omzetten van een oplossing naar de nieuwe orbitalen veel eenvoudiger en computationeel sneller geworden.

Om te testen hoe goed deze methode werkt, passen we ze toe op een aantal testsystemen. Voor een waterstofmolecule vinden we de exacte oplossing, maar als we twee helium atomen uit elkaar trekken gaat er iets grondig mis. We hebben bij dit systeem gebruik gemaakt van de symmetrie: als je bijvoorbeeld de twee helium atomen van plaats verwisselt, verandert er niks aan het systeem. Deze symmetrie blijkt echter de vorm van de orbitalen te sterk te beperken. Als we de symmetrie loslaten en elke vorm van de orbitalen toestaan, dan vinden we de energie die we verwacht hadden. Het volgende systeem dat we onderzoeken is de vervorming van een rechthoek met op elke hoek een waterstof atoom. Hieruit blijkt nogmaals hoe belangrijk het is dat we de orbitalen niet beperken tot een bepaalde symmetrie en dat de keuze van het startpunt cruciaal is. Vervolgens testen we het uit elkaar trekken van

een aantal molecules. Bij N_2 vinden we goede resultaten maar bij CN^- en NO^+ botsen we op een gekend probleem van de techniek. Het aantal elektronen moet mooi verdeeld worden over de atomen, maar onze benadering heeft hier een fout: één elektron zal worden verspreid over beide atomen. Dit lijdt tot een fysisch incorrecte situatie maar door de extra vrijheid is de energie wel lager. Er bestaat een oplossingsmethode voor dit probleem maar ze is complex en traag. De specifieke oplossing suggereert echter dat er misschien een andere snellere methode zou kunnen bestaan om dit op te lossen. Tot slot proberen we nog een CO molecule, en daar zijn de resultaten opnieuw goed.

We hebben in dit werk aangetoond dat door de golffunctie te beperken tot een bepaalde klasse, de voorwaarden voor N-representeerbaarheid veel simpeler worden, en dat de optimalisatie een stuk sneller kan worden uitgerekend. Het nadeel dat de vorm van de orbitalen ook moet worden geoptimaliseerd is aangepakt. De eerst resultaten zijn beloftevol. In de toekomst kunnen we beter optimalisatie technieken voor de orbitalen proberen en de drie-index condities implementeren. Deze zouden de accuraatheid van de methode aanzienlijk moeten verbeteren en de gevonden dichtheidsmatrix zal ook dichter bij de echte liggen.

Abstract

Nothing is as simple as it seems at first.
Or as hopeless as it seems in the middle.
Or as finished as it seems in the end.

The world at the level of the atom is described by the branch of science called quantum mechanics. The world of quantum mechanics is very different from our own macroscopic world. It is governed by probabilities and there is a duality between particles and waves. Its foundations were built in the first half of the twentieth century by a large group of physicists. The crown jewel is given by the Schrödinger equation which describes a system of indistinguishable particles, that interact with each other. However, an equation alone is not enough: the solution is what interests us. This is a problem, because only for the smallest system is the analytical solution known. For other systems we must resort to numerical techniques. And even then we are plagued by an exponential scaling of the Hilbert space.

In the second half of the twentieth century, a wide array of approximations were developed. This dissertation concerns itself with one of the oldest approximations: the variational optimization of the second-order reduced density matrix (v2DM). Its main attractive point at the time was the reduction of the exponential scaling of the wave function to a quadratically scaling matrix. Unfortunately, the computational burden was simple shifted to the so-called N-representability problem: does there exist a wave function that is compatible with the given reduced density matrix? The necessary and sufficient conditions for N-representability are known but not in a practically usable form. To make matters worse, we now know that the problem belongs to the class of the hardest problems we know. A general solution is extremely unlikely to exist. Despite this, we can generate approximate solutions to the N-representability problem by using a set of necessary conditions. This leads to the classical $\mathcal{P}$, $\mathcal{Q}$ and $\mathcal{G}$ conditions. It also gives rise to another unique feature of this method: we always find a strict lower bound on the energy.

A major advance came when it was realized that the variational optimization of the second-order reduced density matrix can be expressed as a semidefinite programming problem. One could now use the vast machinery of the convex optimization world. And for a brief period, the technique flourished. Unfortunately, despite major advances the technique is still not on par with the competition: there exist faster and more accurate methods.

This dissertation tries another approach: we assume that the wave function has a Slater determinant expansion where all orbitals are doubly occupied or empty. Every electron has a pairing partner. This assumption drastically reduces the scaling of the two-index and three-index conditions. The downside is that the energy explicitly depends on the used orbitals and thus an orbital optimizer is needed. The hope is that by using this approximation, we can capture the lion's share of the static correlation and that any missing dynamic correlation can be added through perturbation theory.

We combine a boundary point method to optimize the second-order density matrix with an orbital optimizer based on Jacobi rotations. Finding the optimal orbitals is a very hard problem: it means finding the lowest point in an uncharted energy landscape. All methods that can solve this problem in general have one thing in common: they are slow. We follow the standard approximation: a local minimizer combined with a good guess of the starting point. At each iteration, we look for the optimal pair of orbitals to rotate and the optimal angle. The advantage of this method is that we avoid the expensive transformation of the one- and two-body integrals as the Jacobi rotation only mixes two orbitals at a time. As every unitary transformation can be decomposed into a series of Jacobi rotations, our approach forms no restriction in finding the optimal orbitals.

We test our method on several benchmark systems. For the hydrogen molecule, we can reproduce the exact values as expected. For a helium dimer, the dissociation limit is wrong. The spatial symmetry of the orbitals restricts the orbital optimizer. If we allow it to break the spatial symmetry, the correct dissociation limit is recovered. As a prototype for strong correlation, we test a linear H_8 chain. The choice of the starting point turns out to be crucial: only the symmetry broken, localized orbitals can find the lowest energy curve.

Next we study the dissociation of several diatomic molecules. The results for N_2 are good but the CN^- and NO^+ molecule suffer from a known issue with v2DM. The energy as a function of the number of electrons should be piecewise linear: on two dissociated atoms we should find an integer charge. Unfortunately, in v2DM this curve is convex which causes the algorithm to favour fractional charges. By distributing a single electron over both atoms the energy can be artificially lowered. There is a solution to this problem

in the form of subsystem constraints but it is expensive to use. However, using the orbitals produced by an exact solver in the v2DM algorithm without orbital optimization does give us the correct energy. This suggest that an alternative solution within the orbital optimizer can be found.

We can conclude that the restriction of the N-representability conditions to a doubly-occupied wave function has promise. The lower scaling makes the method competitive with other methods, while the orbital optimization can be handled efficiently. The issue of the fractional charges still requires a fast solution. There are several interesting paths to investigate in the future: several alternative orbital optimizer schemes are worth pursuing, along with improved guesses of the starting points. The conditions on the third-order reduced density matrix still need testing. A good approximation of the energy does not necessary mean that we also have a good approximation of the second-order reduced density matrix itself. The three-index condition should help in this case.

List of Abbreviations and Glossary

1DM

first-order reduced Density Matrix. 6, 7, 17, 19–23, 27, 38, 46, 48, 53, 60, 114, 126, 152

2DM

second-order reduced Density Matrix. 7–9, 11–13, 17, 18, 21–23, 26–30, 32, 35–40, 43–49, 51–53, 60, 68, 69, 74, 84, 85, 88, 89, 91, 99, 104, 111, 116, 125–127, 129, 157, 161

3DM

third-order reduced Density Matrix. 26–28, 46, 52, 53, 58, 60, 61, 126, 129, 157

AP1roG

Antisymmetric Product of one-reference-orbital Geminals. 86–88, 99, 106, 127

APG

Antisymmetric Product of Geminals. 84, 85

BPP

Bounded-Error Probabilistic Polynomial Time. 15–17

BQP

Bounded-Error Quantum Polynomial Time. 17

CASSCF

Complete Active Space Self-Consistent Field. 94

CC

Coupled Cluster. 60, 112

cc-pVDZ

Correlation Consistent Polarized Valence Double Zeta. 44, 101, 103, 107, 111–113, 115, 118, 119, 162

CCD

Coupled Cluster with Double excitations. 86

CCSD(T)

Coupled Cluster with Singles, Doubles and Triples in Perturbation. 9, 87, 111, 112

CI

Configuration Interaction. 5, 11, 60, 83, 86, 101, 126, 127

CID

Configuration Interaction with Double excitations. 86

CIDQ

Configuration Interaction with Double and Quadruple excitations. 86

CISD

Configuration Interaction with Single and Double excitations. 84, 86

DFT

Density Functional Theory. 17, 60, 111, 114–116, 126

DMRG

Density Matrix Renormalization Group. 102, 106, 111–113, 115, 119, 120

DOCI

Doubly Occupied Configuration Interaction. 9, 45–47, 49, 51, 53, 58, 78, 80, 83–88, 91, 92, 100, 104, 105, 107–109, 111–113, 115, 118–120, 126–128, 162

ER

Edmiston-Ruedeberg localized orbitals. 105, 107, 110, 128

FLOPS

Floating-Point Operations per Second. 91

FullCI

Full Configuration Interaction. 5, 6, 45, 60, 83, 85, 86, 88, 97, 98, 102, 105, 106, 112, 118, 121, 127–129

FullDOCI

Full Doubly Occupied Configuration Interaction. 86, 88, 101, 104, 107, 111–121, 127, 128, 162

geminal

A two-particle state. 84, 85, 116

GHF

General Hartree-Fock. 104

GVB

General Valence Bond. 85

HF

Hartree-Fock. 5, 6, 20, 21, 45, 83, 85, 87, 89, 97, 101, 104–107, 109, 110

KKT

Karush–Kuhn–Tucker conditions. 77

MA

Merlin-Arthur. 16, 17

MCSCF

Multi-Configurational Self-Consistent Field. 6, 83, 84, 86, 87, 91, 94

MO

Molecular Orbital theory. 85, 101

MPI

Message Passing Interface. 101

MPS

Matrix Product State. 102

NP

Nondeterministic Polynomial Time. 14–17, 32

P

Deterministic Polynomial Time. 15–17, 19

QMA

Quantum Merlin Arthur. 14, 17, 126

RHF

Restricted Hartree-Fock. 86, 97, 101, 102, 104–106, 121, 128

SA

Simulated Annealing. 87, 99, 100

SDP

Semidefinite Programming. 21, 25, 63–66, 68, 70, 72, 76, 77, 80, 87, 125–127

seniority

The number of unpaired particles in the wave function. 46, 47, 49, 50, 52–54, 56, 58, 60, 84, 86, 126

v2DM

Variational Optimization of the second-order reduced Density Matrix. 7–9, 11, 17, 18, 35, 39, 41, 63, 67, 68, 75, 76, 79, 80, 83, 87–91, 97, 99, 101, 104, 111–116, 118–121, 125–128

v2DM-DOCI

Variational Optimization of the second-order reduced Density Matrix in the DOCI space. 88–91, 100–102, 105–107, 110–121, 128, 161

VB

Valence Bond. 85

VBSCF

Valence Bond Self-Consistent Field. 86, 87

Part I

Variational determination of the two-particle density matrix: the case of doubly-occupied space

Chapter 1

Introduction

> *We must be clear that when it comes to atoms, language can be used only as in poetry. The poet, too, is not nearly so concerned with describing facts as with creating images and establishing mental connections.*
>
> Niels Bohr

Richard Feynman, one of the great physicists of the twentieth century, once asked his students:

> If, in some cataclysm, all of scientific knowledge were to be destroyed, and only one sentence passed on to the next generation of creatures, what statement would contain the most information in the fewest words?

It is an interesting question and a wide range of answers is possible but Feynman's own idea is what is of interest here:

> I believe it is the atomic hypothesis that all things are made of atoms - little particles that move around in perpetual motion, attracting each other when they are a little distance apart, but repelling upon being squeezed into one another. In that one sentence, you will see, there is an enormous amount of information about the world, if just a little imagination and thinking are applied.

The idea that matter is built out of atoms is of a profound importance. The world of the atom is a strange world, many things that are counterintuitive are possible on the small scale of an atom. It took a long time for science

to develop a good understanding of it. The branch of physics that deals with the dynamics of particles on atomic length scales is called quantum mechanics. Its foundations were laid in the beginning of the previous century. One of the many counter-intuitive features of quantum mechanics is that particles are described by a wave equation, the so-called Schrödinger equation. Unfortunately this equation can only be solved exactly for systems which are either very small or have special symmetry properties. For other interesting cases one needs to introduce approximations and use numerical techniques. In this work we will describe and develop one such technique, the variational determination of the two-particle reduced density matrix, and apply it to a number of non-trivial systems. We will use the second quantization formalism as it is the natural language to explain this technique. A short introduction to the formalism can be found in Chapter B on page 147.

1.1 Variational second-order density matrix optimization

An N-particle quantum system with pairwise interactions is governed by a Hamiltonian

$$\hat{H} = \hat{T} + \hat{V}, \tag{1.1}$$

where $\hat{T}$ are the one-body operators and $\hat{V}$ the two-body operators. We want to find the ground state energy and wave function,

$$\hat{H}\Psi(\boldsymbol{x}) = E_0\Psi(\boldsymbol{x}), \tag{1.2}$$

where $\boldsymbol{x}$ is a vector in the space $\mathbb{C}^{3N} \times \{\uparrow, \downarrow\}^{3N}$. There are few restrictions on the wave function Ψ: it needs to belong to the class L^2 of square-integrable functions, it must be antisymmetric under the exchange of (indistinguishable) particles due to the Pauli exclusion principle and it has to be normalized. In ab-initio quantum chemistry methods, the Hilbert space is usually restricted to a space spanned by a finite, non-complete set of basis functions. This has the advantage that eq. (1.2) is reduced to a discrete Hermitian eigenvalue problem. The construction of these basis sets is a science of its own: most commonly used are linear combinations of Gaussian functions because they allow for efficient computation of the one- and two-electron integrals. From now on, we will work in an M-dimensional space built by single-particle orbitals. We will refer to these single-particle states with Greek letters: α, β, γ, … A single-particle state is always the product of a spatial orbital and a spin state. To refer to the spatial orbital we will use Roman letters: a, b, c, etc.

In the second quantization formalism (see Chapter B), the Hamiltonian (1.1) can be written as

$$\hat{H} = \sum_{\alpha\beta} T_{\alpha\beta} \hat{a}^\dagger_\alpha \hat{a}_\beta + \frac{1}{4} \sum_{\alpha\beta\gamma\delta} V_{\alpha\beta;\gamma\delta}\ \hat{a}^\dagger_\alpha \hat{a}^\dagger_\beta \hat{a}_\delta \hat{a}_\gamma, \tag{1.3}$$

where $T_{\alpha\beta} = \langle\alpha|\hat{T}|\beta\rangle$ and $V_{\alpha\beta;\gamma\delta} = \langle\alpha\beta|\hat{V}|\gamma\delta\rangle$ are the one- and two-electron integrals. In this work, we only consider Hamiltonians which are field-free (e.g. no magnetic field), non-relativistic and real. The wave function is always over the field $\mathbb{R}$. These are the default assumptions in quantum chemistry. For atoms and molecules, this means that $\hat{T}$ is the sum of the electronic kinetic energy and the nuclei-electron attraction, whereas $\hat{V}$ represents the interelectronic Coulomb repulsion. We always work within the Born-Oppenheimer approximation [1]: we assume that the wave function can be split in its electronic and nuclear degrees of freedom and we neglect the latter. The associated Schrödinger equation in its matrix form is

$$\hat{H}\,|\psi\rangle = E_0\,|\psi\rangle\,. \tag{1.4}$$

The most simple solution is the mean-field approximation, also known as Hartree-Fock (HF), in which $|\psi\rangle$ is given by a single Slater determinant:

$$|\psi\rangle = \hat{a}^\dagger_{\alpha_1} \hat{a}^\dagger_{\alpha_2} \dots \hat{a}^\dagger_{\alpha_N}\,|\rangle\ . \tag{1.5}$$

A Slater determinant is nothing more than the antisymmetric linear combination of a set of orthogonal single-particle states. There are $\frac{M!}{N!(M-N)!}$ possible Slater determinants if the dimension of the single-particle basis is M and N the number of particles. They form a complete basis in which we can expand the wave function

$$|\psi\rangle = \sum_{\alpha_1\alpha_2\alpha_3\dots\alpha_N} c_{\alpha_1\alpha_2\alpha_3\dots\alpha_N}\ \hat{a}^\dagger_{\alpha_1} \hat{a}^\dagger_{\alpha_2} \hat{a}^\dagger_{\alpha_3} \dots \hat{a}^\dagger_{\alpha_N}\,|\rangle\,. \tag{1.6}$$

In the Configuration Interaction (CI) method [2], the wave function is written as a linear combination of a set of Slater determinants. The coefficients are then optimized to find the lowest energy in eq. (1.4). The difficulty in this method lies in picking a suitable set of Slater determinants. The best possible solution within the basis set limit is found when all possible Slater determinant are used. This is called Full Configuration Interaction (FullCI) and coincides with the exact diagonalization of the Hamiltonian matrix. Unfortunately, this is unfeasible for all but the smallest systems.

In practice, the expansion (1.6) is truncated at some point. The usual approach is to use the Hartree-Fock solution as a reference point and then

add Slater determinants which are excitations of the reference Slater determinant: one or more occupied orbital are replaced with a unoccupied (virtual) orbital. In this way, a hierarchy is found: Slater determinants can be cataloged according to the number of excitations needed starting from the reference point. The number of excitations used is denoted by a letter: S for single excitations, D for double excitations, T for triple excitations, etc. These methods are called single-reference as they use one reference Slater determinant. This is not always a good approximation: for example during bond-breaking, multiple independent Slater determinants in the wave function (1.6) will become important. The solution here is to use multi-reference methods like Multi-Configurational Self-Consistent Field (MCSCF) [1, 2]. In MCSCF, both the coefficients for the Slater determinants as well as the single-particle orbitals in the Slater determinants are optimized.

The contributions to the energy are usually split up into two parts: dynamic correlation and non-dynamic (static) correlation. There is no unambiguous distinction between both but as a rule of thumb: the FullCI wave function will have a (small) number of dominant Slater determinants. These are responsible for the static correlation. The dynamic correlation is given by the Slater determinants which are excitations of the dominant set.

A more natural way to describe the state of an N-particle quantum system is through the so-called Nth-order density matrix [3]. In reality most systems are entangled with their environment and they are described by an ensemble of wave functions. This is elegantly expressed with the Nth-order density matrix D

$$D(\boldsymbol{x};\boldsymbol{x}') = \sum_i w_i \Psi_i(\boldsymbol{x})\Psi_i(\boldsymbol{x}'), \tag{1.7}$$

where $w_i \geq 0$ and $\sum_i w_i = 1$. The Nth-order density matrix is positive semidefinite and normalized to 1. A special case is a "pure state density", where the system is characterized by a single wave function,

$$D(\boldsymbol{x};\boldsymbol{x}') = \Psi(\boldsymbol{x})\Psi(\boldsymbol{x}'). \tag{1.8}$$

It is characterized by the fact that D should be idempotent: $D^2 = D$. The first-order reduced Density Matrix (1DM) is found by integrating out all degrees of freedom except those belonging to a single particle:

$$\rho(x_1;x_1') = N \int D(x_1, x_2, \ldots, x_N; x_1', x_2, \ldots, x_N) dx_2 \ldots dx_N. \tag{1.9}$$

Dirac showed that Hartree-Fock solution can be expressed solely using the 1DM [4]. In other words, the 1DM contains the same information as a single Slater determinant. The pth-order reduced density matrix is defined in a

similar way: all degrees of freedom but p are integrated out. From now on, we will only use the second quantization. In this formalism, the 1DM $\rho_{\alpha\beta}$ and the second-order reduced Density Matrix (2DM) $\Gamma_{\alpha\beta;\gamma\delta}$ are given by

$$\rho_{\alpha\beta} = \sum_i w_i \langle\psi_i|\hat{a}^\dagger_\alpha \hat{a}_\beta|\psi_i\rangle\,, \tag{1.10}$$

$$\Gamma_{\alpha\beta;\gamma\delta} = \sum_i w_i \langle\psi_i|\hat{a}^\dagger_\alpha \hat{a}^\dagger_\beta \hat{a}_\delta \hat{a}_\gamma|\psi_i\rangle\,, \tag{1.11}$$

for an ensemble of wave functions ($w_i \geq 0$ and $\sum_i w_i = 1$). The pure state case is found when all except one $w_i = 0$. The 1DM and 2DM are not independent, for we can extract the 1DM out of the 2DM as:

$$\rho_{\alpha\beta} = \frac{1}{N-1}\sum_\lambda \Gamma_{\alpha\lambda;\beta\lambda}. \tag{1.12}$$

A key observation is that the ground state energy of the Hamiltonian (1.3) can be expressed as a linear function of the 2DM

$$E_0 = \mathrm{Tr}\,(K\Gamma) = \frac{1}{4}\sum_{\alpha\beta\gamma\delta} K_{\alpha\beta;\gamma\delta}\Gamma_{\alpha\beta;\gamma\delta} = \sum_{\alpha<\beta}\sum_{\gamma<\delta} K_{\alpha\beta;\gamma\delta}\Gamma_{\alpha\beta;\gamma\delta}, \tag{1.13}$$

where

$$K_{\alpha\beta;\gamma\delta} = \frac{1}{N-1}\left(T_{\alpha\gamma}\delta_{\beta\delta} - T_{\beta\gamma}\delta_{\alpha\delta} - T_{\alpha\delta}\delta_{\beta\gamma} + T_{\beta\delta}\delta_{\alpha\gamma}\right) + V_{\alpha\beta;\gamma\delta}, \tag{1.14}$$

is the reduced Hamiltonian. Not only the ground state energy but the expectation value of any one- or two-particle operator can be calculating using the 2DM. Husimi [5] was the first to realize this in 1940. The full wave function contains all the information about the system but is a much more complicated object. The 2DM is a much more compact object which for most practical purposes is sufficient. It comes close to the "ultimate reduction" for an interacting many body problem. This compactness is the main attractive feature of the 2DM: the dimension of the 2DM scales quadratically with the single-particle dimension and is independent of the number of particles. It led to the idea of quantum mechanics without wave functions: the linear function (1.13) is used to variationally optimize the 2DM, henceforth called Variational Optimization of the second-order reduced Density Matrix (v2DM). However, when Coleman in 1951 performed the first variational optimization of the 2DM on Lithium, he was astonished to find an energy that was 20% below the ground state energy [6]. He realized that he varied over a too large class of trial 2DM's. Independently, Mayer [7] and Löwdin [8] published similar results in 1955. Tredgold [9] pointed out that the variational calculations done by Mayer lead to unphysical results and concluded

that additional constraints would be needed. In 1963 Coleman called this the N-representability problem [10]: what are the necessary and sufficient conditions on a 2DM to be derivable from a ensemble of wave functions, *i.e.* eq. (1.11) must hold for all trial 2DM's. Coleman derived the necessary and sufficient conditions for N-representability on the 1DM in his paper, and gave several necessary conditions on the 2DM. In 1963 a major step forward was made by Garrod and Percus [11] who derived the $\mathcal{Q}$ and $\mathcal{G}$ conditions. The computational results using these conditions on the Beryllium atom were promising: the obtained results were quite accurate [12, 13]. However, Beryllium turned out to be a special case: due to its simple electronic structure, the $\mathcal{Q}$ and $\mathcal{G}$ conditions performed extremely well. In other systems, the same conditions unfortunately did not perform as well [14, 15]. This led to a 25-year-long period of darkness. While in the 1960's there was still hope that the N-representability problem could be solved, it became clear that it is a very fundamental problem without a clear path forward.

In the 1990's, a renaissance arrived. Through another method, known as the contracted Schrödinger equation [16, 17], several groups were able to approximate the 2DM directly, without need for an underlying wave functions [18, 19]. This renewed interest in the direct variational calculation of the 2DM. In 2001, Nakata *et al.* [20] realized that the variational optimization problem could be written as a semidefinite program [21], which is a class of well-known convex optimization problems [22]. They used an off-the-shelf semidefinite solver [23] to calculate the energies of several atoms and molecules with good accuracy. Mazziotti [24] also jumped on the wagon and the train seemed unstoppable. In 2004, Zhao *et al.* [25] implemented three-index conditions $\mathcal{T}_1$ and $\mathcal{T}_2$ which led to milliHartree accuracy for some systems [26, 27], and Mazziotti [28, 29] introduced a much faster optimization method that extended the method to larger systems. In recent years, the variational optimization of the 2DM has gained a lot of appeal due to it being complementary to other variational methods: it provides a lower bound on the energy instead, of an upper bound that is found by variational methods that focus on the wave function. Also, in stark contrast with most wave function based methods, the v2DM method does not depend on a reference state. The energy function is exact, only the amount N-representability conditions limit the accuracy (and speed) of the method.

To make further progress in the v2DM method, two clear directions exist: (1) the search for new N-representability conditions which are computationally feasible (cheap); and (2) improving the semidefinite program algorithms to exploit the specific structure of v2DM. On the first path, Verstichel *et al.* [30] introduced subsystems constraints to fix the problem of fractional charges [31]. Shenvi and Izmaylov [32] introduced active-space constraints. Stricter

bounds on the two-index conditions were derived [33, 34]. Spin symmetry and point-group symmetry of molecules were exploited [35]. A stronger three-index condition was derived [36]. System-specific constraints were introduced [37, 38]. Even excitation energies were calculated [39] using the variationally optimized 2DM. Additional constraints for non-singlet states were discussed [40]. Linear inequalities for the 2DM were found [41–43]. This list is far from conclusive and only aims to give a glance of the activity on the N-representability front. Several books and review papers are written about v2DM and they provide an excellent overview of the road so far [6, 44–48].

On the semidefinite programming front, several algorithms were tried and customized to v2DM [28, 49–51]. The boundary point method [52] is currently the fastest, but it is not always stable. In the convex optimization literature, v2DM is known under the category 'very large scale': the most common semidefinite programming problems are much smaller. There exist general purpose solvers [23] but they are not efficient enough for our problem size.

Currently, the popularity of v2DM has again stagnated. The method is still not competitive with other popular methods like Coupled Cluster with Singles, Doubles and Triples in Perturbation (CCSD(T)), the so-called golden standard [53] in quantum chemistry. Although at present, much larger systems than in de past can be treated, the fundamental problem remains the N-representability. While the three-index conditions lead to considerably improved accuracy, they are computationally very expensive and thus unfeasible for larger systems. The quest for cheap yet accurate conditions continues.

In Chapter 2 the N-representability problem is introduced and the classical approximation to it. We discuss the use of symmetry to simplify the conditions and end with the restriction to the class of Doubly Occupied Configuration Interaction (DOCI) wave functions. We continue in Chapter 3 with an overview of the methods we use to solve a semidefinite programming problem and how we can tailor the algorithm to the specific case of v2DM. After this we discuss in Chapter 4 the motivation of the restriction to a DOCI wave function and put it to the test on a array of benchmark systems. In the final Chapter 5 we draw some conclusion about the merits of this approach.

1.2 Conventions

Greek letters (α, β, ...) are used to denote a single-particle state. The spatial part of an orbital will be referred to by Roman letters (a, b, ...). Almost all

summations will run over the single-particle states unless explicitly marked otherwise. To lighten the notation, the bounds of the sum over single-particle states will not be shown. The trace of a four-index tensor object is defined as

$$\mathrm{Tr}\,(A) = \sum_{\alpha<\beta}\sum_{\gamma<\delta} A_{\alpha\beta;\gamma\delta} = \frac{1}{4}\sum_{\alpha\beta\gamma\delta} A_{\alpha\beta;\gamma\delta} \tag{1.15}$$

Chapter 2

The N-representability problem

For a given wave function, the second-order reduced Density Matrix (2DM) can be calculated using its definition (1.11). However, when given a random symmetric matrix, is it possible to find a corresponding (ensemble of) wave function which has the given matrix as the 2DM? This is the essence of the N-representability problem. In the early days of Variational Optimization of the second-order reduced Density Matrix (v2DM), there was still hope that this problem could effectively be solved. Coulson [54] stated its importance at a conference about "Molecular Structure Calculations" in Boulder, Colorado in 1959:

> There is an instinctive feeling that matters such as electron correlation should show up in the two-particle reduced density matrix. … but we still do not know the conditions that must be satisfied by the 2DM. Until these conditions have been elucidated, it is going to be very difficult to make much progress along these lines…

In this chapter we will show that the hope of finding a solution for the N-representability problem is idle. A formal theorem about the necessary and sufficient conditions will be presented which we will use to find some practically usable necessary conditions. We also look at what we effectively can impose from the symmetry of the wave function in the 2DM. In the second part of this chapter, we rederive the conditions for a specific kind of Configuration Interaction (CI) wave function which simplifies these conditions greatly.

There are two kinds of N-representability: pure and ensemble, depending on whether the 2DM is derivable from a pure wave function or an ensemble of wave functions. We will only be concerned with ensemble N-representability in what follows. The set of ensemble N-representable 2DM's is a closed convex set (see Chapter C on page 149). This is interesting because a convex set is completely determined by its extreme points due to the Krein-Milman theorem [55]. It can be shown that the extreme points for ensemble N-representability are the pure states [6, 10]. The convexity will turn out to be paramount importance. For a long time, it was believed that the 2DM for the non-degenerate ground state of a Hamiltonian (with at most two-particle interaction) corresponds to a unique wave function or ensemble of wave functions [6] but recently counterexamples were found [56].

2.1 General N-representability theorem

The following theorem states the necessary and sufficient conditions for N-representability of a pth-order reduced density matrix.

Theorem 1. *A pth-order reduced density matrix ${}^p\Gamma$, is N-representability if and only if*

$$\forall H^{(p)} : \qquad \mathrm{Tr}\left({}^p\Gamma H^{(p)}\right) \geq E_0(H^{(p)}) \,, \tag{2.1}$$

where $E_0(H^{(p)})$ is the ground state energy of the Hamiltonian $H^{(p)}$.

A graphical depiction of this theorem can be found in Figure 2.1 on the facing page. The boundary of the convex set of N-representable pth-order reduced density matrices is formed by an infinite number of tangent hyperplanes, where each hyperplane represents a p-particle Hamiltonian and its ground state energy. Proving the necessary statement is easy: in case that the pth-order reduced density matrix is N-representable, this theorem simply states that the expectation value of the reduced density matrix with a Hamiltonian cannot be lower than the ground state energy of that Hamiltonian. To prove the sufficient statement, we first make a detour to the separating hyperplane theorem [22]:

Theorem 2. *Let A and B be two disjunct non-empty convex sets than there exists a hyperplane that separates both sets: there exists an a and b such that $\forall x \in A$, $\langle a, x\rangle \geq b$ and $\forall x \in B$, $\langle a, x\rangle \leq b$.*

Let us now assume that ${}^p\tilde{\Gamma}$ is not N-representable. The separating hyperplane theorem implies that there exists a Hamiltonian $H^{(p)}$ for which

$$\mathrm{Tr}\left({}^p\tilde{\Gamma} H^{(p)}\right) \leq k, \tag{2.2}$$

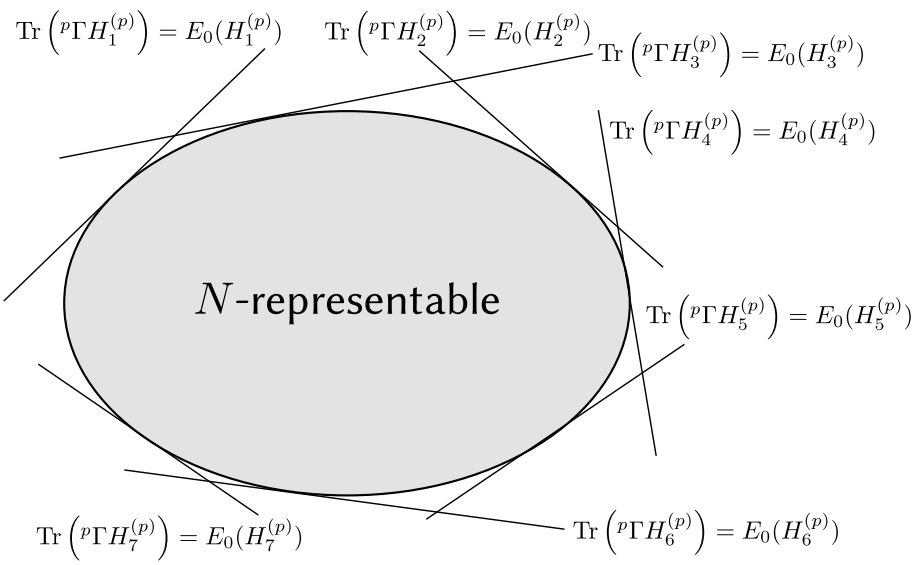

Figure 2.1: Graphical depiction of the necessary and sufficient conditions for N-representability. Every Hamiltonian $H^{(p)}$ can be represented by a hyperplane that bounds the convex set of N-representable ${}^p\Gamma$.

while for all N-representable reduced density matrices ${}^p\Gamma$,

$$\mathrm{Tr}\left({}^p\Gamma H^{(p)}\right) \geq k. \tag{2.3}$$

Now we have

$$\mathrm{Tr}\left({}^p\tilde{\Gamma} H^{(p)}\right) \leq k \leq E_0(H^{(p)}) \leq \mathrm{Tr}\left({}^p\Gamma H^{(p)}\right), \tag{2.4}$$

because $E_0(H^{(p)})$ is the lowest possible value obtainable by the last trace due to the variational principle. We can conclude that if a reduced density matrix is not N-representable, there will be a Hamiltonian for which the reduced density matrix will give a ground state energy which is too low.

This theorem also shows that the 2DM corresponding to the ground state wave function of a Hamiltonian will be on the border of the N-representable convex set [6]. One can even say that every point on the border corresponds to the ground state of some Hamiltonian. Note that this in general is not invertible: a 2DM on the border can correspond to the ground state of multiple Hamiltonians.

A noteworthy fact is the unitary invariance of this theorem. The ground state energy of the p-Hamiltonian $H^{(p)}$ is not dependent on the choice of single-particle basis. Any unitary transformation of the single-particle basis will

lead to the same ground state. This also means that the N-representability conditions must be unitary invariant.

This theorem is not directly usable as a test for N-representability as it requires the ground state energy of every possible Hamiltonian beforehand. It can however be used as a necessary condition as we will show in Section 2.3.

2.2 N-representability is QMA-complete

Although we now have some insight into the problem, we are still no closer to a real solution. And unfortunately, in the general case, we never will: in 2007, it was proven by Liu, Christandl, and Verstraete [57] that the N-representability problem is QMA-complete. This is the quantum generalization of NP-complete. To explain what this means, we will make a short detour into computational complexity theory. First, we will define some commonly used terms:

- Polynomial Time: an algorithm runs in polynomial time if there is an upper bound on the runtime, expressed as a polynomial in the problem size.
- Deterministic Turing machine: a theoretical machine [58, 59] devised by Turing in 1937 for computations. Every non-quantum computer today is a deterministic Turing machine. It consists of an infinitely long tape divided into cells, with in each cell a symbol. These symbols belong to a finite alphabet. There is also a head which can read the symbol in the current cell and move the tape to the next or previous cell. The machine has a state register which holds its state and a finite table of instructions that, given the current state and the current symbol, tells what to do next. It can take three consecutive actions: replace the symbol in the current cell with another, move the head to the next or previous cell, and change the state register to a new state.
- Non-deterministic Turing machine: in a deterministic Turing machine, the action table holds exactly one action for every possible symbol and state. In a non-deterministic Turing machine, multiple actions are possible and it follows them all in parallel. One could think of it as a Turning machine that can clone itself. A non-deterministic Turing machine and a deterministic Turing machine are equivalent in what they can calculate, they differ in the time it takes them to do it. It should be noted that a quantum computer is not a non-deterministic Turing machine.

- Decision problem: a question to which the answer is yes or no. The question can have several inputs. For example: given x, is x a prime number?

- Promise problem: a decision problem along with a promise about the inputs. For example: given a natural number x, is x a prime number?

With that knowledge, we can define the classic complexity classes:

- Deterministic Polynomial Time (P): a decision problem that can be solved in polynomial time on a deterministic Turing machine. For example: given a natural number x, is x a prime number [60]? Or what is the greatest common divisor for two numbers x and y. These are problems which can be solved efficiently.

- Nondeterministic Polynomial Time (NP): a decision problem that can be solved in polynomial time on a non-deterministic Turing machine. However, the proof of the answer can be verified in polynomial time on a deterministic Turing machine. This means that if we are given a specific instance of a problem and a witness (or certificate) that the answer is yes, we can verify that efficiently. For example: integer/prime factorization. Finding the factorization is difficult, but verifying a given factorization is easy.

- NP-hard: a problem is NP-hard, when any problem in NP can be reduced to it in polynomial time. These problems are at least as hard as the hardest problems in NP. Furthermore, if a polynomial time algorithm is found for any NP-hard problem, all NP-hard problems are solved. Notice that not all NP-hard problems are in NP: a NP-hard problem does not have to be a decision problem. For example, the traveling salesmen problem: given a set of places and the distances between them, find the shortest route to visit all the places exactly once.

- NP-complete: a problem is NP-complete when it is in NP and in NP-hard. For example, the decision version of the traveling salesmen: when given a total distance L, is there a path with a shorter total distance? As this is a subset of NP, the solution can be verified in polynomial time.

- Bounded-Error Probabilistic Polynomial Time (BPP): runs in polynomial time on probabilistic Turing machine. This is a deterministic Turing machine together with a random number generator: it is allowed

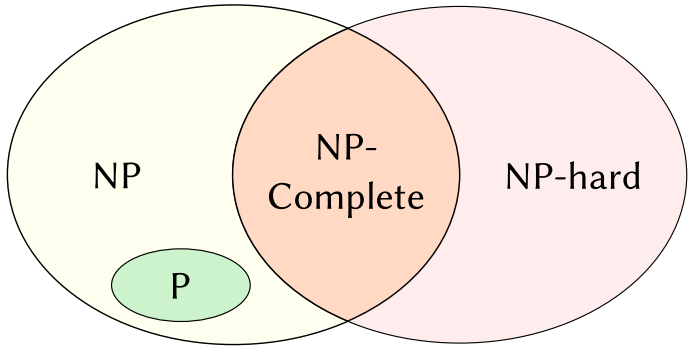

Figure 2.2: The relation between the different complexity classes. The question whether P=NP is one of the unsolved millennium problems and the associated prize is one million dollars [61].

to make random decisions but the probability of giving the wrong answer is at most $1/3$ (bounded error). The certainty of a solution can be improved by doing multiple computations. For example, some Monte-Carlo algorithms fall under this class. The class P is clearly a subset of BPP but its relation to NP is not yet known.

- Merlin-Arthur (MA): a class of decision problems that can only be computed non-deterministically. The Merlin-Arthur protocol is a kind of game: in this system, Merlin has access to unlimited computational power and sends a certificate (or proof) of the problem to Arthur. Using a BPP, Arthur then needs to verify the certificate so that if the answer is yes, he must conclude so with a probability of a least $2/3$. If the answer is no, Arthur must accept all certificates with a probability of at most $1/3$.

The relation between the different classes is shown in Figure 2.2. All of these classes have a quantum version, in which probabilities enter the game. But first we must introduce a quantum computer: quantum computers maximally exploit the non-classical features of a quantum (many-body) system. In analogy with classical information theory, information can be encoded in the quantum states of a quantum system, like the two spin projections of a spin $1/2$ particle, also referred to as a *qu*-bit. A qubit can be in a superposition of both 0 and 1. However in sharp contrast with classical bits, two qubits can become entangled, leading to remarkable quantum algorithms that are impossible on a classical level, such as prime-factorization with a polynomial scaling (in the input size) [62], or $O(\sqrt{N})$ searching in an unsorted database [63].

- Bounded-Error Quantum Polynomial Time (BQP): A quantum version of BPP. It uses a qubit instead of a random number generator. The above mentioned prime-factorization is part of BQP.
- Quantum Merlin Arthur (QMA): the quantum generalization of NP. It is the same as MA but now Arthur has a BQP to help him verify the certificate. The certificate can now take the form of a quantum state. For example, for a given Hamiltonian, is the ground state energy less than $\tilde{E}$? The certificate in this case would be the ground state wave function. Just like the class NP, it is hard to find a solution, but once found, it is easily verified for its correctness.

QMA-hard and QMA-complete have the same relative meaning as in the classical case.

We now return to the original problem of N-representability which was proven to be QMA-complete [57, 64]. Liu, Christandl, and Verstraete [57] proved this first by showing the QMA-hardness of the problem. They did this by reducing the N-representability problem to the 2-local-spin Hamiltonian which was already proven to be QMA-complete [65, 66] (the 2-local refers to a Hamiltonian with spins pairwise interacting). Secondly, they proved that it is part of the QMA class by building a setup in which Arthur can verify the N-representability with the requested accuracy and soundness. The proof for Arthur in this case would be the Nth-order density matrix D. It is easy to verify that the original Γ is reducible from this density.

In this regard, the variational optimization of the second-order density matrix is similar to Density Functional Theory (DFT) [67–69]. Both are exact in principle but depend on an unknown: N-representability for v2DM and the universal functional for DFT. The universal functional has also been shown to be QMA-complete [70].

Note that computational complexity theory deals with worst-case scenarios. It might be that in specific cases, the N-representability problem can be solved due to, for example, symmetry. In the case of $N = 2$ and $N = 3$ [71], the necessary and sufficient conditions for N-representability of the 2DM are known. The ensemble N-representability of the first-order reduced Density Matrix (1DM) is an entirely different matter: it belongs to the complexity class P.

2.2.1 Formal definition

The problem of N-representability is special case of a general set of problems knows as quantum marginal problems [72–74]. The classical marginal

problem [75] is defined as follows: given a set of random variables $X_1, X_2, \ldots, X_n$ and their joint probability distribution, $p(X_1, X_2, \ldots, X_n)$, we can calculate a k marginal distribution. This is done by integrating over a subset of $n-k$ random variables. For example, one of the $\binom{n}{k}$ marginal distributions is

$$g_n^k(X_1, X_2, \ldots, X_k) = \int p(X_{k+1}, X_{k+2}, \ldots, X_n) dX_{k+1} \ldots dX_n. \quad (2.5)$$

The classical marginal problem is the question, when given the set of all k marginal distributions $g_n^k(\ldots)$, does there exist a joint distribution $p(X_1, X_2, \ldots, X_n)$ that is compatible with it in the sense of eq. (2.5)? The quantum version of the marginal problem for identical particles is found when the probability distribution is replaced by the Nth-order density D. The marginal distribution is then the kth-order reduced density matrix

$${}^k\Gamma_{\alpha_1\alpha_2\ldots\alpha_k;\beta_1\beta_2\ldots\beta_k} = \sum_{\alpha_{k+1}\ldots\alpha_N} \sum_{\beta_{k+1}\ldots\beta_N} {}^N D_{\alpha_1\alpha_2\ldots\alpha_N;\beta_1\beta_2\ldots\beta_N} \quad (2.6)$$

Due to the fact that we work with identical particles and that any permutation of them should results in the same density up to a sign, all $\binom{N}{k}$ marginal distribution are the same. The question in the quantum version is then: what are the necessary and sufficient conditions for eq. (2.6) to hold. We can now also see that the necessary and sufficient conditions for N-representability of the ${}^k\Gamma$ in case of $N = k$ are trivial as the ${}^k\Gamma$ is then the Nth-order density D matrix. The conditions on the Nth-order density matrix D are much simpler: it should be positive semidefinite, $D \succeq 0$, and the trace should be one, $\mathrm{Tr}\,(D) = 1$.

2.3 Approximately N-representability conditions

In Section 2.1 on page 12 we showed the necessary and sufficient conditions for N-representability. These required the knowledge of the ground state energy of every possible Hamiltonian and are thus not usable as a sufficient condition. We can, however, use it as a necessary condition: if we restrict (2.1) to Hamiltonians of which we know the ground state energy or a lower bound on it, we can approximate the convex set of N-representable 2DM's. In Figure 2.3 on the next page we give a graphical interpretation of this idea. The approximate set of N-representable 2DM will be larger than the true set: there will be 2DM's which fulfil all the necessary conditions but are still not derivable from an ensemble of wave functions. As a consequence the variational optimization of the 2DM will give a lower bound on the energy. This is one of the highly attractive features of v2DM.

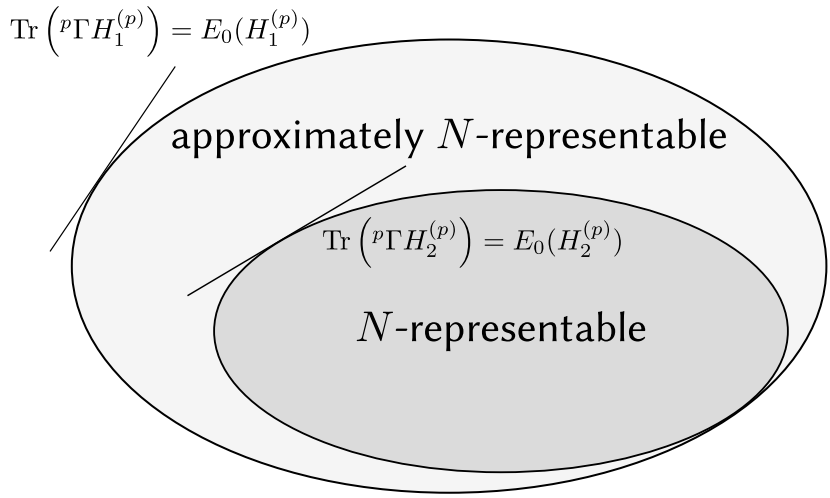

Figure 2.3: Graphical depiction of the necessary conditions for N-representability. $H_1^{(p)}$ belongs to the class of Hamiltonians of which we know a bound on ground state energy while $H_2^{(p)}$ does not. The true convex set of N-representable ${}^{p}\Gamma$ is smaller than the approximate convex set delimited by the Hamiltonians of the class of $H_1^{(p)}$.

2.3.1 The first-order reduced density matrix

The N-representability conditions for the 1DM are in the computational complexity class P as we will show. The 1DM is defined as

$$\rho_{\alpha\beta} = {}^{1}\Gamma = \sum_i w_i \left\langle \psi_i | \hat{a}_\alpha^\dagger \hat{a}_\beta | \psi_i \right\rangle , \tag{2.7}$$

with $\sum_i w_i = 1$ and $w_i \geq 0$. From now on, we will use ρ to denote the 1DM. Several properties can be easily derived from the definition (2.7)

$$\rho_{\alpha\beta} = \rho_{\beta\alpha}, \tag{2.8a}$$

$$\mathrm{Tr}\,(\rho) = \sum_\alpha \rho_{\alpha\alpha} = N, \tag{2.8b}$$

$$\rho \succeq 0. \tag{2.8c}$$

The last equation means that the 1DM must be positive semidefinite (see Chapter C on page 149). This can be understood by thinking of eq. (2.7) as an overlap. If we transform to the single-particle basis which diagonalizes the 1DM, the eigenvalues will be the norm of the states and thus have to be larger or equal to zero. The eigenvalues of the 1DM are called the natural

occupation numbers [8] and the corresponding eigenvectors are the natural orbitals or simply the naturals.

A class of Hamiltonians for which we know a lower bound on the ground state energy is giving by

$$\hat{H} = \hat{B}^\dagger \hat{B}, \tag{2.9}$$

as they are positive semidefinite

$$z^\dagger \hat{H} z = z^\dagger \hat{B}^\dagger \hat{B} z = \|Bz\|^2 \geq 0. \tag{2.10}$$

The operator $\hat{B}$ is a p-particle operator. For the 1DM there are two subclasses,

- $\hat{B}^\dagger = \sum_\alpha p_\alpha \hat{a}_\alpha^\dagger$ leads to

$$\sum_{\alpha\beta} p_\alpha \langle\psi|\hat{a}_\alpha^\dagger \hat{a}_\beta|\psi\rangle\, p_\beta \geq 0. \tag{2.11}$$

  This is equivalent with the already stated condition that the 1DM has to be positive semidefinite.

- $\hat{B}^\dagger = \sum_\alpha q_\alpha \hat{a}_\alpha$ leads to

$$\sum_{\alpha\beta} q_\alpha \langle\psi|\hat{a}_\alpha \hat{a}_\beta^\dagger|\psi\rangle\, q_\beta \geq 0. \tag{2.12}$$

  This can be written as a function of the 1DM using the fundamental anticommutator relations (B.5) to find

$$q = 1 - \rho \succeq 0 \tag{2.13}$$

  This condition means that the occupation number of an orbital cannot be greater than one or that the probability of finding a hole has to be positive.

Both conditions together enforce that the eigenvalues of the 1DM have to lay in the interval $[0, 1]$:

$$0 \preceq \rho \preceq 1 \tag{2.14}$$

This is of course nothing but the Pauli Exclusion principle. The bounds are strict: in the Hartree-Fock solution (a single Slater determinant) the orbitals will have an occupation of either zero or one. This makes us wonder if condition (2.14) is also sufficient for N-representability of the 1DM.

We already showed that the N-representability conditions should be unitary invariant for transformations of the single-particle basis. The eigenvalues of the 1DM form a complete set of unitary invariants for transformations of the

single-particle basis. As a consequence, the N-representability of the 1DM should be expressible solely as a function of its eigenvalues (and the number of particles N). Furthermore, it can be proven that the extreme elements of the convex set of 1DM's are N-representable by a single Slater determinant [10]. Any element in the convex set can be written as a convex combination of the extreme elements. This means that the condition (2.14) is not only necessary but also sufficient for N-representability!

Instead of optimizing the 2DM, we can also optimize the 1DM. To calculate the energy however, we need the 2DM. It is possible to write the 2DM in the cumulant expansion [18, 45, 76–78]

$$^2\Gamma = \rho \wedge \rho + \Delta, \tag{2.15}$$

$$^2\Gamma_{\alpha\beta;\gamma\delta} = \rho_{\alpha\gamma}\rho_{\beta\delta} - \rho_{\alpha\delta}\rho_{\beta\gamma} + \Delta_{\alpha\beta;\gamma\delta}. \tag{2.16}$$

The wedge denotes the Grassmann product (see Chapter C on page 149). The 2DM can be split up into a part expressible in terms of the 1DM and the cumulant Δ, which cannot be expressed as a function of the 1DM. We can approximate the 2DM by setting the cumulant part equal to zero. This boils down to taking an uncorrelated 2DM. The cumulant part holds the two-particle correlations. In fact, the necessary and sufficient conditions for the cumulant to be zero is that the 1DM is idempotent: $\rho^2 = \rho$ [77]. This means that optimizing the 1DM with the cumulant of the 2DM equal to zero is equivalent to Hartree-Fock. The optimization problem for the 1DM is

$$\begin{aligned} E = \min_{\rho} & \operatorname{Tr}\left(H^{(1)}\rho\right) + \operatorname{Tr}\left(\rho V \rho\right) \quad \text{while} \\ & \operatorname{Tr}\left(\rho\right) = N \\ & \rho \succeq 0 \\ & 1 - \rho \succeq 0 \end{aligned} \tag{2.17}$$

The variation is done over all real, symmetric $N \times N$ matrices. The two-particle interaction is represented by V. The energy functional is unfortunately no longer linear in the 1DM, which complicates the optimization. Veeraraghavan and Mazziotti [79, 80] have used this approach to find a global minimum for the Hartree-Fock energy. They rewrote the optimization problem to a Semidefinite Programming form and deduced an upper and lower bound on the Hartree-Fock energy.

2.3.2 The second-order reduced density matrix

The second-order reduced Density Matrix (2DM) is defined by

$$\Gamma_{\alpha\beta;\gamma\delta} = {}^2\Gamma_{\alpha\beta;\gamma\delta} = \sum_i w_i \left\langle \psi_i | \hat{a}^\dagger_\alpha \hat{a}^\dagger_\beta \hat{a}_\delta \hat{a}_\gamma | \psi_i \right\rangle. \tag{2.18}$$

Again $\sum_i w_i = 1$ and $w_i \geq 0$. From now on, we will use Γ to denote the 2DM. As with the 1DM, several properties can be derived directly from the definition (2.18)

$$\Gamma_{\alpha\beta;\gamma\delta} = -\Gamma_{\beta\alpha;\gamma\delta} = -\Gamma_{\alpha\beta;\delta\gamma} = \Gamma_{\beta\alpha;\delta\gamma}, \tag{2.19a}$$

$$\Gamma_{\alpha\beta;\gamma\delta} = \Gamma_{\gamma\delta;\alpha\beta}, \tag{2.19b}$$

$$\mathrm{Tr}\,(\Gamma) = \sum_{\alpha<\beta} \Gamma_{\alpha\beta;\alpha\beta} = \frac{N(N-1)}{2}, \tag{2.19c}$$

$$\Gamma \succeq 0. \tag{2.19d}$$

The last condition can be interpreted in the same way as condition (2.8c) on the 1DM: as the positivity of an overlap matrix in the two-particle space.

As already stated, the N-representability conditions for the 2DM form a much harder problem. While the necessary and sufficient conditions for N-representability on the 1DM can be enforced solely using the spectrum of the 1DM, this cannot be the case for the 2DM. In general, a unitary transformation of the single-particle basis cannot diagonalize the 2DM and thus the spectrum of the 2DM does not form a complete set of unitary invariants. This is one of the reasons why the N-representability problem for the 2DM is so much harder than for the 1DM. Coleman [10] derived upper bounds on the eigenvalues of the 2DM

$$0 \leq \lambda \leq \begin{cases} N-1 & \text{when } N \text{ is odd} \\ N & \text{when } N \text{ is even} \end{cases} \tag{2.20}$$

For the 2DM we can again use the positivity of Hamiltonians of the class (2.9). To lighten the notation, we will not shown the ensemble summation in the conditions. This leads to the following conditions

- $\hat{B}^\dagger = \sum_{\alpha\beta} p_{\alpha\beta} \hat{a}^\dagger_\alpha \hat{a}^\dagger_\beta$ gives

$$\sum_{\alpha\beta\gamma\delta} p_{\alpha\beta} \langle\psi|\hat{a}^\dagger_\alpha \hat{a}^\dagger_\beta \hat{a}_\delta \hat{a}_\gamma|\psi\rangle\, p_{\gamma\delta} \geq 0, \tag{2.21}$$

  which is equivalent with condition (2.19d). This condition has several names in the literature: P, D and $\mathfrak{I}$ condition. We will use the latter. The 1DM can be extracted from the 2DM

$$\rho_{\alpha\beta} = \frac{1}{N-1} \sum_\lambda \Gamma_{\alpha\lambda;\beta\lambda}. \tag{2.22}$$

  If we enforce this condition, the 1DM is also positive semidefinite

$$\sum_{\alpha\beta} z_\alpha \rho_{\alpha\beta} z_\beta = \frac{1}{N-1} \sum_{\alpha\beta} \sum_{\delta\gamma} z_\alpha \delta_{\gamma\delta} \Gamma_{\alpha\gamma;\beta\delta} z_\beta \geq 0, \tag{2.23}$$

as this is a special case of the general condition (2.21).

- $\hat{B}^\dagger = \sum_{\alpha\beta} q_{\alpha\beta}\hat{a}_\alpha\hat{a}_\beta$ gives

$$\sum_{\alpha\beta\gamma\delta} q_{\alpha\beta}\,\langle\psi|\hat{a}_\alpha\hat{a}_\beta\hat{a}_\delta^\dagger\hat{a}_\gamma^\dagger|\psi\rangle\,q_{\gamma\delta} \geq 0, \tag{2.24}$$

which is the $\mathfrak{Q}$ condition of Garrod and Percus [11]. We define the $\mathfrak{Q}$ matrix as

$$\mathfrak{Q}_{\alpha\beta;\gamma\delta} = \langle\psi|\hat{a}_\alpha\hat{a}_\beta\hat{a}_\delta^\dagger\hat{a}_\gamma^\dagger|\psi\rangle\,. \tag{2.25}$$

Condition (2.24) expresses the positive semidefiniteness of the $\mathfrak{Q}$ matrix. The probability of finding a two-hole pair has to be greater than zero. The $\mathfrak{Q}$ matrix has the same symmetry in the indices as the 2DM, e.g. (2.19a) and (2.19b). It can be written as a function of the 2DM using the fundamental anticommutator relations eq. (B.5) on page 147

$$\begin{aligned}\mathfrak{Q}_{\alpha\beta;\gamma\delta}(\Gamma) &= \delta_{\alpha\gamma}\delta_{\beta\delta} - \delta_{\alpha\delta}\delta_{\beta\gamma} + \Gamma_{\alpha\beta;\gamma\delta} \\ &\quad - \delta_{\alpha\gamma}\rho_{\beta\delta} + \delta_{\beta\gamma}\rho_{\alpha\delta} + \delta_{\alpha\delta}\rho_{\beta\gamma} - \delta_{\beta\delta}\rho_{\alpha\gamma},\end{aligned} \tag{2.26a}$$

$$\mathfrak{Q}(\Gamma) = {}^2\mathbb{1} + \Gamma - {}^1\mathbb{1} \wedge \rho. \tag{2.26b}$$

With $\mathbb{1}$ we denote the identity matrix, the superscript denotes the space. This condition enforces the positive semidefiniteness of the q matrix (2.13) in the same way as eq. (2.23). The $\mathfrak{I}$ and $\mathfrak{Q}$ condition are enough to enforce the N-representability of the 1DM as the trace is also fixed by condition (2.19c). However, the set over which the variation is done when using the $\mathfrak{I}$ and $\mathfrak{Q}$ condition is still larger than the true N-representable set of the 2DM and as such the energy be lower than the true ground state energy.

- $\hat{B}^\dagger = \sum_{\alpha\beta} g_{\alpha\beta}\hat{a}_\alpha^\dagger\hat{a}_\beta$ gives

$$\sum_{\alpha\beta\gamma\delta} g_{\alpha\beta}\,\langle\psi|\hat{a}_\alpha^\dagger\hat{a}_\beta\hat{a}_\delta^\dagger\hat{a}_\gamma|\psi\rangle\,g_{\gamma\delta} \geq 0, \tag{2.27}$$

which leads to the $\mathfrak{G}$ condition [11]

$$\mathfrak{G}_{\alpha\beta;\gamma\delta} = \langle\psi|\hat{a}_\alpha^\dagger\hat{a}_\beta\hat{a}_\delta^\dagger\hat{a}_\gamma|\psi\rangle\,. \tag{2.28}$$

This condition enforces the positive semidefiniteness of the $\mathfrak{G}$ matrix which expressed the probability of finding a particle-hole pair must be larger than zero. We can again express the $\mathfrak{G}$ condition as a function of the 2DM using the anticommutator relations (B.5)

$$\mathfrak{G}_{\alpha\beta;\gamma\delta} = \delta_{\beta\delta}\rho_{\alpha\gamma} - \Gamma_{\alpha\delta;\gamma\beta}. \tag{2.29}$$

A major difference with the $\mathcal{I}$ and $\mathcal{Q}$ condition is that the symmetry within a pair state is gone: $\mathcal{G}_{\alpha\beta;\gamma\delta} \neq \mathcal{G}_{\beta\alpha;\gamma\delta}$. The $\mathcal{G}$ matrix is only symmetric under exchange of the pair: $\mathcal{G}_{\alpha\beta;\gamma\delta} = \mathcal{G}_{\gamma\delta;\alpha\beta}$.

- $\hat{B}^\dagger = \sum_{\alpha\beta} \tilde{g}_{\alpha\beta} \hat{a}_\alpha \hat{a}^\dagger_\beta$ gives

$$\sum_{\alpha\beta\gamma\delta} \tilde{g}_{\alpha\beta} \langle\psi|\hat{a}_\alpha \hat{a}^\dagger_\beta \hat{a}_\delta \hat{a}^\dagger_\gamma|\psi\rangle \tilde{g}_{\gamma\delta} \geq 0, \tag{2.30}$$

We will show that this condition is not independent of the $\mathcal{G}$ condition and therefore it is not used. It expresses the probability of finding a hole-particle pair.

It is possible to use a more general form of the $\hat{B}^\dagger$ operator in the Hamiltonian (2.9). For the so-called $\mathcal{G}'$ condition, we use

$$\hat{B}^\dagger = \sum_{\alpha\beta} g'_{\alpha\beta} \hat{a}^\dagger_\alpha \hat{a}_\beta + C, \tag{2.31}$$

where C is a constant operator. This leads to the following condition

$$\begin{aligned}\langle\psi|\hat{B}^\dagger \hat{B}|\psi\rangle = \sum_{\alpha\beta\gamma\delta} g'_{\alpha\beta}\, \mathcal{G}_{\alpha\beta;\gamma\delta}\, g'_{\gamma\delta} + C \sum_{\alpha\beta} g'_{\alpha\beta}\, \rho_{\alpha\beta} \\ + C \sum_{\gamma\delta} g'_{\gamma\delta}\, \rho_{\gamma\delta} + C^2 \geq 0\,. \end{aligned} \tag{2.32}$$

It is clear that we find the $\mathcal{G}$ condition (2.27) when we choose $C = 0$. We can rewrite the $\hat{B}^\dagger$ operator

$$\begin{aligned}\hat{B}^\dagger &= \sum_{\alpha\beta} g'_{\alpha\beta} \hat{a}^\dagger_\alpha \hat{a}_\beta + C \\ &= \sum_{\alpha\beta} -g'_{\alpha\beta} \hat{a}_\beta \hat{a}^\dagger_\alpha + \sum_{\alpha\beta} \delta_{\alpha\beta} g'_{\alpha\beta} + C.\end{aligned}$$

If we choose $C = \sum_\alpha -g'_{\alpha\alpha}$, we find the condition (2.30). The most strict choice of C is

$$C = -\sum_{\alpha\beta} g'_{\alpha\beta} \rho_{\alpha\beta}, \tag{2.33}$$

which can be understood if we rewrite eq. (2.32) to

$$\sum_{\alpha\beta\gamma\delta} g'_{\alpha\beta}\, \mathcal{G}_{\alpha\beta;\gamma\delta}\, g'_{\gamma\delta} + \left(C + \sum_{\alpha\beta} g'_{\alpha\beta}\, \rho_{\alpha\beta} \right)^2 - \sum_{\alpha\beta\gamma\delta} g'_{\alpha\beta} g'_{\gamma\delta}\, \rho_{\alpha\beta} \rho_{\gamma\delta} \geq 0\,.$$

The choice (2.33) will give the lowest upper bound. The major disadvantage is that the condition is not linear in Γ anymore due to the last term. This complicates the Semidefinite Programming problem considerably and is therefore avoided. It turns out that the $\mathcal{G}$ condition will give the same results as using condition (2.31): the nullspace (the eigenspace corresponding to a zero eigenvalue) of both conditions are the same. To understand this, let us look at the condition that the $\mathcal{G}$ matrix has a zero eigenvalue

$$\sum_{\gamma\delta} \mathcal{G}_{\alpha\beta;\gamma\delta}\, v_{\gamma\delta} = \sum_{\gamma} \rho_{\alpha\gamma} v_{\gamma\beta} - \sum_{\gamma\delta} \Gamma_{\alpha\delta;\gamma\beta} v_{\gamma\delta} = 0. \tag{2.34}$$

If we trace this, we find

$$\begin{aligned} \sum_{\alpha}\sum_{\gamma\delta} \mathcal{G}_{\alpha\alpha;\gamma\delta}\, v_{\gamma\delta} &= \sum_{\alpha\gamma} \rho_{\alpha\gamma} v_{\gamma\alpha} + (N-1) \sum_{\gamma\delta} \rho_{\delta\gamma} v_{\gamma\delta} \\ &= N \sum_{\alpha\beta} \rho_{\alpha\beta} v_{\beta\alpha} = 0. \end{aligned} \tag{2.35}$$

The $\mathcal{G}'$ condition with the optimal choice for C (eq. (2.33)) is

$$\mathcal{G}'_{\alpha\beta;\gamma\delta}(\Gamma) = \mathcal{G}_{\alpha\beta;\gamma\delta}(\Gamma) - \rho_{\alpha\beta}\rho_{\gamma\delta}. \tag{2.36}$$

We again look at the condition for a zero eigenvalue

$$\sum_{\gamma\delta} \mathcal{G}'_{\alpha\beta;\gamma\delta} v_{\gamma\delta} = \sum_{\gamma\delta} \mathcal{G}_{\alpha\beta;\gamma\delta} v_{\gamma\delta} - \rho_{\alpha\beta} \sum_{\gamma\delta} \rho_{\gamma\delta} v_{\gamma\delta} = 0. \tag{2.37}$$

This shows that if $\mathcal{G}$ has a zero eigenvalue, than $\mathcal{G}'$ also has a zero eigenvalue with the same eigenvector. The converse is also true. If v is an eigenvector of $\mathcal{G}'$ with zero eigenvalue, then the following vector is an eigenvector of $\mathcal{G}$ with zero eigenvalue

$$v'_{\alpha\beta} = v_{\alpha\beta} - \sum_{\gamma\delta} \rho_{\gamma\delta} v_{\gamma\delta} \frac{\delta_{\alpha\beta}}{N}, \tag{2.38}$$

which can be seen from

$$\begin{aligned} \sum_{\gamma\delta} \mathcal{G}_{\alpha\beta;\gamma\delta} v'_{\gamma\delta} &= \sum_{\gamma\delta} \mathcal{G}'_{\alpha\beta;\gamma\delta} v'_{\gamma\delta} + \sum_{\gamma\delta} \rho_{\alpha\beta}\rho_{\gamma\delta} v'_{\gamma\delta} \\ &= \sum_{\gamma\delta} \rho_{\alpha\beta}\rho_{\gamma\delta} v_{\gamma\delta} - \sum_{\gamma\delta} \mathrm{Tr}\,(\rho v)\, \frac{\delta_{\gamma\delta}}{N} \rho_{\alpha\beta}\rho_{\gamma\delta} \\ &= \rho_{\alpha\beta}\mathrm{Tr}\,(\rho v) - \mathrm{Tr}\,(\rho v)\, \rho_{\alpha\beta} \sum_{\gamma} \frac{\rho_{\gamma\gamma}}{N} = 0. \end{aligned}$$

We have used the fact that v' is also an eigenvector of $\mathcal{G}'$

$$\sum_{\gamma\delta} \mathcal{G}'_{\alpha\beta;\gamma\delta} v'_{\gamma\delta} = \sum_{\gamma\delta} \mathcal{G}'_{\alpha\beta;\gamma\delta} v_{\gamma\delta} - \mathrm{Tr}\,(\rho v)\,\frac{1}{N}\sum_{\gamma} \mathcal{G}'_{\alpha\beta;\gamma\gamma} = 0,$$

because

$$\begin{aligned}\sum_{\gamma} \mathcal{G}'_{\alpha\beta;\gamma\gamma} &= \sum_{\gamma} \delta_{\beta\gamma}\rho_{\alpha\gamma} - \sum_{\gamma} \Gamma_{\alpha\gamma;\gamma\beta} - \sum_{\gamma} \rho_{\alpha\beta}\rho_{\gamma\gamma} \\ &= \rho_{\alpha\beta} + (N-1)\rho_{\alpha\beta} - N\rho_{\alpha\beta} = 0.\end{aligned}$$

We have shown that the nullspaces of $\mathcal{G}$ and $\mathcal{G}'$ coincide. This means that the boundary of the region where $\mathcal{G}$ and $\mathcal{G}'$ are positive semidefinite is the same and both conditions will produce identical results. As $\mathcal{G}'$ is non-linear in Γ, we always use $\mathcal{G}$.

The combination of the $\mathcal{I}$, $\mathcal{Q}$ and $\mathcal{G}$ conditions are called two-index conditions. For some systems, these conditions produce good results [81]. However, we have seen that a good approximation to the energy does not necessarily mean that we have a good approximation to the 2DM itself. This can be seen if we try to calculate other operators, like the spin expectation value or the correlation functions. To fix this, we can use higher order density matrices.

2.3.3 The third-order reduced density matrix

The third-order reduced Density Matrix (3DM) is defined as

$${}^3\Gamma_{\alpha\beta\gamma;\delta\varepsilon\zeta} = \sum_i w_i \left\langle \psi_i | \hat{a}^\dagger_\alpha \hat{a}^\dagger_\beta \hat{a}^\dagger_\gamma \hat{a}_\zeta \hat{a}_\varepsilon \hat{a}_\delta | \psi_i \right\rangle, \tag{2.39}$$

again with $\sum_i w_i = 1$ and $w_i \geq 0$. Several properties can be directly deduced from the definition

$${}^3\Gamma_{\alpha\beta\gamma;\delta\varepsilon\zeta} = \mathrm{sgn}(\sigma)\mathrm{sgn}(\tau)\, {}^3\Gamma_{\sigma(\alpha)\sigma(\beta)\sigma(\gamma);\tau(\delta)\tau(\varepsilon)\tau(\zeta)} \quad \forall \sigma, \tau \in S_3, \tag{2.40a}$$

$${}^3\Gamma_{\alpha\beta\gamma;\delta\varepsilon\zeta} = {}^3\Gamma_{\delta\varepsilon\zeta;\alpha\beta\gamma}, \tag{2.40b}$$

$$\mathrm{Tr}\left({}^3\Gamma\right) = \sum_{\alpha<\beta<\gamma} {}^3\Gamma_{\alpha\beta\gamma;\alpha\beta\gamma} = \frac{N(N-1)(N-2)}{6}, \tag{2.40c}$$

$${}^3\Gamma \succeq 0. \tag{2.40d}$$

Property (2.40a) holds for all elements of the permutation group of 3 elements, S_3. The 2DM can be calculated from the 3DM

$$\Gamma_{\alpha\beta;\gamma\delta} = \frac{1}{N-2}\sum_{\lambda} {}^3\Gamma_{\alpha\beta\lambda;\gamma\delta\lambda}. \tag{2.41}$$

If the 3DM fulfils condition (2.40d) then the 2DM is also be positive semidefinite. In the same way as for the 1DM and 2DM, we can enforce the positive semidefiniteness of the Hamiltonian class (2.9) where $\hat{B}^\dagger$ has three particle operators.

- $\hat{B}^\dagger = \sum_{\alpha\beta\gamma} p_{\alpha\beta\gamma} \hat{a}^\dagger_\alpha \hat{a}^\dagger_\beta \hat{a}^\dagger_\gamma$ leads to

$$\sum_{\alpha\beta\gamma} \sum_{\delta\varepsilon\zeta} p_{\alpha\beta\gamma} \langle\psi|\hat{a}^\dagger_\alpha \hat{a}^\dagger_\beta \hat{a}^\dagger_\gamma \hat{a}_\zeta \hat{a}_\varepsilon \hat{a}_\delta|\psi\rangle \, p_{\delta\varepsilon\zeta} \geq 0, \tag{2.42}$$

  which is equivalent with condition (2.40d). The probability of finding a three-particle triplet must be larger than zero. This is the ${}^3\mathcal{J}$ condition.

- $\hat{B}^\dagger = \sum_{\alpha\beta\gamma} q^1_{\alpha\beta\gamma} \hat{a}^\dagger_\alpha \hat{a}^\dagger_\beta \hat{a}_\gamma$ leads to

$$\sum_{\alpha\beta\gamma} \sum_{\delta\varepsilon\zeta} q^1_{\alpha\beta\gamma} \langle\psi|\hat{a}^\dagger_\alpha \hat{a}^\dagger_\beta \hat{a}_\gamma \hat{a}^\dagger_\zeta \hat{a}_\varepsilon \hat{a}_\delta|\psi\rangle \, q^1_{\delta\varepsilon\zeta} \geq 0. \tag{2.43}$$

  We define the ${}^3\mathcal{E}$ matrix as

$${}^3\mathcal{E}_{\alpha\beta\gamma;\delta\varepsilon\zeta} = \langle\psi|\hat{a}^\dagger_\alpha \hat{a}^\dagger_\beta \hat{a}_\gamma \hat{a}^\dagger_\zeta \hat{a}_\varepsilon \hat{a}_\delta|\psi\rangle, \quad {}^3\mathcal{E} \succeq 0. \tag{2.44}$$

  Rewriting this as a function of the 3DM, we find

$${}^3\mathcal{E}({}^3\Gamma)_{\alpha\beta\gamma;\delta\varepsilon\zeta} = \delta_{\gamma\zeta}\Gamma_{\alpha\beta;\delta\varepsilon} - {}^3\Gamma_{\alpha\beta\zeta;\delta\varepsilon\gamma}. \tag{2.45}$$

- $\hat{B}^\dagger = \sum_{\alpha\beta\gamma} q^2_{\alpha\beta\gamma} \hat{a}^\dagger_\alpha \hat{a}_\beta \hat{a}_\gamma$ leads to

$$\sum_{\alpha\beta\gamma} \sum_{\delta\varepsilon\zeta} q^2_{\alpha\beta\gamma} \langle\psi|\hat{a}^\dagger_\alpha \hat{a}_\beta \hat{a}_\gamma \hat{a}^\dagger_\zeta \hat{a}^\dagger_\varepsilon \hat{a}_\delta|\psi\rangle \, q^2_{\delta\varepsilon\zeta} \geq 0. \tag{2.46}$$

  We define ${}^3\mathcal{F}$ matrix as

$${}^3\mathcal{F}_{\alpha\beta\gamma;\delta\varepsilon\zeta} = \langle\psi|\hat{a}^\dagger_\alpha \hat{a}_\beta \hat{a}_\gamma \hat{a}^\dagger_\zeta \hat{a}^\dagger_\varepsilon \hat{a}_\delta|\psi\rangle, \quad {}^3\mathcal{F} \succeq 0. \tag{2.47}$$

  Rewriting this as a function of the 3DM, we find

$$\begin{aligned} {}^3\mathcal{F}({}^3\Gamma)_{\alpha\beta\gamma;\delta\varepsilon\zeta} = {}^3\Gamma_{\alpha\zeta\varepsilon;\delta\gamma\beta} + \delta_{\gamma\zeta}\mathcal{G}_{\alpha\beta;\delta\varepsilon} - \delta_{\beta\zeta}\mathcal{G}_{\alpha\gamma;\delta\varepsilon} \\ + \delta_{\varepsilon\gamma}\Gamma_{\alpha\zeta;\delta\beta} - \delta_{\beta\varepsilon}\Gamma_{\alpha\zeta;\delta\gamma} \end{aligned} \tag{2.48}$$

  This condition implies the $\mathcal{G}$ condition for the two-index constraint

$$\mathcal{G}_{\alpha\beta;\gamma\delta} = \frac{1}{N+1} \sum_\lambda {}^3\mathcal{F}_{\alpha\beta\lambda;\gamma\delta\lambda}. \tag{2.49}$$

- $\hat{B}^\dagger = \sum_{\alpha\beta\gamma} q^3_{\alpha\beta\gamma} \hat{a}_\alpha \hat{a}_\beta \hat{a}_\gamma$ leads to

$$\sum_{\alpha\beta\gamma} \sum_{\delta\varepsilon\zeta} q^3_{\alpha\beta\gamma} \langle\psi|\hat{a}_\alpha \hat{a}_\beta \hat{a}_\gamma \hat{a}^\dagger_\zeta \hat{a}^\dagger_\varepsilon \hat{a}^\dagger_\delta|\psi\rangle\, q^3_{\delta\varepsilon\zeta} \geq 0. \tag{2.50}$$

We define the ${}^3\mathfrak{Q}$ matrix as

$${}^3\mathfrak{Q} \succeq 0, \quad {}^3\mathfrak{Q}_{\alpha\beta\gamma;\delta\varepsilon\zeta} = \langle\psi|\hat{a}_\alpha \hat{a}_\beta \hat{a}_\gamma \hat{a}^\dagger_\zeta \hat{a}^\dagger_\varepsilon \hat{a}^\dagger_\delta|\psi\rangle\,. \tag{2.51}$$

Rewriting this as a function of the 3DM, we find

$$\begin{aligned}
&{}^3\mathfrak{Q}({}^3\Gamma)_{\alpha\beta\gamma;\delta\varepsilon\zeta} = -{}^3\Gamma_{\alpha\beta\gamma;\delta\varepsilon\zeta} + \\
&\delta_{\gamma\zeta}\delta_{\beta\epsilon}\delta_{\alpha\delta} - \delta_{\gamma\epsilon}\delta_{\alpha\delta}\delta_{\beta\zeta} + \delta_{\alpha\zeta}\delta_{\gamma\epsilon}\delta_{\beta\delta} - \delta_{\gamma\zeta}\delta_{\alpha\epsilon}\delta_{\beta\delta} + \delta_{\beta\zeta}\delta_{\alpha\epsilon}\delta_{\gamma\delta} - \delta_{\alpha\zeta}\delta_{\beta\epsilon}\delta_{\gamma\delta} \\
&- (\delta_{\gamma\zeta}\delta_{\beta\epsilon} - \delta_{\beta\zeta}\delta_{\gamma\epsilon})\,\rho_{\alpha\delta} + (\delta_{\gamma\zeta}\delta_{\alpha\epsilon} - \delta_{\alpha\zeta}\delta_{\gamma\epsilon})\,\rho_{\beta\delta} - (\delta_{\beta\zeta}\delta_{\alpha\epsilon} - \delta_{\alpha\zeta}\delta_{\beta\epsilon})\,\rho_{\gamma\delta} \\
&+ (\delta_{\gamma\zeta}\delta_{\beta\delta} - \delta_{\beta\zeta}\delta_{\gamma\delta})\,\rho_{\alpha\epsilon} - (\delta_{\gamma\zeta}\delta_{\alpha\delta} - \delta_{\alpha\zeta}\delta_{\gamma\delta})\,\rho_{\epsilon\beta} + (\delta_{\beta\zeta}\delta_{\alpha\delta} - \delta_{\alpha\zeta}\delta_{\beta\delta})\,\rho_{\gamma\epsilon} \\
&- (\delta_{\beta\delta}\delta_{\gamma\epsilon} - \delta_{\beta\epsilon}\delta_{\gamma\delta})\,\rho_{\alpha\zeta} + (\delta_{\gamma\epsilon}\delta_{\alpha\delta} - \delta_{\alpha\epsilon}\delta_{\gamma\delta})\,\rho_{\beta\zeta} - (\delta_{\beta\epsilon}\delta_{\alpha\delta} - \delta_{\alpha\epsilon}\delta_{\beta\delta})\,\rho_{\gamma\zeta} \\
&+ \delta_{\gamma\zeta}\Gamma_{\alpha\beta;\delta\epsilon} - \delta_{\beta\zeta}\Gamma_{\alpha\gamma;\delta\epsilon} + \delta_{\alpha\zeta}\Gamma_{\beta\gamma;\delta\epsilon} - \delta_{\gamma\epsilon}\Gamma_{\alpha\beta;\delta\zeta} + \delta_{\beta\epsilon}\Gamma_{\alpha\gamma;\delta\zeta} - \delta_{\alpha\epsilon}\Gamma_{\beta\gamma;\delta\zeta} \\
&+ \delta_{\gamma\delta}\Gamma_{\alpha\beta;\epsilon\zeta} - \delta_{\beta\delta}\Gamma_{\alpha\gamma;\epsilon\zeta} + \delta_{\alpha\delta}\Gamma_{\beta\gamma;\epsilon\zeta},
\end{aligned} \tag{2.52a}$$

$${}^3\mathfrak{Q}({}^3\Gamma) = {}^3\mathbb{1} - {}^2\mathbb{1} \wedge \rho + \Gamma \wedge {}^1\mathbb{1} - {}^3\Gamma. \tag{2.52b}$$

This condition implies the $\mathfrak{Q}$ condition for the two-index constraints

$$\mathfrak{Q}_{\alpha\beta;\gamma\delta} = \frac{1}{2} \sum_\lambda {}^3\mathfrak{Q}_{\alpha\beta\lambda;\gamma\delta\lambda}. \tag{2.53}$$

All other permutations of the operator for the ${}^3\mathcal{E}$ and ${}^3\mathcal{F}$ condition are not independent of these conditions. For example: $\hat{B}^\dagger = \sum_{\alpha\beta\gamma} \tilde{f}_{\alpha\beta\gamma} \hat{a}_\alpha \hat{a}^\dagger_\beta \hat{a}_\gamma = \sum_{\alpha\beta\gamma} -\tilde{f}_{\alpha\beta\gamma} \hat{a}^\dagger_\beta \hat{a}_\alpha \hat{a}_\gamma + \sum_{\alpha\gamma} \delta_{\alpha\beta} \tilde{f}_{\alpha\alpha\gamma} \hat{a}_\gamma$. This will not generate any additional constraints.

The direct optimization of the 3DM with the conditions ${}^3\mathcal{J}$, ${}^3\mathcal{E}$, ${}^3\mathcal{F}$ and ${}^3\mathfrak{Q}$ yields better results than the optimization of the 2DM as all the two-index conditions are included as well [6, 82, 83]. However, due to the computational cost, this is not often done. The middle way is to keep optimizing the 2DM but enforce some three-index constraints which can be written as a function of the 2DM. If we take the anticommutator of a three-index operator, we effectively lower the rank by one and we have something that can be expressed as a function of the 2DM. We enforce the Hamiltonian class

$$\hat{H} = \hat{B}^\dagger \hat{B} + \hat{B} \hat{B}^\dagger. \tag{2.54}$$

We can find three independent conditions from this class. They were first derived by Erdahl [84] and used by Zhao *et al.*, Hammond and Mazziotti [25, 26] in practical calculations.

- $\hat{B}^\dagger = \sum_{\alpha\beta\gamma} t^1_{\alpha\beta\gamma} \hat{a}^\dagger_\alpha \hat{a}^\dagger_\beta \hat{a}^\dagger_\gamma$ leads to

$$\sum_{\alpha\beta\gamma} \sum_{\delta\varepsilon\zeta} t^1_{\alpha\beta\gamma} \left\langle \psi | \hat{a}^\dagger_\alpha \hat{a}^\dagger_\beta \hat{a}^\dagger_\gamma \hat{a}_\zeta \hat{a}_\varepsilon \hat{a}_\delta + \hat{a}_\zeta \hat{a}_\varepsilon \hat{a}_\delta \hat{a}^\dagger_\alpha \hat{a}^\dagger_\beta \hat{a}^\dagger_\gamma | \psi \right\rangle t^1_{\delta\varepsilon\zeta} \geq 0. \quad (2.55)$$

This is the $\mathcal{T}_1$ condition and we define the $\mathcal{T}_1$ matrix as

$$(\mathcal{T}_1)_{\alpha\beta\gamma;\delta\varepsilon\zeta} = \left\langle \psi | \hat{a}^\dagger_\alpha \hat{a}^\dagger_\beta \hat{a}^\dagger_\gamma \hat{a}_\zeta \hat{a}_\varepsilon \hat{a}_\delta + \hat{a}_\zeta \hat{a}_\varepsilon \hat{a}_\delta \hat{a}^\dagger_\alpha \hat{a}^\dagger_\beta \hat{a}^\dagger_\gamma | \psi \right\rangle . \quad (2.56)$$

Notice that $\mathcal{T}_1 = {}^3\mathcal{I} + {}^3\mathcal{Q}$. It can be written as a function of the 2DM using the anticommutator relations (B.5) resulting in

$$\begin{aligned}
&(\mathcal{T}_1(\Gamma))_{\alpha\beta\gamma;\delta\varepsilon\zeta} = \\
&\delta_{\gamma\zeta}\delta_{\beta\epsilon}\delta_{\alpha\delta} - \delta_{\gamma\epsilon}\delta_{\alpha\delta}\delta_{\beta\zeta} + \delta_{\alpha\zeta}\delta_{\gamma\epsilon}\delta_{\beta\delta} - \delta_{\gamma\zeta}\delta_{\alpha\epsilon}\delta_{\beta\delta} + \delta_{\beta\zeta}\delta_{\alpha\epsilon}\delta_{\gamma\delta} - \delta_{\alpha\zeta}\delta_{\beta\epsilon}\delta_{\gamma\delta} \\
&- (\delta_{\gamma\zeta}\delta_{\beta\epsilon} - \delta_{\beta\zeta}\delta_{\gamma\epsilon})\,\rho_{\alpha\delta} + (\delta_{\gamma\zeta}\delta_{\alpha\epsilon} - \delta_{\alpha\zeta}\delta_{\gamma\epsilon})\,\rho_{\beta\delta} - (\delta_{\beta\zeta}\delta_{\alpha\epsilon} - \delta_{\alpha\zeta}\delta_{\beta\epsilon})\,\rho_{\gamma\delta} \\
&+ (\delta_{\gamma\zeta}\delta_{\beta\delta} - \delta_{\beta\zeta}\delta_{\gamma\delta})\,\rho_{\alpha\epsilon} - (\delta_{\gamma\zeta}\delta_{\alpha\delta} - \delta_{\alpha\zeta}\delta_{\gamma\delta})\,\rho_{\epsilon\beta} + (\delta_{\beta\zeta}\delta_{\alpha\delta} - \delta_{\alpha\zeta}\delta_{\beta\delta})\,\rho_{\gamma\epsilon} \\
&- (\delta_{\beta\delta}\delta_{\gamma\epsilon} - \delta_{\beta\epsilon}\delta_{\gamma\delta})\,\rho_{\alpha\zeta} + (\delta_{\gamma\epsilon}\delta_{\alpha\delta} - \delta_{\alpha\epsilon}\delta_{\gamma\delta})\,\rho_{\beta\zeta} - (\delta_{\beta\epsilon}\delta_{\alpha\delta} - \delta_{\alpha\epsilon}\delta_{\beta\delta})\,\rho_{\gamma\zeta} \\
&+ \delta_{\gamma\zeta}\Gamma_{\alpha\beta;\delta\epsilon} - \delta_{\beta\zeta}\Gamma_{\alpha\gamma;\delta\epsilon} + \delta_{\alpha\zeta}\Gamma_{\beta\gamma;\delta\epsilon} - \delta_{\gamma\epsilon}\Gamma_{\alpha\beta;\delta\zeta} + \delta_{\beta\epsilon}\Gamma_{\alpha\gamma;\delta\zeta} - \delta_{\alpha\epsilon}\Gamma_{\beta\gamma;\delta\zeta} \\
&+ \delta_{\gamma\delta}\Gamma_{\alpha\beta;\epsilon\zeta} - \delta_{\beta\delta}\Gamma_{\alpha\gamma;\epsilon\zeta} + \delta_{\alpha\delta}\Gamma_{\beta\gamma;\epsilon\zeta}, \quad (2.57a) \\
&\mathcal{T}_1(\Gamma) = {}^3\mathbb{1} - {}^2\mathbb{1} \wedge \rho + \Gamma \wedge {}^1\mathbb{1}. \quad (2.57b)
\end{aligned}$$

The $\mathbb{1}$ again denotes the identity matrix in the appropriate space.

- $\hat{B}^\dagger = \sum_{\alpha\beta\gamma} t^2_{\alpha\beta\gamma} \hat{a}^\dagger_\alpha \hat{a}^\dagger_\beta \hat{a}_\gamma$ leads to

$$\sum_{\alpha\beta\gamma} \sum_{\delta\varepsilon\zeta} t^2_{\alpha\beta\gamma} \left\langle \psi | \hat{a}^\dagger_\alpha \hat{a}^\dagger_\beta \hat{a}_\gamma \hat{a}^\dagger_\zeta \hat{a}_\varepsilon \hat{a}_\delta + \hat{a}^\dagger_\zeta \hat{a}_\varepsilon \hat{a}_\delta \hat{a}^\dagger_\alpha \hat{a}^\dagger_\beta \hat{a}_\gamma | \psi \right\rangle t^2_{\delta\varepsilon\zeta} \geq 0. \quad (2.58)$$

This is the $\mathcal{T}_2$ condition and we define the $\mathcal{T}_2$ matrix as

$$(\mathcal{T}_2)_{\alpha\beta\gamma;\delta\varepsilon\zeta} = \left\langle \psi | \hat{a}^\dagger_\alpha \hat{a}^\dagger_\beta \hat{a}_\gamma \hat{a}^\dagger_\zeta \hat{a}_\varepsilon \hat{a}_\delta + \hat{a}^\dagger_\zeta \hat{a}_\varepsilon \hat{a}_\delta \hat{a}^\dagger_\alpha \hat{a}^\dagger_\beta \hat{a}_\gamma | \psi \right\rangle . \quad (2.59)$$

Notice that $\mathcal{T}_2 = {}^3\mathcal{E} + {}^3\mathcal{F}$. As a function of the 2DM this becomes

$$\begin{aligned}
(\mathcal{T}_2(\Gamma))_{\alpha\beta\gamma;\delta\varepsilon\zeta} \; &= (\delta_{\alpha\delta}\delta_{\beta\varepsilon} - \delta_{\alpha\varepsilon}\delta_{\beta\delta})\rho_{\gamma\zeta} - \delta_{\alpha\delta}\Gamma_{\gamma\varepsilon;\zeta\beta} + \delta_{\gamma\zeta}\Gamma_{\alpha\beta;\delta\varepsilon} \\
&\quad + \delta_{\beta\delta}\Gamma_{\gamma\varepsilon\zeta\alpha} + \delta_{\alpha\varepsilon}\Gamma_{\gamma\delta;\zeta\beta} - \delta_{\beta\varepsilon}\Gamma_{\gamma\delta\zeta\alpha} \quad (2.60)
\end{aligned}$$

- $\hat{B}^\dagger = \sum_{\alpha\beta\gamma} t^3_{\alpha\beta\gamma} \hat{a}^\dagger_\alpha \hat{a}_\beta \hat{a}^\dagger_\gamma$ leads to

$$\sum_{\alpha\beta\gamma} \sum_{\delta\varepsilon\zeta} t^3_{\alpha\beta\gamma} \left\langle \psi | \hat{a}^\dagger_\alpha \hat{a}_\beta \hat{a}^\dagger_\gamma \hat{a}_\zeta \hat{a}^\dagger_\varepsilon \hat{a}_\delta + \hat{a}_\zeta \hat{a}^\dagger_\varepsilon \hat{a}_\delta \hat{a}^\dagger_\alpha \hat{a}_\beta \hat{a}^\dagger_\gamma | \psi \right\rangle t^3_{\delta\varepsilon\zeta} \geq 0. \quad (2.61)$$

This is the $\mathcal{T}_3$ condition and we define the $\mathcal{T}_3$ matrix as

$$(\mathcal{T}_3)_{\alpha\beta\gamma;\delta\varepsilon\zeta} = \langle\psi|\hat{a}^\dagger_\alpha\hat{a}_\beta\hat{a}^\dagger_\gamma\hat{a}_\zeta\hat{a}^\dagger_\varepsilon\hat{a}_\delta + \hat{a}_\zeta\hat{a}^\dagger_\varepsilon\hat{a}_\delta\hat{a}^\dagger_\alpha\hat{a}_\beta\hat{a}^\dagger_\gamma|\psi\rangle\,. \tag{2.62}$$

As a function of the 2DM this becomes

$$\begin{aligned}(\mathcal{T}_3(\Gamma))_{\alpha\beta\gamma;\delta\varepsilon\zeta} &= \delta_{\alpha\delta}\delta_{\beta\gamma}\delta_{\varepsilon\zeta} - \delta_{\alpha\delta}\Gamma_{\varepsilon\gamma;\beta\zeta} - \delta_{\alpha\zeta}\Gamma_{\varepsilon\zeta;\delta\beta} - \delta_{\gamma\delta}\Gamma_{\alpha\varepsilon;\beta\zeta}\\ &\quad + \delta_{\beta\varepsilon}\Gamma_{\alpha\gamma;\delta\zeta} - \delta_{\gamma\zeta}\Gamma_{\alpha\varepsilon;\delta\beta} - \delta_{\alpha\delta}\delta_{\varepsilon\zeta}\rho_{\beta\gamma} + \delta_{\alpha\zeta}\delta_{\gamma\beta}\rho_{\varepsilon\delta}\\ &\quad + \delta_{\gamma\delta}\delta_{\varepsilon\zeta}\rho_{\alpha\beta} + (\delta_{\alpha\delta}\delta_{\gamma\zeta} - \delta_{\alpha\zeta}\delta_{\gamma\delta})\rho_{\beta\varepsilon}.\end{aligned} \tag{2.63}$$

Like the $\mathcal{G}'$ condition, it is also possible to derive a $\mathcal{T}'_2$ condition. This condition will turn out be more useful than $\mathcal{G}'$. The $\mathcal{T}'_2$ condition is generated by

$$\hat{H} = \hat{B}^\dagger_1\hat{B}_1 + \hat{B}_2\hat{B}^\dagger_2, \tag{2.64}$$

where

$$\hat{B}^\dagger_1 = \sum_{\alpha\beta\gamma} t^2_{\alpha\beta\gamma}\hat{a}^\dagger_\alpha\hat{a}^\dagger_\beta\hat{a}_\gamma + \sum_\lambda \hat{a}^\dagger_\lambda, \tag{2.65a}$$

$$\hat{B}^\dagger_2 = \sum_{\alpha\beta\gamma} t^2_{\alpha\beta\gamma}\hat{a}^\dagger_\alpha\hat{a}^\dagger_\beta\hat{a}_\gamma. \tag{2.65b}$$

As the sum of positive semidefinite operators (2.64) must be positive semidefinite too. The condition consists of the $\mathcal{T}_2$ condition plus additional terms

$$\begin{aligned}\sum_{\alpha\beta\gamma}\sum_{\delta\varepsilon\zeta} t^2_{\alpha\beta\gamma}(\mathcal{T}_2)_{\alpha\beta\gamma;\delta\varepsilon\zeta}\, t^2_{\delta\varepsilon\zeta} + \sum_{\alpha\beta\gamma\lambda} t^2_{\alpha\beta\gamma}\,\langle\psi|\hat{a}^\dagger_\alpha\hat{a}^\dagger_\beta\hat{a}_\gamma\hat{a}_\lambda|\psi\rangle\;\tilde{t}^2_\lambda\\ + \sum_{\mu\delta\varepsilon\zeta}\tilde{t}^2_\mu\,\langle\psi|\hat{a}^\dagger_\delta\hat{a}^\dagger_\varepsilon\hat{a}_\zeta\hat{a}_\mu|\psi\rangle\;t^2_{\delta\varepsilon\zeta} + \sum_{\lambda\mu}\tilde{t}^2_\lambda\rho_{\lambda\mu}\tilde{t}^2_\mu \geq 0.\end{aligned} \tag{2.66}$$

We can write this as a matrix condition

$$\mathcal{T}'_2 = \begin{bmatrix}(\mathcal{T}_2)_{\alpha\beta\gamma;\delta\varepsilon\zeta} & \omega_{\alpha\beta\gamma;\lambda}\\ \omega_{\mu;\delta\varepsilon\zeta} & \rho_{\mu\lambda}\end{bmatrix} \succeq 0, \tag{2.67}$$

with

$$\omega_{\alpha\beta\gamma;\lambda} = \Gamma_{\alpha\beta;\lambda\gamma}. \tag{2.68}$$

The condition (2.67) includes the $\mathcal{T}_2$ condition as a diagonal block of a positive semidefinite matrix must also be positive semidefinite (see Chapter C on page 149). It also encompasses the $\mathcal{T}_3$ condition

$$\begin{aligned}\hat{B}^\dagger &= \sum_{\alpha\beta\gamma} t^3_{\alpha\beta\gamma}\hat{a}^\dagger_\alpha\hat{a}_\beta\hat{a}^\dagger_\gamma\\ &= -\sum_{\alpha\beta\gamma} t^3_{\alpha\beta\gamma}\hat{a}^\dagger_\alpha\hat{a}^\dagger_\gamma\hat{a}_\beta + \sum_{\alpha\beta} t^3_{\alpha\beta\beta}\hat{a}^\dagger_\alpha\end{aligned} \tag{2.69}$$

This is equivalent with condition (2.65a)

$$t^2_{\alpha\beta\gamma} = -t^3_{\alpha\beta\gamma}, \tag{2.70a}$$

$$\tilde{t}^2_{\lambda} = \sum_{\alpha} t^3_{\lambda\alpha\alpha}. \tag{2.70b}$$

In practice, the $\mathcal{T}'_2$ condition is used as it encompasses both the $\mathcal{T}_2$ and the $\mathcal{T}_3$ condition for a negligible additional cost. It has been found that the $\mathcal{T}'_2$ condition produces slightly better results than the combination of $\mathcal{T}_1$ and $\mathcal{T}_2$ [46, 82].

2.3.4 Other Constraints

Until now, we used a class of positive semidefinite Hamiltonians to approximate N-representability. In principle, any knowledge about the ground state of the system can be enforced and can possibly improve the energy or the reduced density matrix. For example, if the ground state should be a singlet ($\hat{S} = 0$), the expectation value of the spin operator can be enforced

$$\mathrm{Tr}\,(S\Gamma) = 0. \tag{2.71}$$

For spin expectation value, we can even do better as will be explained in Section 2.4.1. In general, we are of course interested in constraints that give the largest improvement of the energy. However, only part of all conceivable constraints will actually improve the energy.

I. Sharp conditions

Another straightforward improvement would be to have stricter bounds on the $\mathcal{I}$, $\mathcal{Q}$ and $\mathcal{G}$ conditions. The $\mathcal{I}$ condition reflects that the probability for a given pair to be occupied cannot be negative. If the used basis set is large enough and the filling is below half, it seems fair to assume that the lowest eigenvalue of the $\mathcal{I}$ will be zero. However, this does not mean that there is no room for improvement: we can look for the worst possible violation of this and imposes it. On the other side, we can also derive the maximal eigenvalue of the $\mathcal{I}$ condition: the condition belongs to a class of exactly solvable Hamiltonian known as the Richardson-Gaudin pairing Hamiltonians [85–87]. It is thus possible to efficiently calculate the largest eigenvalue [33]. In practical procedure, we look for the worst possible violation of the upper bound so that the condition is as tight as possible. For the $\mathcal{Q}$ condition, a similar approach is possible for an upper bound. In contrast with the $\mathcal{I}$ condition, the lower bound can also be improved: the $\mathcal{Q}$ condition expresses that the probability

for a given pair to be unoccupied cannot be negative. It seems probable that the lowest eigenvalue will be greater than zero. The $\mathcal{G}$ condition is somewhat different: there is no known way to find stricter upper or lower bounds in the general case, but if we assume that the matrix $g_{\alpha\beta}$ in eq. (2.27) on page 23 is Hermitian ($\hat{B}^\dagger = \hat{B}$), we can [34]. The eigenstates of the $\hat{B}$ operator are now Slater determinants and the eigenvalues simply are the sum of the orbital energies of the occupied orbitals. As we assumed Hermiticity, the eigenvalues of the $\mathcal{G}$ condition are the squares of the eigenvalues of $\hat{B}$. Determining an upper bound is now easy: it is either the sum of the N lowest orbital energies or the N highest. The lower bound is an entirely different story: different eigenvalues can cancel each other. It is basically an integer programming problem. It can be shown to be related to the p-dispersion problems [34, 88], which is NP-hard [89].

These stricter versions of the two-index conditions are know as the sharp condition. For a complete derivation of these sharp constraints, I refer to reference 90. Unfortunately, in practice these conditions do not improve the result for most systems [90], and therefore they are seldom used.

II. Subsystem constraints

Another set of N-representability conditions worth mentioning are the so-called subsystem constraints [30]. The idea is to apply constraints to the 2DM restricted to a subspace of the single-particle Hilbert space. The concept of fractional N-representability is needed for this: using an ensemble of wave functions with a different number of particles, it is possible to give an equivalent definition of fractional N-representability [90]. The full N-representability conditions do not automatically fulfill the same set of conditions for a subsystem. These conditions are needed in the dissociation of diatomic molecules [30, 31, 91].

2.4 Symmetry considerations

Symmetry plays a fundamental role in physics, especially in quantum mechanics [92, 93]. The knowledge of the symmetry of the system allows us to understand a great deal without even knowing the ground state wave function. For example, the existence of the dipole momentum of a molecule can be predicted on symmetry basis alone. There are selection rules for which transitions of energy levels are allowed in a molecule, which are solely based on the symmetry of the molecule. It also simplifies the possible solutions of the Schrödinger equation as every eigenvalue can be labeled on symmetry

grounds. In real life, symmetry is often associated with beauty and harmony. In quantum mechanics, symmetry is also a source of beauty but in the mathematical sense. A symmetry in quantum mechanics means that the system is invariant under an operator. Mathematically this means that the operator must commute with the Hamiltonian of the system: if $\hat{A}$ is the symmetry operator then

$$\hat{H}\hat{A}\left|\psi\right\rangle = \hat{A}\hat{H}\left|\psi\right\rangle = E\hat{A}\left|\psi\right\rangle, \tag{2.72}$$

from which

$$[\hat{H}, \hat{A}] = 0. \tag{2.73}$$

The basic concept in symmetry is the group: this is a set of operations that leave a system invariant, together with following properties. If G is a symmetry group, together with an operation to combine two elements then

- $\forall a \in G$ and $\forall b \in G$ then $ab \in G$.
- There is a unique element $e \in G$ such that $\forall a \in G$, $ae = ea = a$.
- $\forall a \in G$, there exists an element $b \in G$ such that $ab = ba = e$.
- $\forall a, b, c \in G$: $a(bc) = (ab)c$.

There are 2 major categories, discrete symmetries and continuous symmetries. A discrete symmetry has a finite number of operations. An example is the group C_s which contains two operations: the identity operator and a reflection around a plane. A continuous symmetry depends on some continuous parameter. For example, a sphere has a continuous symmetry: the group $O(3)$ of all rotations in $\mathbb{R}^3$ around an axis.

The elements of a group are abstract operations, to use them on a system we need a representation of the elements. This is where representation theory comes in [92, 94, 95]. In representation theory, the elements of a group are represented by linear transformations on a vector space. The dimension of the vector space (or representation space) is called the dimension of the representation. The following relation must hold for a representation, where $\phi : G \to V$ is the image from the group to the vector space: $\forall a, b \in G$: $\phi(ab) = \phi(a)\phi(b)$. An important concept are the irreducible representations, as these are the building blocks for all other representations. A representation is irreducible if the representation space has no subspaces which are also closed under the group operations. If such a subspace would exists, it is called a subrepresentation. If the only subrepresentation of a representation is the trivial subrepresentation (only the identity), the representation is irreducible. Every other (reducible) representation can be expressed as a direct sum of these. Linear transformations on vector spaces can be represented

by matrices. A matrix is non-reducible if there does not exists a similarity transformation that reduces all the matrices in the representation to a block diagonal form. Every group has a trivial representation in which every elements in represented by the identity matrix. For a complete introduction into group theory and representation theory, I refer to references 92, 94–96. In what follows, we will only be concerned with representations of finite groups. We will first look at exploiting the spin symmetry of the system and then the point group symmetry.

2.4.1 Spin symmetry

Spin is a strange, fundamental concept in quantum mechanics. It is the intrinsic angular momentum of a particle [1, 97]. Originally, it was thought be the effect of the particle spinning around its axis, hence the name [98]. Now we understand that spin is a fundamental property of a particle. Wolfgang Pauli is the father of the concept and worked out the mathematical description. Spin also allows us to split all particles into two disjunct groups: fermions and bosons. The latter have an integer spin and are symmetric under particle exchange while the former have a half-integer spin and are antisymmetric under particle exchange (the Pauli exclusion principle). In this work, we are only concerned with fermions and more specifically, electrons with spin $1/2$. In all that follows, we will assume that we are dealing with electrons. We wish to exploit the invariance of the Hamiltonian under rotations in the spin space. The symmetry group for spin $1/2$ fermions is $SU(2)$: the group of all unitary 2×2 matrices with $\det = 1$. The spin operator is given by

$$\hat{S} = \frac{\hbar}{2}\hat{\sigma}, \tag{2.74}$$

with the three Cartesian components

$$S_x = \frac{\hbar}{2}\sigma_x, \qquad S_y = \frac{\hbar}{2}\sigma_y, \qquad S_z = \frac{\hbar}{2}\sigma_z, \tag{2.75}$$

where σ is given by the three Pauli matrices

$$\sigma_x = \begin{pmatrix} 0 & 1 \\ 1 & 0 \end{pmatrix}, \qquad \sigma_y = \begin{pmatrix} 0 & -i \\ i & 0 \end{pmatrix}, \qquad \sigma_z = \begin{pmatrix} 1 & 0 \\ 0 & -1 \end{pmatrix}. \tag{2.76}$$

As angular momentum operators, they have to obey the structure relations of the Lie-algebra of $SU(2)$ [92, 99].

$$[S_x, S_y] = i\hbar S_z, \qquad [S_y, S_z] = i\hbar S_x, \qquad [S_z, S_x] = i\hbar S_y. \tag{2.77}$$

The Hamiltonian is invariant under spin rotations

$$[\hat{H}, \hat{S}^2] = 0, \qquad [\hat{H}, \hat{S}_z] = 0, \tag{2.78}$$

with

$$\hat{S}^2 = \hat{S}_x^2 + \hat{S}_y^2 + \hat{S}_z^2. \tag{2.79}$$

Furthermore, $[\hat{S}^2, \hat{S}_z] = 0$ so that the eigenvalues and eigenvectors of the Hamiltonian can be labeled with the eigenvalues of $\hat{S}^2$ and $\hat{S}_z$. This means that

$$\hat{S}^2 \left|\Psi\right\rangle = S(S+1) \left|\Psi\right\rangle, \tag{2.80}$$

$$\hat{S}_z \left|\Psi\right\rangle = S_z \left|\Psi\right\rangle = M \left|\Psi\right\rangle, \tag{2.81}$$

and we can write

$$\hat{H} \left|\Psi_{SM}\right\rangle = E_{SM} \left|\Psi_{SM}\right\rangle. \tag{2.82}$$

It is also useful to define the ladder operators which can increase or lower M: $\hat{S}_\pm = \hat{S}_x \pm i\hat{S}_y$. Their effect is

$$\hat{S}_\pm \left|\Psi_{SM}\right\rangle = \hbar\sqrt{S(S+1) - M(M \pm 1)} \left|\Psi_{SM\pm1}\right\rangle. \tag{2.83}$$

We now want to exploit this symmetry in v2DM calculations. The idea is to use spin symmetry to reduce the size of the 2DM. In this part, we will explicitly denote the spin in a single-particle state

$$\left|\alpha\right\rangle \rightarrow \left|a\sigma_a\right\rangle. \tag{2.84}$$

Roman letters will be used to denote the spatial part of the single-particle state, and σ will be used for the associated spin state. We want to couple electrons together. For this we need the Clebsch-Gordan coefficients: these coefficients allow us to reduce a coupled representation into the irreducible (uncoupled) representations. We want to find a state that fulfills all the previously mentioned properties of the spin operator. Let us take a look at the case of coupling of two electrons

$$\left|ab; SM_S\right\rangle = \sum_{\sigma_a\sigma_b} \langle \frac{1}{2}\sigma_a \frac{1}{2}\sigma_b | SM_S\rangle \left|a\sigma_a b\sigma_b\right\rangle. \tag{2.85}$$

The factor $\langle \frac{1}{2}\sigma_a \frac{1}{2}\sigma_b | SM_S\rangle$ is a Clebsch-Gordan coefficient for $SU(2)$. They can be found in Chapter D on page 153 together with some properties. Two spin-$1/2$ particles can be coupled together to a singlet ($S = 0$) or a triplet

($S = 1$). If we write out eq. (2.85), we find

$$|ab;00\rangle = \frac{1}{\sqrt{2}}\left(|a\uparrow b\downarrow\rangle - |a\downarrow b\uparrow\rangle\right), \tag{2.86a}$$

$$|ab;1\,{-1}\rangle = |a\downarrow b\downarrow\rangle, \tag{2.86b}$$

$$|ab;10\rangle = \frac{1}{\sqrt{2}}\left(|a\uparrow b\downarrow\rangle + |a\downarrow b\uparrow\rangle\right), \tag{2.86c}$$

$$|ab;11\rangle = |a\uparrow b\uparrow\rangle. \tag{2.86d}$$

Note that state (2.86a) is symmetric under exchange of $a \Leftrightarrow b$ while eqs. (2.86b) to (2.86d) are antisymmetric. The norm of (2.85) is not unity

$$\langle ab;SM_S|cd;S'M'_S\rangle = \delta_{SS'}\delta_{M_SM'_S}\left(\delta_{ac}\delta_{bd} + (-1)^S\,\delta_{ad}\delta_{bc}\right). \tag{2.87}$$

With this knowledge, we can now define the spin-coupled version of the $\hat{B}^\dagger$ operator for the $\mathfrak{I}$ condition

$$\begin{aligned}\hat{B}^{\dagger\,SM_S}_{ab} &= \frac{1}{\sqrt{1+\delta_{ab}}}\left[\hat{a}^\dagger_a \otimes \hat{a}^\dagger_b\right]^S_M \\ &= \frac{1}{\sqrt{1+\delta_{ab}}}\sum_{\sigma_a\sigma_b}\langle\frac{1}{2}\sigma_a\frac{1}{2}\sigma_b|SM_S\rangle\,\hat{a}^\dagger_{a\sigma_a}\hat{a}^\dagger_{b\sigma_b}.\end{aligned} \tag{2.88}$$

Using this definition, the 2DM becomes

$${}^{\mathfrak{S}\mathcal{M}}\Gamma^{SM_S;S'M'_S}_{ab;cd} = \sum_i w_i\,\langle\psi_{\mathfrak{S}\mathcal{M},i}|\hat{B}^{\dagger\,SM_S}_{ab}\,\hat{B}^{S'M'_S}_{cd}|\psi_{\mathfrak{S}\mathcal{M},i}\rangle, \tag{2.89}$$

where the sum runs over an ensemble of wave functions with spin $\mathfrak{S}$ and spin projection $\mathcal{M}$. We now couple both $\hat{B}$ operators together to total spin S_T

$$\begin{aligned}{}^{\mathfrak{S}\mathcal{M}}\Gamma^{SM_S;S'M'_S}_{ab;cd} = (-1)^{S'-M'_S}\sum_i w_i \sum_{S_TM_T}\langle SM_SS'{-}M'_S|S_TM_T\rangle \\ \langle\psi_{\mathfrak{S}\mathcal{M},i}|\left[\hat{B}^{\dagger\,SM_S}_{ab}\otimes\hat{B}^{S'M'_S}_{cd}\right]^{S_T}_{M_T}|\psi_{\mathfrak{S}\mathcal{M},i}\rangle.\end{aligned} \tag{2.90}$$

The prefactor appears because the $\hat{B}$ operators need to be spherical tensor operators (see Chapter D). As the ket and bra wave functions have the same spin projection $\mathcal{M}$, we can deduce that $M_T = 0$. Let us now assume that the ensemble consists of singlet wave functions ($\mathfrak{S} = \mathcal{M} = 0$). It follows that $S_T = 0$ because of spin conservation and thus $S = S'$. The Clebsch-Gordan coefficient in eq. (2.90) reduces to

$$\langle SM_SS{-}M_S|00\rangle = \frac{(-1)^{S-M_S}}{\sqrt{2S+1}}. \tag{2.91}$$

The spin coupled 2DM for the singlet ensemble is

$$ {}^{00}\Gamma^{SM_S;S'M'_S}_{ab;cd} = \frac{\delta_{SS'}\delta_{M_S M'_S}}{2S+1} \sum_i w_i \left\langle \psi_{00,i} \right| \left[\hat{B}^{\dagger\, SM_S}_{ab} \otimes \hat{B}^{SM_S}_{cd} \right]^0_0 \left| \psi_{00,i} \right\rangle . \quad (2.92) $$

Note that this is independent of M_S. The 2DM is split up into a $S = 0$ block and a three-fold degenerate $S = 1$ block. For a singlet state, our notation can be abbreviated to $\Gamma^S_{ab;cd}$.

For higher spin states a similar reduction is possible provided we use a spin-averaged ensemble for the wave function

$$ {}^{\mathcal{S}}\Gamma^{SM_S;S'M_S}_{ab;cd} = (-1)^{S'-M_S} \sum_i w_i \sum_{S_T} \langle SM_S S' {-}M_S | S_T 0 \rangle \frac{1}{2\mathcal{S}+1} \sum_{\mathcal{M}} \left\langle \psi_{\mathcal{SM},i} \right| \left[\hat{B}^{\dagger\, SM_S}_{ab} \otimes \hat{B}^{S'M_S}_{cd} \right]^{S_T}_0 \left| \psi_{\mathcal{SM},i} \right\rangle . \quad (2.93) $$

All members of the spin multiplet have an equal weight in the ensemble. This forms no restriction because of the spin symmetry: the ground state will be degenerate in the multiplet. If we now apply the Wigner-Eckart theorem (see Chapter D on page 153) to the operator in eq. (2.93), we find

$$ \left\langle \psi_{\mathcal{SM},i} \right| \left[\hat{B}^{\dagger\, SM_S}_{ab} \otimes \hat{B}^{S'M_S}_{cd} \right]^{S_T}_0 \left| \psi_{\mathcal{SM},i} \right\rangle = (-1)^{\mathcal{S}-\mathcal{M}} \begin{pmatrix} \mathcal{S} & \mathcal{S} & S_T \\ \mathcal{M} & -\mathcal{M} & 0 \end{pmatrix} \left\langle \psi_{\mathcal{S},i} \right|\!\left| \left[\hat{B}^{\dagger\, SM_S}_{ab} \otimes \hat{B}^{S'M_S}_{cd} \right]^{S_T}_0 \right|\!\left| \psi_{\mathcal{S},i} \right\rangle . \quad (2.94) $$

If we replace the prefactor by following Wigner 3-j symbol (related to Clebsch-Gordan coefficients, see Chapter D)

$$ \begin{pmatrix} \mathcal{S} & \mathcal{S} & 0 \\ \mathcal{M} & -\mathcal{M} & 0 \end{pmatrix} = \frac{(-1)^{\mathcal{S}-\mathcal{M}}}{2\mathcal{S}+1}, \quad (2.95) $$

then we can use the orthogonality relation for Clebsch-Gordan coefficients

$$ \sum_{\mathcal{M}} \begin{pmatrix} \mathcal{S} & \mathcal{S} & 0 \\ \mathcal{M} & -\mathcal{M} & 0 \end{pmatrix} \begin{pmatrix} \mathcal{S} & \mathcal{S} & S_T \\ \mathcal{M} & -\mathcal{M} & 0 \end{pmatrix} = \delta_{S_T 0} \quad (2.96) $$

to find

$$ {}^{\mathcal{S}}\Gamma^{SM_S;S'M_S}_{ab;cd} = \delta_{SS'} \frac{1}{2S+1} \frac{1}{2\mathcal{S}+1} \sum_i w_i \left\langle \psi_{\mathcal{S},i} \right|\!\left| \left[\hat{B}^{\dagger\, SM_S}_{ab} \otimes \hat{B}^{SM_S}_{cd} \right]^0_0 \right|\!\left| \psi_{\mathcal{S},i} \right\rangle . \quad (2.97) $$

Again, we find an expression that is independent of the spin projection. The reduction of the 2DM is the same as for the singlet ensemble: a $S = 0$ block and a three-fold degenerate $S = 1$ block. The same abbreviated notation can be used. The symmetry in the spatial orbital indices is as follows

$$\Gamma^S_{ab;cd} = (-1)^S \Gamma^S_{ba;cd} = (-1)^S \Gamma^S_{ab;dc} = \Gamma^S_{ba;dc}. \tag{2.98}$$

The minus factor is due to the (anti)symmetry in the index, like in eqs. (2.86a) to (2.86d). The $S = 0$ block has dimension $\frac{M}{4}\left(\frac{M}{2}+1\right)$ while the $S = 1$ block has a dimension of $\frac{M}{4}\left(\frac{M}{2}-1\right)$, where M is the number of spin orbitals. If we sum these and keep the three-fold degeneracy in mind, we find the full dimension of the uncoupled 2DM, as expected. To summarize, the couple and uncoupled formulas for the 2DM are

$$\begin{aligned}\Gamma_{a\sigma_a b\sigma_b;c\sigma_c d\sigma_d} =& \sqrt{(1+\delta_{ab})(1+\delta_{cd})} \sum_{SM_S} \langle \frac{1}{2}\sigma_a \frac{1}{2}\sigma_b | SM_S\rangle \\ & \langle \frac{1}{2}\sigma_c \frac{1}{2}\sigma_d | SM_S\rangle \, \Gamma^S_{ab;cd}\end{aligned} \tag{2.99a}$$

$$\begin{aligned}\Gamma^S_{ab;cd} =& \frac{1}{\sqrt{(1+\delta_{ab})(1+\delta_{cd})}} \sum_{\sigma_a\sigma_b} \sum_{\sigma_c\sigma_d} \langle \frac{1}{2}\sigma_a \frac{1}{2}\sigma_b | SM_S\rangle \\ & \langle \frac{1}{2}\sigma_c \frac{1}{2}\sigma_d | SM_S\rangle \, \Gamma_{a\sigma_a b\sigma_b;c\sigma_c d\sigma_d}\end{aligned} \tag{2.99b}$$

The reduction of the 2DM can be seen as

$$\Gamma = \begin{pmatrix} & & \\ & & \\ & & \end{pmatrix} \to \begin{pmatrix} \Gamma^0 & & & \\ & \Gamma^1 & & \\ & & \Gamma^1 & \\ & & & \Gamma^1 \end{pmatrix}. \tag{2.100}$$

In the same way, all conditions can be spin-adapted. The 1DM splits into two degenerate blocks. The $\mathcal{Q}$ reduction is identical to the 2DM and the $\mathcal{G}$ condition has a similar reduction but without the symmetry in the spatial orbital indices. The three-index conditions are more complicated as an intermediary coupling has to take place and there are several possible paths to couple to the total spin. For a complete description of the spin-adapted conditions, we refer to reference 90.

The reduction of the 2DM using spin symmetry can be seen as an N-representability condition which is necessary but not sufficient. The problem of guaranteeing that the wave function has the desired spin is called the S-representability problem [35, 40, 100–103]. It was introduced by Pérez-Romero, Tel, and Valdemoro [100] as: "we say that an ${}^p\Gamma$ is S-representable when there is an N-electron wave function corresponding to a pure spin

quantum number S from which this ${}^p\Gamma$ can be derived." The symmetry reduction due to spin will not alter the energy of the v2DM optimization because both the Hamiltonian and the N-representability conditions already have the correct spin symmetry. This can also be understood from the block structure of the reduced Hamiltonian: any off-block-diagonal element will only increase the energy. It does reduce the optimizing time as it reduces the number of matrix elements. To enforce the spin of the ensemble of wave functions, the most straightforward way is to enforce the expectation value of the $\hat{S}^2$ operator. In the singlet case, we can do even better. Let us take a look at the $\hat{S}_z$ operator.

$$\hat{S}_z = \sum_{a\sigma_a} \sigma_a \hat{a}^\dagger_{a\sigma_a} \hat{a}_{a\sigma_a} = \sum_a \frac{1}{2} \left(\hat{a}^\dagger_{a\uparrow} \hat{a}_{a\uparrow} - \hat{a}^\dagger_{a\downarrow} \hat{a}_{a\downarrow} \right). \tag{2.101}$$

To calculate the $\hat{S}_z$ operator using the 2DM, we must transform it to the two-particle basis

$$\hat{S}_z = \sum_{a\sigma_a} \sigma_a \hat{a}^\dagger_{a\sigma_a} \hat{a}_{a\sigma_a} = \frac{1}{N-1} \sum_{a\sigma_a b\sigma_b} \sigma_a \hat{a}^\dagger_{a\sigma_a} \hat{a}^\dagger_{b\sigma_b} \hat{a}_{b\sigma_b} \hat{a}_{a\sigma_a}, \tag{2.102}$$

the expectation value is

$$S_z = \frac{1}{N-1} \sum_{(a\sigma_a)<(b\sigma_b)} (\sigma_a + \sigma_b) \, \Gamma_{a\sigma_a b\sigma_b; a\sigma_a b\sigma_b}. \tag{2.103}$$

We want to use the spin-coupled version of eq. (2.101). For a particle-hole operator a slight complication arises which is fully explained in Chapter D

$$\begin{aligned} \hat{S}_z &= \sum_{\sigma_a} (-1)^{\frac{1}{2}-\sigma_a} \sigma_a \sum_a \hat{a}^\dagger_{a\sigma_a} \tilde{\hat{a}}_{a-\sigma_a} \\ &= \sum_{\sigma_a} (-1)^{\frac{1}{2}-\sigma_a} \sigma_a \sum_S \langle \frac{1}{2}\sigma_a \frac{1}{2} -\sigma_a | S0 \rangle \sum_a \left[\hat{a}^\dagger_{a\sigma_a} \otimes \tilde{\hat{a}}_{a-\sigma_a} \right]^S_0. \end{aligned} \tag{2.104}$$

The prefactor can again be written as a Clebsch-Gordan coefficient

$$\langle jmj{-}m | 10 \rangle = \frac{\sqrt{3}(-1)^{j-m} m}{\sqrt{2j+1}\sqrt{j(j+1)}}. \tag{2.105}$$

If we use this in eq. (2.104), we get

$$\begin{aligned} \hat{S}_z &= \frac{1}{\sqrt{2}} \sum_{\sigma_a} \sum_S \langle \frac{1}{2}\sigma_a \frac{1}{2} - \sigma_a | 10 \rangle \, \langle \frac{1}{2}\sigma_a \frac{1}{2} -\sigma_a | S0 \rangle \sum_a \left[\hat{a}^\dagger_{a\sigma_a} \otimes \tilde{\hat{a}}_{a-\sigma_a} \right]^S_0 \\ &= \frac{1}{\sqrt{2}} \sum_a \left[\hat{a}^\dagger_a \otimes \tilde{\hat{a}}_a \right]^1_0, \end{aligned} \tag{2.106}$$

where we used the orthogonality properties of Clebsch-Gordan coefficients. If we want the singlet state, the expectation value of $\hat{S}_z$ should be zero. As this operator acts in the particle-hole space, this would mean that the $\mathcal{G}$ matrix has a zero eigenvalue with eigenvector $\frac{1}{\sqrt{2}}\delta_{S1}\delta_{ab}$:

$$\sum_c \mathcal{G}^1_{ab;cc}(\Gamma) = \langle\psi| \left[\hat{a}^\dagger_a \otimes \hat{a}_b\right]^1 \hat{S}_z|\psi\rangle = 0. \tag{2.107}$$

The beauty of the spin symmetry is that by imposing $\hat{S}_z = 0$, we also impose $\hat{S}_x = \hat{S}_y = 0$ due to the three-fold degenerate $S = 1$ block. The total spin will then also be zero as $\hat{S}^2 = \hat{S}^2_x + \hat{S}^2_y + \hat{S}^2_z$. This is a stronger condition than only enforcing $\hat{S}^2 = 0$. If we write eq. (2.107) in function of the 2DM directly, we find

$$\begin{aligned} \forall a < b \qquad \sum_S (2S+1)\left(\frac{1}{2}\frac{1}{N-1} - (-1)^S \begin{Bmatrix} \frac{1}{2} & \frac{1}{2} & 1 \\ \frac{1}{2} & \frac{1}{2} & S \end{Bmatrix}\right) \\ \sum_b \sqrt{(1+\delta_{ab})(1+\delta_{cd})}\Gamma^S_{ab;cb} = 0. \end{aligned} \tag{2.108}$$

This gives us $\frac{M}{4}\left(\frac{M}{2}-1\right)$ linear constraints. The $\mathcal{G}$ condition has a zero eigenvalue and this has to be dealt with accordingly (using a pseudo-inverse for example).

For higher spin states we can only enforce the spin expectation value of $\hat{S}^2$ as a linear constraint $\mathrm{Tr}\left(S^2\Gamma\right) = S(S+1)$. The uncoupled operator can be written as

$$\hat{S}^2 = \hat{S}^2_x + \hat{S}^2_y + \hat{S}^2_z = \frac{1}{2}\left(\hat{S}_+\hat{S}_- + \hat{S}_-\hat{S}_+\right) + \hat{S}^2_z, \tag{2.109}$$

where

$$\hat{S}_+ = \sum_a \hat{a}^\dagger_{a\uparrow}\hat{a}_{a\downarrow}, \tag{2.110a}$$

$$\hat{S}_- = \sum_a \hat{a}^\dagger_{a\downarrow}\hat{a}_{a\uparrow}. \tag{2.110b}$$

Using eqs. (2.110a) and (2.110b) in eq. (2.109), we find

$$\begin{aligned} \hat{S}^2 = \sum_{(a\sigma_a)<(b\sigma_b)} \left(\frac{1}{N-1}\left(1+\sigma^2_a+\sigma^2_b\right) + 2\sigma_a\sigma_b\right)\hat{a}^\dagger_{a\sigma_a}\hat{a}^\dagger_{b\sigma_b}\hat{a}_{b\sigma_b}\hat{a}_{a\sigma_a} \\ + \sum_{ab}\hat{a}^\dagger_{a\uparrow}\hat{a}^\dagger_{b\downarrow}\hat{a}_{b\uparrow}\hat{a}_{a\downarrow}. \end{aligned} \tag{2.111}$$

This gives us one linear constraint. It is fair to assume that this condition is less stringent than in the singlet case. A possible solution is to use an ensemble of the maximal spin projection wave functions ($S_z = S$) [35]. On this ensemble, the same game as for the singlet can be played but with the $\hat{S}_+$ operator. Forcing a zero expectation value will again lead to a zero eigenvalue in the $\mathcal{G}$ matrix. The downside of this is that the symmetry reduction is smaller and computationally more demanding. For the singlet case, the maximal spin-projection ensemble and the spin-weighted ensemble are equivalent.

Angular momentum symmetry is mathematically exactly the same as spin symmetry. If a system has total angular momentum symmetry, meaning it is rotation invariant or there is a rotation axis (all linear molecules), this can also be exploited in v2DM. The approach is very simulair to the spin case. For a complete derivation, we refer the reader to reference 90.

2.4.2 Spatial point group symmetry

Most small to medium sized molecules have a discrete geometric symmetry. For example, a homonuclear diatomic molecule such as N_2, will have a mirror plane orthogonal on the connecting axis. We call this point group symmetry. The given example is C_s symmetry. The group consists of two operators: the identity operation and the mirror operation. The name comes from the fact that these symmetry groups leave at least one point invariant in all operations. We will introduce the most often encountered classes of point groups

- C_n: the group of all rotations that leaves an n-fold axis invariant (meaning rotations of $\frac{360^\circ}{n}$). By convention the z-axis is chosen as rotation axis.
- C_s: reflection around a plane.
- C_i: inversion symmetry.
- C_{nv}: C_n with the addition of n mirror planes containing the axis of rotation.
- C_{nh}: C_n with reflection around the plane perpendicular to the rotation axis. $C_{1h} = C_s$.
- D_n: C_n with n two-fold rotation axis perpendicular on to the n-fold axis.

- D_{nh}: C_{nh} with n reflection planes containing the n-fold rotation axis and one of the two-fold axis.

For example, the C_2H_4 molecule shown in Figure 2.4 has D_{2h} symmetry. The

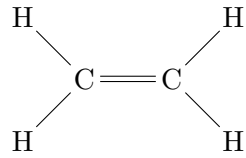

Figure 2.4: The ethylene molecule has D_{2h} symmetry.

main two-fold rotation axis is the connecting axis between the two carbon atoms (the z-axis). The two two-fold rotation axes are the x- and y-axis. The three reflection planes are xy, xz and yz.

In quantum chemistry, we will most often use abelian point groups ($\forall a, b \in G : ab = ba$). Abelian symmetry groups have one-dimensional irreducible representations and this simplifies the mathematics involved considerably as we work with scalars instead of matrices. This also means that we will usually use a subgroup of the real symmetry group of the molecule. For example, H_2 molecule has $D_{\infty h}$ symmetry but we will use D_{2h} because the latter is Abelian. The Abelian groups that can be used are $C_1, C_i, C_2, C_s, C_{2v}, D_2, C_{2h}$ and D_{2h}. The group C_1 is a special case. It is equivalent with no symmetry. Its only operation is the identity operation and thus every molecule has at least C_1 symmetry. In the rest of the text, C_1 and symmetry breaking will be used interchangeably. There is a standard nomenclature for the irreducible representations of point groups. I will give a short overview of what is useful for this work. The irreducible representation are classified according to their action on scalars, vector, etc. If under their action, the sign of the quantity does not change, we call it symmetric and the irreducible representation is denoted with an A. If the sign does change, it is called antisymmetric and the irreducible representation is denoted with a B. As an example, we show the character table and the multiplication table of C_2 group in Table 2.1 on the facing page. The character table contains the trace of the matrices of the irreducible representations. It it split up into conjugacy classes as the trace is invariant under a similarity transformation. These tables are extremely useful for decomposing a representation in its irreducible parts. The first irreducible representation A is called the trivial representation because all the representation matrices (scalars in this case) are one. Every group has this irreducible representation.

The basis functions in which the atomic orbitals are represented are usually not orthogonal. It is possible to transform these basis function to symmetry-

	E	C_2
A	1	1
B	1	-1

(a) Character table of C_2

	A	B
A	A	B
B	B	A

(b) Multiplication table of C_2

Table 2.1: C_2 overview: it has 2 classes of operations. The identity operation and rotations over $180°$. The two irreducible representations are A and B.

adapted basis functions [104–107]: linear combinations are made such that the resulting orbitals all transform according to an irreducible representation of the symmetry group. In other words, every orbital can be labeled according to an irreducible representation. This allows for a serious reduction of the computational cost of calculating the one- and two-electron integrals. Symmetry restricts the number of non-zero integrals: two orbitals can only interact when they belong to the same irreducible representation. This means that in order for a matrix element to be non-zero, the representations of the operators in the matrix element have to couple to the trivial irreducible representation. For the one-particle operator: $\langle\psi|\hat{a}^\dagger_{a\sigma_a}\hat{a}_{b\sigma_b}|\psi\rangle$ can only be non-zero when $I_a \otimes I_b = I_1$, where I_a denotes the irreducible representation of orbital a and I_1 is the trivial representation. This is equivalent with $I_a = I_b$. For two-particle operators, the same condition holds: $\langle\psi|\hat{a}^\dagger_{a\sigma_a}\hat{a}^\dagger_{b\sigma_b}\hat{a}_{d\sigma_d}\hat{a}_{c\sigma_c}|\psi\rangle \neq 0$ when $I_a \otimes I_b \otimes I_c \otimes I_d = I_1$. This is equivalent with $I_a \otimes I_b = I_c \otimes I_d$. This means that a two-particle operator $\hat{B}^\dagger_{a\sigma_a b\sigma_b}$ can be labeled by the irreducible representation $I_a \otimes I_b$: the operator $\hat{B}^\dagger$ can be written as

$$\hat{B}^{\dagger\,I}_{a\sigma_a b\sigma_b} = \delta_{I_a\otimes I_b,I}\ \hat{a}^\dagger_{a\sigma_a}\hat{a}^\dagger_{b\sigma_b}. \tag{2.112}$$

The 2DM thus is

$$\Gamma_{a\sigma_a b\sigma_b;c\sigma_c d\sigma_d} = \delta_{I_1 I_2}\ \langle\psi|\hat{B}^{\dagger\,I_1}_{a\sigma_a b\sigma_b}\hat{B}^{I_2}_{c\sigma_c d\sigma_d}|\psi\rangle\ . \tag{2.113}$$

The 2DM falls apart in blocks per irreducible representation: ${}^I\Gamma_{a\sigma_a b\sigma_b;c\sigma_c d\sigma_d}$. Notice that this in independent of the wave function. Combining point group symmetry with spin symmetry is straightforward as both are unrelated: we simply have to attach a label for the irreducible representation to the operator (2.88):

$$\begin{aligned}\hat{B}^{\dagger\,SM_S;I}_{ab} &= \frac{1}{\sqrt{1+\delta_{ab}}}\delta_{I_a\otimes I_b,I}\left[\hat{a}^\dagger_a\otimes\hat{a}^\dagger_b\right]^S_M \\ &= \frac{1}{\sqrt{1+\delta_{ab}}}\delta_{I_a\otimes I_b,I}\sum_{\sigma_a\sigma_b}\langle\frac{1}{2}\sigma_a\frac{1}{2}\sigma_b|SM_S\rangle\,\hat{a}^\dagger_{a\sigma_a}\hat{a}^\dagger_{b\sigma_b}.\end{aligned} \tag{2.114}$$

Irrep.	$S=0$	$S=1$
A_g	16	6
B_{1g}	2	2
B_{2g}	6	6
B_{3g}	6	6
A_u	2	2
B_{1u}	11	11
B_{2u}	6	6
B_{3u}	6	6
	55	45

Table 2.2: The reduction due to spin and point group symmetry (D_{2h}) for the H_2 molecule.

The entire analysis of Section 2.4.1 on page 34 can now be repeated with the additional label for the irreducible representation and the constraint that both $\hat{B}$ operators should have the same label. Each spin block will split up into blocks per irreducible representation. The transformation formulas are

$$\begin{aligned}\Gamma_{a\sigma_a b\sigma_b;c\sigma_c d\sigma_d} =& \sqrt{(1+\delta_{ab})\,(1+\delta_{cd})}\delta_{I_a\otimes I_b;I_c\otimes I_d} \\ & \sum_{SM} \langle \frac{1}{2}\sigma_a \frac{1}{2}\sigma_b | SM\rangle \, \langle \frac{1}{2}\sigma_c \frac{1}{2}\sigma_d | SM\rangle \, \Gamma^{S;I_a\otimes I_b}_{ab;cd}, \end{aligned} \tag{2.115a}$$

$$\begin{aligned}\Gamma^{S;I}_{ab;cd} =& \frac{1}{\sqrt{(1+\delta_{ab})\,(1+\delta_{cd})}}\delta_{I_a\otimes I_b;I}\delta_{I_c\otimes I_d;I} \sum_{\sigma_a\sigma_b}\sum_{\sigma_c\sigma_d} \\ & \langle \frac{1}{2}\sigma_a \frac{1}{2}\sigma_b | SM\rangle \, \langle \frac{1}{2}\sigma_c \frac{1}{2}\sigma_d | SM\rangle \, \Gamma_{a\sigma_a b\sigma_b;c\sigma_c d\sigma_d}, \end{aligned} \tag{2.115b}$$

where $\Gamma^{S;I}$ denotes the block with spin S and irreducible representation I. The symmetry in the spatial orbital indices is unchanged (see eq. (2.98)). The exact reduction that the point group symmetry gives depends on the specific group. The higher the symmetry, the greater the reduction. As an example we take a look at H_2 in the Correlation Consistent Polarized Valence Double Zeta (cc-pVDZ) basis set [108]. The full symmetry group of H_2 is $D_{\infty h}$ but we use the largest Abelian subgroup which is D_{2h}. In this case, there are 5 orbitals per hydrogen atom: $1s2s2p^3$. The number of pairs per irreducible representation can be found in Table 2.2. The full dimension of the 2DM is $\frac{20(20-1)}{2} = 190$. Utilizing spin symmetry reduces this to a 55×55 and 45×45 block. This is already a 7-fold reduction of the number of matrix elements. If we add the D_{2h} symmetry to the picture, we get another 5-fold reduction:

Instead of $190 \times 190 = 36100$ matrix elements, we have only 942 elements, a 38-fold total reduction!

2.5 The doubly-occupied Hilbert space

In previous sections, we only made general assumptions about the (ensemble of) wave functions from which the 2DM is derivable. All wave functions should be normalized and antisymmetric. For symmetry, we made assumptions on the quantum numbers of the wave function: it should be a singlet wave function, or the wave function should transform according to a certain irreducible representation. But we could make other or additional assumptions. If we take a look at the Full Configuration Interaction (FullCI) expansion of the wave function, we see that a Slater determinant is the basic building block

$$|\Psi\rangle = \sum_{\mathbf{k}} \sum_{\mathbf{s}} c_{\mathbf{k};\mathbf{s}}\, \hat{a}^\dagger_{k_1 s_1} \hat{a}^\dagger_{k_2 s_2} \dots \hat{a}^\dagger_{k_N s_N} |\rangle \,, \tag{2.116}$$

where the summation runs over all possible orbitals ($\mathbf{k}$) and spin configurations ($\mathbf{s}$). Every vector $\mathbf{k} = (k_1, k_2, \dots, k_N)$ with $k_i \in \{1, \dots, L\}$ contains the N orbitals that are occupied and the vector $\mathbf{s} = (s_1, s_2, \dots, s_N)$ with $s_i \in \{\uparrow, \downarrow\}$ contains the spin states for each orbital. Both are not independent as the Pauli exclusion principle must be obeyed. Classic wave function techniques will start from a reference Slater determinant, usually the results of a Hartree-Fock (HF) calculation, and add excitations on top of that [2]. In the limit where all excitations are added, the best possible result within the used basis set is found. However, the number of possible Slater determinants scales exponentially as $\binom{2L}{N}$ and we know that usually a smaller subset will be dominant: many of the $c_{\mathbf{k}}$ coefficients will be negligible. We will make the choice to only keep the Slater determinants where all orbitals are doubly occupied

$$|\Psi\rangle = \sum_{\mathbf{k}} c_{\mathbf{k}}\, \hat{a}^\dagger_{k_1\uparrow} \hat{a}^\dagger_{k_1\downarrow} \dots \hat{a}^\dagger_{k_{\frac{N}{2}}\uparrow} \hat{a}^\dagger_{k_{\frac{N}{2}}\downarrow} |\rangle \,. \tag{2.117}$$

We refer to this class of wave functions as Doubly Occupied Configuration Interaction (DOCI). For the motivation of this choice, we refer to Section 4.3 on page 101. Notice that the number of Slater determinants in the DOCI expansion still scales exponentially as $\binom{L}{\frac{N}{2}}$. We examine the consequence of restricting the ensemble of wave function to DOCI wave functions on the N-representability constraints derived so far. This was originally done by Weinhold and Wilson [109, 110][1] but to the best of my knowledge, they were

1. E. Bright Wilson, Jr. is the father of Kenneth G. Wilson, who won the Nobel Prize for his work on the renormalisation group.

never used in a practical calculations. They make a reference to a third paper but it never appeared. However, not all conditions on the 3DM were derived by them. We shall present all of them. Notice that the wave function (2.117) is a singlet state by definition: the expectation value of the operators $\hat{S}_z$, $\hat{S}_+$ and $\hat{S}_-$ are all zero. We denote the pair partner by a bar symbol: $a\uparrow = a$ and $a\downarrow = \bar{a}$ (or vice versa). In this context, the concept of seniority [111] is also very useful: the seniority number is the number of unpaired particles. DOCI is a seniority-zero wave function.

2.5.1 The first-order reduced density matrix

The 1DM derivable from a DOCI ensemble is much simpler

$$\rho_{a\sigma_a b\sigma_b} = \delta_{\sigma_a\sigma_b}\delta_{ab}\sum_i w_i \langle\psi_i|\hat{a}^\dagger_{a\sigma_a}\hat{a}_{a\sigma_a}|\psi_i\rangle = \rho_a = \rho_{\bar{a}}, \tag{2.118}$$

where $w_i \geq 0$ and $\sum_i w_i = 1$. Due to spin symmetry (see Section 2.4.1 on page 34), we known that the 1DM is diagonal in the spin indices, but in the case of DOCI, the 1DM must be diagonal in the spatial orbital index too: we can only break the same pair states in the ket and bra. It even becomes degenerate in the spin. This can be understood because of the number operators: in the DOCI case, $\hat{n}_a = \hat{n}_{\bar{a}}$. The number of particles in a spin-up and spin-down state is equal. The 1DM is reduced from a $2L \times 2L$ matrix to a vector of length L. The properties of the 1DM now are

$$\rho_a \geq 0, \tag{2.119a}$$

$$\sum_a \rho_a = \frac{N}{2}. \tag{2.119b}$$

The necessary and sufficient conditions for N-representability dictate that each element ρ_a should be in the interval $[0, 1]$. Notice that in the DOCI case, the used orbitals are automatically the natural orbitals and the elements of vector ρ_a are the natural occupation numbers. However, DOCI is orbital dependent: the orbital need to be optimized to find the lowest energy. This will be further explained in Section 4.3.

2.5.2 The second-order reduced density matrix

The 2DM is a bit more complex. It is important to realize that all operators need to couple to seniority zero if evaluated between two DOCI wave functions. An operator cannot change the number of broken pairs. This makes the 1DM diagonal as seen above. The $\hat{B}^\dagger$ operator can do two things: created

or annihilate a doubly-occupied state (seniority zero), or break two doubly-occupied states (seniority two). As seniority must be conserved, the 2DM is block diagonal in the seniority number. Let us first look at the seniority-zero block. We define the $L \times L$ pair matrix as

$$\Pi_{ab} = \Gamma_{a\bar{a};b\bar{b}} = \langle\psi|\hat{a}_a^\dagger \hat{a}_{\bar{a}}^\dagger \hat{a}_{\bar{b}} \hat{a}_b|\psi\rangle\,, \tag{2.120}$$

where we have left out the ensemble summation to lighten the notation. From the positivity of the Hamiltonian $\hat{B}^\dagger \hat{B}$ with

$$\hat{B}^\dagger = \sum_a p_a \hat{a}_a^\dagger \hat{a}_{\bar{a}}^\dagger, \tag{2.121}$$

it follows that the pair matrix (2.120) must be positive semidefinite

$$\Pi \succeq 0. \tag{2.122}$$

This simply implies that the overlap of the wave function with one pair removed must be positive. The seniority-two block is part of the diagonal of the 2DM: as we break two pairs, the left and right operator must be equal. For $a < b$

$$D_{ab} = \Gamma_{ab;ab} = \langle\psi|\hat{a}_a^\dagger \hat{a}_b^\dagger \hat{a}_b \hat{a}_a|\psi\rangle\,, \tag{2.123a}$$
$$= \Gamma_{a\bar{b};a\bar{b}} = \langle\psi|\hat{a}_a^\dagger \hat{a}_{\bar{b}}^\dagger \hat{a}_{\bar{b}} \hat{a}_a|\psi\rangle\,, \tag{2.123b}$$
$$= \Gamma_{\bar{a}b;\bar{a}b} = \langle\psi|\hat{a}_{\bar{a}}^\dagger \hat{a}_b^\dagger \hat{a}_b \hat{a}_{\bar{a}}|\psi\rangle\,, \tag{2.123c}$$
$$= \Gamma_{\bar{a}\bar{b};\bar{a}\bar{b}} = \langle\psi|\hat{a}_{\bar{a}}^\dagger \hat{a}_{\bar{b}}^\dagger \hat{a}_{\bar{b}} \hat{a}_{\bar{a}}|\psi\rangle\,. \tag{2.123d}$$

Notice that eqs. (2.123a) and (2.123d) imply $D_{aa} = 0$ while eqs. (2.123b) and (2.123c) do not. As eq. (2.123b) in the case of $a = b$ is equal to Π_{aa}, we will pick $D_{aa} = 0$ from now on. The equality between eqs. (2.123a) to (2.123d) can be understood from

$$\hat{a}_a^\dagger \hat{a}_a = \hat{n}_a = \hat{n}_{\bar{a}} = \hat{a}_{\bar{a}}^\dagger \hat{a}_{\bar{a}} = \hat{a}_a^\dagger \hat{a}_{\bar{a}}^\dagger \hat{a}_{\bar{a}} \hat{a}_a, \tag{2.124}$$

for DOCI wave functions and the fundamental anticommutator relations eq. (B.5) on page 147. The diagonal D_{ab} is fourfold degenerate, corresponding to $S_z = -1, 0, 1$. A positive semidefinite matrix must have positive elements on its diagonal (see Chapter C on page 149) and thus the N-representability conditions on eq. (2.123) are

$$D_{ab} \geq 0. \tag{2.125}$$

This gives us a set of $\frac{L(L-1)}{2}$ linear inequalities to impose. The general 2DM is now reduced to a $L \times L$ matrix inequality and a set of linear inequalities.

There are now three ways of obtaining the 1DM out of the 2DM: via the general relation eq. (2.22) on page 22

$$\rho_a = \frac{1}{N-1}\sum_b \left(\Gamma_{ab;ab} + \Gamma_{a\bar{b};a\bar{b}}\right) = \frac{1}{N-1}\left(\Pi_{aa} + 2\sum_b D_{ab}\right), \quad (2.126)$$

via the seniority-two diagonal D

$$\begin{aligned}\rho_a &= \frac{1}{\frac{N}{2}-1}\sum_b D_{ab} = \frac{2}{N-2}\sum_b D_{ab} \\ &= \frac{2}{N-2}\sum_b \langle\psi|\hat{a}_a^\dagger \hat{a}_b^\dagger \hat{a}_b \hat{a}_a|\psi\rangle\,,\end{aligned} \quad (2.127)$$

and via the pairing matrix Π

$$\rho_a = \Pi_{aa} = \langle\psi|\hat{a}_a^\dagger \hat{a}_{\bar{a}}^\dagger \hat{a}_{\bar{a}} \hat{a}_a|\psi\rangle\,. \quad (2.128)$$

These are not independent of each other. To have a consistent 2DM, the equivalence of eq. (2.127) and eq. (2.128) will have to be enforced. The trace of the 2DM remains unaltered but we can now split it over Π and D

$$\mathrm{Tr}\,(\Pi) = \sum_a \Pi_{aa} = \frac{N}{2}, \quad (2.129)$$

$$\mathrm{Tr}\,(D) = \sum_{a<b} D_{ab} = \frac{1}{2}\sum_{ab} D_{ab} = \frac{N}{8}(N-2)\,, \quad (2.130)$$

$$\mathrm{Tr}\,(\Gamma) = \mathrm{Tr}\,(\Pi) + 4\mathrm{Tr}\,(D) = \frac{N(N-1)}{2},$$

where we keep the fourfold degeneracy of D in mind.

I. The $\mathcal{Q}$ condition

The $\mathcal{Q}$ matrix has the same structure as the 2DM itself. The seniority-zero block is derived from the positivity of

$$\sum_{ab} q_a \langle\psi|\hat{a}_a \hat{a}_{\bar{a}} \hat{a}_{\bar{b}}^\dagger \hat{a}_b^\dagger|\psi\rangle\, q_b \geq 0. \quad (2.131)$$

We define the $L \times L$ matrix $\mathcal{Q}^\Pi$ as

$$\mathcal{Q}^\Pi_{ab} = \langle\psi|\hat{a}_a \hat{a}_{\bar{a}} \hat{a}_{\bar{b}}^\dagger \hat{a}_b^\dagger|\psi\rangle\,. \quad (2.132)$$

Equation (2.129) means that $\mathcal{Q}^{\Pi}$ should be positive semidefinite: $\mathcal{Q}^{\Pi} \succeq 0$. The $\mathcal{Q}^{\Pi}$ can again be expressed as a function of the Π and D matrices

$$\mathcal{Q}^{\Pi}_{ab}(\Pi, D) = \delta_{ab}(1 - \rho_a - \rho_b) + \Pi_{ab}. \tag{2.133}$$

The seniority two part is on the diagonal of the $\mathcal{Q}$ matrix and given by

$$a < b: \qquad \langle\psi|\hat{a}_a\hat{a}_b\hat{a}^\dagger_b\hat{a}^\dagger_a|\psi\rangle = 1 - \rho_a - \rho_b + D_{ab} \geq 0. \tag{2.134}$$

Just like for the 2DM, this forms a set of $\frac{L(L-1)}{2}$ linear inequalities.

II. The $\mathcal{G}$ condition

The $\mathcal{G}$ condition is somewhat more elaborate as more combinations are nonzero. We work systematically according to seniority and spin. The full operator $\hat{B}^\dagger$ for the $\mathcal{G}$ condition is

$$\hat{B}^\dagger = \sum_{\alpha\beta} g_{\alpha\beta}\hat{a}^\dagger_\alpha\hat{a}_\beta \tag{2.135}$$

$$= \sum_{ab}\left(g^1_{ab}\hat{a}^\dagger_a\hat{a}_b + g^2_{ab}\hat{a}^\dagger_a\hat{a}_{\bar{b}} + g^3_{ab}\hat{a}^\dagger_{\bar{a}}\hat{a}_b + g^4_{ab}\hat{a}^\dagger_{\bar{a}}\hat{a}_{\bar{b}}\right). \tag{2.136}$$

Spin projections $S_z = \pm 1$ are equivalent, so we only consider the $S_z = +1$ case: the g^2 and g^3 terms will generate equivalent constraints. We always assume $a \neq b$, since for a DOCI wave function $\hat{a}^\dagger_a\hat{a}_{\bar{a}} = 0$. The particle-hole operators generating this constraint are of the form

$$\hat{B}^\dagger = \sum_{ab} g^2_{ab}\hat{a}^\dagger_a\hat{a}_{\bar{b}}, \tag{2.137}$$

which leads to the following seniority-2 positivity condition:

$$\begin{aligned}
&\sum_{abcd} g^2_{ab}\,\langle\psi|\hat{a}^\dagger_a\hat{a}_{\bar{b}}\hat{a}^\dagger_{\bar{d}}\hat{a}_c|\psi\rangle\, g^2_{cd} = \\
&\sum_{abcd} g^2_{ab}\left[\delta_{bd}\delta_{ac}(\rho_a - D_{ab}) - \delta_{ad}\delta_{bc}\Pi_{ab}\right] g^2_{cd} = \\
&\sum_{ab} g^2_{ab}\left[(\rho_a - D_{ab})g^2_{ab} - \Pi_{ab}g^2_{ba}\right] \geq 0
\end{aligned} \tag{2.138}$$

This condition is almost diagonal, as g^2_{ab} is only connected with itself and g^2_{ba}. If we order the summation

$$\sum_{a<b} g^2_{ab}(\rho_a - D_{ab})g^2_{ab} - g^2_{ab}\Pi_{ab}g^2_{ba} + g^2_{ba}(\rho_b - D_{ab})g^2_{ba} - g^2_{ba}\Pi_{ab}g^2_{ab} \geq 0, \tag{2.139}$$

we can see that this is equivalent with the positive semidefiniteness of the following set of 2×2 matrices

$$\forall a < b \qquad \begin{bmatrix} \rho_a - D_{ab} & -\Pi_{ab} \\ -\Pi_{ab} & \rho_b - D_{ab} \end{bmatrix} \succeq 0 \,. \tag{2.140}$$

For the $S_z = 0$ and seniority-two case, the particle-hole operators are of the form

$$\hat{B}_1^\dagger = \sum_{ab} g_{ab}^1 \hat{a}_a^\dagger \hat{a}_b, \tag{2.141a}$$

$$\hat{B}_4^\dagger = \sum_{ab} g_{ab}^4 \hat{a}_{\bar{a}}^\dagger \hat{a}_{\bar{b}}, \tag{2.141b}$$

with $a \neq b$. These terms are coupled to each other. The diagonal terms, $\hat{B}_1^\dagger \hat{B}_1$ and $\hat{B}_4^\dagger \hat{B}_4$, are

$$\langle\psi|\hat{a}_a^\dagger \hat{a}_b \hat{a}_d^\dagger \hat{a}_c|\psi\rangle = \delta_{ac}\delta_{bd}(\rho_a - D_{ab}) = \langle\psi|\hat{a}_{\bar{a}}^\dagger \hat{a}_{\bar{b}} \hat{a}_{\bar{d}}^\dagger \hat{a}_{\bar{c}}|\psi\rangle \,. \tag{2.142}$$

The off-diagonal terms, $\hat{B}_1^\dagger \hat{B}_4$ and $\hat{B}_4^\dagger \hat{B}_1$, are

$$\langle\psi|\hat{a}_a^\dagger \hat{a}_b \hat{a}_{\bar{d}}^\dagger \hat{a}_{\bar{c}}|\psi\rangle = \delta_{ad}\delta_{bc}\Pi_{ab} = \langle\psi|\hat{a}_{\bar{a}}^\dagger \hat{a}_{\bar{b}} \hat{a}_d^\dagger \hat{a}_c|\psi\rangle \,, \tag{2.143}$$

which in the same way leads to the set of 2×2 constraint matrices

$$\forall a < b \qquad \begin{bmatrix} \rho_a - D_{ab} & \Pi_{ab} \\ \Pi_{ab} & \rho_b - D_{ab} \end{bmatrix} \succeq 0 \,. \tag{2.144}$$

These only differ with (2.140) in the sign of the off-diagonal elements but the characteristic polynomial of both is the same and thus the conditions are equivalent.

The $S_z = 0$ and seniority-zero part is built by two particle-hole operators

$$\hat{B}_1^\dagger = \sum_a g_a \hat{a}_a^\dagger \hat{a}_a, \tag{2.145a}$$

$$\hat{B}_2^\dagger = \sum_b g_b \hat{a}_{\bar{b}}^\dagger \hat{a}_{\bar{b}}. \tag{2.145b}$$

This leads to a $2L \times 2L$ matrix with diagonal elements, $\hat{B}_1^\dagger \hat{B}_1$ and $\hat{B}_2^\dagger \hat{B}_2$,

$$\langle\psi|\hat{a}_a^\dagger \hat{a}_a \hat{a}_b^\dagger \hat{a}_b|\psi\rangle = \delta_{ab}\rho_a + D_{ab} = \langle\psi|\hat{a}_{\bar{a}}^\dagger \hat{a}_{\bar{a}} \hat{a}_{\bar{b}}^\dagger \hat{a}_{\bar{b}}|\psi\rangle \,, \tag{2.146}$$

and off-diagonal elements, $\hat{B}_1^\dagger \hat{B}_2$ and $\hat{B}_2^\dagger \hat{B}_1$,

$$\begin{aligned} \langle\psi|\hat{a}_a^\dagger \hat{a}_a \hat{a}_{\bar{b}}^\dagger \hat{a}_{\bar{b}}|\psi\rangle &= D_{ab} + \delta_{ab}\Pi_{ab} \\ &= \delta_{ab}\rho_a + D_{ab} \\ &= \langle\psi|\hat{a}_{\bar{a}}^\dagger \hat{a}_{\bar{a}} \hat{a}_b^\dagger \hat{a}_b|\psi\rangle \,. \end{aligned} \tag{2.147}$$

Both blocks are identical. This means we have a positivity condition on a block matrix of the form

$$\begin{bmatrix} A & A \\ A & A \end{bmatrix}. \tag{2.148}$$

Using the following block matrix property of determinants (see Chapter C on page 149)

$$\begin{vmatrix} A & B \\ B & A \end{vmatrix} = \left|A - B\right| \left|A + B\right|, \tag{2.149}$$

we can see that we only have to impose the positivity of one block to obey the constraint. This leads to the matrix condition $\mathcal{G}^{\Pi} \succeq 0$ of a $L \times L$ matrix:

$$\mathcal{G}^{\Pi}_{ab}(\Pi, D) = \delta_{ab}\rho_a + D_{ab}\,. \tag{2.150}$$

Unlike the $\mathcal{I}$ and $\mathcal{Q}$ conditions, the original $\mathcal{G}$ matrix is never used. We have derived a simpler set of conditions which are equivalent.

Compared to the full $\mathcal{P}$, $\mathcal{Q}$ and $\mathcal{G}$ conditions, these constraints have a much lower scaling. The matrix dimensions are reduced from L^2 to L.

A DOCI wave function is a singlet state by definition. In Section 2.4.1 on page 34 we derived a set of necessary conditions for the singlet state on the 2DM. In the case of DOCI derived 2DM, this condition is automatically fulfilled. The $\hat{S}_z$ operator is

$$\hat{S}_z = \frac{1}{2}\sum_a \left(\hat{a}^\dagger_a \hat{a}_a - \hat{a}^\dagger_{\bar{a}} \hat{a}_{\bar{a}}\right). \tag{2.151}$$

We reevaluated the condition eq. (2.107) on page 40,

$$\begin{aligned}
\langle\psi|\hat{a}^\dagger_c \hat{a}_d \hat{S}_z|\psi\rangle = & \\
&= \frac{1}{2}\delta_{cd}\sum_a^L \left(\langle\psi|\hat{a}^\dagger_c \hat{a}_d \hat{a}^\dagger_a \hat{a}_a|\psi\rangle - \langle\psi|\hat{a}^\dagger_c \hat{a}_d \hat{a}^\dagger_{\bar{a}} \hat{a}_{\bar{a}}|\psi\rangle\right) \\
&= \frac{1}{2}\sum_a^L \left(\langle\psi|\hat{a}^\dagger_a \hat{a}_a|\psi\rangle - \langle\psi|\hat{a}^\dagger_c \hat{a}^\dagger_a \hat{a}_c \hat{a}_a|\psi\rangle - \langle\psi|\hat{a}^\dagger_c \hat{a}^\dagger_{\bar{a}} \hat{a}_c \hat{a}_{\bar{a}}|\psi\rangle\right) \\
&= \frac{1}{2}\sum_a^L \left(\rho_a + (1-\delta_{ac})D_{ac} - \Pi_{ac}\delta_{ac} - (1-\delta_{ac})D_{ca}\right) \\
&= 0\,.
\end{aligned}$$

This shows no additional constraints are needed to ensure the singlet state.

2.5.3 The third-order reduced density matrix

The 3DM falls apart in blocks labeled by S_z and the seniority number: we have seniority one and three, combined with $S_z = \pm\frac{1}{2}, \pm\frac{3}{2}$.

The seniority-three part, which breaks up three pairs, must be diagonal so that the three pairs can recombine. The diagonal elements of a positive semidefinite matrix must be positive leading to

$$D^3_{abc} = \langle\psi|\hat{a}^\dagger_a\hat{a}^\dagger_b\hat{a}^\dagger_c\hat{a}_c\hat{a}_b\hat{a}_a|\psi\rangle \geq 0. \tag{2.152}$$

It is clear that D^3_{abc} will be zero when any two indices are equal. Furthermore, the different permutations of spin-up and spin-down will lead to the same constraint: D^3_{abc} is fourfold degenerate for the different values of S_z. There is also permutation symmetry in the indices

$$\forall\sigma \in S_3: \quad D^3_{abc} = D^3_{\sigma(a)\sigma(b)\sigma(c)}, \tag{2.153}$$

where S_3 is the symmetric group of three elements. This condition gives us a set of $\frac{L(L-1)(L-2)}{6}$ linear constraints. If we sum over the different indices, we find

$$\sum_c D^3_{abc} = \left(\frac{N}{2} - 2\right) D_{ab}, \tag{2.154a}$$

$$\sum_{bc} D^3_{abc} = \left(\frac{N}{2} - 1\right)\left(\frac{N}{2} - 2\right)\rho_a, \tag{2.154b}$$

$$\sum_{abc} D^3_{abc} = \frac{N}{2}\left(\frac{N}{2} - 1\right)\left(\frac{N}{2} - 2\right). \tag{2.154c}$$

The condition (2.152) implies the condition (2.125) on the 2DM.

The seniority-one part means removing an entire pair and breaking another resulting in

$$\begin{aligned}\Pi^b_{ac} = \Pi^b_{ca} &= \langle\psi|\hat{a}^\dagger_a\hat{a}^\dagger_{\bar{a}}\hat{a}^\dagger_b\hat{a}_b\hat{a}_{\bar{c}}\hat{a}_c|\psi\rangle = \Pi^{\bar{b}}_{ac} = \Pi^{\bar{b}}_{ca} \\ &= \langle\psi|\hat{a}^\dagger_b\hat{a}^\dagger_{\bar{a}}\hat{a}^\dagger_a\hat{a}_c\hat{a}_{\bar{c}}\hat{a}_b|\psi\rangle\end{aligned} \tag{2.155}$$

This set of L symmetric matrices is twofold degenerate in the upper index. It belongs to $S_z = \pm\frac{1}{2}$. Furthermore, $\Pi^a_{ab} = \Pi^b_{ab} = 0$. The operator

$$\hat{B}^\dagger = \sum_{ab} t_{ab}\hat{a}^\dagger_a\hat{a}^\dagger_{\bar{a}}\hat{a}^\dagger_b \tag{2.156}$$

leads to the condition

$$\forall b: \quad \Pi^b \succeq 0. \tag{2.157}$$

We have a set of L positive semidefinite constraints on $(L-1)\times(L-1)$ matrices. Similar as the 2DM, there are some consistency conditions that need to be fulfilled. We have,

$$\Pi^b_{aa} = D_{ab} = D_{ba}, \tag{2.158}$$

which means following 'lifting' and consistency conditions have be enforced

$$\Pi^b_{aa} = \Pi^a_{bb}, \tag{2.159}$$

$$\sum_c D^3_{abc} = \left(\frac{N}{2} - 2\right)\Pi^b_{aa}, \tag{2.160}$$

where we used eq. (2.154a) on page 52. Furthermore, the following sums are known

$$\sum_b \Pi^b_{ac} = \left(\frac{N}{2} - 1\right)\Pi_{ac}, \tag{2.161}$$

$$\sum_{ab} \Pi^b_{aa} = \frac{N}{2}\left(\frac{N}{2} - 1\right). \tag{2.162}$$

Every part of the 1DM and 2DM can be calculated by summing over indices. These conditions imply the necessary N-representability conditions for DOCI on the 1DM and 2DM.

I. The ${}^3\mathcal{Q}$ condition

The ${}^3\mathcal{Q}$ condition has the same structure as the 3DM. The seniority-three condition leads to

$$\langle\psi|\hat{a}_a\hat{a}_b\hat{a}_c\hat{a}^\dagger_c\hat{a}^\dagger_b\hat{a}^\dagger_a|\psi\rangle = 1-\rho_a-\rho_b-\rho_c+D_{ab}+D_{bc}+D_{ac}-D^3_{abc} \geq 0. \tag{2.163}$$

This gives us a set of $\frac{L(L-1)(L-2)}{6}$ linear constraints. The equivalent of the $\mathcal{T}_1$ condition is found by the sum of the ${}^3\mathcal{J}$ and ${}^3\mathcal{Q}$ matrix which generates

$$1 - \rho_a - \rho_b - \rho_c + D_{ab} + D_{bc} + D_{ac} \geq 0. \tag{2.164}$$

This is a constraint on the diagonal of the $\mathcal{T}_1$ matrix.

The seniority-one condition produces a set of L matrices of dimension $(L-1)\times(L-1)$. The generating operator is

$$\hat{B}^\dagger = \sum_{ab} q_{ab}\hat{a}_a\hat{a}_{\bar{a}}\hat{a}_b, \tag{2.165}$$

which leads to

$$\mathcal{Q}^b_{ac} = \langle\psi|\hat{a}_a\hat{a}_{\bar{a}}\hat{a}_b\hat{a}^\dagger_b\hat{a}^\dagger_{\bar{c}}\hat{a}^\dagger_c|\psi\rangle \tag{2.166}$$

$$= \delta_{ac}\left(1 - 2\rho_a - \rho_b + 2D_{ab}\right) + \Pi_{ac} - \Pi^b_{ac}, \tag{2.167}$$

and this set of matrices has to positive semidefinite

$$\forall b: \quad \mathcal{Q}^b \succeq 0. \tag{2.168}$$

We can again find an equivalent $\mathcal{T}_1$ condition by adding Π^b to (2.167)

$$(\mathcal{T}_1)^b_{ac} = \delta_{ac}\left(1 - 2\rho_a - \rho_b + 2D_{ab}\right) + \Pi_{ac}, \tag{2.169}$$

$$\forall b: \quad (\mathcal{T}_1)^b \succeq 0.$$

II. The ${}^3\mathcal{E}$ condition

The ${}^3\mathcal{E}$ is more involved. We are looking for a set of conditions that are equivalent with the full ${}^3\mathcal{E}$ as shown derived in Section 2.3.3. The condition will split in blocks labeled by S_z and seniority number. Within such a block, not all states will be coupled to each other. This is what we are looking for.

The generating operator for the ${}^3\mathcal{E}$ is

$$\hat{B}^\dagger = \sum_{\alpha\beta\gamma} q^1_{\alpha\beta\gamma}\hat{a}^\dagger_\alpha\hat{a}^\dagger_\beta\hat{a}_\gamma, \tag{2.170}$$

which again leads to a seniority one and three combined with $S_z = \pm\frac{1}{2}, \pm\frac{3}{2}$. Just like the $\mathcal{G}$ condition, much more combination are possible, as different terms will be connected.

We begin with the seniority-three sector. This means that we have to break three *different* pairs. For $S_z = \pm\frac{3}{2}$ the generator is $\hat{B}^\dagger = \sum_{abc} q^1_{abc}\hat{a}^\dagger_a\hat{a}^\dagger_b\hat{a}_{\bar{c}}$ ($a \neq b \neq c$) which leads to

$$\langle\psi|\hat{a}^\dagger_a\hat{a}^\dagger_b\hat{a}_{\bar{c}}\hat{a}^\dagger_{\bar{f}}\hat{a}_e\hat{a}_d|\psi\rangle = \\ \delta_{cf}\delta_{ad}\delta_{be}\left(D_{ab} - D^3_{abc}\right) - \delta_{af}\delta_{be}\delta_{cd}\Pi^b_{ac} - \delta_{bf}\delta_{ce}\delta_{ad}\Pi^a_{bc}. \tag{2.171}$$

This connects three states with the same spatial orbitals, $ab\bar{c}$, $bc\bar{a}$ and $ca\bar{b}$. For $bc\bar{a}$ we find

$$\langle\psi|\hat{a}^\dagger_b\hat{a}^\dagger_c\hat{a}_{\bar{a}}\hat{a}^\dagger_{\bar{d}}\hat{a}_f\hat{a}_e|\psi\rangle = \\ \delta_{cf}\delta_{ad}\delta_{be}\left(D_{bc} - D^3_{bac}\right) - \delta_{af}\delta_{be}\delta_{cd}\Pi^b_{ac} - \delta_{bd}\delta_{cf}\delta_{ae}\Pi^c_{ab}, \tag{2.172}$$

while for $ca\bar{b}$

$$\langle\psi|\hat{a}_c^\dagger\hat{a}_a^\dagger\hat{a}_{\bar{b}}\hat{a}_{\bar{e}}^\dagger\hat{a}_d\hat{a}_f|\psi\rangle = \delta_{cf}\delta_{ad}\delta_{be}\left(D_{ac} - D^3_{abc}\right) - \delta_{ad}\delta_{ce}\delta_{bf}\Pi^a_{bc} - \delta_{bd}\delta_{cf}\delta_{ae}\Pi^c_{ab}. \quad (2.173)$$

Combining this will eventually give us a 3×3 matrix condition

$$\begin{array}{c} \\ ab\bar{c} \\ bc\bar{a} \\ ca\bar{b} \end{array} \begin{array}{c} \begin{array}{ccc} ab\bar{c} & bc\bar{a} & ca\bar{b} \end{array} \\ \begin{bmatrix} D_{ab} - D^3_{abc} & -\Pi^b_{ac} & -\Pi^a_{bc} \\ -\Pi^b_{ac} & D_{bc} - D^3_{abc} & -\Pi^c_{ab} \\ -\Pi^a_{bc} & -\Pi^c_{ab} & D_{ac} - D^3_{abc} \end{bmatrix} \end{array} \succeq 0, \quad (2.174)$$

for $a < b$ and $a \neq b \neq c$. The row and column set of indices are the indices for the left and right. There are $\frac{L(L-1)(L-2)}{2}$ such matrix conditions. We continue with the $S_z = \pm\frac{1}{2}$ sector. There are two generating operators

$$\hat{B}_1^\dagger = \sum_{abc} q^1_{abc}\hat{a}_a^\dagger\hat{a}_b^\dagger\hat{a}_c, \quad (2.175a)$$

$$\hat{B}_2^\dagger = \sum_{abc} q^1_{abc}\hat{a}_a^\dagger\hat{a}_{\bar{b}}^\dagger\hat{a}_{\bar{c}}, \quad (2.175b)$$

with $a \neq b \neq c$. The direct term $\hat{B}_1^\dagger\hat{B}_1$ gives us

$$\langle\psi|\hat{a}_a^\dagger\hat{a}_b^\dagger\hat{a}_c\hat{a}_f^\dagger\hat{a}_e\hat{a}_d|\psi\rangle = \delta_{ad}\delta_{be}\delta_{cf}\left(D_{ab} - D^3_{abc}\right), \quad (2.176)$$

while the other direct term $\hat{B}_2^\dagger\hat{B}_2$ leads to

$$\langle\psi|\hat{a}_a^\dagger\hat{a}_{\bar{b}}^\dagger\hat{a}_{\bar{c}}\hat{a}_{\bar{f}}^\dagger\hat{a}_{\bar{e}}\hat{a}_d|\psi\rangle = \delta_{ad}\delta_{be}\delta_{cf}\left(D_{ab} - D^3_{abc}\right) - \delta_{af}\delta_{be}\delta_{cd}\Pi^b_{ac}. \quad (2.177)$$

For the mixed term we obtain

$$\langle\psi|\hat{a}_a^\dagger\hat{a}_b^\dagger\hat{a}_c\hat{a}_{\bar{f}}^\dagger\hat{a}_{\bar{e}}\hat{a}_d|\psi\rangle = \delta_{ad}\delta_{bf}\delta_{ce}\Pi^a_{bc} - \delta_{bd}\delta_{af}\delta_{ce}\Pi^b_{ac} \quad (2.178)$$

$$= \left(\delta_{ad}\delta_{bf} - \delta_{bd}\delta_{af}\right)\delta_{ce}\Pi^d_{fe} \quad (2.179)$$

The second term in eq. (2.178) comes from $a \leftrightarrow b$. Again we see that this couples three terms for a, b and c.

$$\begin{array}{c} \\ abc \\ cba \\ cab \end{array} \begin{array}{c} \begin{array}{ccc} abc & cba & cab \end{array} \\ \begin{bmatrix} D_{ab} - D^3_{abc} & -\Pi^b_{ac} & -\Pi^a_{bc} \\ -\Pi^b_{ac} & D_{bc} - D^3_{abc} & \Pi^c_{ab} \\ -\Pi^a_{bc} & \Pi^c_{ab} & D_{ac} - D^3_{abc} \end{bmatrix} \end{array} \succeq 0, \quad (2.180)$$

This condition is equivalent with (2.174): by multiplying the first row and column with -1 we find matrix (2.174) with the sign of the off-diagonal

elements flipped. As shown in Chapter C, these gives us matrices with the same spectrum.

For the seniority-one sector, only $S_z = \pm\frac{1}{2}$ is possible as only one pair is broken. The generating operators are

$$\hat{B}_1^\dagger = \sum_{ab} q_{ab} \hat{a}_a^\dagger \hat{a}_{\bar{a}}^\dagger \hat{a}_{\bar{b}}, \tag{2.181a}$$

$$\hat{B}_2^\dagger = \sum_{ab} q_{ab} \hat{a}_b^\dagger \hat{a}_{\bar{a}}^\dagger \hat{a}_{\bar{a}}, \tag{2.181b}$$

$$\hat{B}_3^\dagger = \sum_{ab} q_{ab} \hat{a}_b^\dagger \hat{a}_a^\dagger \hat{a}_a, \tag{2.181c}$$

with $a \neq b$. We begin with the diagonal terms:

- $B_1^\dagger B_1$ leads to

$$\langle\psi|\hat{a}_a^\dagger \hat{a}_{\bar{a}}^\dagger \hat{a}_{\bar{b}} \hat{a}_{\bar{d}}^\dagger \hat{a}_{\bar{c}} \hat{a}_c|\psi\rangle = \delta_{bd}\left(\Pi_{ac} - \Pi_{ac}^b\right). \tag{2.182}$$

  This gives a set of L matrices of size $(L-1)\times(L-1)$. It can be extended by realizing that the missing element (when $a = b$ in eq. (2.181a)) is part of a primed condition with $\hat{B}^\dagger = \sum_c q_c \hat{a}_c^\dagger$

$$\langle\psi|\hat{a}_a^\dagger \hat{a}_{\bar{a}}^\dagger \hat{a}_{\bar{b}} \hat{a}_c|\psi\rangle = \delta_{bc}\Pi_{ab}, \tag{2.183}$$

$$\langle\psi|\hat{a}_b^\dagger \hat{a}_c|\psi\rangle = \delta_{bc}\rho_b. \tag{2.184}$$

  If we included this element, we find for every b the $L \times L$ matrix

$$\begin{bmatrix} \Pi_{ac} - \Pi_{ac}^b & \Pi_{ab} \\ \Pi_{cb} & \rho_b \end{bmatrix} \succeq 0, \tag{2.185}$$

  where the index a runs over the columns and c over the rows.

- $B_2^\dagger B_2$ gives us

$$\langle\psi|\hat{a}_b^\dagger \hat{a}_{\bar{a}}^\dagger \hat{a}_{\bar{a}} \hat{a}_{\bar{d}}^\dagger \hat{a}_{\bar{d}} \hat{a}_c|\psi\rangle = \delta_{bc}\left(\delta_{ad} D_{ab} + D_{abd}^3\right). \tag{2.186}$$

- $B_3^\dagger B_3$ produces

$$\langle\psi|\hat{a}_b^\dagger \hat{a}_a^\dagger \hat{a}_a \hat{a}_d^\dagger \hat{a}_d \hat{a}_c|\psi\rangle = \delta_{bc}\left(\delta_{ad} D_{ab} + D_{abd}^3\right). \tag{2.187}$$

The mixed terms:

- $B_1^\dagger B_2$ leads to

$$\langle\psi|\hat{a}_a^\dagger\hat{a}_{\bar{a}}^\dagger\hat{a}_{\bar{b}}\hat{a}_{\bar{d}}^\dagger\hat{a}_{\bar{d}}\hat{a}_c|\psi\rangle = \delta_{bc}\Pi_{ab}^d \tag{2.188}$$

- $B_1^\dagger B_3$ gives us

$$\langle\psi|\hat{a}_a^\dagger\hat{a}_{\bar{a}}^\dagger\hat{a}_{\bar{b}}\hat{a}_d^\dagger\hat{a}_d\hat{a}_c|\psi\rangle = \delta_{bc}\Pi_{ab}^d. \tag{2.189}$$

- $B_2^\dagger B_3$ produces

$$\begin{aligned}\langle\psi|\hat{a}_b^\dagger\hat{a}_{\bar{a}}^\dagger\hat{a}_{\bar{a}}\hat{a}_d^\dagger\hat{a}_d\hat{a}_c|\psi\rangle &= \delta_{bc}\delta_{ad}\Pi_{aa}^b + \delta_{bc}D_{abd}^3 \\ &= \delta_{bc}\left(\delta_{ad}D_{ab} + D_{abd}^3\right)\end{aligned} \tag{2.190}$$

- the overlap of the primed condition results in

$$\langle\psi|\hat{a}_b^\dagger\hat{a}_a^\dagger\hat{a}_a\hat{a}_c|\psi\rangle = \delta_{bc}D_{ab}. \tag{2.191}$$

As the $B_2^\dagger B_2$, $B_3^\dagger B_3$ and $B_2^\dagger B_3$ all produces the same element, we can reduce this $2L\times 2L$ matrix to a $L\times L$ matrix in the same way as with the $\mathcal{G}$ condition. This conditions reduces to a set of L matrices

$$[\delta_{ad}D_{ab} + D_{abd}^3] \succeq 0. \tag{2.192}$$

Combining all these results in a set of L matrices with dimensions $(2L-1)\times(2L-1)$. We could write it down as

$$\begin{bmatrix} \hat{a}_a^\dagger\hat{a}_{\bar{a}}^\dagger\hat{a}_{\bar{b}}\hat{a}_{\bar{b}}^\dagger\hat{a}_{\bar{c}}\hat{a}_c & \hat{a}_a^\dagger\hat{a}_{\bar{a}}^\dagger\hat{a}_{\bar{b}}\hat{a}_{\bar{c}}^\dagger\hat{a}_c\hat{a}_b & \hat{a}_a^\dagger\hat{a}_{\bar{a}}^\dagger\hat{a}_{\bar{b}}\hat{a}_b \\ \hat{a}_b^\dagger\hat{a}_a^\dagger\hat{a}_a\hat{a}_{\bar{b}}^\dagger\hat{a}_{\bar{c}}\hat{a}_c & \hat{a}_b^\dagger\hat{a}_{\bar{a}}^\dagger\hat{a}_{\bar{a}}\hat{a}_{\bar{c}}^\dagger\hat{a}_{\bar{c}}\hat{a}_b & \hat{a}_b^\dagger\hat{a}_a^\dagger\hat{a}_a\hat{a}_b \\ \hat{a}_b^\dagger\hat{a}_{\bar{b}}^\dagger\hat{a}_{\bar{c}}\hat{a}_c & \hat{a}_b^\dagger\hat{a}_{\bar{c}}^\dagger\hat{a}_{\bar{c}}\hat{a}_b & \hat{a}_b^\dagger\hat{a}_b \end{bmatrix} \succeq 0, \tag{2.193}$$

but using the results from above leads to

$$\forall b \neq a, \neq c, \quad \begin{bmatrix} \Pi_{ac} - \Pi_{ac}^b & \Pi_{ab}^c & \Pi_{ab} \\ \Pi_{cb}^a & \delta_{ac}D_{ab} + D_{abc}^3 & D_{ab} \\ \Pi_{bc} & D_{bc} & \rho_b \end{bmatrix} \succeq 0. \tag{2.194}$$

This might not look as a symmetric matrix because it has to be expanded: the index a is column index and c the row index.

III. The ${}^3\mathcal{F}$ condition

The generating operator for the ${}^3\mathcal{F}$ is

$$\hat{B}^\dagger = \sum_{\alpha\beta\gamma} q^1_{\alpha\beta\gamma} \hat{a}^\dagger_\alpha \hat{a}_\beta \hat{a}_\gamma. \tag{2.195}$$

We expect that this condition will be similar to the ${}^3\mathcal{E}$ condition. Again we have seniority one and three combined with $S_z = \pm\frac{1}{2}, \pm\frac{3}{2}$. We start with seniority-three and $S_z = \pm\frac{3}{2}$. The generator is $\hat{B}^\dagger = \sum_{abc} q^1_{abc} \hat{a}^\dagger_a \hat{a}_{\bar{b}} \hat{a}_{\bar{c}}$ with $a \neq b \neq c$ which leads to

$$\begin{aligned}\langle\psi|\hat{a}^\dagger_a \hat{a}_{\bar{b}} \hat{a}_{\bar{c}} \hat{a}^\dagger_{\bar{f}} \hat{a}^\dagger_{\bar{e}} \hat{a}_d|\psi\rangle &= \delta_{ad}\delta_{be}\delta_{cf}\left(\rho_a - D_{ab} - D_{ac} + D^3_{abc}\right) \\ &+ \delta_{af}\delta_{be}\delta_{cd}\left(\Pi^b_{ac} - \Pi_{ac}\right) + \delta_{ae}\delta_{cf}\delta_{bd}\left(\Pi^c_{ab} - \Pi_{ab}\right)\end{aligned} \tag{2.196}$$

when we choice an ordering in the indices $a \neq b < c$ (meaning some terms drop out). In the same fashion as for the ${}^3\mathcal{E}$ condition, this couples three terms (abc, cba and bac) leading to a set of 3×3 matrix conditions

$$\begin{bmatrix} \rho_a - D_{ab} - D_{ac} + D^3_{abc} & \Pi^b_{ac} - \Pi_{ac} & \Pi^c_{ab} - \Pi_{ab} \\ \Pi^b_{ac} - \Pi_{ac} & \rho_c - D_{bc} - D_{ac} + D^3_{abc} & \Pi^a_{bc} - \Pi_{bc} \\ \Pi^c_{ab} - \Pi_{ab} & \Pi^a_{bc} - \Pi_{bc} & \rho_b - D_{ab} - D_{bc} + D^3_{abc} \end{bmatrix} \succeq 0, \tag{2.197}$$

for $a \neq b \neq c$ and $b < c$. We can combine the seniority-three, $S_z = +\frac{3}{2}$ matrix of the ${}^3\mathcal{F}$ condition with its $S_z = -\frac{3}{2}$ counterpart of the ${}^3\mathcal{E}$ condition to find a DOCI version of the $\mathcal{T}_2$ condition. If we permute the rows and columns of the matrix (2.174) to the order $bc\bar{a}$, $ab\bar{c}$ and $ca\bar{b}$ and add it to (2.197), the resulting matrix has no elements of the 3DM:

$$\begin{bmatrix} \rho_a - D_{ab} - D_{ac} + D_{bc} & -\Pi_{ac} & -\Pi_{ab} \\ -\Pi_{ac} & \rho_c - D_{bc} - D_{ac} + D_{ab} & -\Pi_{bc} \\ -\Pi_{ab} & -\Pi_{bc} & \rho_b - D_{ab} - D_{bc} + D_{ab} \end{bmatrix} \succeq 0. \tag{2.198}$$

We continue with the $S_z = \pm\frac{1}{2}$ sector. The generating operator is

$$\hat{B}^\dagger = \sum_{ab} q_{ab} \hat{a}^\dagger_a \hat{a}_b \hat{a}_{\bar{c}}, \tag{2.199a}$$

with $a \neq b \neq c$ which leads to

$$\begin{aligned}\langle\psi|\hat{a}^\dagger_a \hat{a}_b \hat{a}_{\bar{c}} \hat{a}^\dagger_{\bar{f}} \hat{a}^\dagger_e \hat{a}_d|\psi\rangle &= \delta_{ad}\delta_{be}\delta_{cf}\left(\rho_a - D_{ab} - D_{ac} + D^3_{abc}\right) \\ &+ \delta_{af}\delta_{be}\delta_{cd}\left(\Pi^b_{ac} - \Pi_{ac}\right) + \delta_{ae}\delta_{cf}\delta_{bd}\left(\Pi^c_{ab} - \Pi_{ab}\right)\end{aligned} \tag{2.200}$$

This will generate an equivalent constraint as the $S_z = \pm\frac{3}{2}$ case.

For the seniority-one, again only $S_z = \pm\frac{1}{2}$ is possible. The same structure as for the ${}^3\mathcal{E}$ is expected. The generating operators are

$$\hat{B}_1^\dagger = \sum_{ab} q_{ab} \hat{a}_a^\dagger \hat{a}_a \hat{a}_{\bar{b}}, \tag{2.201a}$$

$$\hat{B}_2^\dagger = \sum_{ab} q_{ab} \hat{a}_b^\dagger \hat{a}_a \hat{a}_{\bar{a}}, \tag{2.201b}$$

with $a \neq b$. The primed operator is $B^\dagger = \sum_a q_a \hat{a}_{\bar{a}}$.

- $B_1^\dagger B_1$ leads to

  $$\langle\psi|\hat{a}_a^\dagger \hat{a}_a \hat{a}_{\bar{b}} \hat{a}_{\bar{d}}^\dagger \hat{a}_c^\dagger \hat{a}_c|\psi\rangle = \delta_{bd}\delta_{ac}\left(\rho_c - D_{ab}\right) + \delta_{bd} D_{ac} - \delta_{bd} D^3_{abc}. \tag{2.202}$$

  Combined with the prime term this gives

  $$\langle\psi|\hat{a}_a^\dagger \hat{a}_a \hat{a}_{\bar{b}} \hat{a}_{\bar{d}}^\dagger|\psi\rangle = \delta_{bd}\rho_a - \delta_{bd} D_{ab}. \tag{2.203}$$

- $B_2^\dagger B_2$ produces

  $$\langle\psi|\hat{a}_b^\dagger \hat{a}_a \hat{a}_{\bar{a}} \hat{a}_{\bar{c}}^\dagger \hat{a}_c^\dagger \hat{a}_d|\psi\rangle = \delta_{bd}\delta_{ac}(\rho_b - 2D_{bc}) + \delta_{bd}\Pi^b_{ac}. \tag{2.204}$$

  The combination with the primed term leads to

  $$\langle\psi|\hat{a}_b^\dagger \hat{a}_a \hat{a}_{\bar{a}} \hat{a}_{\bar{d}}^\dagger|\psi\rangle = -\delta_{bd}\Pi_{ab}. \tag{2.205}$$

The mixed term between B_1 and B_2 is

$$\langle\psi|\hat{a}_a^\dagger \hat{a}_a \hat{a}_{\bar{b}} \hat{a}_{\bar{c}}^\dagger \hat{a}_c^\dagger \hat{a}_d|\psi\rangle = \delta_{bd}\delta_{ac}\Pi_{ab} - \delta_{bd}\Pi^a_{bc}. \tag{2.206}$$

Combining this all gives us a set of L positivity conditions on matrices of dimensions $2L-1$

$$\begin{bmatrix} \delta_{ac}\left(\rho_c - D_{ab}\right) + D_{ac} - D^3_{abc} & \delta_{ac}\Pi_{ab} - \Pi^a_{bc} & \rho_a - D_{ab} \\ \delta_{ac}\Pi_{cb} - \Pi^c_{ab} & \delta_{ac}(\rho_b - 2D_{bc}) + \Pi^b_{ac} & -\Pi_{ab} \\ \rho_c - D_{bc} & -\Pi_{bc} & 1 - \rho_b \end{bmatrix} \succeq 0, \tag{2.207}$$

for $\forall b$, $a \neq b$ and $c \neq b$. Using its counterpart in the ${}^3\mathcal{E}$ condition, again a $\mathcal{T}_2$ condition can be derived

$$\begin{bmatrix} \delta_{ac}\rho_c + D_{ac} & \delta_{ac}\Pi_{ab} & \rho_a \\ \delta_{ac}\Pi_{bc} & \delta_{ac}(\rho_b - 2D_{bc}) - \Pi_{ac} & 0 \\ \rho_c & 0 & 1 \end{bmatrix} \succeq 0, \tag{2.208}$$

where the first row and column of (2.194) are interchanged before adding it to (2.207).

2.6 Conclusion

In this chapter, we have introduced the N-representability problem and a set of necessary but in general not sufficient conditions for it. We gave the general conditions on the 1DM, 2DM and 3DM. The conditions were also rederived in the specific case that the ensemble of wave functions consistent only of seniority-zero wave functions. This lead to a considerably reduction of the dimensions of the conditions. We further showed that symmetry can also lead help to reduce the computational complexity of the conditions.

In classical wave function based methods such as Configuration Interaction or Coupled Cluster, there is a systematic way to improve the result: by including higher orders of excitations, they will eventually reach the Full Configuration Interaction (FullCI) limit. In stark contrast, there is no such hierarchy in the necessary N-representability conditions. The three-index condition will improve the results over the two-index condition but beyond that, there are no known conditions that can be expressed as a function of the 2DM. One could use a higher reduced density matrix: the ${}^{p+1}\Gamma$ and all $p+1$ index conditions will included all positivity conditions on the ${}^{p}\Gamma$. However, this is not computationally feasible and the 2DM already contains all the information for two-particle operators. Claims have been made about a hierarchical solution to the N-representability problem [112, 113] but it remains unclear if this solutions is complete. Furthermore, the condition that could be where derived in the framework have never been put to the test. In this regard, the similarity with DFT can again be pointed out: there is also no systematic way of improving a functional.

It also been shown that the two- and three-index conditions are expressible as Grassmann integrals [114] but so far, this has not lead to a new insights.

The N-representability problem has been proven to belong to the hardest kind of problems we know and so far we are "stuck" on the two- and three-index conditions.

To summarize, the optimization problem of the reduced density matrix can now be formulated as

$$\begin{aligned} E_0 = & \min_{\Gamma} \operatorname{Tr}(K\Gamma) \\ \text{while} \quad & \operatorname{Tr}(\Gamma) = \frac{N(N-1)}{2} \\ & \bigoplus_i \mathcal{L}_i(\Gamma) \succeq 0. \end{aligned} \tag{2.209}$$

The minimization goes over all symmetry matrices, while the direct sum in the constraints goes over the enforced N-representability conditions. The $\oplus$

notation means the direct sum of block matrices. For example, for the two-index conditions, this would mean: $\mathcal{L}_i \in \{\mathcal{I}, \mathcal{Q}, \mathcal{G}\}$. The optimization problem for the 3DM is identical in form but the trace has to be adjusted. In the next chapter we will discuss how to solve this optimization problem.

Chapter 3

Semidefinite Programming

> *Science is knowledge which we understand so well that we can teach it to a computer; and if we don't fully understand something, it is an art to deal with it.*
>
> Donald E. Knuth

The world of convex optimization is a rich and interesting world. Due to the convexity, it has many nice features: the nicest one is probably the guarantee that there are no local extrema. In this chapter, we will introduce Semidefinite Programming (SDP), a subclass within convex optimization. Do not let the word programming deceive you, SDP is a convex optimization problem. Even linear programming problems can be expressed as a SDP problem. More importantly, an SDP problem can be solved efficiently, both in theory and practice. After introducing the problem and several of its properties, we discuss several methods to solve it. These methods are then adapted to maximally exploit the specific problem structure of v2DM. There are general purpose codes available to solve the standard form of an SDP problem [23, 115–119], but they are in general too slow for us. SDP problems are encountered in a wide range of fields: control theory [120], combinatorial optimization [121] and statistics [122], to name just a few.

3.1 Primal-dual formalism

Before we continue, let us first repeat the definition of convexity. A set S in a linear space is convex if and only if for every $x_1, x_2 \in S$ holds that $\alpha x_1 + \beta x_2 \in S$ with $\alpha, \beta \geq 0$ and $\alpha + \beta = 1$. This means that the line segment connecting any two points in the set must also be part of the set. A

function $f : \mathbb{R}^n \to \mathbb{R}$ is convex if the domain of f is a convex set and for any two points x and y in the domain of f must hold

$$f(\alpha x + \beta y) \leq \alpha f(x) + \beta f(y), \tag{3.1}$$

with $\alpha, \beta \geq 0$ and $\alpha + \beta = 1$. One can prove that a function is convex if on a convex set its Hessian is positive semidefinite. Furthermore, we will use S^n to denote the set of $n \times n$ symmetric matrices and S^n_+ to mark the subset of positive semidefinite matrices. The set S^n_+ has the mathematical structure of a cone: for every $A \in S^n_+$ we have that $\lambda A \in S^n_+$, when $\lambda > 0$[1].

The standard SDP problem is defined as minimizing a linear function in $x \in \mathbb{R}^n$ subjected to a matrix inequality

$$\begin{aligned} &\min c^T x \\ \text{while} \quad &F(x) \succeq 0, \end{aligned} \tag{3.2}$$

where

$$F(x) = F_0 + \sum_{i=1}^{n} x_i F_i. \tag{3.3}$$

An SDP problem is defined by a vector $c \in \mathbb{R}^n$ and $n+1$ symmetric matrices $F_0, F_i \in S^m$. Both the objective ($c^T x$) and constraint ($F(x)$) are convex

$$\alpha \geq 0, \qquad F(\alpha x + (1-\alpha)y) = \alpha F(x) + (1-\alpha)F(y) \succeq 0. \tag{3.4}$$

To demonstrate what the solution of this problem is, we can examine an example for $x \in \mathbb{R}^2$ in Figure 3.1 on the next page, the value of m is not relevant at the moment. The region where the matrix inequality is satisfied is called the feasible region. The solution of the SDP problem is found by moving as far as possible in the direction $-c$ within the feasible region. The solution or optimal point x_{opt} will always be found on the boundary of the feasible region. This means that $F(x)$ will have at least one zero eigenvalue. Due to the convexity of the feasible region, it is clearly impossible to have a local minimum: in that case it would be impossible to draw a line between the local minimum and global minimum that stays within the feasible region. Note that in the case $m = 1$ one has a linear program.

We will now introduce the dual problem. The problem (3.2) is called the primal problem. The Lagrangian of the primal problem (3.2) is

$$L(x, Z) = c^T x + \operatorname{Tr}\left(\left(F_0 + \sum_{i=1}^{n} x_i F_i\right) Z\right), \tag{3.5}$$

1. For completeness we should note that the cone of positive semidefinite matrices is self-dual [22]. This will only be used indirectly in this chapter and can be mostly ignored.

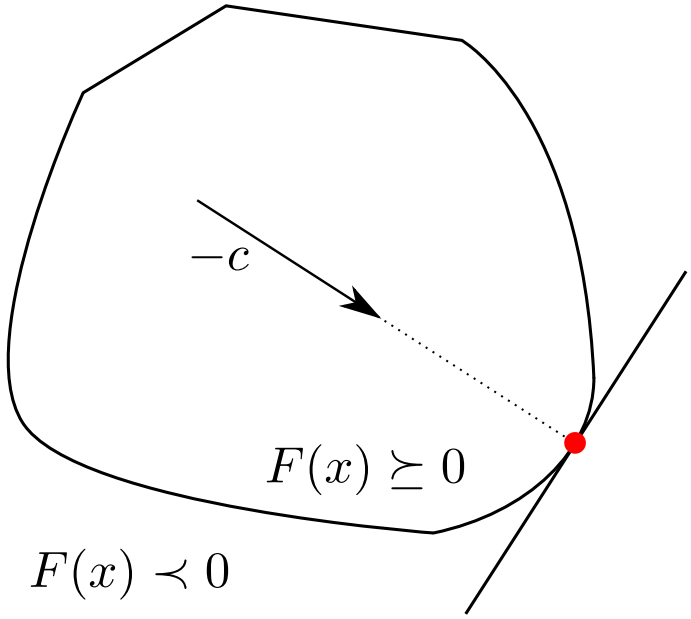

Figure 3.1: A graphical depiction of a SDP problem in two variables. The red dot marks the optimal point. It is found by following the direction $-c$ until the boundary of the feasible region is hit.

where $Z \in S^n$ is called the dual variable (or Lagrange multiplier [123, 124]). It has to be negative semidefinite $Z \preceq 0$ because it is the Lagrange multiplier of an inequality: if $F(x)$ is positive and Z negative, the second term in (3.5) will be negative and thus decrease the Lagrangian. If $F(x)$ would be negative, it would increase the Lagrangian. As we prefer to work with positive semidefinite matrices, we will replace Z by $-Z$.

$$L(x, Z) = c^T x - \operatorname{Tr}\left(\left(F_0 + \sum_{i=1}^{n} x_i F_i\right) Z\right) \tag{3.6}$$

$$= x_1 \left(c_1 - \operatorname{Tr}\left(F_1 Z\right)\right) + x_2 \left(c_2 - \operatorname{Tr}\left(F_2 Z\right)\right) + \ldots$$
$$x_n \left(c_n - \operatorname{Tr}\left(F_n Z\right)\right) - \operatorname{Tr}\left(F_0 Z\right) \tag{3.7}$$

We can now define the dual function as

$$g(Z) = \inf_x L(x, Z) = \begin{cases} -\operatorname{Tr}\left(F_0 Z\right) & c_i - \operatorname{Tr}\left(F_i Z\right) = 0, \quad i = 1 \ldots n \\ -\infty & \text{otherwise.} \end{cases} \tag{3.8}$$

We minimize over the primal variables to find a problem in the dual variables.

The associated dual problem is

$$\begin{aligned} & \max \quad -\mathrm{Tr}\left(F_0 Z\right) \\ \text{while} \quad & Z \succeq 0 \\ & \mathrm{Tr}\left(F_i Z\right) = c_i, \quad i = 1 \dots n. \end{aligned} \tag{3.9}$$

This is again an SDP problem and can be rewritten to the standard form in (3.2) [21]. Furthermore, we call Z dual feasible if $Z \succeq 0$ and $\mathrm{Tr}\left(F_i Z\right) = c_i$ ($i = 1 \dots n$), and x primal feasible if $F(x) \succeq 0$. Feasible means that the constraints of the problem are fulfilled.

Now, what is the point of all this? The dual problem is very powerful as it provides a lower bound on the primal problem and vice versa. If we assume that x is primal feasible and Z is dual feasible then

$$c^T x + \mathrm{Tr}\left(F_0 Z\right) = \sum_{i=1}^{n} \mathrm{Tr}\left(Z F_i\right) x_i + \mathrm{Tr}\left(F_0 Z\right) = \mathrm{Tr}\left(Z F(x)\right) \geq 0. \tag{3.10}$$

The last inequality follows from the positive semidefiniteness of $F(x)$ and Z (see Chapter C). We now have

$$-\mathrm{Tr}\left(F_0 Z\right) \leq c^T x, \tag{3.11}$$

for any feasible value of Z and x, including the optimal points of both. This is called weak duality [22]. The difference between both sides of eq. (3.11) is called the duality gap (or primal-dual gap)

$$\eta = c^T x + \mathrm{Tr}\left(F_0 Z\right) = \mathrm{Tr}\left(Z F(x)\right) \geq 0. \tag{3.12}$$

The duality gap is zero if we use the optimal points of both the primal and dual problem; in that case we have strong duality. For SDP problems this is the case when the Slater condition is fulfilled [21, 22]: there must be strictly feasible points for either the primal or dual problem. This means that there must be an x for which $F(x) \succ 0$ or a Z for which $Z \succ 0$ and $\mathrm{Tr}\left(F_i Z\right) = c_i$ ($i = 1 \dots n$). If the Slater condition holds, we have at the optimal points

$$c^T x = -\mathrm{Tr}\left(F_0 Z\right), \tag{3.13}$$

from which it follows that $\mathrm{Tr}\left(F(x) Z\right) = 0$ and thus

$$F(x) Z = 0, \tag{3.14}$$

as $F(x) \succeq 0$ and $Z \succeq 0$ (see Chapter C). This is called the complementary slackness condition and can be interpreted as saying that the space spanned by the columns of Z and $F(x)$ must be orthogonal. The duality gap gives

us a powerful convergence measure. If we use an iterative algorithm to solve both the primal and dual problem, we have at iteration k the current optimal value x^k and Z^k and we know that

$$c^T x^k - x_{\text{opt}} \leq \eta^k = c^T x^k + \text{Tr}\left(F_0 Z^k\right). \tag{3.15}$$

If we use, as the stopping criterion $\epsilon > 0$ on the duality gap, then

$$c^T x^k - x_{\text{opt}} \leq c^T x^k + \text{Tr}\left(F_0 Z^k\right) \leq \epsilon. \tag{3.16}$$

In other words, we know (it is guaranteed) that the current optimal value x^k is ϵ suboptimal. This is much more powerful than just converging to a certain tolerance.

3.1.1 Problem definition

The perceptive reader has probably already recognized the similarity between the dual problem (3.9) and v2DM optimization problem (2.209) from Chapter 2. For the two-index optimization, the obvious choice seems to be

$$Z = \Gamma \oplus \mathfrak{Q}(\Gamma) \oplus \mathfrak{G}(\Gamma), \tag{3.17a}$$
$$F_0 = K \oplus 0 \oplus 0, \tag{3.17b}$$
$$F_1 = \mathbb{1} \oplus 0 \oplus 0, \tag{3.17c}$$
$$c_1 = \frac{N(N-1)}{2}. \tag{3.17d}$$

However, this is not sufficient: Z contains all free variables and the $\mathfrak{Q}$ and $\mathfrak{G}$ conditions are of course not independent. We need to use the equality constraints to enforce the form of (3.17a). We will write Z as $\oplus_i \mathcal{L}_i$ to have an expression independent of the exact N-representability constraints used and we introduce $\{e_i\}$ as an orthonormal basis in the space of the Z matrix. Let us focus on constraint $\mathcal{L}$. We need to enforce that

$$\text{Tr}\left(Z^{\mathcal{L}} e_i^{\mathcal{L}}\right) = \text{Tr}\left(\mathcal{L}(\Gamma) e_i^{\mathcal{L}}\right), \tag{3.18}$$

where the superscript $\mathcal{L}$ denotes the part of Z corresponding to the constraint $\mathcal{L}$. Before we continue, we must introduce an extremely helpful tool: the Hermitian adjoint map. It is defined as

$$\text{Tr}\left(\mathcal{L}_i(\Gamma) A\right) = \text{Tr}\left(\mathcal{L}_i^\dagger(A)\Gamma\right), \tag{3.19}$$

where A is a symmetric matrix in the same space as the constraint $\mathcal{L}_i$ and the Hermitian adjoint is $\mathcal{L}_i^\dagger$. Using its definition (3.19), it is possible to derive the

adjoint map of all N-representability conditions introduced in Chapter 2. In Chapter F on page 157 we give a list of expressions for the Hermitian adjoint images used in this work. We also require that every N-representability constraint map is homogeneous[2] as this makes the mathematics involved a lot easier. Using the Hermitian adjoint, we can rewrite eq. (3.18) to

$$\mathrm{Tr}\left(Z^{\mathcal{L}} e_i^{\mathcal{L}}\right) = \mathrm{Tr}\left(\Gamma \mathcal{L}^\dagger(e_i^{\mathcal{L}})\right). \tag{3.20}$$

We can now express this as an equality constraint for the dual problem:

$$\mathrm{Tr}\left(Z F_i^{\mathcal{L}}\right) = 0, \tag{3.21}$$

where $F_i^{\mathcal{L}}$ is a block matrix with two non-zero blocks

$$\left(F_i^{\mathcal{L}}\right)_\Gamma = -\mathcal{L}^\dagger(e_i^{\mathcal{L}}), \tag{3.22a}$$

$$\left(F_i^{\mathcal{L}}\right)_{\mathcal{L}} = e_i^{\mathcal{L}}. \tag{3.22b}$$

In this way, we enforce the $\mathcal{Q}$, $\mathcal{G}$, … conditions. The number of F_i matrices will be equal to the number of independent variables in the conditions (plus the trace condition). Using this formalism, Nakata *et al.* [20] implemented the v2DM optimizing problem as an SDP problem and used the SDPA [116] program to solve it. We will use a slightly different formalism.

The core object we want to optimize is the 2DM. There are matrix inequalities and one equality constraint that need to be enforced. We can eliminate the trace condition by choosing a feasible starting point and restrict the optimizing to the space orthogonal to this condition. In this case, we should restrict the optimizing to the traceless space. Let the set $\{f^i\}$ be a complete, orthogonal basis of traceless, symmetric matrices in the two-particle space. Following properties will hold

$$\mathrm{Tr}\left(f^i\right) = 0, \tag{3.23a}$$

$$\mathrm{Tr}\left(f^i f^j\right) = \delta_{ij}, \tag{3.23b}$$

$$f^i_{\alpha\beta;\gamma\delta} = -f^i_{\beta\alpha;\gamma\delta} = -f^i_{\alpha\beta;\delta\gamma} = f^i_{\beta\alpha;\delta\gamma} = f^i_{\delta\gamma;\beta\alpha}. \tag{3.23c}$$

We can write the 2DM in this basis as

$$\Gamma = \frac{2\mathrm{Tr}\left(\Gamma\right)}{M(M-1)}\mathbb{1} + \sum_i \underbrace{\mathrm{Tr}\left(\Gamma f^i\right)}_{\gamma_i} f^i, \tag{3.24}$$

2. A function is homogeneous with degree k when it is scale invariant: $f(\alpha x) = \alpha^k f(x)$.

where M is used to denote the dimension of the single-particle space (including spin). The energy function can be rewritten as

$$E = \mathrm{Tr}\left(K\Gamma\right) = \frac{2\mathrm{Tr}\left(\Gamma\right)\mathrm{Tr}\left(K\right)}{M(M-1)} + \sum_i \gamma_i h^i, \tag{3.25}$$

where

$$\gamma_i = \mathrm{Tr}\left(\Gamma f^i\right), \tag{3.26a}$$
$$h^i = \mathrm{Tr}\left(K f^i\right), \tag{3.26b}$$

are the expansion coefficients of the 2DM and reduced Hamiltonian in the traceless basis. We can now restrict the optimization to the set $\{\gamma_i\}$ without having to worry about the trace condition. Using this, our objective function is now

$$\min_{\gamma} \sum_i h^i \gamma_i. \tag{3.27}$$

The matrix constraints can be written as

$$\mathcal{L}(\Gamma) = \frac{2\mathrm{Tr}\left(\Gamma\right)}{M(M-1)}\mathcal{L}(\mathbb{1}) + \sum_i \gamma_i \mathcal{L}(f^i), \tag{3.28}$$

which can be simplified by defining

$$u^0 = \frac{N(N-1)}{M(M-1)} \bigoplus_j \mathcal{L}_j(\mathbb{1}), \tag{3.29}$$
$$u^i = \bigoplus_j \mathcal{L}_j(f^i), \tag{3.30}$$

to

$$\mathcal{L}(\Gamma) = u^0 + \sum_i \gamma_i u^i \succeq 0. \tag{3.31}$$

This clearly has the form of the primal problem (3.2). From now on, we will use $X(\Gamma) = \mathcal{L}(\Gamma)$ to specify the constraint matrix in the primal problem. Our optimization is now

$$\begin{aligned} &\min_{\gamma} h^T \gamma \\ \text{while} \quad &X(\gamma) = u^0 + \sum_i \gamma_i u^i \succeq 0. \end{aligned} \tag{3.32}$$

This is a much more compact and elegant expression than the previously derived dual variant of the problem. The dual problem of (3.32) is given by

$$\begin{aligned} &\max \quad -\mathrm{Tr}\left(Z u_0\right) \\ \text{while} \quad &Z \succeq 0 \\ &\mathrm{Tr}\left(Z u_i\right) = h^i, \forall i \end{aligned} \tag{3.33}$$

Now the optimization problem is clearly defined, we will continue with techniques to solve it[3].

3.2 Potential Reduction method

The so-called interior point methods [125] are the standard workhorse of Semidefinite Programming. They try to remain in the feasible region as they approach the optimal point. The convergence properties of these methods have been thoroughly examined and they tend to be very stable. To remain within the feasible region, a barrier function is used

$$\phi(\gamma) = \begin{cases} -\ln\det X(\gamma) & X(\gamma) \succ 0 \\ +\infty & \text{otherwise} \end{cases} \tag{3.34}$$

This barrier function is analytic, strictly convex and self-concordant[4] [126]. It is $+\infty$ when there is a zero eigenvalue in $X(\gamma)$ and thus forces us to remain inside the feasible region. The point that minimizes the barrier function $\phi(\gamma)$ is called the analytic center of the constraint $X(\gamma) \succ 0$. Using this we can define the central path: the central path is formed by the solution of the following optimization problem

$$\begin{aligned} & \min_{\gamma} \phi(\gamma) \\ \text{while} \quad & h^T\gamma = e \\ & X(\gamma) \succ 0, \end{aligned} \tag{3.35}$$

where $E_{\text{min}} \leq e \leq E_{\text{max}}$. If we solve this problem for all allowed values of e we find the central path. A solution of (3.35) is called the analytic center of the primal feasible set. It is clear that all those analytic centers lie on the central path, including the optimal point of our original SDP problem. An interior point method will try to follow the central path to find the solution. By doing this, it avoids the edge of the feasible region as long as possible, as the problem becomes singular near it. In Figure 3.2 on the next page we show the central path of the previous graphical example of an SDP problem. Furthermore, there is a connection between the points on the central path of the primal and dual problem. If we write down the Lagrangian of the problem (3.35), we find

$$L = -\ln\det X(\gamma) + \lambda(h^T\gamma - e). \tag{3.36}$$

3. We should note that compared to reference 90, we have switched the primal and dual problem. Everything is equivalent, but the notation is different.
4. This is a property that is key in proving the convergence of these methods but unimportant for what we do. A function $f(x)$ is self-concordant when $|f'''(x)| \leq 2f''(x)^{\frac{3}{2}}$.

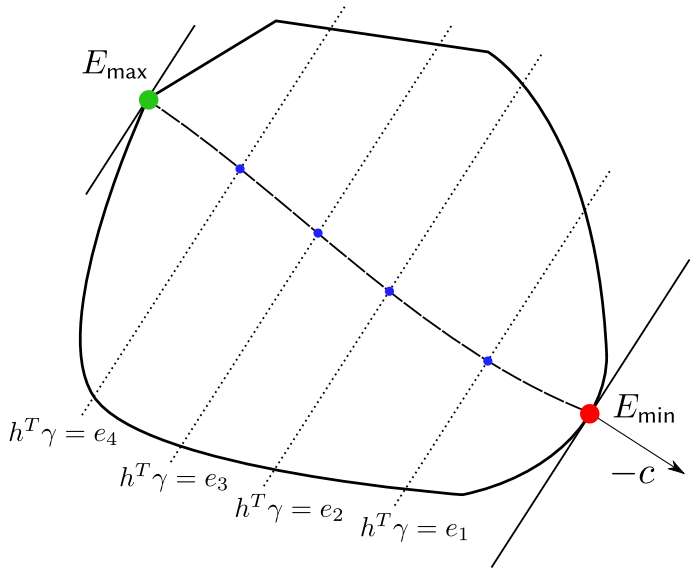

Figure 3.2: Illustration of the central path. Both the minimal value and the maximal value lie on the central path. It is formed by all analytic centers (marked with blue dots).

The optimality condition for this Lagrangian is

$$\operatorname{Tr}\left(X(\gamma)^{-1}u^i\right) = \lambda h^i, \quad i = 1, \ldots, n. \tag{3.37}$$

The derivative of the barrier function can found in Chapter C. It is interesting to see that the matrix $X(\gamma)^{-1}/\lambda$ is dual feasible when $\lambda > 0$. The associated duality gap is

$$\eta = \operatorname{Tr}\left(X(\gamma)Z\right) = \operatorname{Tr}\left(X(\gamma)\frac{X(\gamma)^{-1}}{\lambda}\right) = \frac{m}{\lambda}, \tag{3.38}$$

where m is the dimension of the $X(\gamma)$ matrix. We see that the Lagrange multiplier is directly related to the duality gap. It can even be shown that $X(\gamma)^{-1}/\lambda$ is an analytic center of the dual problem [21]. In other words, if we have a point on the central path of the primal problem, we can derive its partner point on the central path of the dual problem. It is even so that the optimal points $X(\gamma)$ and Z will be each other's inverse, up to a factor.

We will now focus on potential reduction techniques to solve the primal problem. The idea is simple: we add the barrier function (3.34) to the objective function, but scaled with a parameter t. During the calculation, we will iteratively solve the unconstrained problem. After every iteration we will decrease the barrier, until at convergence the barrier is non-existing and we find the

optimal point on the boundary of the feasible region. Our unconstrained objective function is

$$\phi(\gamma) = h^T\gamma - t\ln\det X(\gamma). \tag{3.39}$$

By optimizing the γ_i coefficients, we automatically enforce the trace condition and the barrier function will make sure that the N-representability conditions are positive semidefinite. As a function of t, eq. (3.39) lies on the central path. For $t \to \infty$, we should find the analytic center of $X(\gamma) \succ 0$ and for $t \to 0$ we should find the optimal point of the SDP problem. We now look for the minimum of $\phi(\gamma)$ for a fixed value of t. The standard way to minimize an unconstrained objective function is to use the Newton-Raphson method [127]. Under the right conditions (good starting point, well behaving derivatives), it has quadratic convergence. First, we need a second-order Taylor expansion of eq. (3.39)

$$\phi(\gamma_0 + \Delta\gamma) \approx \phi(\gamma_0) + \sum_i \Delta\gamma_i \frac{\partial\phi(\gamma)}{\partial\gamma_i} + \sum_{ij} \frac{1}{2}\Delta\gamma_i \frac{\partial^2\phi(\gamma)}{\partial\gamma_i\gamma_j}\Delta\gamma_j. \tag{3.40}$$

We search for a step $\Delta\gamma$ that minimize eq. (3.40). By taking the derivative we find

$$\sum_j \frac{\partial^2\phi(\gamma)}{\partial\gamma_i\gamma_j}\Delta\gamma_j = -\frac{\partial\phi(\gamma)}{\partial\gamma_i}, \tag{3.41a}$$

$$\sum_j \mathcal{H}^{ij}\Delta\gamma_j = -\nabla\phi^i, \tag{3.41b}$$

where the second equation introduces the symbols for the gradient and Hessian of eq. (3.40). If we solve this linear system of equations, we know the optimal update step $\Delta\gamma$. All that is left is finding an expression for the gradient and the Hessian.

The gradient of eq. (3.40) is

$$\nabla\phi^i = \frac{\partial\phi(\gamma)}{\partial\gamma_i} = h^i - t\,\mathrm{Tr}\left(X(\gamma)^{-1}u^i\right). \tag{3.42}$$

By using the adjoint images (see Chapter F) and the structure of $X(\gamma)$ we can simplify this to

$$\nabla\phi^i = h^i - t\sum_j \mathrm{Tr}\left(\mathcal{L}_j(\Gamma)^{-1}\mathcal{L}_j(f^i)\right) \tag{3.43}$$

$$= \mathrm{Tr}\left(\left[K - t\sum_j \mathcal{L}_j^\dagger(\mathcal{L}_j(\Gamma)^{-1})\right] f^i\right), \tag{3.44}$$

where we used the definition of the traceless basis (eq. (3.26)). We used $\mathcal{L}_j(\Gamma)$ where we actually should use $\mathcal{L}_j(\gamma)$, but the former simplifies the notation. The gradient can be written as the projection of a matrix on the traceless two-particle space

$$\nabla\phi = \hat{P}_{\text{Tr}}\left(K - t\sum_j \mathcal{L}_j^\dagger(\mathcal{L}_j(\Gamma)^{-1})\right), \tag{3.45}$$

with the traceless projection operator

$$\hat{P}_{\text{Tr}}(A) = A - \frac{\text{Tr}\,(A)}{\dim A}\mathbb{1}. \tag{3.46}$$

The nice thing about this approach is that we never need the traceless basis explicitly! We can simply construct the matrix in eq. (3.45) and do the projection.

The Hessian is a bit more complicated. By taking the derivative of eq. (3.42) we find

$$\mathcal{H}^{ij} = \frac{\partial^2\phi(\gamma)}{\partial\gamma_i\gamma_j} = t\,\text{Tr}\left(X(\gamma)^{-1}u^iX(\gamma)^{-1}u^j\right) \tag{3.47}$$

$$= t\sum_k \text{Tr}\left(\mathcal{L}_k(\Gamma)^{-1}\mathcal{L}_k(f^i)\mathcal{L}_k(\Gamma)^{-1}\mathcal{L}_k(f^j)\right). \tag{3.48}$$

We decompose our update step $\Delta\gamma$ in the traceless basis

$$\Delta\gamma = \sum_i \delta\gamma_i f^i, \tag{3.49}$$

and examine the action of the Hessian on this

$$\sum_j \mathcal{H}^{ij}\delta\gamma_j = t\sum_k \text{Tr}\left(\mathcal{L}_k(\Gamma)^{-1}\left[\sum_j \mathcal{L}_k(f^j)\delta\gamma_j\right]\mathcal{L}_k(\Gamma)^{-1}\mathcal{L}_k(f^i)\right)$$

$$= t\sum_k \text{Tr}\left(\mathcal{L}_k^\dagger\left(\mathcal{L}_k(\Gamma)^{-1}\mathcal{L}_k(\Delta\gamma)\mathcal{L}_k(\Gamma)^{-1}\right)f^i\right). \tag{3.50}$$

We see that the action of the Hessian on a traceless matrix can be expressed as

$$\mathcal{H}\Delta\gamma = t\,\hat{P}_{\text{Tr}}\left(\sum_k \mathcal{L}_k^\dagger\left(\mathcal{L}_k(\Gamma)^{-1}\mathcal{L}_k(\Delta\gamma)\mathcal{L}_k(\Gamma)^{-1}\right)\right). \tag{3.51}$$

Again, no explicit reference to the traceless basis is used. Notice that eq. (3.51) actually gives us an efficient matrix-vector product to solve eq. (3.41b). The

dimension of the 2DM scales as M^2 (with M the size of the single-particle basis) and the dimension of the traceless basis $\{\gamma_i\}$ scales as M^4, leading to an M^8 scaling for the matrix-vector product of the Hessian. However, eq. (3.51) only scales as M^6: we work directly without the matrix in the two-particle space with using the traceless basis explicitly. Now that we have an efficient matrix-vector product, we can use a Krylov subspace method to solve the linear system in eq. (3.41b). The idea is that the inverse of a matrix can be expressed as a linear combination of powers of the matrix[5]. The Hessian is positive semidefinite, which leads us to the Conjugate gradient method [127, 128]: this is an iterative method to solve a linear system using only matrix-vector operations. This means that we never have to explicitly construct the Hessian, we only use its action on a vector.

Although the problem is now solved and we can calculate the update step $\Delta\gamma$ for eq. (3.40), we can speed up the convergence process by optimizing the step size. This means calculating α such that $\tilde{\phi}(\alpha) = \phi(\gamma_0 + \alpha\Delta\gamma)$ is minimal. The optimality condition is

$$\frac{\mathrm{d}\tilde{\phi}(\alpha)}{\mathrm{d}\alpha} = \frac{\partial\phi(\gamma_0 + \alpha\Delta\gamma)}{\partial\alpha} = 0. \tag{3.52}$$

If we use eq. (3.39), we find

$$\frac{\mathrm{d}\tilde{\phi}(\alpha)}{\mathrm{d}\alpha} = \mathrm{Tr}\,(K) - t\,\sum_j \mathrm{Tr}\left(\mathcal{L}_j(\gamma_0 + \alpha\Delta\gamma)^{-1}\mathcal{L}_j(\Delta\gamma)\right). \tag{3.53}$$

Every evaluation of this would require calculating the inverse of a matrix. Luckily, this can be avoided. First, we must calculate the eigenvalues of following generalized eigenvalue problem

$$\mathcal{L}(\Delta\gamma)w = \lambda^{\mathcal{L}}\mathcal{L}(\Gamma)w, \tag{3.54}$$

which can be transformed to an ordinary symmetric eigenvalue problem as

$$\left(\mathcal{L}(\Gamma)^{-\frac{1}{2}}\mathcal{L}(\Delta\gamma)\mathcal{L}(\Gamma)^{-\frac{1}{2}}\right)v = \lambda^{\mathcal{L}}v, \qquad v = \mathcal{L}^{\frac{1}{2}}w. \tag{3.55}$$

It can be shown that eq. (3.53) can be expressed as [90]

$$\frac{\mathrm{d}\tilde{\phi}(\alpha)}{\mathrm{d}\alpha} = \mathrm{Tr}\,(K) - t\,\sum_j\left(\sum_i \frac{\lambda_i^{\mathcal{L}_j}}{1 + \alpha\lambda_i^{\mathcal{L}_j}}\right). \tag{3.56}$$

The summation over i runs over all eigenvalues of eq. (3.54), while j runs over all enforced matrix constraints. This way is much cheaper to calculate

5. This is a direct consequence of the Cayley–Hamilton theorem.

the optimal value of α as the eigenvalues only have to be calculated once and then a simple bisection method [127] can be used to find the roots of eq. (3.56).

To estimate the duality gap, we need an (approximate) solution to the dual problem. If we have found the solution to eq. (3.40), the gradient will be zero

$$0 = h^i - t \operatorname{Tr}\left(X(\gamma)^{-1} u^i\right). \tag{3.57}$$

We see that $Z = tX(\gamma)^{-1}$ is dual feasible and using eqs. (3.37) and (3.38) we can estimate the duality gap to be

$$\eta = \operatorname{Tr}\left(X(\gamma)Z\right) = mt, \tag{3.58}$$

with m the dimension of $X(\gamma)$ or Z. We use this as our convergence criterion. To conclude the expose about the potential reduction method, we give an

Algorithm 1 The potential reduction algorithm to solve the primal problem tailored for v2DM.

```
Set ε > 0, ε_NR > 0 and β ∈ [0, 1]
Γ = N(N−1)/M(M−1) 𝟙; t = 1
while nt > ε do                                  ▷ The barrier reduction loop
    while δ > ε_NR do                            ▷ The Newton-Raphson loop
        ∇φ = P̂_Tr ( K − t Σ_j L_j^†(L_j(Γ)^{-1}) )
        Solve HΔγ = −∇φ                          ▷ Solved with Conjugate Gradient
        Solve dφ̃(α)/dα = 0
        Γ ← Γ + αΔγ
        δ ← α ‖Δγ‖
    end while
    t ← βt
end while
```

overview of the algorithm in pseudocode in Algorithm 1.

3.3 Boundary Point method

One of the problems with the barrier function method is that the problem gets harder to solve as the barrier is reduced. When we approach the boundary of the feasible region, the condition number of the Hessian will become worse. As we use an iterative technique to solve the linear system of equations, the number of iterations will sharply increase towards the boundary. For this reason it is not even interesting to start from a better guess: a good

guess will be close to the boundary and we want to avoid that as long as possible by walking on the central path. One possible solution to this is to use an Augmented Lagrangian method [123], which adds an additional term to the unconstrained optimization that should help to improve the convergence. This led to the so-called Boundary Point method [129–131] in which the complementary slackness condition (3.14) is always fulfilled. This method jumps between the cone of positive semidefinite matrices and the space of the other constraints until convergence: at this point the solution is primal and dual feasible. It was first used by Mazziotti [51] in the context of v2DM.

The augmented Lagrangian for the primal SDP problem (3.32) is

$$L = h^T\gamma + \mathrm{Tr}\left(Z\left(X - u^0 - \sum_i \gamma_i u^i\right)\right) + \frac{\sigma}{2}\left\|X - u^0 - \sum_i \gamma_i u^i\right\|^2. \tag{3.59}$$

This has a slightly different form than eq. (3.5) as we include the primal matrix X explicitly, not as a function of γ. Remember that the Lagrangian multiplier Z is the primary variable of the dual problem. Compared to the regular Lagrangian, we added an additional term that adds a quadratic penalty for infeasibility, where $\sigma > 0$ determines the strength of the penalty. In contrast with penalty or barrier functions, σ should not go to ∞ (or 0) to reach the optimal point. Before we continue, let us review the optimality conditions for the primal and dual problem. A solution γ, X and Z is optimal (assuming the Slater condition holds) when

$$X \succeq 0, \tag{3.60a}$$
$$X = u^0 + \sum_i \gamma_i u^i, \tag{3.60b}$$
$$Z \succeq 0, \tag{3.60c}$$
$$\mathrm{Tr}\,(Zu_i) = h^i, \tag{3.60d}$$
$$XZ = 0. \tag{3.60e}$$

The first four conditions demand the feasibility of the solution and the last condition ensures that the duality gap is zero.

By introducing a new matrix

$$W(\gamma) = u^0 + \sum_i \gamma_i u^i - \frac{1}{\sigma}Z, \tag{3.61}$$

we can rewrite the eq. (3.59) to

$$L = h^T\gamma + \frac{1}{2\sigma}\|Z\|^2 + \frac{\sigma}{2}\|X - W(\gamma)\|^2. \tag{3.62}$$

We now define

$$f(\gamma, X) = h^T\gamma + \frac{\sigma}{2}\left\|X - W(\gamma)\right\|^2. \tag{3.63}$$

The method then consists of first minimizing $f(\gamma, X)$ under the constraint $X \succeq 0$, while keeping Z constant. After this, we use the solutions γ and X obtained in the previous step to update Z as

$$Z = \sigma(X - u^0 - \sum_i \gamma_i u^i). \tag{3.64}$$

We first focus on the so-called inner problem

$$\begin{aligned} &\min_{\gamma, X} \; h^T\gamma + \frac{\sigma}{2}\left\|X - W(\gamma)\right\|^2 \\ &\text{while} \quad X \succeq 0. \end{aligned} \tag{3.65}$$

This is a quadratic SDP problem. Its Lagrangian is

$$L = h^T\gamma + \frac{\sigma}{2}\left\|X - W(\gamma)\right\|^2 - \mathrm{Tr}\left(VX\right), \tag{3.66}$$

where $V \succ 0$ is the Lagrangian multiplier for the constraint $X \succeq 0$. The necessary set of conditions for optimality, the so-called Karush–Kuhn–Tucker (KKT) conditions [22, 132, 133] for (3.65) are

$$\frac{\partial L}{\partial \gamma_i} = h_i - \sigma \mathrm{Tr}\left(\left(X - W(\gamma)\right)u^i\right) = 0, \tag{3.67a}$$

$$\frac{\partial L}{\partial X} = \sigma\left(X - W(\gamma)\right) - V = 0, \tag{3.67b}$$

$$V \succ 0, \tag{3.67c}$$

$$X \succeq 0, \tag{3.67d}$$

$$VX = 0. \tag{3.67e}$$

Due to the Slater condition, this set of conditions is also sufficient [22]. We will now try to solve these directly. The gradient conditions eqs. (3.67a) and (3.67b) can be rewritten to

$$\sum_j \gamma_j \mathrm{Tr}\left(u^i u^j\right) = \mathrm{Tr}\left(\left(X - u^0 + \frac{1}{\sigma}Z\right)u^i\right) - \frac{h^i}{\sigma}, \tag{3.68}$$

$$V = \sigma\left(X - W(\gamma)\right). \tag{3.69}$$

Now, if we keep γ fixed, the optimization problem (3.65) is reduced to the projection of the matrix X on the cone of positive semidefinite matrices

$$\min_{X \succeq 0} \left\|X - W(\gamma)\right\|. \tag{3.70}$$

The solution is straightforward: we have to split up $W(\gamma)$ into a positive and negative part. This can be done through a spectral decomposition

$$\begin{aligned} W(\gamma) &= \sum_i \lambda_i U_i U_i^T \\ &= \sum_i \lambda_i^+ U_i U_i^T + \sum_i \lambda_i^- U_i U_i^T \\ &= W^+(\gamma) + W^-(\gamma), \end{aligned} \tag{3.71}$$

where λ_i^+ and λ_i^- denote the positive and negative eigenvalues respectively and U is the associated eigenvector. For a fixed value of γ, the optimal value of $X = W^+(\gamma)$. The optimal value of V follows from eq. (3.69)

$$V = -\sigma W^-(\gamma) \succeq 0. \tag{3.72}$$

The complimentary slackness condition $VX = 0$ is fulfilled as the eigenspaces are orthogonal. For a fixed value of X (and V), the optimal γ can be found by solving the linear system in eq. (3.68). This can be done very efficiently by using the overlap formalism from Verstichel [90]. The set $u^\alpha = \{u^0, u^i\}$ is non-orthogonal and has an overlap S

$$S_{\alpha\beta} = \mathrm{Tr}\left(u^\alpha u^\beta\right) = \sum_k \mathrm{Tr}\left(\mathcal{L}_k\left(f^\alpha\right)\mathcal{L}_k\left(f^\beta\right)\right). \tag{3.73}$$

Using the Hermitian adjoint images, this can be expressed as

$$S_{\alpha\beta} = \sum_k \mathrm{Tr}\left(\mathcal{L}_k^\dagger\left(\mathcal{L}_k\left(f^\alpha\right)\right) f^\beta\right). \tag{3.74}$$

In other words, the overlap can be considered as a linear map from two-particle to two-particle space,

$$S(\Gamma) = \sum_k \mathcal{L}_k^\dagger\left(\mathcal{L}_k\left(\Gamma\right)\right). \tag{3.75}$$

It can be shown that the overlap map can be expressed as a generalized $\mathfrak{Q}$ map for all two- and three-index N-representability conditions [90][6]. In the DOCI case, this does not hold. The inverse of the map (3.75) can again be expressed as a generalized $\mathfrak{Q}$ matrix. Compared to the time spent calculating the eigenvalues and eigenvectors of $W(\gamma)$, solving the linear system in eq. (3.68) is negligible.

We see that the inner problem (3.65) can be solved by alternating between solving for X (with γ constant) through eq. (3.70) and solving for γ (with X

6. The complete expressions for the overlap can be found in reference 90

constant) through eq. (3.68). When the linear system in eq. (3.68) is satisfied after projection on the cone of positive semidefinite matrices, we have reached convergence for the inner problem. The convergence criteria can be rewritten as

$$h_i - \sigma \mathrm{Tr}\left(\left(X - W(\gamma)\right) u^i\right) = h_i - \mathrm{Tr}\left(V u^i\right) \leq \varepsilon_{\text{inner}}. \tag{3.76}$$

If we compare this to eq. (3.60d), we see that V is dual feasible. By setting $Z = V$, all conditions in eq. (3.60) are fulfilled. In other words, we can consider the inner loop to be a projection on the dual feasibility. The outer loop in which we update Z, can be interpreted as projecting on the primal feasibility. As convergence criteria, we use the primal infeasibility,

$$\left\| X - u^0 - \sum_i \gamma_i u^i \right\| \leq \varepsilon_{\text{outer}}. \tag{3.77}$$

During the whole optimization we have $XZ = 0$ meaning that the duality gap is always zero. This interpretation also explains the name "Boundary Point method": during the entire optimization, we keep the duality gap zero and alternately project on the primal and dual feasibility conditions until at convergence both primal and dual feasible are fulfilled. In Algorithm 2 we

Algorithm 2 The boundary point algorithm to solve the primal and dual problem tailored for v2DM.

Set $\varepsilon_{\text{inner}} > 0,\ \varepsilon_{\text{outer}} > 0$ and $\sigma > 0$
$X = 0,\ Z = 0,\ k = 0$
while $\delta_{\text{outer}} > \varepsilon_{\text{outer}}$ **do** ▷ The outer loop
  while $\delta_{\text{inner}} > \varepsilon_{\text{inner}}$ **do** ▷ The inner loop
    Solve for γ^k: $\sum_j \gamma_j^k \mathrm{Tr}\left(u^i u^j\right) = \mathrm{Tr}\left(\left(X^k - u^0 + \frac{1}{\sigma} Z^k\right) u^i\right) - \frac{h^i}{\sigma}$
    $W(\gamma) = u^0 + \sum_i \gamma_i u^i - \frac{1}{\sigma} Z^k$
    $X^k = W^+,\ \ V^k = -\sigma W^-$
    $\delta_{\text{inner}} = \sum_i \left| h_i - \mathrm{Tr}\left(V^k u^i\right)\right|$ ▷ Dual infeasibility
  end while
  $Z^{k+1} \leftarrow V^k$
  $k \leftarrow k + 1$
  $\delta_{\text{outer}} = \left\| X^k - u^0 - \sum_i \gamma_i u^i \right\|$ ▷ Primal infeasibility
end while

show the boundary point algorithm that we have implemented. The bottleneck in the algorithm is the computation of the eigenvalues and eigenvectors of $W(\gamma)$. This scales as the third power of the matrix dimension, giving us an algorithm that scales as M^6, with M the dimension of the single-particle

space. The linear system can be solved very efficiently for the classic two-index and three-index conditions. In the DOCI case, we do not have a closed form for the inverse but a Conjugate gradient algorithm can be used. The number of iterations required to solve the linear system is small and the bottleneck remains the computation of W^+ and W^-.

Compared to other methods to solve SDP problems, the boundary point method is faster but less stable. While the potential reduction method can almost be used as a black box, this is certainly not the case for the boundary point method. By tweaking the parameters, a speedup factor of $5-10\times$ can be achieved compared to classic primal-dual methods. In our experience, the following practical considerations have to be taken in account when using the algorithm. It turns out that it is best to limit the number of iterations of the inner loop. We limit it to 1-5 iterations. The penalty parameter σ in the augmented Lagrangian has to be chosen carefully. The algorithm works best when the primal and dual infeasibility are comparable. If the primal infeasibility is greater than the dual feasibility, then we multiply σ with a factor $\tau > 1$. If the primal infeasibility is smaller than the dual feasibility, we divide σ by τ. When starting the algorithm, there is a great variation in σ until the primal and dual problem are in equilibrium and then we have a monotonic convergence rate to primal and dual feasibility. In reference 51, an additional parameter is introduced in the calculation of $W(\gamma)$

$$W(\gamma) = u^0 + \sum_i \gamma_i u^i - \frac{\tau_{\mathrm{m}}}{\sigma} Z. \tag{3.78}$$

We have named this factor τ_{m} the Mazziotti factor. Setting it to a value in the range $[1, 1.6]$ can speedup the algorithm but also influenes the stability of the algorithm. It alters the sensitivity of the $\{\gamma_i\}$ on the dual infeasibility of Z.

3.4 Conclusion

In this chapter, we have introduced a class of convex optimization problems called Semidefinite Programming. The primal and dual formalism of these problems was explored. Our v2DM problem was translated to a primal and dual SDP. We investigate an interior-point method to solve the problem by adding a barrier function to the objective function. This led to the potential reduction algorithm tailored to v2DM. This algorithm is robust, stable and has a scaling of M^6 for the two-index conditions and M^9 for the three-index conditions. Unfortunately, this method becomes slower and slower as we approach the solution. At every iteration, a linear system of the Hessian has to

be solved. We have implemented this efficiently using a Conjugate gradient algorithm which avoids building the Hessian: we only need a matrix-vector product. Near the boundary of the feasible set, the condition number of the Hessian gets worse and the number of iterations needed to solve the linear system increases sharply. In practice we see that the first steps are very quick and most of the calculating time is spent near the boundary. This algorithm can be used as a black box and it has only one parameter that might need tweaking: the factor by which the barrier is decreased after every iteration.

An alternative to avoid the downsides of the potential reduction algorithm is the augmented Lagrangian approach. In this method, an additional term is added to the Lagrangian to stabilize the convergence. It leads to the boundary point method which has the same theoretical scaling of M^6 (two-index) or M^9 (three-index) as the potential reduction method, but is nonetheless much faster in reality. This speedup comes at a cost: the boundary point method is much less stable. The parameters of the algorithm need careful tweaking to ensure convergence. The boundary point method was specifically designed for systems with a large number of variables and is at its best in these systems.

As it is the fastest method we have, it will be our preferred method for the rest of this work.

Chapter 4

Results

In the previous chapters, we have introduced the concept of the Variational Optimization of the second-order reduced Density Matrix. In Chapter 2, a necessary set of N-representability conditions were derived and in Chapter 3 we have shown the computational methods that can be used to do the actual optimization. It is time to use this knowledge. First we look into DOCI and explain the motivation for the DOCI N-representability conditions derived in Section 2.5. Next, we explore orbital optimization with the goal to combine it with v2DM restricted to DOCI. We then try our method on several benchmark systems to assess its merits.

4.1 Introduction

Before we begin the story of the marriage between DOCI and v2DM, let us take a step back and consider the origins of DOCI. First we will introduce some classic concepts of wavefunction-based methods [2].

In Configuration Interaction (CI) methods, the wave function is expanded in a (complete) basis of Slater determinants. The classical approach is to pick a reference Slater determinant and add excitations on top. This reference is usually obtained by a Hartree-Fock (HF) calculation. This works well when one Slater determinant is dominant in the expansion of all possible Slater determinants (FullCI), and we speak of a single-reference method. However, this is far from always the case: in a bond-breaking process, multiple Slater determinants become equally important. These are called multi-reference effects and to correctly describe this situation, one can use a method like Multi-Configurational Self-Consistent Field (MCSCF). In this method, both

the orbitals in the Slater determinants and the coefficients of the Slater determinants are optimized.

Another important distinction to introduce is static and dynamic correlation. The static correlation is the contribution due to the different dominant Slater determinants and you need a method such as MCSCF to correctly describe it. Dynamic correlation on the other hand is well described by a single reference Slater determinant and the excitations of this reference. A method like Configuration Interaction with Single and Double excitations (CISD) is very well suited to capture this part of the energy. The difference between these two is not always well defined and both concepts are often used rather loosely in the literature.

After this short introduction, we can introduce a new partitioning of the Slater determinants based on the seniority number. As introduced in Section 2.5, the seniority number is the number of unpaired electrons in a Slater determinant. Notice that it is not a proper quantum number: the seniority operator does not commute with the electronic structure Hamiltonian [111]. It finds its origin in nuclear and condensed matter physics where it is a good quantum number for the pairing Hamiltonian [134]. The seniority operator is defined as

$$\hat{\Omega} = \sum_{a\sigma} \hat{a}^\dagger_{a\sigma}\hat{a}_{a\sigma} - 2\sum_{a} \hat{a}^\dagger_{a\uparrow}\hat{a}^\dagger_{a\downarrow}\hat{a}_{a\downarrow}\hat{a}_{a\uparrow}, \tag{4.1}$$

which can be calculated with the 2DM as

$$\begin{aligned}\langle\hat{\Omega}\rangle &= \langle\psi|\hat{\Omega}|\psi\rangle \\ &= \sum_{a\sigma}\rho_{a\sigma;a\sigma} - 2\sum_{a}\Gamma_{a\uparrow a\downarrow;a\uparrow a\downarrow} \\ &= N - 2\sum_{a}\Gamma_{a\uparrow a\downarrow;a\uparrow a\downarrow}.\end{aligned} \tag{4.2}$$

We are interested in Doubly Occupied Configuration Interaction (DOCI) wave functions or, equivalently, seniority-zero wave functions. The building blocks of DOCI are electron pair states or geminals. The idea of working with electron pairs is very old. It predates the concept of orbitals [135] and is somewhat deviating from the orbital picture [136, 137]. It has links to the concept of a Lewis structure [135], which is still being taught in most high-school chemistry classes. One can build a class of wave functions based on this: the so-called Antisymmetric Product of Geminals (APG) [138, 139]

$$|\psi_{\text{APG}}\rangle = \prod_{p=1}^{P}\left(\sum_{k=1}^{L} c_{p;k}\hat{a}^\dagger_{p;k}\hat{a}^\dagger_{p;\bar{k}}\right)|\rangle\,, \tag{4.3}$$

where $P = {}^{N}/_{2}$ is the number of pairs. The geminals are not necessarily orthogonal to each other. In this concept the pairs of electrons can be regarded as weakly correlated to each other, since the wave function has a mean-field product structure in the geminals. Notice that the pairing scheme is not fixed with APG: each geminal has its own pairing scheme. However, the APG wave function is computationally intractable [138, 140]. An often used approach to circumvent this problem is to enforce an orthogonality restriction to the geminals (separated pair restriction). The pairing scheme is usually also enforced to be the same for all geminals. Although in principle any pairing scheme can be exploited, the obvious choice is the most used one: we pair electrons of different spin together in the same spatial orbital. For the rest of this work, we use this pairing scheme. As shown in Section 2.5, this leads to a serious simplification in the structure of the 2DM. For a random pairing scheme, this is not the case. Within the spin-pairing scheme DOCI is the most general type of wave function, built from Slater determinants in which every orbital is either unoccupied or doubly occupied. It was first mentioned in Weinhold and Wilson [141]. The wave function has the form

$$|\psi_{\text{DOCI}}\rangle = \sum_{\substack{m_i=\{0,1\} \\ \sum m_i = P}} c_{m_1 m_2 \ldots m_L} \left(\hat{a}_1^\dagger \hat{a}_{\bar{1}}^\dagger\right)^{m_1} \left(\hat{a}_2^\dagger \hat{a}_{\bar{2}}^\dagger\right)^{m_2} \ldots \left(\hat{a}_L^\dagger \hat{a}_{\bar{L}}^\dagger\right)^{m_L} |\rangle \quad (4.4)$$

DOCI is FullCI-like but uses only the doubly occupied Slater determinants. It is computationally cheaper than FullCI but still has a factorial scaling: $\binom{L}{N/2}$ vs $\binom{L}{N/2}^2$ for FullCI with $S_z = 0$. This makes it computationally unfeasible for all but the smallest systems. The geminal idea can also be linked to Valence Bond (VB) theory [142, 143]: in VB, one has to pair orbitals together manually in so-called VB structures, which are similar to Lewis structures. The theory had/has a large traction in the chemical community due to its more intuitive character. Unlike Molecular Orbital theory (MO), the orbitals are localized, making it easier to use chemical intuition in building the wave function. It was very popular in the early days of quantum mechanics but eventually MO became dominant. Due to the use of non-orthogonal orbitals, the computational cost was unfavorable compared to MO. Furthermore, it is much easier to use MO as a black box: a HF calculation is used as starting point and excitations are added on top of this, to improve the result. It turns out that General Valence Bond (GVB) with Perfect Pairing (PP) [144] is a special case of DOCI [145]. In this theory, the valence bond orbitals are expanded in the atomic orbital basis set and they are optimized in a self-consistent way. The perfect pairing refers to the coupling of the two electrons in the pair to a singlet state: only the VB structure with the largest coefficient is used.

DOCI is the most general closed-shell wave function available. Although it received quite some attention in the early days of quantum chemistry, it remained dormant for a very long time due to its scaling. In 2011, Bytautas *et al.* [146] re-examined DOCI as part of a seniority hierarchy-based approximation to the wave function. They found that DOCI or the seniority-zero sector is capable of capturing the lion's share of the static correlation. When adding higher seniority sectors, the result quickly convergences to the FullCI result. It was realized that DOCI is the lowest rung on a ladder of the seniority hierarchy which eventually leads to FullCI: by adding Slater determinants with two, four, ... unpaired electrons, we will eventually use all Slater determinants in the Hilbert space. Given the large number of Slater determinants in the DOCI wave function, it cannot really come as a surprise that it is quite good for describing static correlation. Dynamic correlation is better described in *e.g.* CISD. However, using pair excitations on the DOCI wave function, one can recover most of the dynamic correlation [147]. In essence, a single pair excitation is a subclass of Configuration Interaction with Double excitations (CID), a double pair excitation is subclass of Configuration Interaction with Double and Quadruple excitations (CIDQ), etc.

The renewed interest in DOCI led to the construction of mean-field scaling approximations of DOCI wave function, the so-called Antisymmetric Product of one-reference-orbital Geminals (AP1roG) [145, 148, 149] or equivalently Coupled Cluster with Double excitations (CCD) [150, 151]. The wave function has the form

$$|\psi_{\text{AP1roG}}\rangle = \exp\left(\sum_{i=1}^{P}\sum_{a=P+1}^{L} t_i^a \hat{a}_a^\dagger \hat{a}_{\bar{a}}^\dagger \hat{a}_{\bar{i}} \hat{a}_i\right)|\phi\rangle\,, \tag{4.5}$$

where $|\phi\rangle$ is the reference state, usually a Restricted Hartree-Fock (RHF) state. The coefficients t_i^a needs to be optimized for a given single-particle basis. This approximation can generate results which are virtually indistinguishable from Full Doubly Occupied Configuration Interaction (FullDOCI) [145]. FullDOCI refers to the equivalent of FullCI but restricted to the space of all doubly occupied Slater determinants.

A major downside of DOCI is its orbital dependence. Any truncated CI wave function will be dependent on the orbitals: as part of the Hilbert space is missing, the shape of the orbitals needs to be optimized to find the (ground state) energy. In DOCI for example, only the diagonal one-particle matrix elements $\langle\alpha|\hat{T}|\alpha\rangle$ are used. This greatly complicates matters: one needs an algorithm to find the optimal shape, and the matrix elements for the one- and two-particle integrals need to be transformed to the optimal basis. In MCSCF and Valence Bond Self-Consistent Field (VBSCF), a similar issue arises. The

'full' problem is very challenging to solve: it means finding the global minimum in an uncharted energy landscape. We know that the DOCI landscape is riddled with local minima [152]. The methods that exist and can potentially find the global minima, such as Simulated Annealing (SA) [127, 153, 154], are slow. The situation is grave but not hopeless: given a suitable starting point, a local minimization can bring us to the desired minimum. This is the approach used by most MCSCF and VBSCF methods. In most cases, the HF orbitals are a good choice to start the minimization. The disadvantage is of course that one can never be sure that the lowest energy has been found, but in practice this approach seems to work. However, it comes at a steep computational cost: a gradient and a Hessian matrix have to be calculated, followed by a unitary transformation of the four-index tensor with the two-electron integrals. The latter operation scales as $O(L^5)$. A general unitary transformation U of a single element is

$$V_{abcd} = \sum_{a\tilde{a}} \sum_{b\tilde{b}} \sum_{c\tilde{c}} \sum_{d\tilde{d}} U_{a\tilde{a}} U_{b\tilde{b}} U_{c\tilde{c}} U_{d\tilde{d}} V_{\tilde{a}\tilde{b}\tilde{c}\tilde{d}}. \tag{4.6}$$

This scales as $O(L^4)$. Combined with the loop over all elements, this would give a total scaling of $O(L^8)$. Luckily, this can be reduced to $O(L^5)$ by rewriting eq. (4.6) as

$$\begin{aligned}
V_{a\tilde{b}\tilde{c}\tilde{d}} &= \sum_{a\tilde{a}} U_{a\tilde{a}} V_{\tilde{a}\tilde{b}\tilde{c}\tilde{d}}, \\
V_{ab\tilde{c}\tilde{d}} &= \sum_{b\tilde{b}} U_{b\tilde{b}} V_{a\tilde{b}\tilde{c}\tilde{d}}, \\
V_{abc\tilde{d}} &= \sum_{c\tilde{c}} U_{c\tilde{c}} V_{ab\tilde{c}\tilde{d}}, \\
V_{abcd} &= \sum_{d\tilde{d}} U_{d\tilde{d}} V_{abc\tilde{d}}.
\end{aligned}$$

We transform index per index and thus have a scaling of $O(L)$ instead of $O(L^4)$. However, this is still computationally more expensive than an energy evaluation in AP1roG (which has L^3 mean-field scaling). In Section 4.2 on page 91, our solution to this problem is discussed.

We can now go back to the marriage of DOCI and v2DM. A general v2DM calculation, using one of the SDP methods from Chapter 3 with two-index conditions, scales as $O(L^6)$. However, the results found by these are not always accurate enough: in many cases, the three-index conditions are needed to capture the correct physics in the system. If we use the three-index commutator conditions, this increases to $O(L^9)$. If we compare this to the so-called 'golden standard' Coupled Cluster with Singles, Doubles and Triples in

Perturbation (CCSD(T)) [53], which scales as $O(L^7)$ [155], we must conclude that v2DM is not competitive in terms of accuracy and time. The benefit we have is that v2DM finds a lower bound on the energy while other variational methods will find an upper bound. If we make the assumption that the ensemble of wave functions from which our 2DM should be derivable only consists of DOCI wave functions, we can use the DOCI N-representability conditions shown in Section 2.5. These have the advantage that the matrix dimensions of the two-index conditions are reduced from L^2 to L. We additionally have a set of linear inequalities and 2×2 matrix conditions but those are cheap to enforce. This changes the scaling of v2DM from $O(L^6)$ to $O(L^3)$. In other words, it suddenly puts us in an entirely different ballpark. Of course, the wave function based approximations of DOCI such as AP1roG also have mean-field scaling. The combination of v2DM and the DOCI N-representability constraints will be called Variational Optimization of the second-order reduced Density Matrix in the DOCI space (v2DM-DOCI)[1] [156] from now on. We will show that v2DM-DOCI is a better approximation to FullDOCI than v2DM is to FullCI. Unfortunately, we lose the advantage of the lower bound on the energy: with the same set of orbitals, v2DM-DOCI still produces a lower bound on the FullDOCI energy, but as we have to optimize the orbitals separately, this is meaningless. One thing that remains is that v2DM-DOCI is exact for a two-particle system: DOCI produces the exact energy for a system with only one pair when the orbitals are optimized [146]. This can be seen as follows: the exact wave function for two particles in the singlet ($S = 0$) state is

$$|\psi\rangle = \sum_{ab} c_{ab}\, \hat{a}^\dagger_{a\uparrow} \hat{a}^\dagger_{b\downarrow} |\rangle\,. \tag{4.7}$$

In the singlet case, the wave function is antisymmetric when swapping the spin indices and symmetric when swapping the orbital indices (see eq. (2.86a) on page 36): this means that c is a symmetric (real) matrix. When we diagonalize c and transform to the basis of the eigenvectors, the wave function becomes

$$|\psi\rangle = \sum_{k} \sqrt{\lambda^c_k}\, \hat{a}^\dagger_{k\uparrow} \hat{a}^\dagger_{k\downarrow} |\rangle\,. \tag{4.8}$$

From the physical point of view, this can be interpreted as first performing rotations between the occupied and virtual orbitals until all single excitations disappear and one finds the Brueckner determinant [157, 158]. Next, one can rotate the virtual orbitals among each other until all double excitations no longer contribute to the wave function. Notice that in this case, the D part

1. An alternative name is vOODo-2DM: variational, Orbital Optimized, Doubly occupied second order Density Matrix.

of the 2DM will be identically zero and the eigenvalues λ_k^c are the natural occupation numbers, doubly degenerate and summing to one (two when the degeneracy is accounted for). The transformation in eq. (4.8) is equivalent with transforming to the basis spanned by the natural orbitals.

The reduced Hamiltonian (see Equation (1.14) on page 7) for v2DM-DOCI is

$$K_{ab}^{\Pi} = \frac{2}{N-1} T_{aa}\delta_{ab} + V_{aabb}, \tag{4.9a}$$

$$K_{ab}^{D} = \frac{1}{N-1}\left(T_{aa} + T_{bb}\right) + V_{abab} - \frac{1}{2}V_{abba}, \tag{4.9b}$$

where $T_{ab} = \langle a|\hat{T}|b\rangle$ and $V_{abcd} = (ab|\hat{V}|cd)$. Notice the round brackets (see eq. (B.10)). The energy function becomes

$$E_{\text{DOCI}} = \sum_{ab}\left(K_{ab}^{\Pi}\Pi_{ab} + 2K_{ab}^{D}D_{ab}\right). \tag{4.10}$$

We have implemented v2DM-DOCI using both a Potential Reduction Method and a Boundary Point method (see Chapter 3). As already said, the latter is much faster. In contrary to general v2DM, the Potential Reduction method is often difficult to converge. It is often necessary to tweak the speed at which the barrier drops and the point where convergence is reached seems to vary greatly. Therefore we have mostly focused on the Boundary Point method. Note that there are some default settings from general v2DM which have to be changed in v2DM-DOCI, for instance the Mazziotti factor is always set to one. We always used primal and dual convergence criteria 10^{-7} and primal-dual criteria of 10^{-3}. The Boundary Point method is fast but not very stable: we added a convergence monitor that checks if the primal convergence keeps going down. If too many steps do not decrease the primal convergence value (typically 2000-3000 steps), the algorithm will halt. This has consequences in the orbital optimizer on which we will expand later.

We have done a scaling test using a linear chain of hydrogen atoms in the STO-3G basis [159]. We used a minimal basis set as this gives us a system which we can let grow linearly: for every additional hydrogen atom, one additional orbital is used. The interatomic distance was kept fixed at 2 Bohr while we increased the chain length. At this distance, the individual hydrogen atoms are still within the interacting region [160]. No orbital optimizations are performed, we directly use the HF orbitals. As reference, we calculated the same chain with general v2DM and the Boundary Point method using spin symmetry and the singlet constraints (see eq. (2.108)). The convergence criteria were the same for both programs. Both were run on a single core of Intel® Xeon® E5-2680 v3 CPU. In Figure 4.1 on the next page we show the calculation time for all chain lengths on a log-log scale. The timings were

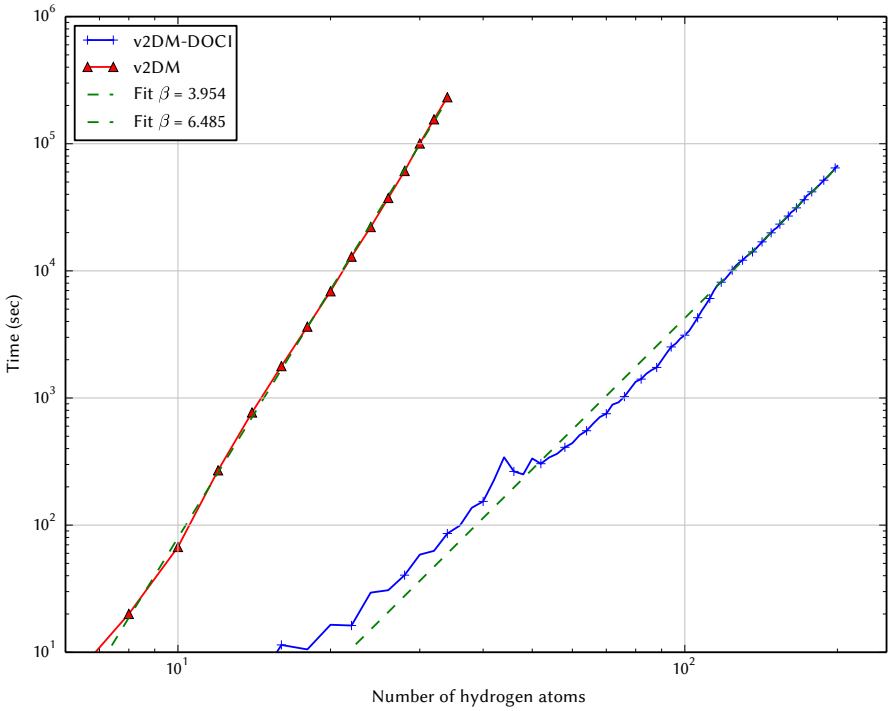

Figure 4.1: The scaling of v2DM vs v2DM-DOCI on a log-log scale. The test system is a linear hydrogen chain in the STO-3G basis. We fitted a linear curve $\beta x + \alpha$ to the data.

checked to be reproducible. Notice that for a chain of 34 hydrogen atoms, the difference in runtime between v2DM-DOCI and v2DM is three orders of magnitude. For the v2DM curve (red) all calculated data points are marked, while for the v2DM-DOCI curve (blue) only every third data point is marked. To find the leading power in scaling, we performed a linear fit on the log-log data. The code scales as $f(x) = \alpha x^\beta + \ldots$, where we neglect all terms expect for the highest power. On a log-log scale, this becomes

$$\log f(x) = \beta \log x + \log \alpha, \tag{4.11}$$

or a simple linear curve. We used a least squares fit [127] which means minimizing

$$e = \sum_i |\beta \log x_i + \log \alpha - t_i|^2 \tag{4.12}$$

with respect to α and β (the sum goes over the data points). For the v2DM, we used a threshold of 600 seconds resulting in 11 data points for the fit. The v2DM-DOCI fit used a threshold of 10^4 seconds, giving us 35 data points for

	α	β
v2DM	$2.602\ 10^{-5}$	6.485
v2DM-DOCI	$5.268\ 10^{-5}$	3.954

Table 4.1: The resulting coefficients of the linear fit in Figure 4.1

the fit. Both choices are motivated by Figure 4.1: it is visually clear that both curves only reach a constant scaling when the problem size is sufficiently large. It is interesting to see that v2DM-DOCI needs a much larger chain to have a constant scaling. In Table 4.1, the results of the fit can be found: v2DM-DOCI is two orders faster than v2DM while the leading coefficient changes little. The results deviate from our prediction of $O(L^3)$ for v2DM-DOCI and $O(L^6)$ for v2DM. This can be explained by the internal loop of the Boundary Point method. The actual scaling is iterative $O(L^3)$: for one loop, the number of Floating-Point Operations per Second (FLOPS) scales as $O(L^3)$ but its main loop adds an additional power to this. It is interesting to notice that the additional cost is higher for v2DM-DOCI than for v2DM. Despite its simpler structure, the DOCI N-representability constraints are more difficult to converge than their general counterpart. This agrees with our experience with the code: the Boundary Point method in v2DM-DOCI seems to be more unstable than in general v2DM.

4.2 Orbital Optimization

We now turn our attention to the orbital optimization of the DOCI orbitals. Like most MCSCF methods, we will use an iterative two-step algorithm: first we optimize the 2DM for a given set of orbitals and secondly we optimize the orbitals using the optimal 2DM. We look for the unitary transformation ($UU^\dagger = U^\dagger U = \mathbb{1}$) of the orbitals that gives us the lowest energy. Notice that as we have restricted ourself to real orbitals, the transformations are actually orthogonal ($UU^T = U^T U = \mathbb{1}$). We want to calculate the energy under a unitary transformation. In general v2DM this would give

$$E' = \frac{1}{4} \sum_{\alpha\beta\gamma\delta} \sum_{\alpha'\beta'\gamma'\delta'} K_{\alpha\beta;\gamma\delta} U_{\alpha\alpha'} U_{\beta\beta'} U_{\gamma\gamma'} U_{\delta\delta'} \Gamma_{\alpha'\beta';\gamma'\delta'}. \tag{4.13}$$

One can both transform the 2DM or the reduced Hamiltonian K. However, this does not hold for DOCI, since a unitary transformation will moves us out of the DOCI space: the one- and two-electron integrals need to be transformed directly. If one transforms the 2DM as in eq. (4.13), then it can

only use the current DOCI space, while we want to rotate new information from outside into the DOCI space. The transformation of the one- and two-electron integrals is

$$T'_{ab} = \sum_{a'b'} U_{aa'} U_{bb'} T_{a'b'}, \tag{4.14a}$$

$$V'_{abcd} = \sum_{a'b'c'd'} U_{aa'} U_{bb'} U_{cc'} U_{dd'} V_{a'b'c'd'}. \tag{4.14b}$$

If we substitute this in the reduced Hamiltonian (4.9), we find

$$K^{\Pi}_{ab} = \frac{2}{N-1} \delta_{ab} \sum_{a'b'} U_{aa'} U_{ab'} T_{a'b'} + \sum_{a'b'c'd'} U_{aa'} U_{ab'} U_{bc'} U_{bd'} V_{a'b'c'd'}, \tag{4.15a}$$

$$K^{D}_{ab} = \frac{1}{N-1} \sum_{a'b'} \left(U_{aa'} U_{ab'} + U_{ba'} U_{bb'} \right) T_{a'b'} + \sum_{a'b'c'd'} U_{aa'} U_{bb'} \left(U_{ac'} U_{bd'} - \frac{1}{2} U_{bc'} U_{ad'} \right) V_{a'b'c'd'}. \tag{4.15b}$$

The energy function (4.10) now is

$$\begin{aligned} E' = & \frac{2}{N-1} \sum_{ab} \sum_{a'b'} \left(\delta_{ab} U_{aa'} U_{ab'} \Pi_{aa} + \left(U_{aa'} U_{ab'} + U_{ba'} U_{bb'} \right) D_{ab} \right) T_{a'b'} + \\ & \sum_{ab} \sum_{a'b'c'd'} U_{aa'} U_{ab'} U_{bc'} U_{bd'} V_{a'b'c'd'} \Pi_{ab} + \\ & \sum_{ab} \sum_{a'b'c'd'} U_{aa'} U_{bb'} \left(2 U_{ac'} U_{bd'} - U_{bc'} U_{ad'}. \right) V_{a'b'c'd'} D_{ab}. \end{aligned} \tag{4.16}$$

An $n \times n$ unitary matrix can be parameterised by a antisymmetric $n \times n$ matrix X as [161]

$$U = \exp X = \mathbb{1} + X + \frac{1}{2} X^2 + \frac{1}{6} X^3 + \ldots = \sum_{n=0}^{\infty} \frac{1}{n!} X^n \tag{4.17}$$
$$\text{with} \quad X^T = -X.$$

This parameterization is used since otherwise we would need a Lagrange multiplier [123, 124] to ensure the unitarity of U in a minimization. The most often used approach is to use the second-order approximation of U

and substitute it in the energy function (4.16). We then rewrite the energy as

$$E(\mathbf{x}) = E(\mathbf{0}) + \sum_{ab} x_{ab} \frac{\partial E}{\partial x_{ab}} + \frac{1}{2} \sum_{abcd} x_{ab} \frac{\partial^2 E}{\partial x_{ab} \partial x_{cd}} x_{cd} \tag{4.18a}$$

$$= E(\mathbf{0}) + \mathbf{g}^T \mathbf{x} + \frac{1}{2} \mathbf{x}^T H \mathbf{x}, \tag{4.18b}$$

where $\mathbf{x} = (X_{12}, X_{13}, \ldots)$ is the vector with the non-redundant elements of the antisymmetric matrix X, while $\mathbf{g}$ and H are the gradient and Hessian of the orbital optimization. The straightforward way is to use a Newton-Raphson method [127] to find the local minimum starting from an educated guess. Often the Hessian is approximated in some way to speed up the minimization [162]. In the end we still need to transform the one- and two-electron integrals using the found unitary matrix, which scales as $O(L^5)$. We will try to avoid this.

One of the simplest unitary transformations are Jacobi rotations [163]: it is a rotation in the two-dimensional subspace of two orbitals. It is also referred to as a Givens rotation[2]. The Jacobi rotation of orbitals k and l over an angle θ is given by

$$\left(Q^{kl}(\theta)\right)_{ij} = \delta_{ij} + (\delta_{ik}\delta_{jk} + \delta_{il}\delta_{jl})(\cos\theta - 1) + (\delta_{ik}\delta_{jl} - \delta_{il}\delta_{jk}) \sin\theta, \tag{4.19}$$

or in matrix form

$$Q^{kl}(\theta) = \begin{array}{c} \\ \\ k \\ \\ l \\ \\ \\ \end{array} \begin{array}{c} \begin{array}{ccccccc} & & & k & & l & \\ \end{array} \\ \begin{pmatrix} 1 & & & & & & \\ & \ddots & & & & & \\ & & \cos\theta & \cdots & \sin\theta & & \\ & & \vdots & \ddots & \vdots & & \\ & & -\sin\theta & \cdots & \cos\theta & & \\ & & & & & \ddots & \\ & & & & & & 1 \end{pmatrix} \end{array}. \tag{4.20}$$

Originally, it was used in the Jacobi Eigenvalue algorithm [127, 164]: a sequence of Jacobi rotations were used to zero out all off-diagonal elements of a matrix. Although it is considered not to be competitive with the QR algorithm [164], it has the advantage of being inherently parallelizable. To understand this, let us look at what happens when we perform a Jacobi rotation on a

2. The correct name would be a Givens rotation but in the Quantum Chemistry literature, the name Jacobi rotation is used consistently.

symmetric matrix T

$$T' = Q^{kl}(\theta)T \tag{4.21}$$

$$T'_{ab} = \sum_c \left(Q^{kl}(\theta)\right)_{ac} T_{cb} \tag{4.22}$$

$$\begin{aligned} &= T_{ab} + \delta_{ak}\left(T_{kb}\left(\cos\theta - 1\right) + T_{lb}\sin\theta\right) + \\ &\quad \delta_{al}\left(T_{lb}\left(\cos\theta - 1\right) - T_{kb}\sin\theta\right). \end{aligned} \tag{4.23}$$

We can see that only row/column k and l are changed. This is also the reason why we are interested in Jacobi rotations: if T is the matrix with the one-particle integrals, only 2 row/columns need to be updated at each step. For the two-particle matrix elements V_{abcd} the situation is slightly more complicated, but it boils down to the same: only if at least one of the 4 indices is equal to k or l does an update have to occur. If point group symmetry is used, the simplification is even bigger. We always assume that the orbitals k and l belong to the same irreducible representation. Another advantage is that no Taylor expansion is needed: we use the exact unitary transformation instead of a second-order approximation. The antisymmetric parameterization X of U also has a distinct form for a Jacobi rotation: all elements are zero expect $X_{kl} = \theta$. With this form, eq. (4.17) will generate the series expansion of a $\cos$ and $\sin$. Furthermore, using a sequence of only Jacobi rotations forms no limitation: any orthogonal transformation can be uniquely decomposed as a series of Jacobi rotations [165]. This leads to a generalization of the Euler angles [166, 167]. There exist MCSCF and Complete Active Space Self-Consistent Field (CASSCF) algorithms that use Jacobi rotations for the orbital optimization step [168, 169].

If we substitute the unitary transformation (4.19) in the energy function (4.16) we find a lengthy expression, which can be simplified as

$$\begin{aligned} E(\theta) = \tilde{A}\cos^4\theta + \tilde{B}\sin^4\theta + \tilde{C}\cos^2\theta + \tilde{D}\sin^2\theta + 2\tilde{E}\cos\theta\sin\theta \\ + 2\tilde{F}\cos^2\theta\sin^2\theta + 4\tilde{G}\sin\theta\cos^3\theta + 4\tilde{H}\sin^3\theta\cos\theta + \tilde{I}, \end{aligned} \tag{4.24}$$

where

$$\tilde{A} = V_{kkkk}\Gamma_{k\bar{k};k\bar{k}} + V_{llll}\Gamma_{l\bar{l};l\bar{l}} + 2V_{kkll}\Gamma_{k\bar{k};l\bar{l}} + 2\left(2V_{klkl} - V_{kkll}\right)\Gamma_{kl;kl} \tag{4.25a}$$

$$\tilde{B} = V_{kkkk}\Gamma_{l\bar{l};l\bar{l}} + V_{llll}\Gamma_{k\bar{k};k\bar{k}} + 2V_{kkll}\Gamma_{k\bar{k};l\bar{l}} + 2\left(2V_{klkl} - V_{kkll}\right)\Gamma_{kl;kl} \tag{4.25b}$$

$$\begin{aligned} \tilde{C} = \sum_{\substack{a \\ a\notin\{k,l\}}} \Bigg\{ &2V_{kkaa}\Gamma_{k\bar{k};a\bar{a}} + 2V_{llaa}\Gamma_{l\bar{l};a\bar{a}} + 2\left(2V_{kaka} - V_{kaak} + \frac{2}{N-1}T_{kk}\right)\Gamma_{ka;ka} \\ &+ 2\left(2V_{lala} - V_{laal} + \frac{2}{N-1}T_{ll}\right)\Gamma_{la;la}\Bigg\} + \frac{2}{N-1}\left(T_{kk}\Gamma_{k\bar{k};k\bar{k}} + T_{ll}\Gamma_{l\bar{l};l\bar{l}}\right) \end{aligned} \tag{4.25c}$$

$$\tilde{D} = \sum_{\substack{a \\ a\notin\{k,l\}}} \Big\{ 2V_{kkaa}\Gamma_{l\bar{l};a\bar{a}} + 2V_{llaa}\Gamma_{k\bar{k};a\bar{a}} + 2\left(2V_{kaka} - V_{kaak} + \frac{2}{N-1}T_{kk}\right)\Gamma_{la;la} + 2\left(2V_{lala} - V_{laal} + \frac{2}{N-1}T_{ll}\right)\Gamma_{ka;ka}\Big\} + \frac{2}{N-1}\left(T_{ll}\Gamma_{k\bar{k};k\bar{k}} + T_{kk}\Gamma_{l\bar{l};l\bar{l}}\right)\Big] \tag{5.25d}$$

$$\tilde{E} = \sum_{\substack{a \\ a\notin\{k,l\}}} \Big\{ 2V_{klaa}\left(\Gamma_{l\bar{l};a\bar{a}} - \Gamma_{k\bar{k};a\bar{a}}\right) + 2\left(2V_{kala} - V_{kaal} + \frac{2}{N-1}T_{kl}\right) \left(\Gamma_{la;la} - \Gamma_{ka;ka}\right)\Big\} + \frac{2}{N-1}T_{kl}\left(\Gamma_{l\bar{l};l\bar{l}} - \Gamma_{k\bar{k};k\bar{k}}\right) \tag{5.25e}$$

$$\tilde{F} = \left(2V_{kkll} + V_{klkl}\right)\left(\Gamma_{k\bar{k};k\bar{k}} + \Gamma_{l\bar{l};l\bar{l}}\right) + \left(V_{kkkk} + V_{llll} - 2\left(V_{kkll} + V_{klkl}\right)\right)\Gamma_{k\bar{k};l\bar{l}} + \left(V_{kkkk} + V_{llll} - 6V_{kkll} + 2V_{klkl}\right)\Gamma_{kl;kl} \tag{5.25f}$$

$$\tilde{G} = V_{klll}\Gamma_{l\bar{l};l\bar{l}} - V_{klkk}\Gamma_{k\bar{k};k\bar{k}} + \left(V_{klkk} - V_{klll}\right)\left(\Gamma_{k\bar{k};l\bar{l}} + \Gamma_{kl;kl}\right) \tag{5.25g}$$

$$\tilde{H} = V_{klkk}\Gamma_{l\bar{l};l\bar{l}} - V_{klll}\Gamma_{k\bar{k};k\bar{k}} - \left(V_{klkk} - V_{klll}\right)\left(\Gamma_{k\bar{k};l\bar{l}} + \Gamma_{kl;kl}\right) \tag{5.25h}$$

$$\tilde{I} = \sum_{\substack{ab \\ a,b\notin\{k,l\}}} \left\{ V_{aabb}\Gamma_{a\bar{a};b\bar{b}} + \left(2V_{abab} - V_{abba} + \frac{2}{N-1}\left(T_{aa} + T_{bb}\right)\right)\Gamma_{ab;ab}\right\} \tag{5.25i}$$

The energy expression (4.24) can be simplified even more using trigonometric identities to

$$E(\theta) = A\cos 4\theta + B\cos 2\theta + C\sin 4\theta + D\sin 2\theta + F, \tag{4.26}$$

where the constants are

$$A = \frac{\tilde{A} + \tilde{B}}{8} - \frac{\tilde{F}}{4}, \tag{4.27a}$$

$$B = \frac{\tilde{G} - \tilde{H}}{2}, \tag{4.27b}$$

$$C = \frac{\tilde{A} - \tilde{B} + \tilde{C}}{2} - \frac{\tilde{D}}{2}, \tag{4.27c}$$

$$D = \tilde{E} + \tilde{G} + \tilde{H}, \tag{4.27d}$$

$$F = \frac{3}{8}\left(\tilde{A} + \tilde{B}\right) + \frac{\tilde{C} + \tilde{D}}{2} + \frac{\tilde{F}}{4} + \tilde{I}. \tag{4.27e}$$

We now want to know the minima of this one-dimensional function. A direct analytical result seems not feasible, so we resort to numerical techniques: we

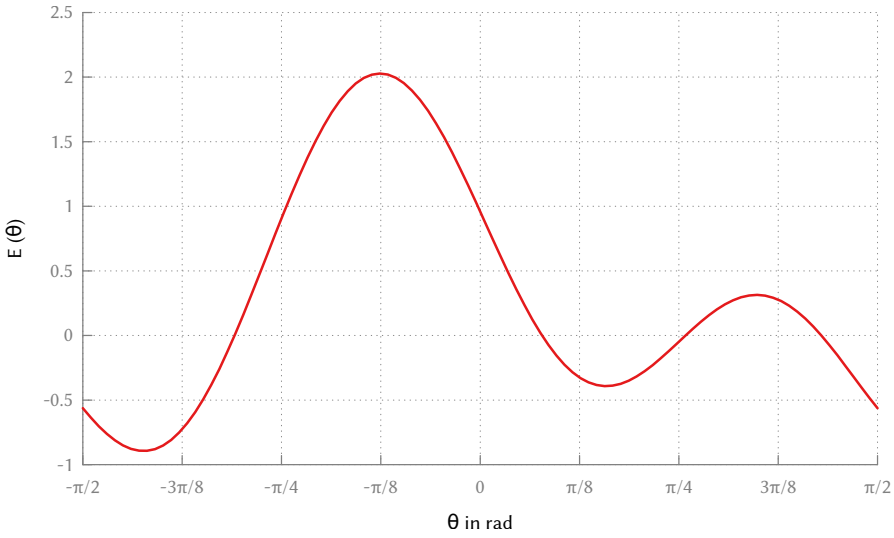

Figure 4.2: Equation (4.26) for the case $A \approx -0.115$, $B \approx -0.839$, $C \approx 0.761$, $D \approx -0.477$ and $F \approx 0.313$.

use the Newton-Raphson method [127], for which we require the gradient and Hessian:

$$\frac{\mathrm{d}E(\theta)}{\mathrm{d}\theta} = -4A\sin 4\theta - 2B\sin 2\theta + 4C\cos 4\theta + 2D\cos 2\theta, \tag{4.28a}$$

$$\frac{\mathrm{d}^2E(\theta)}{\mathrm{d}\theta^2} = -16A\cos 4\theta - 4B\cos 2\theta - 16C\sin 4\theta - 4D\sin 2\theta. \tag{4.28b}$$

It is interesting to note here that it is cheaper to compute the gradient or Hessian than it is to evaluating the energy (4.26). This is a direct consequence of the Jacobi rotations: the constant term in eq. (4.26), *e.g.* the I term in eq. (5.25i), has a double summation over all orbitals except k and l, while all other terms have at most a summation over one index. Thus calculating the energy scales as $O(L^2)$ while calculating the gradient and Hessian only scale as $O(L)$. The actual Newton-Raphson will be very fast as it only requires the evaluation of four sine and cosine values. We always start from $\theta = 0$ to find a minimum. Using the Hessian (4.28b) we can make sure that we have a minimum. It is clear that eq. (4.26) is periodic with a period of π, so we limit our search to the interval $\left[-\frac{\pi}{2}, \frac{\pi}{2}\right]$. Note that in case of $\theta = \frac{\pi}{2}$, we simply switch two orbitals. It is possible that eq. (4.26) has multiple minima and that we will not find the lowest one when starting from $\theta = 0$. Such a situation can be seen in Figure 4.2. We looked for a pattern in the coefficients to discover this kind of situation, but found none. The easiest way is simply to perform two minimizations starting from two different starting points. This

Doubly occupied orbitals					
$1A_1$	-7.339428	$2A_1$	-0.573370	$3A_1$	-0.246546
Virtual orbitals					
$1B_1$	0.269938	$1B_2$	0.269938	$4A_1$	0.701123

Table 4.2: The restricted Hartree-Fock solution for BH in STO-3G. The orbital energies are in Hartree. We use C_{2v} symmetry, the orbitals are labelled according to irreducible representations A_1, B_1 or B_2.

approach works well as each minimization is very fast. In case of a positive Hessian (or maximum), we also simply restart from $\theta = \frac{\pi}{4}$.

We still need to know which pair of orbitals to consider. Looping over all possible pairs of orbitals within an irreducible representation will scale as $O(L^2)$. Combining this with the Newton-Raphson minimization, we have a $O(L^3)$ algorithm to find the optimal set of orbitals. As already said, the update of the one- and two-electron integrals scales as $O(L)$. Explicit formulas to directly calculate the reduced Hamiltonian can be found in Chapter E on page 155. Note that the minimal energy found by eq. (4.26) is not necessarily the actual minimum: the N-representability conditions are unitarily invariant but the v2DM minimum is not. Let us take a look at an example: the BH molecule in the STO-3G [159] basis with an interatomic distance of 2.33 Bohr. This molecule has C_{2v} symmetry with four orbitals transforming according to irreducible representation A_1, one according to B_1 and one according to B_2. The result of eq. (4.26) with and without a v2DM optimization can be seen in Figure 4.3 on the next page. As we hoped, around $\theta = 0$, both curves coincide. Most orbital pairs have a minimum very close to $\theta = 0$ except one: the rotation between orbitals $2A_1$ and $3A_1$. But even there, the minimum predicted by the Jacobi rotations is very close to the optimized one: the difference is 0.039 rad. A single Jacobi rotation already brings us very close to the FullCI energy of -24.810 Hartree. This can be understood from the HF solution of BH: the orbital energies (in Hartree) of the RHF solution are given in Table 4.2. The $1A_1$ orbital is the $1s$ orbital on the Bohr atom while the $2A_1$ and $3A_1$ are a mixture of the $1s$ orbital on the hydrogen atom and the $2s$ and $2p_z$ orbital on the Bohr atom. The largest energy gain can be achieved by mixing these orbitals.

It turns out that the picture painted in Figure 4.3 is correct for most molecules: most orbital pairs will have a minimum very close to $\theta = 0$, while a select group will lower the energy. We present our algorithm to find the optimal Jacobi rotation in pseudocode in Algorithm 3.

One of the downsides of using Jacobi rotations versus a procedure with the

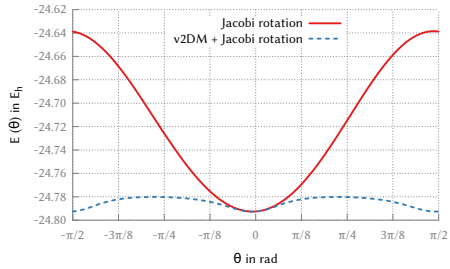

(a) Orbitals $1A_1$ and $2A_1$, min ≈ -0.027 rad

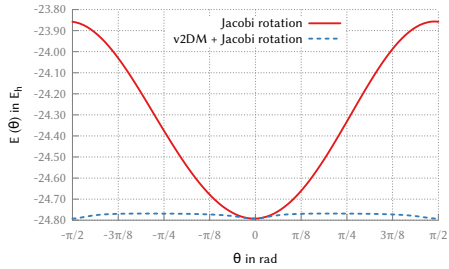

(b) Orbitals $1A_1$ and $3A_1$, min ≈ -0.011 rad

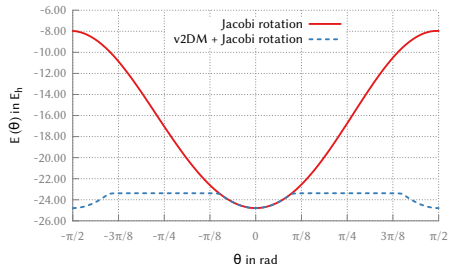

(c) Orbitals $1A_1$ and $4A_1$, min ≈ 0.000 rad

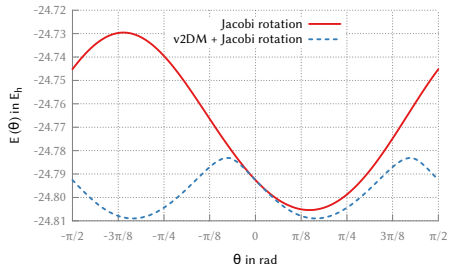

(d) Orbitals $2A_1$ and $3A_1$, min ≈ 0.463 rad

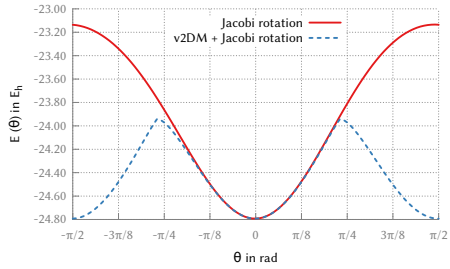

(e) Orbitals $2A_1$ and $4A_1$, min ≈ -0.005 rad

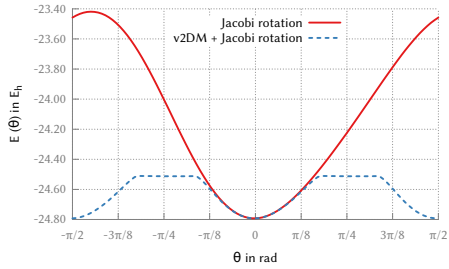

(f) Orbitals $3A_1$ and $4A_1$, min ≈ -0.010 rad

Figure 4.3: The red curve has been calculated using eq. (4.26), while the dashed blue curve uses the same transformed reduced Hamiltonian but an optimized 2DM. The min refers to the minimum of the red curve. The FullCI energy is -24.810 E_h.

Algorithm 3 The algorithm used to find the optimal Jacobi rotation in pseudocode. The inputs are the 2DM, and the one- and two-electron integrals. It returns the optimal orbital pair and angle.

```
procedure FindOptimalRotation(Γ, T, V)
    for i ← 1, n_irrep do                ▷ Loop over all irreducible representations
        for all (a, b) ∈ irrep_i do      ▷ Loop over all orbital pairs in irrep_i
            (E_ab, θ_ab) = FindMinimum(Γ, T, V, a, b)   ▷ Minimum of (4.26)
        end for
    end for
    (k, l, θ) = min (E, θ)               ▷ Find the lowest energy over all pairs
    return (k, l, θ_kl)                  ▷ Return the pair of orbitals and the angle
end procedure
```

full gradient and Hessian, is that it can only update two orbitals at a time, whereas a gradient-based method can update all orbitals at the same time. We can partially circumvent this: we found that the first sequence of Jacobi rotations decreases the energy clearly, and is then followed by a long sequence of Jacobi rotations over small angles. For small angles, the 2DM does not change much and we can skip the actual optimization. This leads to a hybrid algorithm: first we combine the Jacobi rotations with the optimization of the 2DM until the energy change in consecutive steps is small enough, then we perform a sequence of Jacobi rotations with an occasional optimization of the 2DM. After the energy decrease is small enough, we restart the original Jacobi rotation with 2DM optimization until convergence has been reached. This procedure can give a considerable speed boost. Let us now revisit our previous test system to fit the scaling. We will use the same linear hydrogen chain as in Figure 4.1 on page 90 but now include orbital optimization. For the linear fit, a threshold of 10^4 seconds was used, resulting in $27.256\,10^{-5}\,x^{4.200}$. If we compare this to the values in Table 4.1, we see that the orbital optimization costs us an additional 0.25 in the leading power. This is still clearly faster than v2DM and AP1roG. It is difficult to draw general conclusions from this because a hydrogen chain in STO-3G [159] is such as special case: only the $1s$ orbital is present.

As reference, we have also implemented a Simulated Annealing (SA) algorithm [127, 153, 154] for the orbital optimization. As already stated, SA is a slow method, but it is able to find the global minimum. It is not often used in the context of electronic structure calculations [170–173] but it has been successfully applied to protein folding [174, 175]. It is a kind of Monte Carlo algorithm but the idea is inspired by annealing in metallurgy. The material is slowly cooled and, once in a while, slightly reheated to minimize the number

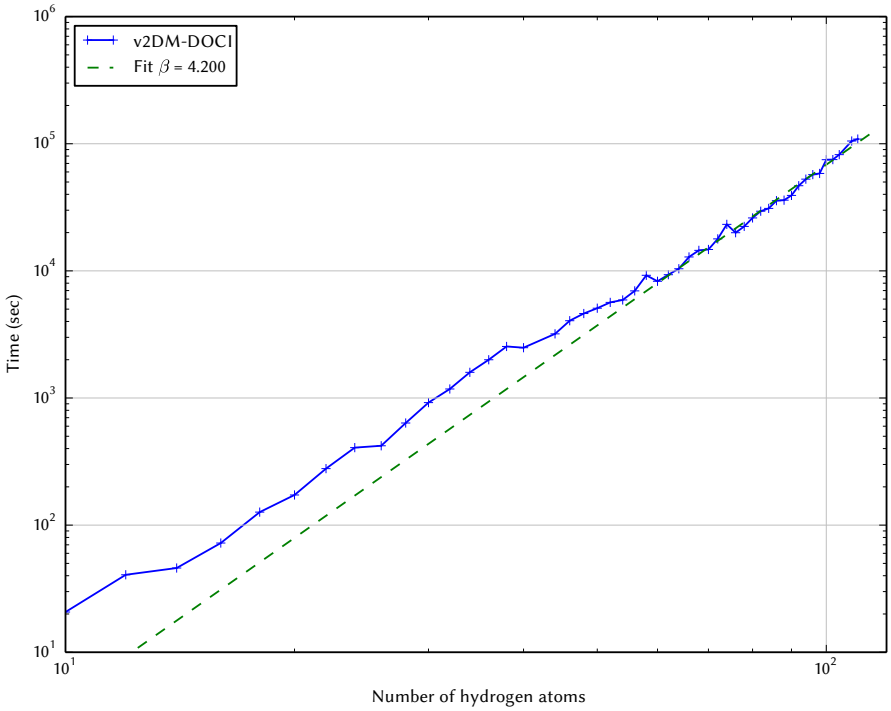

Figure 4.4: The scaling of v2DM-DOCI with orbital optimization on a log-log scale. The test system is a linear hydrogen chain in the STO-3G basis. We fitted a linear curve $\beta x + \alpha$ to the data.

of defects in the material. In SA, there is an artificial temperature which determinates the probability of accepting a new solution with a higher energy than the previous solution. In a nutshell, the SA algorithm can start at any random point (but a guess close to the actual solution is of course better), it will then make a random move on the DOCI surface and calculate the energy with the new set of orbitals. If the new energy is lower, the algorithm will accept the solution and the cycle restarts. If the new energy is higher, the algorithm will accept it with a probability depending on the temperature: the higher the temperature, the higher the probability it will be accepted. During the cycles, the temperature is slowly decreased until higher energy solutions have a negligible probability of acceptance. We use Jacobi rotations for the random perturbation on the orbitals: a pair of orbitals and the rotation angle are chosen at random at each cycle. As acceptance probability function, we will use a Boltzmann function: $\exp \frac{E_{\text{old}} - E_{\text{new}}}{T}$. There are many parameters that need customizing in a SA algorithm: the acceptance probability function, the temperature change function and the random perturbation generator.

Our algorithm is heavily inspired by that of Van Raemdonck *et al.* [147]. Unfortunately, this algorithm is slow: depending on the starting point, many cycles are needed before convergence is reached. As it is a Monte Carlo algorithm, several runs are needed to ensure that we have actually found the correct global minimum. Our algorithm starts several "walkers" in parallel which communicate with each other through the Message Passing Interface (MPI) [176, 177]. They all start again from the lowest energy walker after a certain number of steps. We will only use this algorithm when there is doubt that the Jacobi rotation-based local minimizer finds the correct minimum.

4.3 DOCI tailored v2DM

Before we embark on our tour through the v2DM-DOCI results, let us first sketch the boundary conditions. From now on, we will always use the cc-pVDZ basis [108] unless explicitly specified otherwise. All HF calculations were done with PSI4 [178], an open-source ab initio electronic structure program. The symmetry-adapted molecular one- and two-particle integrals also were extracted from PSI4. As v2DM always needs an orthogonal basis, we work in the symmetry-adapted basis where we applied a Löwdin orthogonalization [179]. This transformation has the interesting property that the orthogonalized orbitals are, in a least-squares sense, the closest to the original orbitals [180, 181]. When we use the RHF orbitals, we use the transformation from the orthogonalized symmetry-adapted basis to the MO orbitals. By doing this, we can use the optimal set of orbitals from one configuration to the next.

We use atomic units [182], namely Bohr for distances and Hartree for energies. The symmetries to which we refer always mean the largest Abelian subgroup of the full point group symmetry. When we refer to FullDOCI, we mean a CI solver which is restricted to all Doubly-occupied Slater determinants within the basis. The code is GPLv3-licensed [183] and available online [184]. We use the same starting point and orbital optimization algorithm in FullDOCI and v2DM-DOCI. All calculations were done on an Intel® Xeon® E5-2680 v3 CPU with 64 GB of RAM. The v2DM-DOCI code is single threaded while the FullDOCI code is parallelized: the sparse Hamiltonian is constructed explicitly and the lowest eigenvalue and eigenvector are found by an implicit restarted Arnoldi algorithm [185, 186]. It is only because of this parallelization that we can find the FullDOCI results in a reasonable time. More details about the working of both codes can be found in Chapter G on page 161. In Algorithm 4 on the following page we show a schematic overview of the entire program.

Algorithm 4 Schematic overview of the complete v2DM-DOCI algorithm

converged $\leftarrow 0$
while converged < 25 **do** ▷ Do 25 steps within convergence criteria
  $E_{\text{new}}, \Gamma = \text{v2DM}(T, V)$ ▷ Do a v2DM-DOCI optimization with electron integrals T and V
  $(k, l, \theta) = \textsc{FindOptimalRotation}(\Gamma, T, V)$ ▷ Find the optimal rotation
  $T, V = \textsc{TransformIntegrals}(k, l, \theta, T, V)$ ▷ Rotate the integrals
  if $|E_{\text{new}} - E_{\text{old}}| < 10^{-6}$ **then** ▷ Check convergence
    converged $\leftarrow$ converged $+ 1$
  end if
  $E_{\text{old}} \leftarrow E_{\text{new}}$
end while

When the size of the problem allowed it, we used the FullCI solver from PSI4 to generate the reference results. For larger problems, we used CheMPS2 [187–190], an open-source spin-adapted implementation of Density Matrix Renormalization Group (DMRG) [191–194] for ab initio quantum chemistry. It uses a Matrix Product State (MPS) [195] as ansatz for the wave function which is then iteratively optimized during a number of sweeps. The size or bond dimension of the matrices in the MPS determine the accuracy and speed. We have always started with a bond dimension of 500 and increased this in steps to 2500. CheMPS2 also fully exploits spin symmetry and point group symmetry. For all practical purposes in this work, we can consider the energy found by CheMPS2 to be FullCI accurate.

4.3.1 Few electron systems

We first investigate a couple of special cases as reference: H_2, He and He_2. The first two have only two electrons, and thus we should find the FullCI value using only the $\mathbb{J}$ condition. The latter dissociates in two two-electron systems, and we should thus recover the correct dissociation energy. In Figure 4.5 on the next page the result for H_2 can be seen. As expected, the v2DM-DOCI curve and the FullCI curve coincide. For the neutral atom Helium, we find a ground state energy of -2.8875948297 Hartree with v2DM-DOCI while FullCI gives us -2.8875948311 Hartree. The difference between both is 1.400 nanoHartree. In both cases we started from the RHF solution. The number of orbital optimization steps was small (< 10). A more interesting case is the Helium dimer in Figure 4.6 on the facing page. This system has D_{2h} symmetry and if we calculate v2DM-DOCI using this symmetry, the dissociation limit produces too high an energy. It is only when we break the symmetry (and use C_1 symmetry) that we recover the correct dissociation

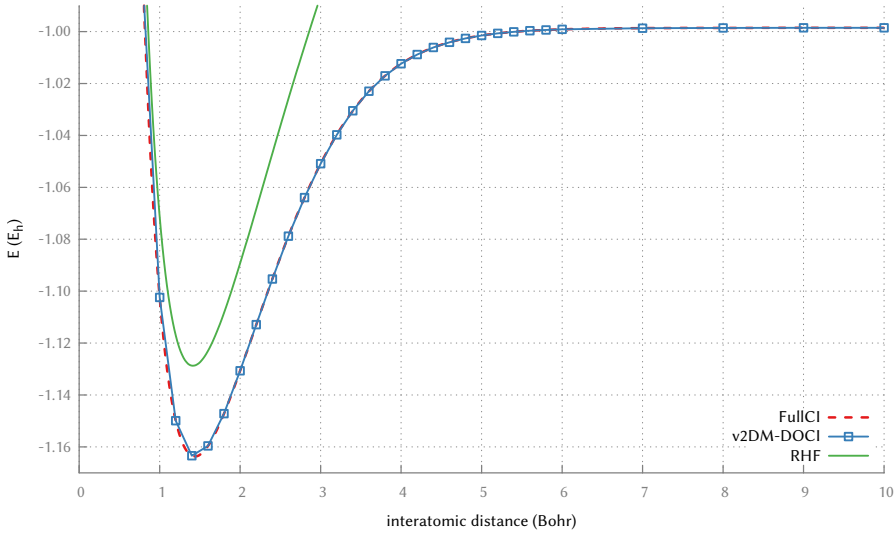

Figure 4.5: The dissociation of H_2 in the cc-pVDZ basis.

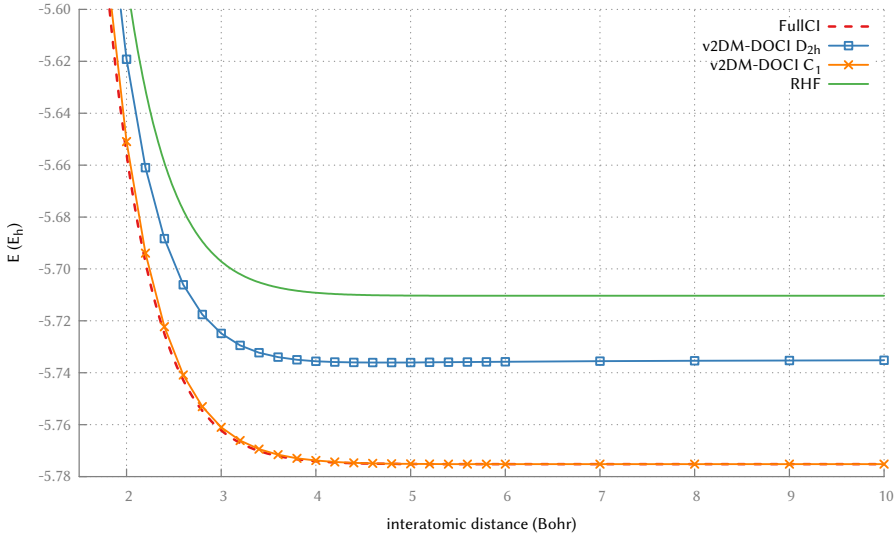

Figure 4.6: The dissociation of He_2 in the cc-pVDZ basis. Both the symmetry-adapted (D_{2h}) and symmetry-broken (C_1) results are shown.

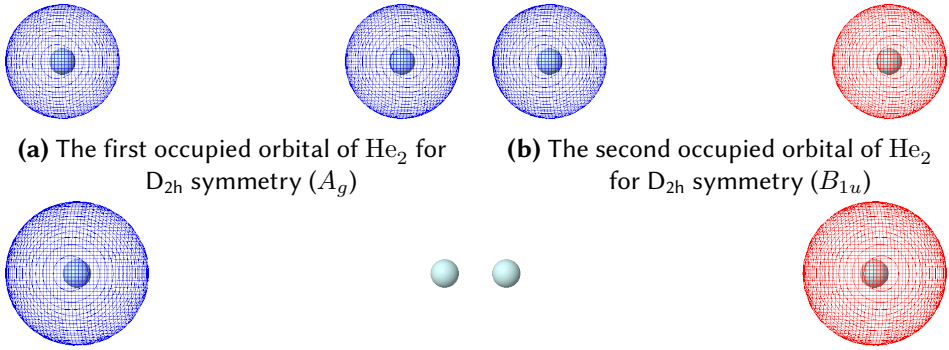

(a) The first occupied orbital of He_2 for D_{2h} symmetry (A_g)

(b) The second occupied orbital of He_2 for D_{2h} symmetry (B_{1u})

(c) The first occupied orbital of He_2 for C_1 symmetry

(d) The second occupied orbital of He_2 for C_1 symmetry

Figure 4.7: The occupied natural orbitals of He_2 at an interatomic distance of 10 Bohr, for both D_{2h} and C_1 symmetry. The colors indicate the relative sign.

energy. We tried random starting points for the D_{2h} calculation but never found an energy lower than the one depicted in Figure 4.6. If we look at the occupation numbers, we see exactly what we expect: two orbitals which are doubly occupied. This example shows the importance of symmetry breaking for DOCI. Symmetry breaking has a long history in physics [196–198]. The exact ground state wave function (or 2DM) of a Hamiltonian needs to exhibit the symmetry of the system but this does not hold for the approximated wave function. On the contrary, if we use the classic variational principle, every additional constraint on the wave function will only increase the energy. This was called the symmetry dilemma by Lödwin [199]. The most strict approximation in HF theory is symmetry-adapted RHF: all symmetries are conversed. Each symmetry that is broken leads to a flavour of HF [200, 201], with the most general one being complex General Hartree-Fock (GHF) [202]. In GHF, none of the symmetries of the system are used in the variation, leading to a potentially much lower energy. Afterwards, a projection is done to restore some symmetries such as particle number. However, it turns out that it is difficult to recover a good quantum number once it is lost. In HF theory, this can be solved by a self-consistent variation after projection approach [203]. In the present case of DOCI, we will only break the spatial point-group symmetry. It is important to note that this is not related to v2DM. If we use FullDOCI exactly the same issues arises. It is the DOCI space itself that requires the symmetry breaking.

In Figure 4.7 we have visualized the natural orbitals using Jmol [204, 205]: an isosurface of the natural orbital is plotted. We show the isosurface $f(x, y, z) =$

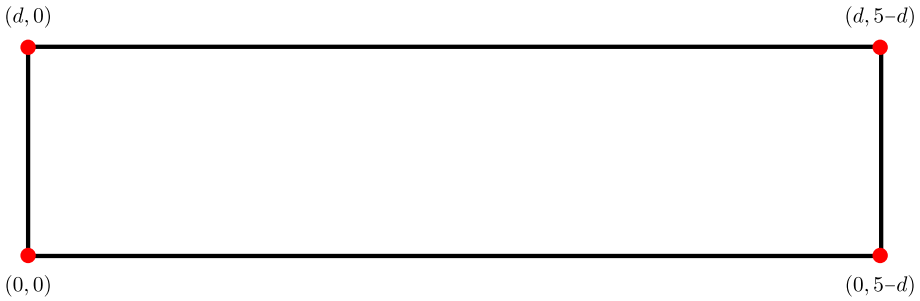

Figure 4.8: The deformation of a planar H_4 system. The parameter d is varied from $1 \ldots 4$ Bohr.

0.05 in red and $f(x, y, z) = -0.05$ in blue, where $f(x, y, z)$ is a linear combination of the atom-centered, Gaussian-type orbitals. The atoms are shown at 15% of the van der Waals radius [206]. The effect of symmetry breaking is clear: in the D_{2h} case, both occupied orbitals are a linear combination of the $1s$ and $2s$ of both He atoms, while for C_1 only the s orbital of a single He atom is used for each natural orbital. The DOCI wave function needs this additional degree of freedom to find the correct ground-state energy.

The next molecular system which we examine is a planar configuration of four hydrogen atoms. We will deform a rectangle of 4×1 to 1×4 Bohr. The coordinates of the four hydrogen atoms are $(0, 0)$, $(d, 0)$, $(0, 5 - d)$ and $(d, 5 - d)$ where d is varied in steps from 1 to 4 Bohr. The configuration is depicted in Figure 4.8. Similar systems have already been studied extensively [207–212]. The reason for the interest in this system is the degeneracy in the square configuration: two Slater determinants become equivalent in this case and we have a strongly correlated system. This system has D_{2h} symmetry as the full point group symmetry (instead of as an Abelian subgroup). For the symmetry-broken v2DM-DOCI calculations, we used the Edmiston-Ruedeberg (ER) localized orbitals [213]. These are found by maximizing the self-interaction: the unitary transformation which causes the terms V_{iiii} of two-electron integrals to be maximal. We need the symmetry-broken orbitals to find the lowest energy which is very close to the FullCI energy. Both minima are found when two hydrogen atoms are at their equilibrium distance of 1.437 Bohr: in that case, we have two almost uncoupled H_2 molecules which are 3.563 Bohr apart. When $d = 2.5$ Bohr, we have a perfect square and the system is degenerate. The RHF energy has a cusp indicating that a single Slater determinant cannot adequately describe the system. This is also the point where the largest deviation from FullCI is found for v2DM-DOCI. The C_1 curve has a cusp while the D_{2h} curve is smoother. We usually start from the HF orbital around equilibrium and use the optimal orbitals from one

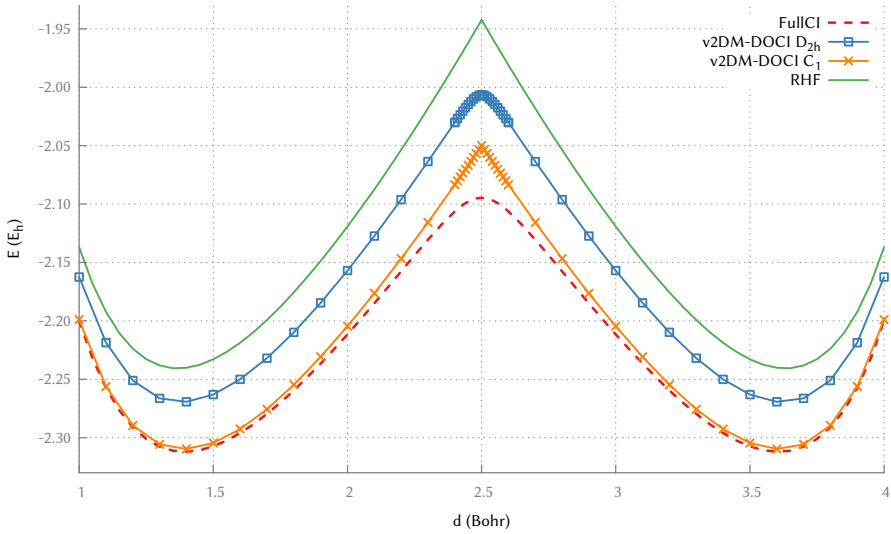

Figure 4.9: The energy of the deformation of a planar H_4 system.

calculation as start point for the next calculation. This fails around the peak: the transition is very steep and it is not possible to have a smooth transition using a set of orbitals from one side to the other. Just like the RHF curve, there is a cusp in the energy at the square configuration. These results seem to indicate that the seniority-two sector plays an important role. If we also add the seniority-four sector, we find the FullCI result.

Another interesting system is the symmetric stretch of an equidistant H_8 chain. It is simple yet challenging, because of the strong correlation effects in the transition from metallic hydrogen to dissociated hydrogen. It is often used as a benchmark system for methods (e.g. AP1roG [145]) and it is one of the systems studied by Bytautas *et al.* [146]. Practically every method which claims to have a good description of strong correlation has been tested on this system or a variant of it [214–218]. In Figure 4.10 on the next page the results can be found. This system has D_{2h} symmetry, which in this context is equivalent with parity symmetry with respect to the middle of the chain. In the limit of dissociated hydrogen, the v2DM-DOCI results coincide with the DMRG results. However, in the transition from metallic hydrogen to dissociated hydrogen, something interesting happens: the symmetry-adapted optimization does not produce a smooth curve between both regimes. The blue curve is the result when starting from the HF orbitals at the equilibrium distance, and then using the optimal set of orbitals as a starting point for the next distance. On the other hand, the green curve was found by a random search at an interatomic distance of 10 Bohr. The

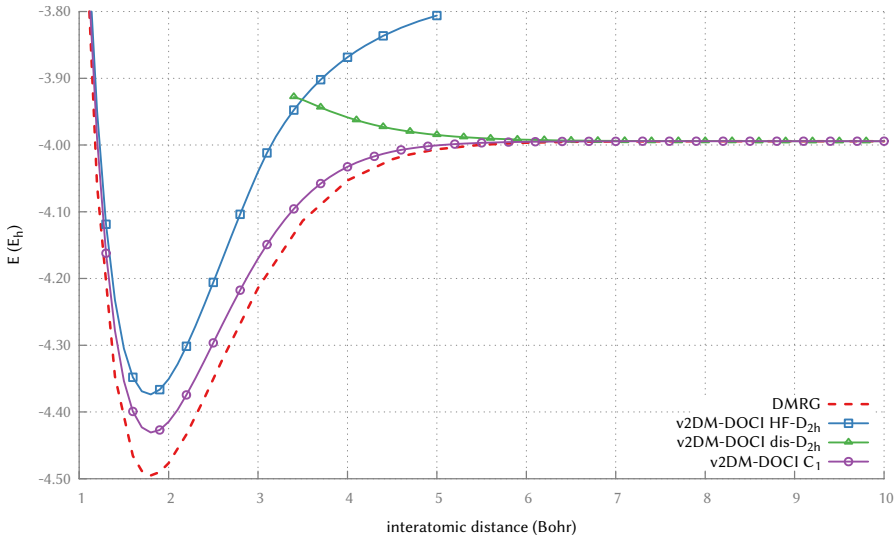

Figure 4.10: The symmetric stretch of a linear H_8 chain in the cc-pVDZ basis. Not all calculated points are marked on the curves.

symmetry prevents the smooth transition between the orbitals. The energy when starting from the HF orbitals even gives a much higher energy when going to the non-interacting region. Furthermore, the symmetry-adapted orbitals do not find the lowest energy at the equilibrium distance. We tried a random search at this point but no lower energy was found. The pictures changes when we use the symmetry-broken orbitals. As a starting point we used the ER localized orbitals. v2DM-DOCI now gives a physically correct picture of the system. Similar results were found by Bytautas *et al.* [146]. They investigated whether the result might be due to an avoided-crossing or a two-state crossing between the ground state and an excited state, but found nothing. In Figure 4.11 on the following page, we have plotted the first excited DOCI state using the optimal set of orbitals found by v2DM-DOCI. This has been calculated using the FullDOCI program. It is clear that the ground state and the first excited state are separated, and no crossings are present.

To better understand what is happening, we have plotted the occupation numbers for both symmetries in Figure 4.12 on the next page. The colors of the curves match those in Figure 4.10. In Figure 4.12b on the following page for the C_1 symmetry, we find the picture we expect: doubly-occupied orbitals which split into single-occupied hydrogen in the dissociation limit. However, in the D_{2h} case (Figure 4.12a), there is an unphysical branch of single-occupied orbitals. There are also orphan branches: they have no con-

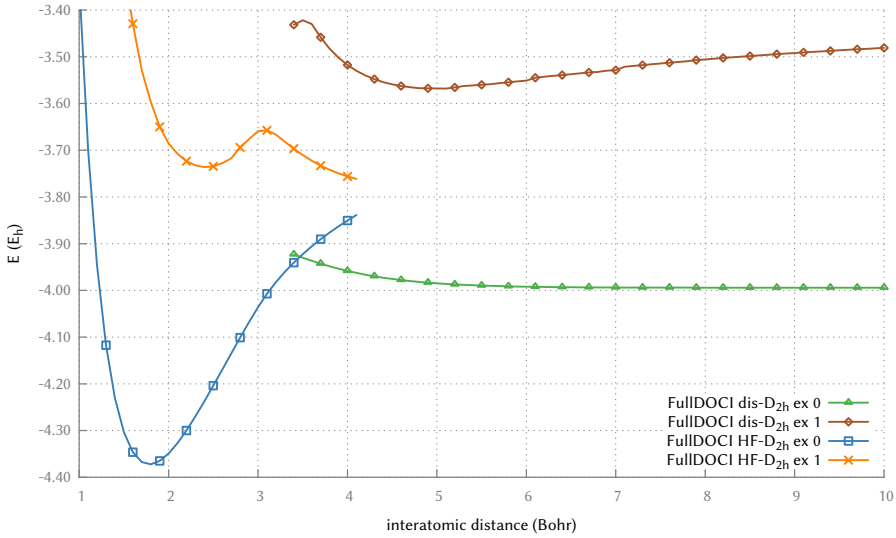

Figure 4.11: The DOCI ground state and the first excited DOCI state of the linear H_8 chain.

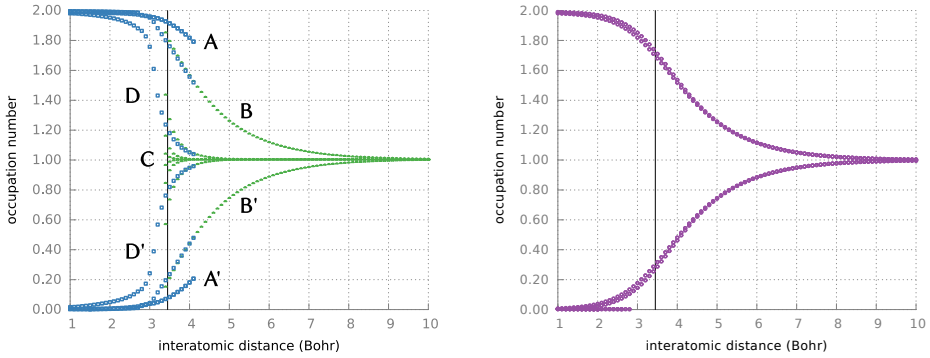

(a) The natural occupation numbers of the H_8 chain in D_{2h} symmetry. The different curves are labeled to easily identify them in the text.

(b) The natural occupation numbers of the H_8 chain in C_1 symmetry.

Figure 4.12: The natural occupied numbers of the H_8 chain. The black line indicates the crossing of the two D_{2h} curves in Figure 4.10. Only points with an occupation $> 10^{-3}$ are shown. The colors match those in Figure 4.10.

nection from the dissociated regime to the metallic regime (and vice versa). Let us examine the situation where all three curves are active: in Figure 4.13 on the next page we have plotted the occupied natural orbitals of the H_8 chain with an interatomic distance of 4 Bohr for the different curves. In the case of symmetry-broken orbitals we see a familiar picture: the highest-occupied orbitals are the bonding combination of the $1s$ orbitals of two adjacent hydrogen atoms. As we are already near the dissociation, the antibonding orbitals also have a non-negligible occupation. This is in essence what can also be seen in fig. 4.12b: as the interatomic distance increases, the occupation of the bonding orbital decreases and the occupation of the antibonding orbital is increases, until they are degenerate. In the symmetry-adapted calculation, it is not possible to form these combinations due to the mirror plane in the middle. The only possibility to form direct bonding and antibonding orbitals is for the two hydrogen atoms in the center. Indeed, these combinations are present in both fig. 4.13a and fig. 4.13b and the occupations match those in fig. 4.13c. These orbitals are responsible for the curve marked with B and B′ in Figure 4.12a: it is possible to have a smooth transition for these from one regime to the other. If we look at the highest occupied orbitals in fig. 4.13a, we see that these correspond to two bonding hydrogen atoms on each side of the chain. The corresponding lower branch in fig. 4.12a (marked with A′), has the antibonding combination on the same hydrogens. In the dissociated solution Figure 4.13b, the orbitals are localized and a bonding/antibonding combination does not happen due to symmetry. It consists of all combinations of two localized hydrogen orbitals that are allowed due to the mirror symmetry. The combination of outermost hydrogen atoms leads to the unphysical branch (marked with C) in fig. 4.12a, with no corresponding branch in the other regime. The connecting branch between the two regimes which starts from occupation 1 (marked with D and D′) is caused by the set of orbitals present in both fig. 4.13a and fig. 4.13b: the bonding and antibonding combination of atoms three and six. This all shows how the D_{2h} symmetry prevents the orbitals from reaching the lowest energy state shown in fig. 4.13c. We can now also better understand the energy curves in fig. 4.10. With a larger interatomic distance, the localized orbital are the most accurate description of the chain and therefore, they have the lowest energy. However, as the interatomic distance decreases, the orbitals want to delocalize, and the symmetry constraints make this hard to do. In fact, we know that this delocalized description must lie in a different valley in the DOCI landscape, as the orbital optimizer cannot reach it. From the other side, the HF orbitals are delocalized and provide a better starting point for small interatomic distances. In the same way as before, if we increase the interatomic distance, the symmetry prevents the orbitals from delocalizing and therefore the energy keeps on rising. This system is not stable: a Peierls

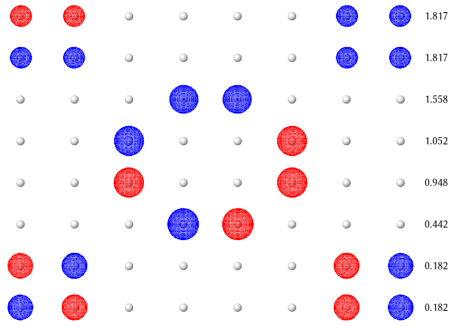

(a) The natural orbitals of H_8 with D_{2h} symmetry starting from the HF orbitals (the blue curve in fig. 4.10).

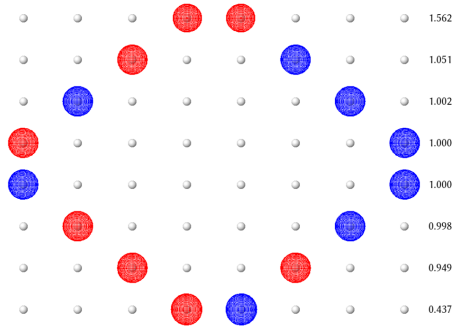

(b) The natural orbitals of H_8 with D_{2h} symmetry starting from the dissociated orbitals (the green curve in fig. 4.10).

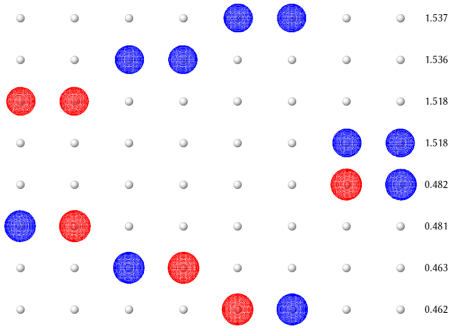

(c) The natural orbitals of H_8 with C_1 symmetry starting from the ER localized orbitals (the purple curve in fig. 4.10).

Figure 4.13: The occupied natural orbitals of the H_8 chain at an interatomic distance of 4 Bohr for the different v2DM-DOCI calculations. The occupation numbers are shown on the right of the orbitals. All symmetry-adapted orbitals transform according to either A_g or B_{1u}, depending on whether the orbital changes sign under a mirror operation.

d	Sym.	DMRG	Δv2DM	Δv2DM-DOCI	ΔFullDOCI
2.2	D_{2h}	-109.278	-77.375	222.578	224.455
2.2	C_1	-109.278	-77.375	209.891	214.787
4.0	D_{2h}	-108.975	-96.213	257.013	258.842
4.0	C_1	-108.975	-96.213	248.396	250.991
10.0	D_{2h}	-108.960	-66.384	282.966	283.108
10.0	C_1	-108.960	-66.384	273.371	273.464

Table 4.3: Some points on the N_2 curve from Figure 4.14. The interatomic distance (d) is in Bohr. The DMRG energy is in Hartree. For v2DM, v2DM-DOCI and FullDOCI, the deviation from DMRG is given in milliHartree.

transition [219] will break the symmetry and there will be two alternative distances between the atoms. The system will break down into four separate H_2 molecules.

This example shows the Achilles heel of our orbital optimizer: it cannot jump to a different valley in the DOCI landscape. Given a suitable starting point it will duly find the minimum in the corresponding valley, but one never be sure.

4.3.2 Molecular systems

Another interesting application is the dissociation of a diatomic molecule in which static correlation is of paramount importance at dissociation. First we must introduce some addional nomenclature for the results: v2DM-DOCI refers to v2DM with the DOCI constraints on the 2DM and with the Jacobi orbital optimization. FullDOCI uses the same orbital optimization algorithm. v2DM-DOCI/FullDOCI is a single-shot v2DM-DOCI calculation using the optimal set of orbitals from a FullDOCI calculation. FullDOCI/v2DM-DOCI is exactly the opposite: a single-shot FullDOCI calculation using the optimal set of orbitals from v2DM-DOCI.

The first system we study is the dissociation of N_2. This is a challenging system due to the breaking of a triple bond and is often used as a test case [146, 212, 220–222]. In the cc-pVDZ basis, N_2 has 28 orbitals. The results can be seen in Figure 4.14 on the following page. In order to appreciate the performance of v2DM-DOCI, results of other methods such as CCSD(T)[53] and DFT with B3LYP functional[223, 224] are also presented. All DOCI curves give a qualitatively correct description of the dissociation process. In Table 4.3

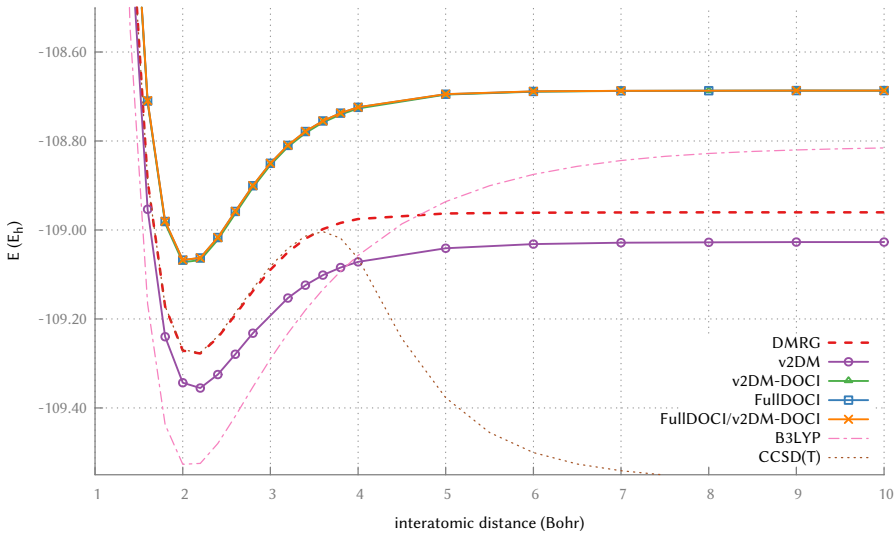

Figure 4.14: The dissociation of N_2 in the cc-pVDZ basis. The DOCI curves shown are for the C_1 symmetry. Note that three curves (v2DM-DOCI, FullDOCI, FullDOCI/v2DM-DOCI) coincide visually.

we show the exact values of some selected data points. Unlike the previous examples, symmetry breaking does not significantly alter the energy: the symmetry-broken energy is always lower than the symmetry-adapted value but the difference is in the ≤ 10 milliHartree region. More interesting to see is that the energy difference between v2DM-DOCI and FullDOCI is very small. It seems that v2DM-DOCI is a better approximation to FullDOCI than v2DM is to FullCI: the difference is 2-3 milliHartree while v2DM usually deviates from FullCI in the dozens of milliHartree. The CCSD(T) curve fails completely in the dissociation limit. This is a known failure and it can be fixed within Coupled Cluster (CC) theory [212]. Note that N_2 dissociates into two N atoms with an odd number of electrons. This forms no problem for DOCI as the orbital optimization can handle this[152]. The difference between the DOCI curves and the DMRG reference is due to dynamical correlations and can be added in a subsequent stage, as shown in reference 225.

Another interesting case is cyanide, CN^-. This heteronuclear molecule also has a triple bond and dissociates in C^- and N. The effect of breaking the C_{2v} symmetry is again minimal (see results in Table 4.4 on the facing page), so in Figure 4.15 we restrict ourself to the C_1 curve. For this heteronuclear molecule, the dissociation limit for v2DM and v2DM-DOCI is incorrect. This is a known failure for v2DM-based techniques [31]: the energy of the isolated atoms as a function of fractional charge is a convex curve in v2DM whereas

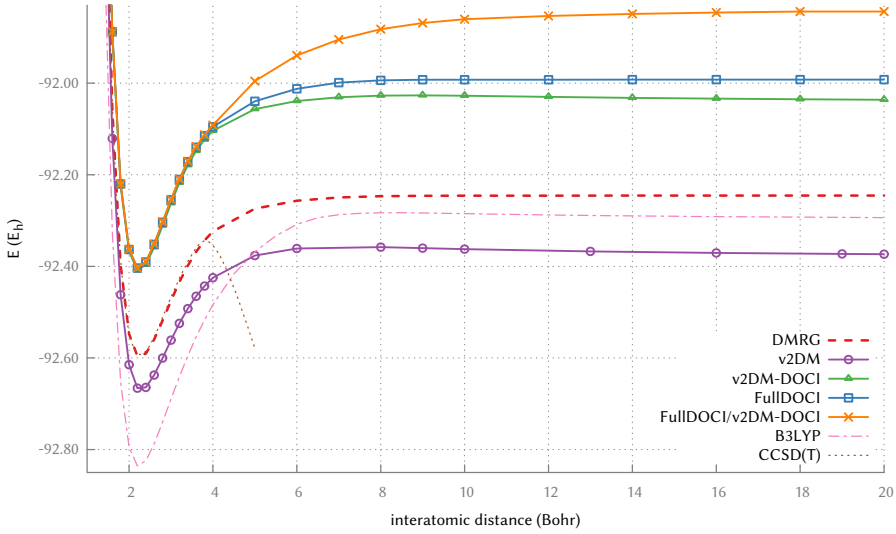

Figure 4.15: The dissociation of CN^- in the cc-pVDZ basis. The DOCI curves shown are for the C_1 symmetry.

d	Sym.	DMRG	Δv2DM	Δv2DM-DOCI	ΔFullDOCI
2.2	C_{2v}	-92.596	-70.208	186.967	192.202
2.2	C_1	-92.596	-70.208	186.967	192.192
4.0	C_{2v}	-92.324	-101.281	219.639	228.307
4.0	C_1	-92.324	-101.281	219.639	228.300
10.0	C_{2v}	-92.246	-116.686	218.333	253.131
10.0	C_1	-92.246	-116.686	218.333	253.130
20.0	C_{2v}	-92.246	-127.996	209.275	253.135
20.0	C_1	-92.246	-127.996	209.275	253.133

Table 4.4: Some points on the CN^- curve from Figure 4.15. The interatomic distance (d) is in Bohr. The DMRG energy is in Hartree. For v2DM, v2DM-DOCI and FullDOCI, the deviation from DMRG is given in milliHartree.

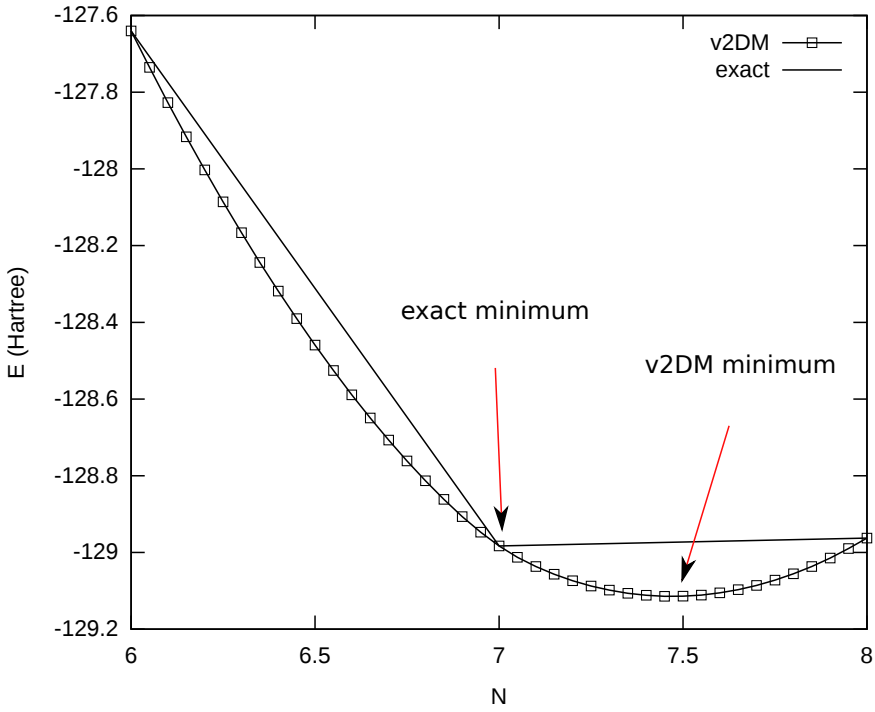

Figure 4.16: The energy as a function of number of electrons on the oxygen atom for the NO^+ molecule. Reproduced from Reference 90 with permission of B. Verstichel.

it should be a piecewise linear curve [226, 227]. We have plotted the energy as a function of the charge in Figure 4.16 for the NO^+ molecule: the problem of the convexity can be clearly seen. It will lead to a too low energy. It is the same problem from which DFT suffers [228] and is more commonly referred to as the delocalization error. In DFT the approximate functionals also favour a fractional distribution of the electrons. It can explain the underestimation of the band-gap in DFT calculations [228]. For the same reason, v2DM will favour fractional charges on dissociated atoms and thus give a physically incorrect picture. This can be seen clearly on the FullDOCI/v2DM-DOCI curve: if we use the optimal basis of v2DM-DOCI calculation, the FullDOCI energy is much higher than the true FullDOCI energy, as the FullDOCI solution is far from optimal with the artificial non-integer atomic charges from v2DM-DOCI. The problem can be confirmed through a population analysis. We will perform a Mulliken population analysis [229] at an interatomic distance of 20 Bohr. In this case, the overlap between orbitals centered on the carbon and the oxygen will be negligible. The diagonal elements of 1DM can then be

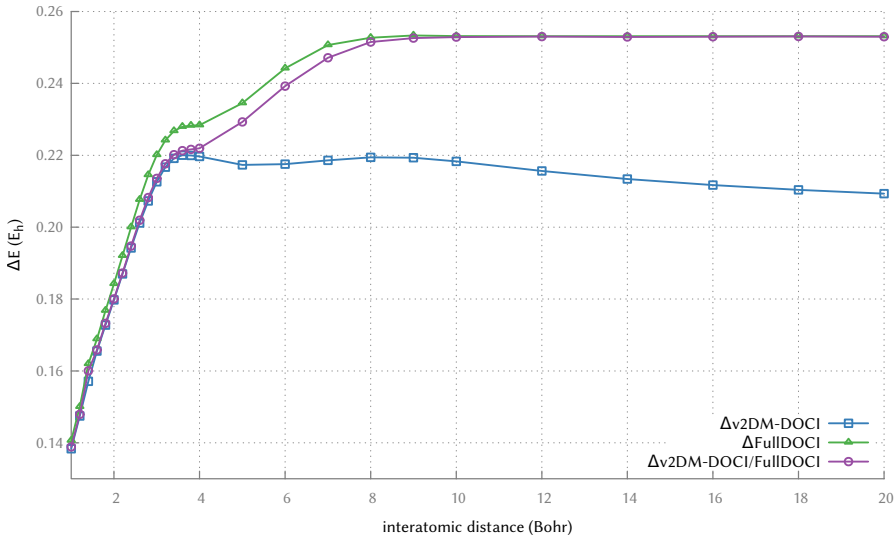

Figure 4.17: The dissociation of CN^- in the cc-pVDZ basis: comparing the v2DM-DOCI/FullDOCI results with v2DM-DOCI and FullDOCI. The deviation from DMRG is plotted.

distributed as belonging to either the carbon or oxygen atom. The sum will be the total particle number. When we do this, we find that the net charges are $C^{-0.43}N^{-0.57}$ for the v2DM-DOCI calculation. At the same distance, DFT with B3LYP produces $C^{-0.42}N^{-0.58}$ while v2DM finds $C^{-0.60}N^{-0.40}$. The physical correct dissociation would be $C^{-1.0}N^{0.0}$.

Using so-called subsystem constraints [30, 91] (see Section 2.3.4 on page 31), one can force the E vs N curve to be piecewise linear. However, this would require a v2DM(-DOCI) optimization at each nearby integer value of N. This makes it a costly solution with the additional downside that although it fixes the energy in the dissociation limit, the transition to this limit remains unphysical: at the point when the subsystem constraints become active the energy curve is 'pulled' towards the correct limit (examples can be found in reference 90). However, there might be another solution. In Figure 4.17, we have used the FullDOCI optimal orbitals for the v2DM-DOCI calculation. In this case, v2DM-DOCI gives the correct DOCI dissociation limit. This suggests that it might be possible to find specific DOCI constraints to solve the problem of fractional charges in v2DM-DOCI.

In Figure 4.19 on page 117, we have plotted the occupied natural orbitals of both v2DM-DOCI and FullDOCI. Unfortunately, this does not learn us much. While in the FullDOCI case all orbitals have an occupation of either approximately two or one, the valence orbitals of v2DM-DOCI do not. For

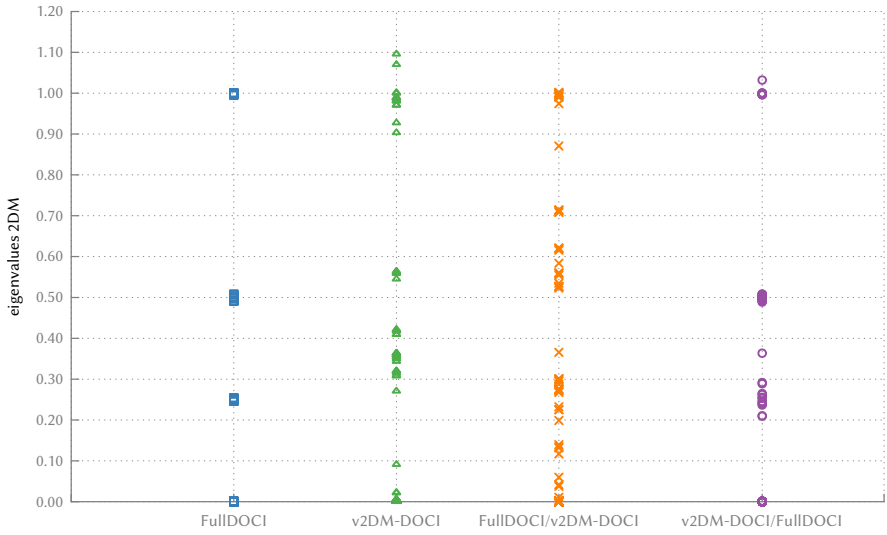

Figure 4.18: The eigenvalues of all the calculated 2DM's for CN^- with an interatomic distance of 20 Bohr.

the core s orbitals, there is no difference. For the p orbitals, an electron is spread out over several orbitals, leading to fractional charges. We also examined the eigenvalues of the 2DM. These present the occupation numbers of the natural geminals. If we look at the eigenvalues of the 2DM from the FullDOCI calculation at an interatomic distance of 20 Bohr, there is a clear structure. The eigenvalues are separated in 4 groups: $[0.995, 1.001]$, $[0.491, 0.508]$, $[0.246, 0.254]$ and $[0, 0.001]$. The number of eigenvalues in each group is 13, 24, 12 and 356. This is not the case in the 2DM from v2DM-DOCI: the eigenvalues are spread over the entire $[0, 1.1]$ range. We have plotted these in Figure 4.18, in order to indicate what goes wrong. Figure 4.17 seems to suggest that the problem can be solved without constraints on the 2DM but purely in the orbital optimization: given a suitable set of orbitals, v2DM-DOCI does not necessarily use fractional charges. Although the picture of the eigenvalues of the 2DM in Figure 4.18 may suggest otherwise, there are no fractional charges found in the resulting 2DM for the v2DM-DOCI/FullDOCI optimization. Unfortunately, we have not yet found the necessary constraint on the orbital optimization.

We did a calculation for the NO^+ molecule but the same problem occurs here. In Figure 4.20 on page 118 the energy curves are shown while Table 4.5 on page 119 has the exact value of several selected data points. If we repeat the Mulliken analysis at an interatomic distance of 20 Bohr, we find $N^{0.45}O^{0.55}$ for v2DM-DOCI, $N^{0.67}O^{0.33}$ for DFT with B3LYP and $N^{0.47}O^{0.53}$ for v2DM.

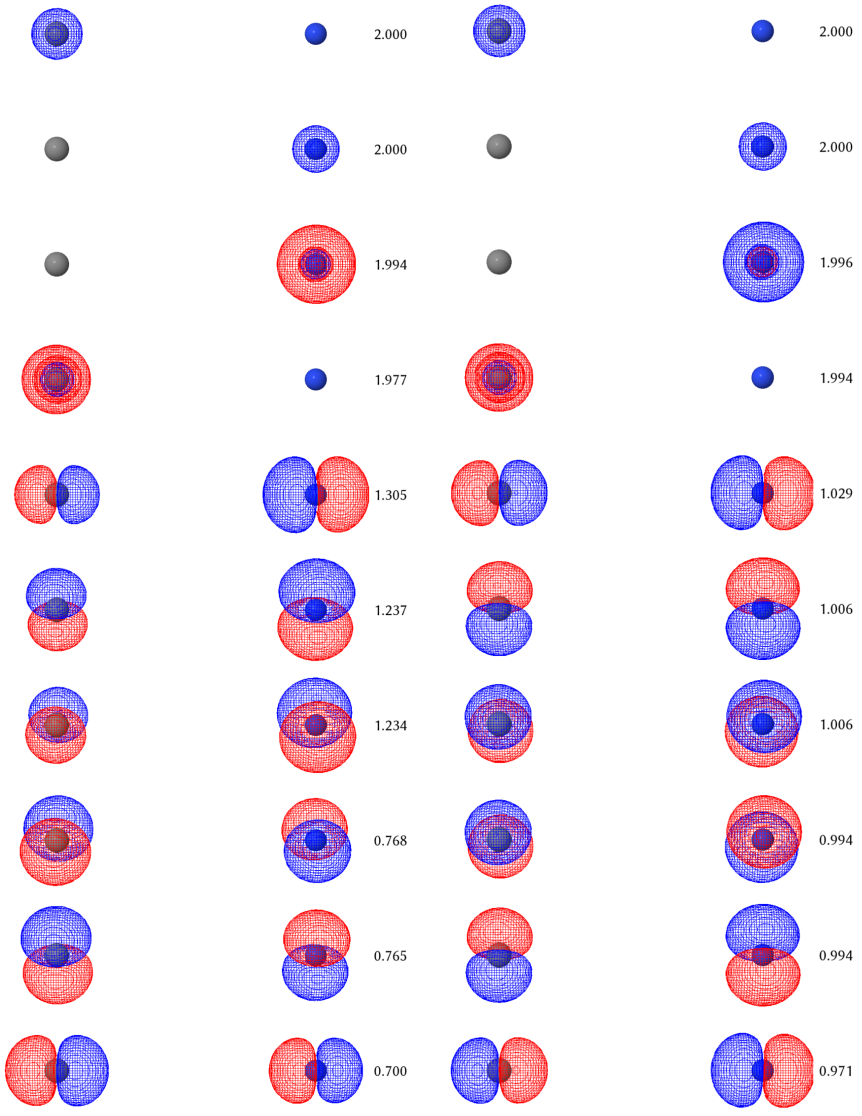

(a) The natural orbitals of CN^- calculated by v2DM-DOCI.

(b) The natural orbitals of CN^- calculated by FullDOCI.

Figure 4.19: The occupied natural orbitals of the CN^- with C_1 symmetry at an interatomic distance of 10 Bohr for v2DM-DOCI and FullDOCI. The occupation number is shown on the right of the orbitals.

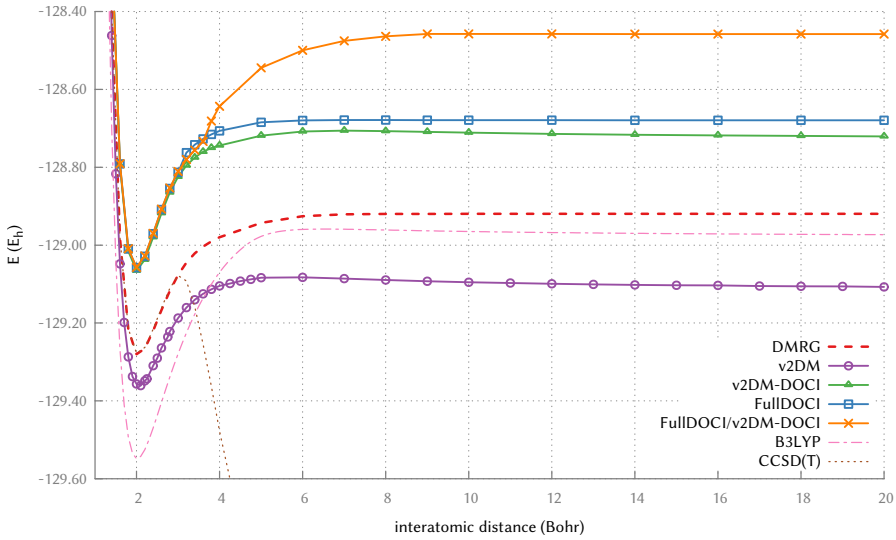

Figure 4.20: The dissociation of NO^+ in the cc-pVDZ basis. The DOCI curves shown are for the C_1 symmetry.

The physical correct disocciation would be $N^{0.0}O^{1.0}$.

The last system we examined is another member of the isoelectronic series: CO. The results of the calculations can be found in Figure 4.21 on the facing page and Table 4.6 on page 120. Unlike the previous two cases, fractional charges do not seem to be an issue here. A Mulliken population analysis finds $C^{0.003}O^{-0.003}$ for the v2DM-DOCI calculation at an interatomic distance of 10 Bohr. However, the ground state of the oxygen atom is a triplet ($S = 1$) state while the carbon atom is a singlet. This means that the total spin of the wave function of the dissociated system should be $S = 1$. The DOCI space is singlet by nature, which means that our resulting solution will have the wrong total spin. Despite this, the results are in agreement with the previous results. We find a energy deviation form FullCI in the range of 200 milliHartree. Although we enforce the singlet constraints (see Section 2.4.1), the v2DM optimization still has the necessary freedom to enter the triplet domain. The singlet constraints are only necessary conditions and not sufficient for the singlet state. But looking at the results, v2DM-DOCI does not use this freedom as FullDOCI produces an energy very close to it.

4.3.3 The Hubbard model

The Fermi-Hubbard model [230] is a model that possesses some of the non-trivial correlations present in a solid. Originally it was formulated as a simple

d	Sym.	DMRG	Δv2DM	Δv2DM-DOCI	ΔFullDOCI
2.2	C_{2v}	-129.266	-82.860	228.039	236.820
2.2	C_1	-129.266	-82.860	228.082	236.934
4.0	C_{2v}	-128.980	-124.913	235.704	424.907
4.0	C_1	-128.980	-124.913	235.708	273.176
10.0	C_{2v}	-128.920	-175.533	208.614	340.015
10.0	C_1	-128.920	-175.533	208.652	240.620
20.0	C_{2v}	-128.920	-187.722	199.268	344.949
20.0	C_1	-128.920	-187.722	198.773	357.722

Table 4.5: Some points on the NO^+ curve from Figure 4.20. The interatomic distance (d) is in Bohr. The DMRG energy is in Hartree. For v2DM, v2DM-DOCI and FullDOCI, the deviation from DMRG is given in milliHartree.

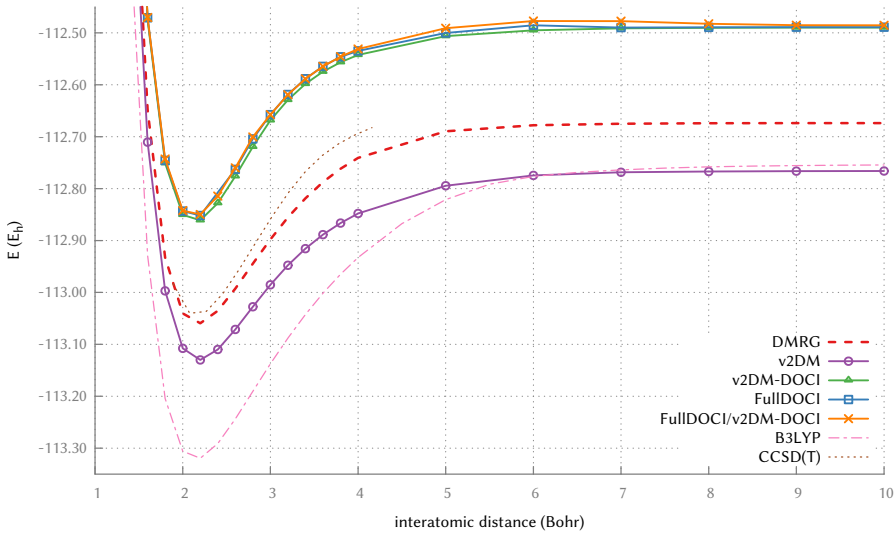

Figure 4.21: The dissociation of CO in the cc-pVDZ basis. The DOCI curves shown are for the C_1 symmetry.

d	Sym.	DMRG	Δv2DM	Δv2DM-DOCI	ΔFullDOCI
2.2	C_{2v}	-113.059	-70.607	198.729	207.680
2.2	C_1	-113.059	-70.607	198.416	207.680
4.0	C_{2v}	-112.741	-107.071	201.542	208.968
4.0	C_1	-112.741	-107.071	198.536	206.093
10.0	C_{2v}	-112.673	-92.418	187.388	187.871
10.0	C_1	-112.673	-92.418	183.954	184.604
19.0	C_{2v}	-112.674	-91.970	187.348	188.261
19.0	C_1	-112.674	-91.970	187.262	187.789

Table 4.6: Some points on the CO curve from Figure 4.21. The interatomic distance (d) is in Bohr. The DMRG energy is in Hartree. For v2DM, v2DM-DOCI and FullDOCI, the deviation from DMRG is given in milliHartree.

model to study the correlations of d-electrons in transition metals. Since then it has been the subject of intensive research. It is believed that the two-dimensional version holds the key to understanding high temperature superconductivity [231]. It is also an excellent model to study the effects of strong correlation and this is why we will examine the DOCI results of a one-dimensional Hubbard model. The Hamiltonian is given by

$$\hat{H} = -t \sum_{a\sigma_a} \left(\hat{a}^\dagger_{a\sigma_a} \hat{a}_{a-1\sigma_a} + \hat{a}^\dagger_{a+1\sigma_a} \hat{a}_{a\sigma_a} \right) + U \sum_a \hat{n}_{a\uparrow} \hat{n}_{a\downarrow}, \tag{4.29}$$

where the ratio $\frac{U}{t}$ is the only degree of freedom and $\hat{n}_{a\uparrow}$ is the number operator. We assume periodic boundary conditions on the chain.

The Hamiltonian has two competing terms: the first term, called the hopping term favours delocalization of the electrons while the second term, called the on-site repulsion, favours localization. In the site basis the second term is diagonal while in the pseudo-momentum basis the first term is diagonal. It is very interesting how such a simple model can give rise to such complex physics. To fully appreciate this, an illustration of complexity is depicted in the final pages of this chapter.

The one-dimensional model at half filling (one electron per site) has a known solution given by the Lieb-Wu equations [232–234]. We examine a chain of 22 sites as we increase the on-site interaction strength with a fixed $t = 1$. In Figure 4.22 on the facing page the result is plotted. As the starting point for the orbital optimizer the pseudo-momentum basis was used as this is already a mixture of all sites. At $U = 0$ the exact wave function is given by a single

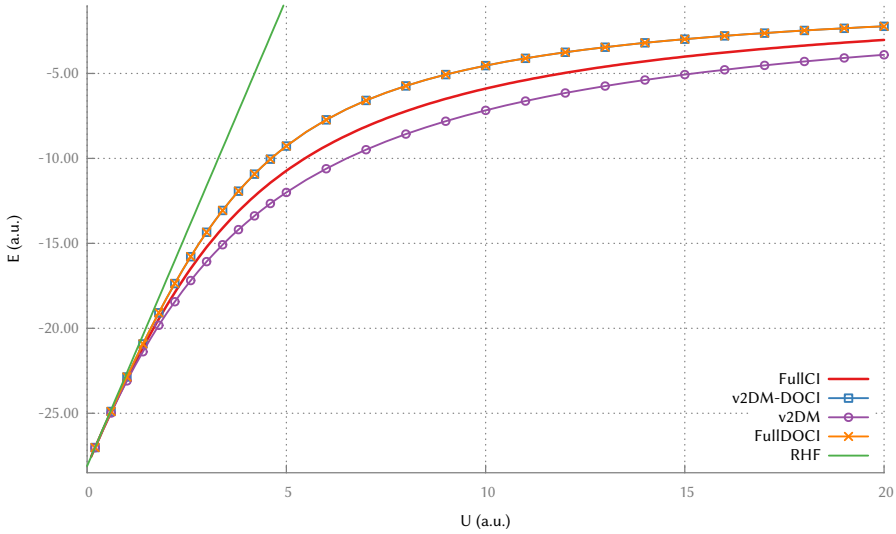

Figure 4.22: The results of a one-dimensional Fermi-Hubbard model with 22 sites. The energy is plotted for increasing interaction strength.

Slater determinant and both v2DM-DOCI and RHF produce the correct energy. At intermediate interaction strength, the deviation from FullCI is the largest. In the limit $U \to \infty$ the Hubbard model is reduced to a Heisenberg antiferromagnet [235]: every electron is frozen at a site and not a single site will be doubly occupied. Despite this, v2DM-DOCI gives a reasonable approximation to the energy. This result demonstrates the power of orbital optimization.

Notice that over the entire range, the deviation from FullCI for both v2DM and v2DM-DOCI is roughly equal.

We tried a 50 sites Hubbard model but hit a wall with the orbital optimizer. The Hilbert space becomes so large that the number of Jacobi rotations required to find the optimal orbitals becomes unmanageable. In this case, a full Hessian approach would be more beneficial, despite the associated expensive two-body integral transformation.

We end this chapter with the remark that v2DM-DOCI indeed seems like a very good approximation to FullDOCI, when using the same set of orbitals. The major difficulty is finding the optimal set of orbitals: the choice of the starting point is crucial.

QUANTUM & PIXEL

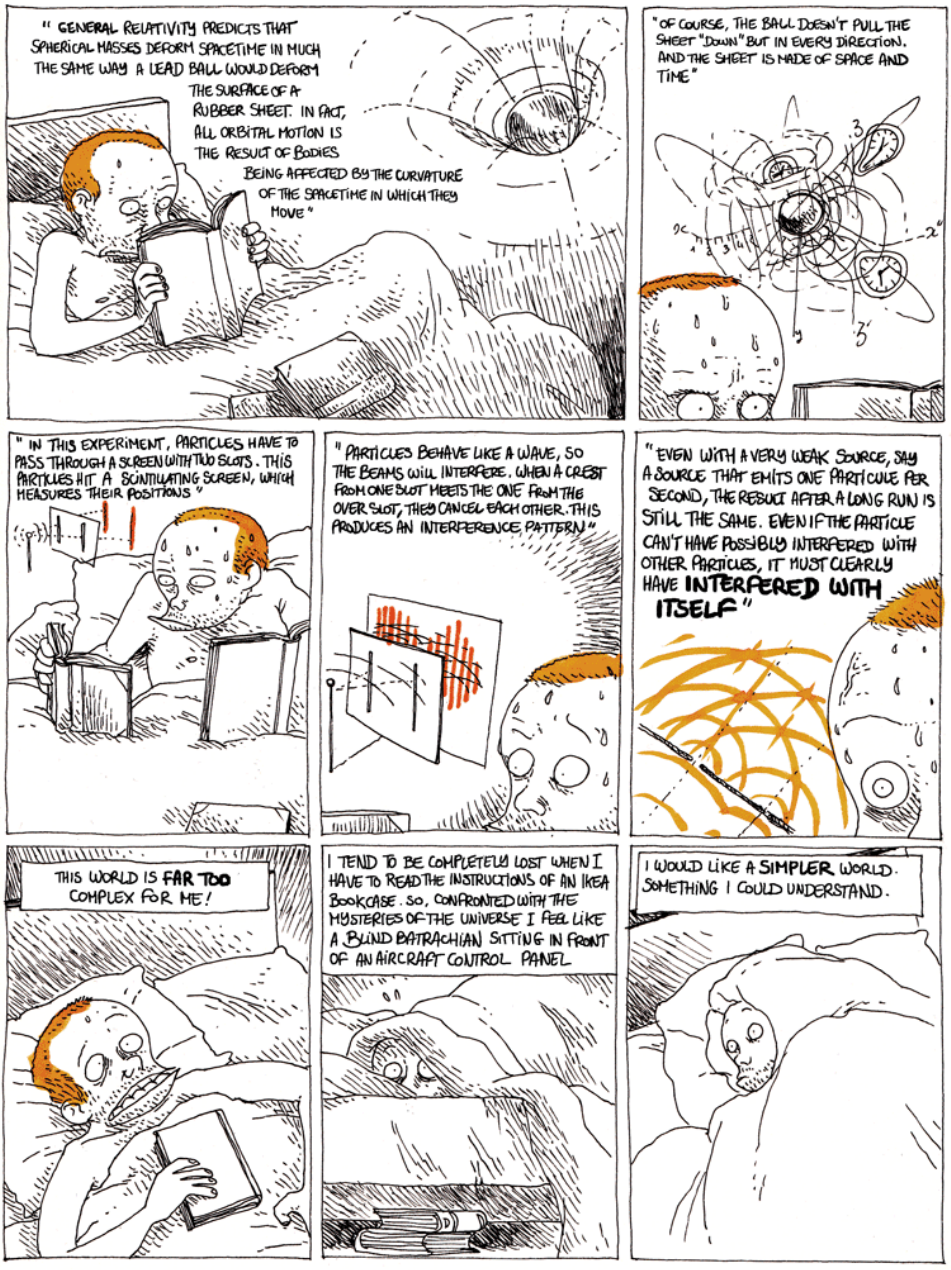


Something like that, yeah ! Nothing too complex ! No bending spacetime, no freaking lead balls on some rubber sheet !
Nothing's wrong with a bit of bidimensionality ! A cool world, with natural laws you can understand at first sight !
Oh ! Professor Hawking ! Thanks for coming ! Alas, I'm afraid you won't have much to study in here ! Ha ! Ha ! Ha !
I wouldn't say so, Boulet my friend ! I'm studying pixelic relativity, this is fascinating !
Er... Uh ?
Allow me to explain. I discovered that the pixel was relative: It depends of the observer's point of view. I call that the «Relative Definition». For example: at close range, an object will appear composed of hundreds of pixels...
... But from some distance, the same object will appear composed by only a few pixels.
The pixel is the smallest particle we know, but it contains a lot of information. It's very strange. Take a look in this microscope, you will see the minimum resolution of the universe.
These creatures are the smallest we know. They are made with only a very few pixels, however they can have very elaborate behaviors. We think they hide a lot of hidden data, beyond their pixels: the famous «bits» whose existence we try to prove in giant pixel accelerators.
But calculations are impossible ! At this scale, mathematic laws don't apply any more ! For example, in a square of side = x, we know that the diagonal equals x√2... But at pixellic scale it doesn't ! the diagonal is made of THE SAME NUMBER OF PIXELS AS ITS SIDE !

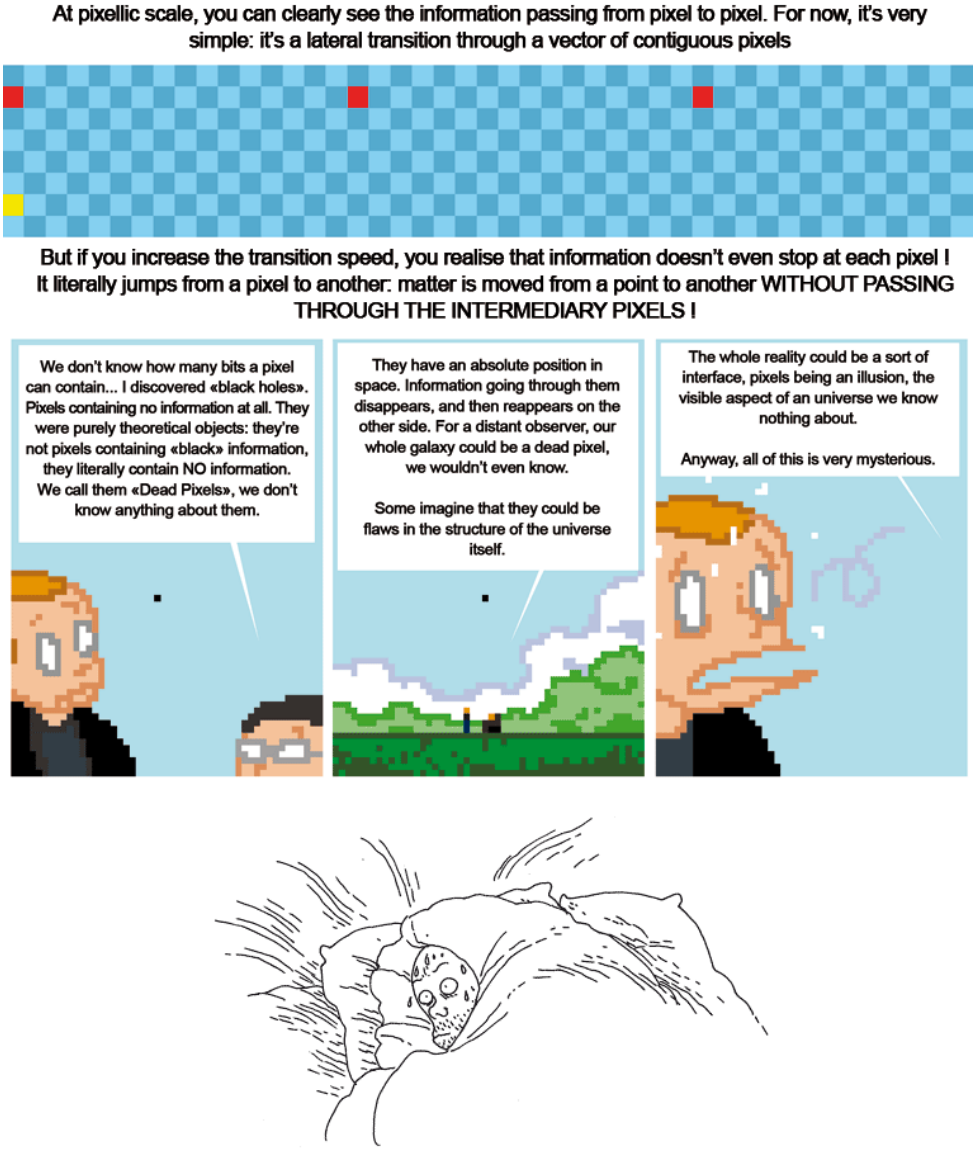

Reproduced with permission from my favorite cartoonist, Boulet. Copyright Boulet, from http://english.bouletcorp.com.

Chapter 5

Conclusions

The true delight is in the finding out rather than in the knowing.
Isaac Asimov

In this work we have introduced the Variational Optimization of the second-order reduced Density Matrix to solve the many-body problem. The second-order reduced Density Matrix (2DM) contains all necessary information to describe such a system, and the expectation value of one- or two-particle operators can be expressed as a linear function of the 2DM. Unlike the more conventional quantum mechanical methods, the wave function is never used. This method itself has a long history and attracted quite some attention in the second half of the previous century. At first glance, it has many interesting properties: the 2DM has a much better scaling than the wave function, and the method is strictly variational. Unlike wavefunction-based methods, it produces a strict lower bound on the energy (instead of an upper bound). Unfortunately, the complexity of the many-body problem has not disappeared, but is shifted to the N-representability problem: what are the necessary and sufficient conditions for a 2DM to be derivable from an ensemble of many-fermion wave functions? In the 1960's, there was still hope that this problem could be solved in some way, but time has learned that it is a very hard problem (see later).

A major breakthrough came when it was realized that the v2DM problem could be formulated as a Semidefinite Programming problem. This opened a whole new toolbox of methods to perform the optimization. It resparked interest, leading to numerous extensions and improvements to the method. However, the difficulty of the N-representability problem reared its ugly head again, and interest in the method is fading. The technique has been called a dead end several times. One of the goals of this work is to show

the flexibility of the method: by using a subclass of N-representability conditions, we can increases the performance of the method considerably while still finding a good approximation to the energy. We hope that after reading this work, the reader will agree that there are still interesting paths left to discover. We will first iterate over the contents of the chapters in this work, to end with a general conclusion and outlook.

In Chapter 2 we formally introduced the N-representability problem. A theorem about the necessary and sufficient conditions for N-representability was shown and proven. Unfortunately, this theorem does not give us a practical way to enforce N-representability. We introduced the formal complexity class of the N-representability problem: Quantum Merlin Arthur. This means that in general it is very hard to find a solution to the problem but once a solution has been found, it is easy to verify the correctness of the solution. This scatters all hope of finding a general solution to the N-representability problem. It may be possible to find a solution in specific instances of the problem. This does not necessarily mean that the situation is hopeless, after all Density Functional Theory belongs to the same complexity class and this has not held its practical usage back.

Next we showed how the N-representability theorem can be used to generate a set of necessary conditions. The necessary conditions on the 1DM turn out to be also sufficient. For the 2DM we derive a set of two-index and three-index conditions. Using the same formalism, we derive all three-index conditions with the 3DM as the basic object. These conditions can be simplified by exploiting the symmetry of the system. We show that by utilizing the spin freedom we can reduce the 2DM into a singlet and a (three-fold degenerate) triplet block. The spatial point-group symmetry of a system reduces the 2DM into blocks per irreducible representation. The actual gain is dependent on the specific spatial symmetry.

Until now, the only assumptions we made about the fermionic wave function was that it is normalized and antisymmetric. Now we will restrict ourself to Doubly Occupied Configuration Interaction-type wave functions: in the Configuration Interaction expansion only the Slater determinants were all orbitals are either doubly occupied or empty are used. This is a so-called seniority-zero approximation to the wave function. The structure of all density matrices is greatly simplified by this assumption. The matrix positivity of the 2DM is equivalent with the matrix positivity of an $L \times L$ block (with the L the number of spatial orbitals), combined with a set of linear inequalities. A similar reduction is possible for the 3DM. Finally we formulate the v2DM problem we want to solve using the derived N-representability conditions.

In Chapter 3 we introduce a convex optimization problem called Semidefinite

Programming. Its so-called primal and dual formulation are derived, and the relationship between both is shown. We reformulate our v2DM problem as a primal SDP problem. An interior-point method is introduced to solve the problem. By adding a barrier function to the objective function, we cannot leave the feasible region and the problem is reduced to an unconstrained optimization for which we use a Newton-Raphson method. We steadily decrease the barrier until we have found the optimal solution. In every iteration a linear system of equations must be solved. We have implemented this efficiently by using a matrix-vector product of the Hessian without ever constructing the Hessian itself. As we approach the optimal point on the boundary of the feasible region, the condition number of the matrix gets worse and the number of iterations required to solve the linear system increases. This limits the usability of this method for large systems.

As a possible solution, we discuss an augmented Lagrangian technique: the boundary point method. In this method, the duality gap is always zero and we alternately project on the primal and dual feasibility until at convergence we find a point that is both primal and dual feasible. This method was developed for large systems and it is noticeably faster than other methods, although the principal scaling is the same: L^6 for the two-index conditions and L^9 for the three-index conditions. The disadvantage of the boundary point method is that it is much less stable than the potential reduction method. While the potential reduction method can be used as a black box routine, this is certainly not the case for the boundary point method.

In Chapter 4 we motivate our interest in DOCI wave functions. The idea of using electron pairs as the basic building blocks for wave functions is old. Many types of pairing-based wave functions exist, but if the spin-pairing scheme is used, DOCI is the most general type. It can be considered as the lowest rung on the ladder in the seniority hierarchy. When seniority-two, four, etc. Slater determinants are added, the result quickly convergences to FullCI. The hope is that DOCI can capture the bulk of the static correlation. Unfortunately FullDOCI still has a factorial scaling. A mean-field scaling wave function-based approximation to it was developed: AP1roG. We approximate the 2DM as being derivable from a DOCI wave function.

An important aspect of DOCI is its orbital dependence: any truncated CI wave function is orbital dependent. However, finding the optimal set of orbitals is a hard problem: it means finding the global minimum in an uncharted energy landscape. The associated transformation to the new orbitals scales as L^5 and forms the bottleneck in the entire algorithm. Our solution to this is to use Jacobi rotations. As they only mix two orbitals at a time, the integral transformation can be done very efficiently. As any orthogonal transformation can be decomposed in a series of Jacobi rotations, this

presents no limitations. The usual approach for orbital optimization is to work with a second order Taylor series for the unitary transformation. Using Jacobi rotations avoids this second-order approximation.

After having derived the necessary transformation formulas and discussed the fine details of the orbital optimizer, we use our new algorithm, v2DM-DOCI, on a few test cases. The DOCI wave function is exact for a two-electron system, as is v2DM: for the H_2 molecule we find the FullCI energy, as expected. However, the dissociation of the He dimer fails. This shows the importance of spatial symmetry breaking. To find the optimal set of orbitals, DOCI needs to break the spatial symmetry of the system. When we perform the calculation using C_1 symmetry, the FullCI energy is recovered by v2DM-DOCI in the limit of full dissociation. A visualization of the natural orbitals shows that by breaking the symmetry, the orbitals on each atom of the dissociated system of two He atoms can optimize separately. The next system we try is the deformation of a H_4 rectangle. At the square configuration, the four hydrogen atoms are degenerate. This leads to a cusp in the RHF energy and the symmetry-broken v2DM-DOCI energy. The symmetry broken solution is found by starting from Edmiston-Ruedeberg localized orbitals.

As a prototype for strong correlation, we test our method on the symmetric dissociation of an H_8 chain. Again the symmetry-adapted v2DM-DOCI energy gives a wrong description of the system. There even seem to be two different regimes. However, looking at the occupation numbers and the shape of the orbitals, the differences can be fully understood. The D_{2h} symmetry of the system forbids the system to go in a state of 4 H_2 atoms.

We continue by testing v2DM-DOCI on the dissociation of N_2, CN^-, NO^+ and CO. The results for N_2 are good: v2DM-DOCI is consistently a better approximation to FullDOCI than v2DM to FullCI. However, in case of the CN^- and NO^+ molecule we suffer from a known failure of v2DM *i.e.* fractional charges on the dissociated atoms. As the particle vs energy curve for v2DM is convex instead of piecewise linear, we end up with a fractional electron partitioning over two dissociated atoms. A solution exists in the form of subsystem constraints, but these are expensive to add. The v2DM-DOCI calculation using the optimal set of orbitals from FullDOCI does produce the correct energy. This seems to hint that a solution to this problem can be found in the orbital optimization. The CO molecule does not suffer from this problem, and we see the same picture as in the N_2 case: v2DM-DOCI is a very good approximations to FullDOCI.

We hope that the reader is convinced that there still is a future for v2DM in the form of v2DM-DOCI. It does not suffer from the bad scaling of v2DM and it seems to be a better approximation to FullDOCI than v2DM is to FullCI.

However, the story is not yet over. The orbital optimizer still has room for improvement: better starting points still need to be sought. An approximation to the Brueckner determinant might yield a good starting point. It would also be interesting to investigate other methods for finding the optimal orbitals: the basin-hopping method[236] seems interesting. It works by performing a series of local minimizations to approximate the energy landscape. However, it requires a good metric on the landscape to 'jump' to the next valley.

A practical implementation of the 3DM conditions has not yet been realized. It seems reasonable to assume that their effect will be similar to the general case: increase the energy to milliHartree accuracy. Furthermore, we did not verify the correctness of the 2DM itself: a good approximation to the energy does not necessarily produce a good approximation to the 2DM. Using the 3DM conditions will certainly improve this.

As a last step we can use perturbation theory to add the missing dynamic correlation to the energy. This should give us an good approximation to the FullCI energy.

Part II

Papers

Paper 1

Variational Two-Particle Density Matrix Calculation for the Hubbard Model Below Half Filling Using Spin-Adapted Lifting Conditions

https://dx.doi.org/10.1103/PhysRevLett.108.213001

Paper 2

Extensive v2DM study of the one-dimensional Hubbard model for large lattice sizes: Exploiting translational invariance and parity

https://dx.doi.org/10.1016/j.comptc.2012.09.014

Paper 3

Variational optimization of the 2DM: approaching three-index accuracy using extended cluster constraints

https://dx.doi.org/10.1140/epjb/e2014-40788-x

Paper 4

Variational Optimization of the Second-Order Density Matrix Corresponding to a Seniority-Zero Configuration Interaction Wave Function

https://dx.doi.org/10.1021/acs.jctc.5b00378

Paper 5

Polynomial scaling approximations and Dynamic Correlation Corrections to Doubly Occupied Configuration Interaction wave functions

https://dx.doi.org/10.1063/1.4930260

Appendices

Appendix A

List of publications

- B. Verstichel, H. van Aggelen, W. Poelmans, D. Van Neck, "Variational Two-Particle Density Matrix Calculation for the Hubbard Model Below Half Filling Using Spin-Adapted Lifting Conditions", *Physical Review Letters* **108**, 213001 (2012)

- B. Verstichel, H. van Aggelen, W. Poelmans, S. Wouters, D. Van Neck, "Extensive v2DM study of the one-dimensional Hubbard model for large lattice sizes: Exploiting translational invariance and parity", *Computational and Theoretical Chemistry* **1003**, 12-21 (2013)

- B. Verstichel, W. Poelmans, S. De Baerdemacker, S. Wouters, D. Van Neck, "Variational optimization of the 2DM: approaching three-index accuracy using extended cluster constraints", *The European Physical Journal B* **87**, 59 (2014)

- S. Wouters, W. Poelmans, P.W. Ayers, D. Van Neck, "CheMPS2: a free open-source spin-adapted implementation of the density matrix renormalization group for ab initio quantum chemistry", *Computer Physics Communications*, **185**, 1501-1514 (2014)

- M. Van Houteghem, A. Ghysels, T. Verstraelen, W. Poelmans, M. Waroquier, V. Van Speybroeck, "Critical analysis of the accuracy of models predicting or extracting liquid structure information", *Journal of Physical Chemistry B*, **118**, 2451–2470, (2014)

- S. Wouters, W. Poelmans, S. De Baerdemacker, P.W. Ayers, D. Van Neck, "CheMPS2: Improved DMRG-SCF routine and correlation functions", *Computer Physics Communications*, **191**, 235-237, (2015)

- W. Poelmans, M. Van Raemdonck, B. Verstichel, S. De Baerdemacker, A. Torre, L. Lain, G. Massaccesi, D. Alcoba, P. Bultinck, D. Van Neck, "Variational optimization of the second order density matrix corresponding to a seniority-zero configuration interaction wave function", *Journal of Chemical Theory and Computation*, **11**, 4064-4076, (2015)

- M. Van Raemdonck, D. Alcoba, W. Poelmans, S. De Baerdemacker, A. Torre, L. Lain, G. Massaccesi, P. Bultinck, D. Van Neck, "Polynomial scaling approximations and Dynamic Correlation Corrections to Doubly Occupied Configuration Interaction wave functions", *Journal of Chemical Physics*, **143**, 104106 (2015)

- K. Lejaeghere, G. Bihlmayer, T. Björkman, P. Blaha, S. Blügel, V. Blum, D. Caliste, I. E. Castelli, S. J. Clark, A. Dal Corso, S. de Gironcoli, T. Deutsch, J. Kay Dewhurst, I. Di Marco, C. Draxl, M. Dułak, O. Eriksson, J. A. Flores-Livas, K. F. Garrity, L. Genovese, P. Giannozzi, M. Giantomassi, S. Goedecker, X. Gonze, O. Grånäs, E. K. U. Gross, A. Gulans, F. Gygi, D. R. Hamann, P. J. Hasnip, N. A. W. Holzwarth, D. Iuşan, D. B. Jochym, F. Jollet, D. Jones, G. Kresse, K. Koepernik, E. Küçükbenli, Y. O. Kvashnin, I. L. M. Locht, S. Lubeck, M. Marsman, N. Marzari, U. Nitzsche, L. Nordström, T. Ozaki, L. Paulatto, C. J. Pickard, W. Poelmans, M. I. J. Probert, K. Refson, M. Richter, G. Rignanese, S. Saha, M. Scheffler, M. Schlipf, K. Schwarz, S. Sharma, F. Tavazza, P. Thunström, A. Tkatchenko, M. Torrent, D. Vanderbilt, M. J. van Setten, V. Van Speybroeck, J. M. Wills, J. R. Yates, G. Zhang, S. Cottenier, "The Kohn-Sham equation of state for elemental solids: a solved problem", *Science* (2015) (submitted)

Appendix B

Second quantization

The second quantization formalism is used in this work. This appendix will give a very short introduction to the fermionic case. A complete introduction can be found in references 237 and 2. The state on which the operators acts is the antisymmetric N particle state,

$$|\alpha_1\alpha_2\ldots\alpha_N\rangle = -|\alpha_2\alpha_1\ldots\alpha_N\rangle\,. \tag{B.1}$$

The operator $\hat{a}^\dagger_\alpha$ creates a particle in the single-particle state α

$$\hat{a}^\dagger_\alpha\,|\alpha_1\alpha_2\alpha_N\rangle = |\alpha\alpha_1\alpha_2\ldots\alpha_N\rangle\,, \tag{B.2}$$

while the annihilation operator, $\hat{a}_\alpha$, does the opposite

$$\hat{a}_\alpha\,|\alpha\alpha_1\alpha_2\alpha_N\rangle = |\alpha_1\alpha_2\ldots\alpha_N\rangle\,. \tag{B.3}$$

We will use $|\rangle$ to denote the particle vacuum,

$$\hat{a}_\alpha\,|\rangle = 0. \tag{B.4}$$

The addition and removal operators obey the fundamental anticommutation relations:

$$\{\hat{a}_\alpha, \hat{a}^\dagger_\beta\} = \hat{a}_\alpha\hat{a}^\dagger_\beta + \hat{a}^\dagger_\beta\hat{a}_\alpha = \delta_{\alpha\beta}, \tag{B.5a}$$

$$\{\hat{a}_\alpha, \hat{a}_\beta\} = \{\hat{a}^\dagger_\alpha, \hat{a}^\dagger_\beta\} = 0. \tag{B.5b}$$

Note that the Pauli exclusion principle nicely follows from this:

$$\hat{a}^\dagger_\alpha\hat{a}^\dagger_\alpha = -\hat{a}^\dagger_\alpha\hat{a}^\dagger_\alpha = 0, \tag{B.6}$$

i.e. every single-particle state can be occupied by at most one fermion. A one-body operator $\hat{T}$ can be written in this formalism as

$$\hat{T} = \sum_{\alpha\beta} \langle \alpha | T | \beta \rangle \, \hat{a}^\dagger_\alpha \hat{a}_\beta. \tag{B.7}$$

For a two-body operator $\hat{V}$, this becomes

$$\hat{V} = \frac{1}{4} \sum_{\alpha\beta\gamma\delta} \langle \alpha\beta | V | \gamma\delta \rangle \, \hat{a}^\dagger_\alpha \hat{a}^\dagger_\beta \hat{a}_\delta \hat{a}_\gamma. \tag{B.8}$$

Note that the order for γ and δ in the operators and the two-body matrix element is different. An alternative form for eq. (B.8) is

$$\hat{V} = \frac{1}{2} \sum_{\alpha\beta\gamma\delta} (\alpha\beta | V | \gamma\delta) \hat{a}^\dagger_\alpha \hat{a}^\dagger_\beta \hat{a}_\delta \hat{a}_\gamma, \tag{B.9}$$

where

$$\langle \alpha\beta | V | \gamma\delta \rangle = (\alpha\beta | V | \gamma\delta) - (\alpha\beta | V | \delta\gamma), \tag{B.10}$$

and $|\alpha\beta)$ is a direct product state (not antisymmetric). A much used operator is the number operator

$$\hat{n} = \sum_\alpha \hat{a}^\dagger_\alpha \hat{a}_\alpha, \tag{B.11}$$

which simply counts the number of particles in a state:

$$\hat{n} \, |\alpha_1 \alpha_2 \dots \alpha_N \rangle = N \, |\alpha_1 \alpha_2 \dots \alpha_N \rangle \tag{B.12}$$

Appendix C

Mathematics

All results shown here can be found in references 22, 161, 164.

C.1 Convexity

A set S in a linear space is convex if and only if for every $x_1, x_2 \in S$ holds

$$\alpha x_1 + \beta x_2 \in S, \tag{C.1}$$

with $\alpha, \beta \geq 0$ and $\alpha + \beta = 1$. This means that the line segment connecting any two points in the set must also be part of the set.

A function $f : \mathbb{R}^n \to \mathbb{R}$ is convex if the domain of f is a convex set and for any two points x and y in the domain of f must hold

$$f(\alpha x + \beta y) \leq \alpha f(x) + \beta f(y), \tag{C.2}$$

with $\alpha, \beta \geq 0$ and $\alpha + \beta = 1$. One can prove that a function is convex if on a convex set its Hessian is positive semidefinite.

C.2 Positive semidefinite matrices

We now restrict ourself to symmetric matrices. A symmetric matrix is always diagonalizable by a orthogonal matrix and has real eigenvalues. We call a symmetric matrix $A \in \mathbb{R}^{n \times n}$ positive semidefinite when

$$\forall z \in \mathbb{R}^n : \quad z^T A z \geq 0. \tag{C.3}$$

When the inequality is strict, the symmetric matrix is positive definite. In exactly the same way a negative (semi)definite matrix can be introduced. When a matrix is neither positive or negative, it is called indefinite. From now on, we will use $\succeq$ to denote that a matrix is positive semidefinite.

In a sense, a positive semidefinite matrix is the equivalent of a positive number. The most important property of a positive semidefinite matrix is that all its eigenvalues are real and non-negative. From this follows, if $A \succeq 0$ then

$$\det A \geq 0, \tag{C.4}$$
$$\mathrm{Tr}\,(A) \geq 0, \tag{C.5}$$
$$A_{ii} \geq 0, \tag{C.6}$$
$$\exists! S \succeq 0 \quad A = SS. \tag{C.7}$$

Furthermore, when $A \succeq 0$ and $B \succeq 0$ then

$$A \succeq 0, B \succeq 0 \Rightarrow A + B \succeq 0, \tag{C.8}$$
$$[A, B] = 0 \Rightarrow AB \succeq 0, \tag{C.9}$$
$$ABA \succeq 0,\ BAB \succeq 0, \tag{C.10}$$
$$\mathrm{Tr}\,(AB) = 0 \Rightarrow AB = 0, \tag{C.11}$$

The set of positive semidefinite matrices has the mathematical structure of a cone: for every $A \succeq 0$ we have that $\lambda A \succeq 0$, when $\lambda > 0$. A cone is a substructure of a vector space. It is convex when any combination $\alpha A + \beta B$ is also an element of the cone for $\alpha > 0$ and $\beta > 0$. Every cone has a dual cone. Let C be the cone and V the underlying vector space of real-symmetric matrices, then the set

$$v \in V : \forall w \in C, \mathrm{Tr}\,(vw) \geq 0, \tag{C.12}$$

is the dual cone of C. The dual cone is not important for this work as the cone of positive semidefinite matrices is self-dual: the cone and the dual cone are the same.

C.3 Eigenvalues of symmetric matrices

A real symmetric $n \times n$ matrix A will have the same spectrum as a matrix B if they only differ in the sign of the off-diagonal matrix elements:

$$A = \begin{bmatrix} a_{11} & a_{12} & \dots & a_{1n} \\ a_{21} & a_{22} & \dots & a_{2n} \\ \vdots & \vdots & \ddots & \vdots \\ a_{n1} & a_{n2} & \dots & a_{nn} \end{bmatrix} \qquad B = \begin{bmatrix} a_{11} & -a_{12} & \dots & -a_{1n} \\ -a_{21} & a_{22} & \dots & -a_{2n} \\ \vdots & \vdots & \ddots & \vdots \\ -a_{n1} & -a_{n2} & \dots & a_{nn} \end{bmatrix}$$

We call this the Verstichel-Claeys theorem. It is trivial in the case of a 2×2 matrix. For a 3×3 matrix it can be proven by first diagonalizing the upper 2×2 block:

$$A = \begin{bmatrix} \lambda_1 & 0 & a_{13} \\ 0 & \lambda_2 & a_{23} \\ a_{31} & a_{32} & a_{33} \end{bmatrix} \qquad B = \begin{bmatrix} \lambda_1 & 0 & -a_{13} \\ 0 & \lambda_2 & -a_{23} \\ -a_{31} & -a_{32} & a_{33} \end{bmatrix}$$

If we multiple the last row/column of B with -1, its determinant remains unchanged. As the determinant of A and B are now the same, they will have the same spectrum (as the first two eigenvalues are already equal). In this fashion, the 4×4 case can also be proven. By induction it can be proven for arbitrary n.

C.4 Useful results for determinants

- Let M be a symmetric block matrix of the form

$$M = \begin{bmatrix} A & B \\ B & A \end{bmatrix}, \tag{C.13}$$

  then the determinant of M is

$$\det M = \det (A + B) \det (A - B). \tag{C.14}$$

- For any real symmetric matrix function $A(x)$, we can define the function $\phi(x)$ as

$$\phi(x) = -\log \det A(x). \tag{C.15}$$

  The derivative is given by

$$\frac{\partial \phi(x)}{\partial x} = -\mathrm{Tr} \left(A(x)^{-1} \frac{\partial A(x)}{\partial x} \right). \tag{C.16}$$

C.5 Wedge product

The wedge product of two antisymmetric maps $a : \mathbb{R}^n \to \mathbb{R}$ and $b : \mathbb{R}^m \to \mathbb{R}$ is given by

$$a \wedge b(x_1, \ldots, x_n, x_{n+1}, \ldots, x_{m+n}) = \sum_{\sigma \in Sh_{k,m}} \mathrm{sgn}\sigma \; a(x_{\sigma(1)}, \ldots, x_{\sigma(n)}) \; b(x_{\sigma(n+1)}, \ldots, x_{\sigma(n+m)}), \tag{C.17}$$

where the summation runs over all so-called n, m shuffles. This the set of permutations on $n+m$ objects, such that the first n elements and the last m elements are ordered: $\sigma(1) \leq \ldots \leq \sigma(n)$ and $\sigma(n+1) \leq \ldots \leq \sigma(n+m)$. As an example, let us look at the wedge product of two 1DM's

$$(\rho \wedge \rho)_{\alpha\beta;\gamma\delta} = \rho_{\alpha\gamma}\rho_{\beta\delta} - \rho_{\alpha\delta}\rho_{\beta\gamma}. \tag{C.18}$$

Appendix D

Clebsch-Gordan coefficients

In general Clebsch-Gordan coefficients are the coefficients needed to couple multiple irreducible representations of a group. This appendix is about the Clebsch-Gordan coefficients for the $SU(2)$ group, which are needed to couple the fermion spins. We refer to references 99, 238 and 92 for a full overview.

We want to couple two spins j_1 and j_2 together to good total spin J

$$|j_1 j_2; JM\rangle = \sum_{m_1 m_2} \langle j_1 m_1 j_2 m_2 | JM\rangle \, |j_1 m_1\rangle \, |j_2 m_2\rangle \,, \tag{D.1}$$

where $\langle j_1 m_1 j_2 m_2 | JM\rangle$ is the Clebsch-Gordan coefficient. The inverse transformation is

$$|j_1 m_1\rangle \, |j_2 m_2\rangle = \sum_{JM} \langle j_1 m_1 j_2 m_2 | JM\rangle \, |j_1 j_2; JM\rangle \,. \tag{D.2}$$

There are orthogonality relations

$$\sum_{m_1 m_2} \langle j_1 m_1 j_2 m_2 | JM\rangle \, \langle j_1 m_1 j_2 m_2 | J'M'\rangle = \delta_{JJ'} \delta_{MM'}, \tag{D.3}$$

$$\sum_{JM} \langle j_1 m_1 j_2 m_2 | JM\rangle \, \langle j_1 m_1' j_2 m_2' | JM\rangle = \delta_{m_1 m_1'} \delta_{m_2 m_2'}. \tag{D.4}$$

An alternative notation are the Wigner 3j-symbols

$$\langle j_1 m_1 j_2 m_2 | j_3 m_3\rangle = (-1)^{j_1 - j_2 + m_3} \frac{1}{\sqrt{2j_3 + 1}} \begin{pmatrix} j_1 & j_2 & j_3 \\ m_1 & m_2 & -m_3 \end{pmatrix}. \tag{D.5}$$

In this case, the orthogonality relations eqs. (D.3) and (D.4) become

$$\sum_{m_1 m_2} \begin{pmatrix} j_1 & j_2 & j_3 \\ m_1 & m_2 & m_3 \end{pmatrix} \begin{pmatrix} j_1 & j_2 & j_3' \\ m_1 & m_2 & m_3' \end{pmatrix} = \delta_{j_3 j_3'} \delta_{m_3 m_3'} \frac{1}{2j_3+1}, \tag{D.6}$$

$$\sum_{j_3 m_3} (2j_3+1) \begin{pmatrix} j_1 & j_2 & j_3 \\ m_1 & m_2 & m_3 \end{pmatrix} \begin{pmatrix} j_1 & j_2 & j_3 \\ m_1' & m_2' & m_3 \end{pmatrix} = \delta_{m_1 m_1'} \delta_{m_2 m_2'}. \tag{D.7}$$

The Clebsch-Gordan coefficients have the following symmetry,

$$\langle j_1 m_1 j_2 m_2 | JM \rangle = (-1)^{j_1+j_2-J} \langle j_2 m_2 j_1 m_1 | JM \rangle, \tag{D.8}$$

$$= (-1)^{j_1+j_2-J} \langle j_1 {-m_1} j_2 {-m_2} | J {-M} \rangle. \tag{D.9}$$

In the case of $J = 0$, we have

$$\langle j_1 m_1 j_2 m_2 | 00 \rangle = \delta_{j_1 j_2} \delta_{m_1 -m_2} \frac{(-1)^{j_1-m_1}}{\sqrt{2j_1+1}}. \tag{D.10}$$

In the case of $j_1 = j_2 = 1/2$, we have

$$\langle \frac{1}{2} \frac{1}{2} \frac{1}{2} \frac{1}{2} | 11 \rangle = \langle \frac{1}{2} {-\frac{1}{2}} \frac{1}{2} {-\frac{1}{2}} | 1{-1} \rangle = 1, \tag{D.11}$$

$$\langle \frac{1}{2} {-\frac{1}{2}} \frac{1}{2} \frac{1}{2} | 10 \rangle = \langle \frac{1}{2} \frac{1}{2} \frac{1}{2} {-\frac{1}{2}} | 10 \rangle = \sqrt{\frac{1}{2}}, \tag{D.12}$$

$$\langle \frac{1}{2} {-\frac{1}{2}} \frac{1}{2} \frac{1}{2} | 00 \rangle = -\sqrt{\frac{1}{2}}, \tag{D.13}$$

$$\langle \frac{1}{2} \frac{1}{2} \frac{1}{2} {-\frac{1}{2}} | 00 \rangle = \sqrt{\frac{1}{2}}. \tag{D.14}$$

In a Hilbert space with an angular momentum operator $\hat{\boldsymbol{J}}$, one can define a spherical tensor operator $\hat{A}^j_m$ as an operator that obeys the following commutator relations

$$[\hat{J}_+, \hat{A}^j_m] = \sqrt{(j \pm m + 1)(j \mp m)} \hat{A}^j_{m\pm 1}, \tag{D.15}$$

$$[\hat{J}_z, \hat{A}^j_m] = m \hat{A}^j_m. \tag{D.16}$$

It is a generalization of the eigenstates $|jm\rangle$ for the $\hat{J}_z$ operator. Spherical tensor operators are important in the context of the Wigner-Eckart theorem. What is important to note, is that the Hermitian adjoint of a spherical tensor operator is not a spherical tensor operator, but needs an additional factor

$$\tilde{A}^j_m = (-1)^{j+m} \left(A^j_{-m} \right)^\dagger. \tag{D.17}$$

The spherical tensor operators used in this work are

$$\hat{a}^\dagger_{jm}, \qquad \tilde{\hat{a}}_{jm} = (-1)^{j+m} \, \hat{a}_{j\ -m}. \tag{D.18}$$

Appendix E

Formulas for Jacobi rotations

In Section 4.2 on page 91 we have introduced an orbital optimizer based on Jacobi rotations. The energy change under a Jacobi rotation can be calculated using Equation (4.24). In this appendix we give the formula to update the reduced Hamiltonian for a Jacobi rotation. If we rotate between orbitals k and l over an angle θ than the update formulas are for the case $\forall a, b \notin \{k, l\}$

$$K'_{a\bar{a};b\bar{b}} = K_{a\bar{a};b\bar{b}},\ K'_{ab;ab} = K_{ab;ab}, \tag{E.1}$$

while for the case $\forall b \notin \{k, l\}$

$$K'_{k\bar{k};b\bar{b}} = \cos^2\theta V_{kkbb} - 2\cos\theta\sin\theta V_{klpp} + \sin^2\theta V_{llpp}, \tag{E.2}$$

$$K'_{l\bar{l};b\bar{b}} = \cos^2\theta V_{llbb} + 2\cos\theta\sin\theta V_{klpp} + \sin^2\theta V_{kkpp}, \tag{E.3}$$

$$\begin{aligned} K'_{kb;kb} = {} & \frac{1}{N-1}\left(T_{bb} + \cos^2\theta T_{kk} - 2\sin\theta\cos\theta T_{kl} + \sin^2\theta T_{ll}\right) + \\ & \cos^2\theta\left(V_{kbkb} - \frac{1}{2}V_{kbbk}\right) - 2\cos\theta\sin\theta\left(V_{kblb} - \frac{1}{2}V_{kbbl}\right) + \\ & \sin^2\theta\left(V_{lblb} - \frac{1}{2}V_{lbbl}\right), \end{aligned} \tag{E.4}$$

$$\begin{aligned} K'_{lb;lb} = {} & \frac{1}{N-1}\left(T_{bb} + \cos^2\theta T_{ll} - 2\sin\theta\cos\theta T_{kl} + \sin^2\theta T_{kk}\right) + \\ & \cos^2\theta\left(V_{lblb} - \frac{1}{2}V_{lbbl}\right) + 2\cos\theta\sin\theta\left(V_{kblb} - \frac{1}{2}V_{kbbl}\right) + \\ & \sin^2\theta\left(V_{kbkb} - \frac{1}{2}V_{kbbk}\right). \end{aligned} \tag{E.5}$$

The remaining cases are

$$K'_{k\bar{k};k\bar{k}} = \frac{2}{N-1}\left(\cos^2\theta T_{kk} - 2\sin\theta\cos\theta T_{kl} + \sin^2\theta T_{ll}\right) + \cos^4\theta V_{kkkk} + \sin^4\theta V_{llll} + \cos^2\theta\sin^2\theta\left(4V_{kkll} + 2V_{klkl}\right) - 4\cos\theta\sin^3\theta V_{klll} - 4\cos^3\theta\sin\theta V_{klkk}, \tag{E.6}$$

$$K'_{l\bar{l};l\bar{l}} = \frac{2}{N-1}\left(\cos^2\theta T_{ll} + 2\sin\theta\cos\theta T_{kl} + \sin^2\theta T_{kk}\right) + \cos^4\theta V_{llll} + \sin^4\theta V_{kkkk} + \cos^2\theta\sin^2\theta\left(4V_{kkll} + 2V_{klkl}\right) + 4\cos\theta\sin^3\theta V_{klkk} + 3\cos^3\theta\sin\theta V_{klll}, \tag{E.7}$$

$$K'_{k\bar{k};l\bar{l}} = \left(\cos^4\theta + \sin^4\theta\right)V_{kkll} + \cos^2\theta\sin^2\theta\left(V_{kkkk} + V_{llll} - 2V_{klkl} + V_{kkll}\right) + 2\left(\cos^3\theta\sin\theta - \cos\theta\sin^3\theta\right)\left(V_{klkk} - V_{klll}\right), \tag{E.8}$$

$$K'_{kl;kl} = \frac{1}{N-1}\left(T_{kk} + T_{ll}\right) + \cos^2\theta\sin^2\theta\left(\frac{1}{2}V_{kkkk} + V_{llll} - 3V_{kkll} + V_{klkl}\right) + \left(\cos^4\theta + \sin^4\theta\right)\left(V_{klkl} - \frac{1}{2}V_{kkll}\right) + \left(\cos^3\theta\sin\theta - \cos\theta\sin^3\theta\right)\left(V_{klkk} - V_{klll}\right). \tag{E.9}$$

Appendix F

Hermitian adjoint images

All N-representability constraints are expressed as an image of the 2DM (or 3DM). We require that these images are homogeneous[1], as it simplifies the mathematical treatment. This means that they must be scale invariant. In our case, they are even linear. We require that for $\alpha \in \mathbb{R}$

$$\mathcal{L}_i(\alpha\Gamma) = \alpha\mathcal{L}_i(\Gamma), \tag{F.1}$$

where $\mathcal{L}_i$ can be any N-representability constraint. As a consequence we have to change the $\mathfrak{Q}$ condition: the first term is simply the unity matrix which can be rewritten in homogeneous form using the trace condition

$$\begin{aligned}\mathfrak{Q}_{\alpha\beta;\gamma\delta}(\Gamma) = {} & \left(\delta_{\alpha\gamma}\delta_{\beta\delta} - \delta_{\alpha\delta}\delta_{\beta\gamma}\right)\frac{2\mathrm{Tr}\left(\Gamma\right)}{N(N-1)} + \Gamma_{\alpha\beta;\gamma\delta} \\ & - \delta_{\alpha\gamma}\rho_{\beta\delta} + \delta_{\beta\gamma}\rho_{\alpha\delta} + \delta_{\alpha\delta}\rho_{\beta\gamma} - \delta_{\beta\delta}\rho_{\alpha\gamma}.\end{aligned} \tag{F.2}$$

Any non-homogeneous image can be adapted in the same way.

Another very important and helpful concept are the Hermitian adjoint images which are defined by

$$\mathrm{Tr}\left(\mathcal{L}_i(\Gamma)A\right) = \mathrm{Tr}\left(\mathcal{L}_i^\dagger(A)\Gamma\right). \tag{F.3}$$

The adjoint image transforms from the constraint space to the 2DM space. The easiest way to derive them is to use the definition eq. (F.3). For the $\mathfrak{I}$ and $\mathfrak{Q}$ images, this is simple: they are self-adjoint, meaning that the image is also its adjoint. For the $\mathfrak{G}$ condition, we have

$$\begin{aligned}\mathfrak{G}^\dagger\left(A\right)_{\alpha\beta;\gamma\delta} = {} & \frac{1}{N-1}\left[\delta_{\beta\delta}\overline{A}_{\alpha\gamma} - \delta_{\alpha\delta}\overline{A}_{\beta\gamma} - \delta_{\beta\gamma}\overline{A}_{\alpha\delta} + \delta_{\alpha\gamma}\overline{A}_{\beta\delta}\right] \\ & - A_{\alpha\delta;\gamma\beta} + A_{\beta\delta;\gamma\alpha} + A_{\alpha\gamma;\delta\beta} - A_{\beta\gamma;\delta\alpha},\end{aligned} \tag{F.4}$$

1. A function is homogeneous with degree k when it is scale invariant: $f(\alpha x) = \alpha^k f(x)$.

where

$$\overline{A}_{\alpha\gamma} = \sum_{\lambda} A_{\alpha\lambda;\gamma\lambda} \,. \tag{F.5}$$

For the $\mathcal{T}_1$ image, it gets a bit more complicated. The adjoint transform from the three-particle space to the two-particle space. For the Hermitian adjoint image, we find

$$\begin{aligned} \mathcal{T}_1^\dagger\left(A\right)_{\alpha\beta;\gamma\delta} = \frac{2}{N(N-1)}\left(\delta_{\alpha\gamma}\delta_{\beta\delta} - \delta_{\alpha\delta}\delta_{\beta\gamma}\right)\mathrm{Tr}\; A + \overline{A}_{\alpha\beta;\gamma\delta} \\ - \frac{1}{2(N-1)}\left[\delta_{\beta\delta}\overline{\overline{A}}_{\alpha\gamma} - \delta_{\alpha\delta}\overline{\overline{A}}_{\beta\gamma} - \delta_{\beta\gamma}\overline{\overline{A}}_{\alpha\delta} + \delta_{\alpha\gamma}\overline{\overline{A}}_{\beta\delta}\right], \end{aligned} \tag{F.6}$$

with

$$\overline{A}_{\alpha\beta;\gamma\delta} = \sum_{\lambda} A_{\alpha\beta\lambda;\gamma\delta\lambda}, \tag{F.7}$$

$$\overline{\overline{A}}_{\alpha\gamma} = \sum_{\lambda\kappa} A_{\alpha\lambda\kappa;\gamma\lambda\kappa}. \tag{F.8}$$

The Hermitian adjoint for the $\mathcal{T}_2$ image is

$$\begin{aligned} \mathcal{T}_2^\dagger(A)_{\alpha\beta;\gamma\delta} = \frac{1}{2(N-1)}\left[\delta_{\beta\delta}\tilde{\tilde{A}}_{\alpha\gamma} - \delta_{\alpha\delta}\tilde{\tilde{A}}_{\beta\gamma} - \delta_{\beta\gamma}\tilde{\tilde{A}}_{\alpha\delta} + \delta_{\alpha\gamma}\tilde{\tilde{A}}_{\beta\delta}\right] \\ + \overline{A}_{\alpha\beta;\gamma\delta} - \left[\tilde{A}_{\delta\alpha;\beta\gamma} - \tilde{A}_{\delta\beta;\alpha\gamma} - \tilde{A}_{\gamma\alpha;\beta\delta} + \tilde{A}_{\gamma\beta;\alpha\delta}\right], \end{aligned} \tag{F.9}$$

where

$$\tilde{\tilde{A}}_{\alpha\gamma} = \sum_{\lambda\kappa} A_{\lambda\kappa\alpha;\lambda\kappa\gamma}, \tag{F.10}$$

$$\overline{A}_{\alpha\beta;\gamma\delta} = \sum_{\lambda} A_{\alpha\beta\lambda;\gamma\delta\lambda}, \tag{F.11}$$

$$\tilde{A}_{\alpha\beta;\gamma\delta} = \sum_{\lambda} A_{\lambda\alpha\beta;\lambda\gamma\delta}. \tag{F.12}$$

The Hermitian adjoint image for the $\mathcal{T}_2'$ condition is a bit more complex. It is found by requiring that

$$\begin{aligned} \mathrm{Tr}\left(\mathcal{T}_2'(\Gamma)A\right) &= \mathrm{Tr}\left(\left[\begin{pmatrix} \mathcal{T}_2\left(\Gamma\right) & \omega \\ \omega^\dagger & \rho \end{pmatrix}\begin{pmatrix} A_{\mathcal{T}} & A_\omega \\ A_\omega^\dagger & A_\rho \end{pmatrix}\right]\right) \\ &= \mathrm{Tr}\left(\left(\mathcal{T}_2'\right)^\dagger\left(A\right)\Gamma\right). \end{aligned} \tag{F.13}$$

This leads to

$$\begin{aligned} \mathcal{T}_2'^\dagger\left(A\right)_{\alpha\beta;\gamma\delta} = \mathcal{T}_2^\dagger(A_{\mathcal{T}}) + \left(A_\omega\right)_{\alpha\beta\delta;\gamma} + \left(A_\omega\right)_{\gamma\delta\beta;\alpha} \\ - \left(A_\omega\right)_{\alpha\beta\gamma;\delta} - \left(A_\omega\right)_{\gamma\delta\alpha;\beta} \\ + \frac{1}{N-1}\left(\delta_{\beta\delta}\left(A_\rho\right)_{\gamma\alpha} - \delta_{\alpha\delta}\left(A_\rho\right)_{\gamma\beta} - \delta_{\beta\gamma}\left(A_\rho\right)_{\delta\alpha} + \delta_{\alpha\gamma}\left(A_\rho\right)_{\delta\beta}\right). \end{aligned} \tag{F.14}$$

F.1 Spin symmetry

Since the matrices $\mathcal{L}^\dagger(A)$ are two-particle matrices, the spin-coupled version of the Hermitian adjoint maps is defined as:

$$\mathcal{L}^\dagger(A)^S_{ab;cd} = \frac{1}{\sqrt{(1+\delta_{ab})(1+\delta_{cd})}} \sum_{\sigma_a\sigma_b} \sum_{\sigma_c\sigma_d} \langle \frac{1}{2}\sigma_a \frac{1}{2}\sigma_b | SM \rangle \langle \frac{1}{2}\sigma_c \frac{1}{2}\sigma_d | SM \rangle \, \mathcal{L}^\dagger(A)_{a\sigma_a b\sigma_b; c\sigma_c d\sigma_d} \,. \quad \text{(F.15)}$$

The $\mathcal{G}^\dagger$ map: the first non-trivial Hermitian adjoint map is the $\mathcal{G}^\dagger$. Its spin-coupled form can be derived by substituting eq. (F.4) in eq. (F.15) and performing the necessary angular momentum algebra. This leads to:

$$\begin{aligned}\mathcal{G}^\dagger(\Gamma)^S_{ab;cd} = \frac{1}{\sqrt{(1+\delta_{ab})(1+\delta_{cd})}} \Bigg(& \frac{1}{N-1} \left[\delta_{ac} \overline{A}_{bd} + (-1)^S \delta_{ad} \overline{A}_{bc} \right. \\ & \left. + (-1)^S \delta_{bc} \overline{A}_{ad} + \delta_{bd} \overline{A}_{ac} \right] - \sum_{S'} (2S'+1) \begin{Bmatrix} \frac{1}{2} & \frac{1}{2} & S \\ \frac{1}{2} & \frac{1}{2} & S' \end{Bmatrix} \\ & \left[A^{S'}_{ad;cb} + (-1)^S A^{S'}_{bd;ca} + (-1)^S A^{S'}_{ac;db} + A^{S'}_{bc;da} \right] \Bigg) \,, \quad \text{(F.16)}\end{aligned}$$

in which the bar function for spin-coupled particle-hole matrices is defined as:

$$\overline{A}_{ac} = \frac{1}{2} \sum_S (2S+1) \sum_b A^S_{ab;cb} \,. \quad \text{(F.17)}$$

The spin-coupled Hermitian adjoint maps for the three-index conditions can be derived in a similar but more complicated fashion. We refer to reference 90 for the full expressions.

Appendix G

Computer codes

In this appendix we give some background on the computer codes used in this work. All codes are open source under the GPLv3-license [183] and available online [184, 239]. They are written in C++ using the BLAS and LAPACK libraries for linear algebra operations and the HDF5[1] library for storing data. The one- and two-electron integrals are calculated using PSI4 [178] and stored in a HDF5 file using the Hamiltonian class of CheMPS2 [187–190].

G.1 doci_sdp-atom

The program `doci_sdp-atom` [239] implements the v2DM-DOCI method using both the boundary point method and the potential reduction method. It can use a Jacobi-based orbital optimizer or a simulated annealing-based orbital optimizer. The code is single-threaded as it is very difficult to parallelize a boundary point method: you can only parallelize within a single step and every step is already very fast. The boundary point method has a convergence checker: if the algorithm gets stuck, it will stop it. This has consequences for all the following steps: if the 2DM is not properly convergence, the orbital optimizer might not make a good decision about which orbital to rotate next. It can take a while for the program recovers from this.

1. http://www.hdfgroup.org

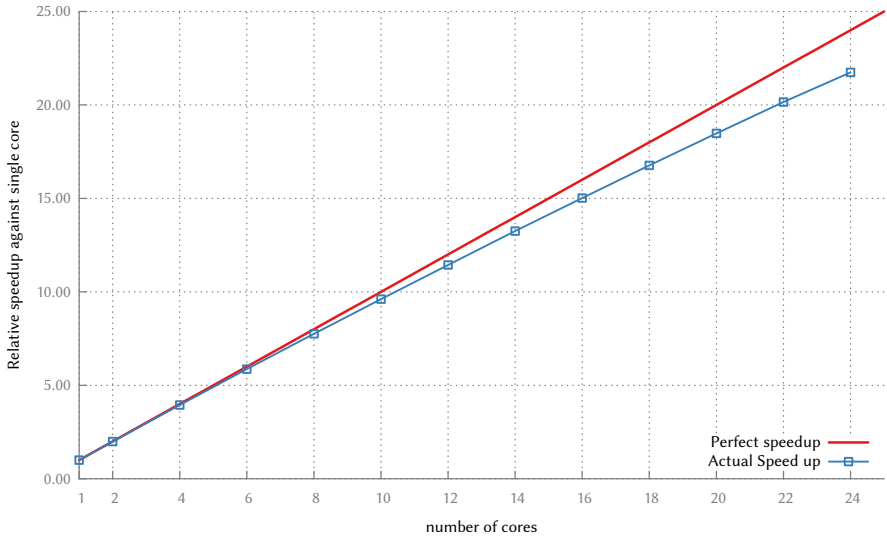

Figure G.1: The speedup of parallelizing the FullDOCI program.

G.2 DOCI-Exact

The program `DOCI-Exact` [184] implements a FullDOCI algorithm. The DOCI Hamiltonian is build and then diagonalized to find the groundstate energy and state. It can build and store the Hamiltonian as a sparse matrix and then utilize a implicit restarted Arnoldi algorithm [185, 186] to find the groundstate energy using only a sparse matrix-vector product. Every N-particle state is represented by a bit string. Calculating a single element of the Hamiltonian is very quick and as all elements are independent, this is very well suited for parallelization. In Figure G.1 the speed up is shown. It is this parallelization that makes it possible to do DOCI calculations in the cc-pVDZ basis. The same orbital optimization algorithm as for `doci_sdp-atom` program are used.

Bibliography

[1] A. Szabo and N. S. Ostlund, *Modern Quantum Chemistry: Introduction to Advanced Electronic Structure Theory* (Dover Publications, 1996).

[2] T. Helgaker, P. Jorgensen, and J. Olsen, *Molecular Electronic-Structure Theory* (Wiley, 2014).

[3] J. v. Neumann, *Mathematische Grundlagen der Quantenmechanik* (Springer-Verlag, Berlin, 1932).

[4] P. A. M. Dirac, "Quantum mechanics of many-electron systems," *Proceedings of the Royal Society of London A: Mathematical, Physical and Engineering Sciences* **123**, 714 (1929).

[5] K. Husimi, "Some formal properties of the density matrix," *Proceedings of the Physico-Mathematical Society of Japan* **22**, 264 (1940).

[6] A. J. Coleman, *Many-electron densities and reduced density matrices*, edited by J. Cioslowski, mathematical and computational chemistry (Kluwer Academic/Plenum Publishers, 2000).

[7] J. Mayer, "Electron correlation," *Physical Review* **100**, 6 (1955).

[8] P.-O. Löwdin, "Quantum theory of many-particle systems. I. physical interpretations by means of density matrices, natural spin-orbitals, and convergence problems in the method of configurational interaction," *Physical Review* **97**, 1474 (1955).

[9] R. H. Tredgold, "Density matrix and the many-body problem," *Physical Review* **105**, 5 (1957).

[10] A. J. Coleman, "Structure of fermion density matrices," *Reviews of Modern Physics* **35**, 668 (1963).

[11] C. Garrod and J. K. Percus, "Reduction of the N-particle variational problem," *Journal of Mathematics and Physics* **5**, 1756 (1964).

[12] C. Garrod, M. V. Mihailovic, and M. Rosina, "The variational approach to the two - body density matrix," *Journal of Mathematical Physics* **16**, 868 (1975).

[13] C. Garrod and M. A. Fusco, "A density matrix variational calculation for atomic be," *International Journal of Quantum Chemistry* **10**, 495 (1976).

[14] M. Mihailovic and M. Rosina, "The variational approach to the density matrix for light nuclei," *Nuclear Physics A* **237**, 221 (1974).

[15] M. Rosina and C. Garrod, "The variational calculation of reduced density matrices," *Journal of Computational Physics* **18**, 300 (1975).

[16] C. Valdemoro, "Theory and methodology of the contracted schrödinger equation," in *Reduced-Density-Matrix Mechanics: With Application to Many-Electron Atoms and Molecules* (John Wiley & Sons, Inc., 2007) pp. 119–164.

[17] D. A. Mazziotti, "Contracted schrödinger equation," in *Reduced-Density-Matrix Mechanics: With Application to Many-Electron Atoms and Molecules* (John Wiley & Sons, Inc., 2007) pp. 165–203.

[18] F. Colmenero, C. Pérez del Valle, and C. Valdemoro, "Approximating *q*-order reduced density matrices in terms of the lower-order ones. I. general relations," *Physical Review A* **47**, 971 (1993).

[19] F. Colmenero and C. Valdemoro, "Approximating *q*-order reduced density matrices in terms of the lower-order ones. II. applications," *Physical Review A* **47**, 979 (1993).

[20] M. Nakata, H. Nakatsuji, M. Ehara, M. Fukuda, K. Nakata, and K. Fujisawa, "Variational calculations of fermion second-order reduced density matrices by semidefinite programming algorithm," *Journal of Chemical Physics* **114**, 8282 (2001).

[21] L. Vandenberghe and S. Boyd, "Semidefinite programming," *SIAM Review* **38**, 49 (1996).

[22] S. Boyd and L. Vandenberghe, *Convex Optimization* (Cambridge University Press, 2006).

[23] M. Yamashita, K. Fujisawa, M. Fukuda, K. Kobayashi, K. Nakata, and M. Nakata, *Handbook on Semidefinite, Conic and Polynomial Optimization*, edited by M. F. Anjos and J. B. Lasserre, International Series in Operations Research & Management Science, Vol. 166 (Springer US, 2012) pp. 687–713.

[24] D. A. Mazziotti, "Variational minimization of atomic and molecular ground-state energies via the two-particle density matrix," *Physical Review A* **65**, 062511 (2002).

[25] Z. Zhao, B. J. Braams, M. Fukuda, M. L. Overton, and J. K. Percus, "The reduced density matrix method for electronic structure calculations and the role of three-index representability conditions," *Journal of Chemical Physics* **120**, 5 (2004).

[26] J. R. Hammond and D. A. Mazziotti, "Variational two-electron reduced-density-matrix theory: Partial 3-positivity conditions for N-representability," *Physical Review A* **71**, 062503 (2005).

[27] D. A. Mazziotti, "Variational two-electron reduced density matrix theory for many-electron atoms and molecules: Implementation of the spin- and symmetry-adapted T2 condition to non-equilibrium geometries." *Physical Review A* **72**, 032510 (2005).

[28] D. A. Mazziotti, "Realization of quantum chemistry without wave functions through first-order semidefinite programming," *Physical Review Letters* **93**, 213001 (2004).

[29] D. A. Mazziotti, "First-order semidefinite programming for the direct determination of two-electron reduced density matrices with application to many-electron atoms and molecules," *Journal of Chemical Physics* **121**, 10957 (2004).

[30] B. Verstichel, H. van Aggelen, D. Van Neck, P. W. Ayers, and P. Bultinck, "Subsystem constraints in variational second order density matrix optimization: Curing the dissociative behavior," *Journal of Chemical Physics* **132**, 114113 (2010).

[31] H. Van Aggelen, P. Bultinck, B. Verstichel, D. Van Neck, and P. W. Ayers, "Incorrect diatomic dissociation in variational reduced density matrix theory arises from the flawed description of fractionally charged atoms," *Physical Chemistry Chemical Physics* **11**, 5558 (2009).

[32] N. Shenvi and A. F. Izmaylov, "Active-space n-representability constraints for variational two-particle reduced density matrix calculations," *Physical Review Letters* **105**, 213003 (2010).

[33] D. Van Neck and P. W. Ayers, "Necessary conditions for the N-representability of the second-order reduced density matrix: Upper bounds on the P and Q matrices." *Physical Review A* **75**, 032502 (2007).

[34] P. A. Johnson, P. W. Ayers, B. Verstichel, D. Van Neck, and H. van Aggelen, "The sharp-g n-representability condition," *Computational and Theoretical Chemistry* **1003**, 32 (2013).

[35] G. Gidofalvi and D. A. Mazziotti, "Spin and symmetry adaptation of the variational two-electron reduced-density-matrix method," *Physical Review A* **72**, 052505 (2005).

[36] D. A. Mazziotti, "Variational reduced-density-matrix method using three-particle n-representability conditions with application to many-electron molecules," *Physical Review A* **74**, 032501 (2006).

[37] G. Gidofalvi and D. A. Mazziotti, "Variational reduced-density-matrix theory: strenght of hamiltonian-dependent positivity condtions," *Chemical Physics Letters* **398**, 434 (2004).

[38] B. Verstichel, H. van Aggelen, W. Poelmans, and D. Van Neck, "Variational two-particle density matrix calculation for the hubbard model below half filling using spin-adapted lifting conditions," *Physical Review Letters* **108**, 213001 (2012).

[39] H. van Aggelen, B. Verstichel, G. Acke, M. Degroote, P. Bultinck, P. W. Ayers, and D. Van Neck, "Extended random phase approximation method for atomic excitation energies from correlated and variationally optimized second-order density matrices," *Computational and Theoretical Chemistry* **1003**, 50 (2013).

[40] H. van Aggelen, B. Verstichel, P. Bultinck, D. Van Neck, and P. W. Ayers, "Considerations on describing non-singlet spin states in variational second order density matrix methods," *Journal of Chemical Physics* **136**, 014110 (2012).

[41] E. R. Davidson, "Linear inequalities for density matrices: III," *International Journal of Quantum Chemistry* **91**, 1 (2003).

[42] W. B. McRae and E. R. Davidson, "Linear inequalities for density matrices. II," *Journal of Mathematical Physics* **13**, 1527 (1972).

[43] E. R. Davidson, "Linear inequalities for density matrices," *Journal of Mathematical Physics* **10**, 725 (1969).

[44] A. J. Coleman and V. I. Yukalov, *Reduced Density Matrices: Coulson's Challange* (Springer-Verlag, New York, 2000).

[45] D. A. Mazziotti, *Reduced-Density-Matrix Mechanics: With Aplication to Many-Electron Atoms and Molecules*, edited by D. A. Mazziotti, Vol. 134 (Wiley: New York, 2007) p. 93.

[46] B. J. Braams, J. K. Percus, and Z. Zhao, "Reduced-Density-Matrix Mechanics: With Aplication to Many-Electron Atoms and Molecules," (Wiley: New York, 2007) p. 93.

[47] D. A. Mazziotti, "Two-electron reduced density matrix as the basic variable in many-electron quantum chemistry and physics," *Chemical Reviews* **112**, 244 (2012), pMID: 21863900.

[48] P. Ayers and A. Thakkar, "Forward for special issue," *Computational and Theoretical Chemistry* **1003**, 1 (2013), reduced Density Matrices: A Simpler Approach to Many-Electron Problems?

[49] B. Verstichel, H. van Aggelen, D. Van Neck, P. W. Ayers, and P. Bultinck, "Variational density matrix optimization using semidefinite programming," *Computer Physics Communications* **182**, 2025 (2011).

[50] B. Verstichel, H. van Aggelen, D. Van Neck, P. Bultinck, and S. De Baerdemacker, "A primal-dual semidefinite programming algorithm tailored to the variational determination of the two-body density matrix," *Computer Physics Communications* **182**, 1235 (2011).

[51] D. A. Mazziotti, "Large-Scale Semidefinite Programming for Many-Electron Quantum Mechanics," *Physical Review Letters* **106**, 083001 (2011).

[52] D. A. Mazziotti, "Large-scale semidefinite programming for many-electron quantum mechanics," *Physical Review Letters* **106**, 083001 (2011).

[53] K. Raghavachari, G. W. Trucks, J. A. Pople, and M. Head-Gordon, "A fifth-order perturbation comparison of electron correlation theories," *Chemical Physics Letters* **157**, 479 (1989).

[54] C. A. Coulson, "Present state of molecular structure calculations," *Reviews of Modern Physics* **32**, 170 (1960).

[55] M. Krein and D. Milman, "On extreme points of regular convex sets," *Studia Mathematica* **9**, 133 (1940).

[56] S. A. Ocko, X. Chen, B. Zeng, B. Yoshida, Z. Ji, M. B. Ruskai, and I. L. Chuang, "Quantum codes give counterexamples to the unique preimage conjecture of the n-representability problem," *Physical Review Letters* **106**, 110501 (2011).

[57] Y.-K. Liu, M. Christandl, and F. Verstraete, "Quantum computational complexity of the N-representability problem: QMA complete," *Physical Review Letters* **98**, 110503 (2007).

[58] A. M. Turing, "On computable numbers, with an application to the entscheidungsproblem," *Proceedings of the London Mathematical Society* **s2-42**, 230 (1937).

[59] A. M. Turing, "On computable numbers, with an application to the entscheidungsproblem. a correction," *Proceedings of the London Mathematical Society* **s2-43**, 544 (1938).

[60] M. Agrawal, N. Kayal, and N. Saxena, "PRIMES is in P," *Annals of Mathematics* Second Series, **160**, pp. 781 (2004).

[61] J. Carlson, *The Millennium Prize Problems*, edited by A. Jaffe and A. Wiles (American Mathematical Society, 2006).

[62] P. W. Shor, "Polynomial-time algorithms for prime factorization and discrete logarithms on a quantum computer," *SIAM Review* **41**, 303–332 (1999).

[63] L. K. Grover, in *Proceedings of the Twenty-eighth Annual ACM Symposium on Theory of Computing*, STOC '96 (ACM, New York, NY, USA, 1996) pp. 212–219.

[64] J. D. Whitfield, P. J. Love, and A. Aspuru-Guzik, "Computational complexity in electronic structure," *Physical Chemistry Chemical Physics* **15**, 397 (2013).

[65] A. Y. Kitaev, A. H. Shen, and M. N. Vyalyi, *Classical and Quantum Computation* (American Mathematical Society, Boston, MA, USA, 2002).

[66] J. Kempe, A. Kitaev, and O. Regev, "The complexity of the local hamiltonian problem," *SIAM Journal on Computing* **35**, 1070 (2006).

[67] P. Hohenberg and W. Kohn, "Inhomogeneous electron gas," *Physical Review* **136**, B864 (1964).

[68] W. Kohn and L. J. Sham, "Self-consistent equations including exchange and correlation effects," *Physical Review* **140**, A1133 (1965).

[69] R. G. Parr and Y. Weitao, *Density-Functional Theory of Atoms and Molecules* (Oxford University Press, New York, NY, 1994).

[70] N. Schuch and F. Verstraete, "Computational complexity of interacting electrons and fundamental limitations of density functional theory," *Nature Physics* **5**, 732 (2009).

[71] D. W. Smith, "N-representability problem for fermion density matrices. I. the second-order density matrix with $N = 3$," *Journal of Chemical Physics* **43**, S258 (1965).

[72] A. A. Klyachko, "Quantum marginal problem and n-representability," *Journal of Physics: Conference Series* **36**, 72 (2006).

[73] A. Klyachko, "Quantum marginal problem and representations of the symmetric group," *arXiv:quant-ph/0409113* (2004), arXiv: quant-ph/0409113.

[74] C. Schilling, "The Quantum Marginal Problem," *arXiv:1404.1085 [math-ph, physics:quant-ph]* (2014), arXiv: 1404.1085.

[75] J. Hoffmann-Jørgensen, in *Functional Analysis II*, Lecture Notes in Mathematics, Vol. 1242, edited by D. Butković, S. Kurepa, and H. Kraljević (Springer Berlin Heidelberg, 1987) pp. 77–367.

[76] R. Kubo, "Generalized cumulant expansion method," *Journal of the Physical Society of Japan* **17**, 1100 (1962).

[77] W. Kutzelnigg and D. Mukherjee, "Cumulant expansion of the reduced density matrices," *Journal of Chemical Physics* **110**, 2800 (1999).

[78] D. A. Mazziotti, "Approximate solution for electron correlation through the use of schwinger probes," *Chemical Physics Letters* **289**, 419 (1998).

[79] S. Veeraraghavan and D. A. Mazziotti, "Global solutions of hartree-fock theory and their consequences for strongly correlated quantum systems," *Physical Review A* **89**, 010502 (2014).

[80] S. Veeraraghavan and D. A. Mazziotti, "Global solutions of restricted open-shell hartree-fock theory from semidefinite programming with applications to strongly correlated quantum systems," *Journal of Chemical Physics* **140**, 124106 (2014).

[81] B. Verstichel, H. van Aggelen, D. Van Neck, P. W. Ayers, and P. Bultinck, "Variational determination of the second-order density matrix for the isoelectronic series of beryllium, neon, and silicon," *Physical Review A* **80**, 032508 (2009).

[82] D. A. Mazziotti, "Variational reduced-density-matrix method using three-particle n-representability conditions with application to many-electron molecules," *Physical Review A* **74**, 032501 (2006).

[83] G. Gidofalvi and D. A. Mazziotti, "Molecular properties from variational reduced-density-matrix theory with three-particle n-representability conditions," *Journal of Chemical Physics* **126**, 024105 (2007).

[84] R. M. Erdahl, "Representability," *International Journal of Quantum Chemistry* **13**, 697 (1978).

[85] R. W. Richardson, "A restricted class of exact eigenstates of the pairing-force hamiltonian," *Physics Letters* **3**, 277 (1963).

[86] R. W. Richardson and N. Sherman, "Exact eigenstates of the pairing-force hamiltonian," *Nuclear Physics* **52**, 221 (1964).

[87] M. Gaudin, "Diagonalisation d'une classe d'hamiltoniens de spin," *Journal de Physique France* **37**, 1087 (1976).

[88] D. Pisinger, "Upper bounds and exact algorithms for p-dispersion problems," *Computers & Operations Research* **33**, 1380 (2006).

[89] S. S. Ravi, D. J. Rosenkrantz, and G. K. Tayi, "Heuristic and special case algorithms for dispersion problems," *Operations Research* **42**, 299 (1994).

[90] B. Verstichel, *Variational determination of the two-particle density matrix as a quantum many-body technique*, Ph.D. thesis, Ghent University (2012).

[91] H. van Aggelen, B. Verstichel, P. Bultinck, D. V. Neck, P. W. Ayers, and D. L. Cooper, "Variational second order density matrix study of F_3^-: Importance of subspace constraints for size-consistency," *Journal of Chemical Physics* **134**, 054115 (2011).

[92] J. F. Cornwell, *Group Theory in Physics, Volume 1: An Introduction*, abridged edition ed. (Academic Press, San Diego, 1997).

[93] D. J. Gross, "The role of symmetry in fundamental physics," *Proceedings of the National Academy of Sciences* **93**, 14256 (1996).

[94] J. P. Elliott and P. G. Dawber, *Symmetry in Physics: Principles and Simple Applications Volume 1* (Oxford University Press, New York, 1985).

[95] J. P. Elliott and P. G. Dawber, *Symmetry in Physics: Further Applications Volume 2* (Oxford University Press, New York, 1985).

[96] J. F. Cornwell, *Group Theory in Physics, Volume 2* (Academic Press, London ; Orlando, 1984).

[97] B. H. Bransden and C. J. Joachain, *Quantum Mechanics*, 2nd ed. (Addison-Wesley, Harlow, England ; New York, 2000).

[98] S.-i. Tomonaga, *The Story of Spin*, 1st ed. (University Of Chicago Press, Chicago, 1998).

[99] A. R. Edmonds, *Angular Momentum in Quantum Mechanics*, revised edition ed. (Princeton University Press, Princeton, N.J, 1957).

[100] E. Pérez-Romero, L. M. Tel, and C. Valdemoro, "Traces of spin-adapted reduced density matrices," *International Journal of Quantum Chemistry* **61**, 55 (1997).

[101] D. R. Alcoba and C. Valdemoro, "Spin structure and properties of the correlation matrices corresponding to pure spin states: Controlling the s-representability of these matrices," *International Journal of Quantum Chemistry* **102**, 629 (2005).

[102] D. R. Alcoba, C. Valdemoro, L. M. Tel, and E. Pérez-Romero, "Controlling the n- and s-representability of the second-order reduced density matrix: The doublet-state case," *Physical Review A* **77**, 042508 (2008).

[103] H. van Aggelen, *Variational optimization of second order density matrices for electronic structure calculation*, Ph.D. thesis, Ghent University (2011).

[104] E. R. Davidson, "Use of double cosets in constructing integrals over symmetry orbitals," *Journal of Chemical Physics* **62**, 400 (1975).

[105] S. Wilson, ed., *Methods in Computational Chemistry: Volume 3: Concurrent Computation in Chemical Calculations*, 1989th ed. (Springer, 2013).

[106] H. F. Schaefer, *Methods of Electronic Structure Theory*, first edition edition ed. (Springer, 1977).

[107] D. Yarkony, ed., *Modern Electronic Structure Theory* (World Scientific Pub Co Inc, 1995).

[108] J. Thom H. Dunning, "Gaussian basis sets for use in correlated molecular calculations. I. the atoms boron through neon and hydrogen," *Journal of Chemical Physics* **90**, 1007 (1989).

[109] F. Weinhold and E. B. Wilson, "Reduced density matrices of atoms and molecules. II. on the N-representability problem," *Journal of Chemical Physics* **47**, 2298 (1967).

[110] F. Weinhold and E. B. Wilson, "Reduced density matrices of atoms and molecules. I. the 2 matrix of double-occupancy, configuration-interaction wavefunctions for singlet states," *Journal of Chemical Physics* **46**, 2752 (1967).

[111] P. Ring and P. Schuck, *The Nuclear Many-Body Problem* (Springer, 2005).

[112] D. A. Mazziotti, "Structure of fermionic density matrices: Complete N-representability conditions," *Physical Review Letters* **108** (2012), 10.1103/physrevlett.108.263002.

[113] D. A. Mazziotti, "Significant conditions for the two-electron reduced density matrix from the constructive solution of n representability," *Physical Review A* **85**, 062507 (2012).

[114] V. Bach, H. K. Knörr, and E. Menge, "Representability conditions by grassmann integration," *arXiv* (2013), 1307.0465 .

[115] M. Yamashita, K. Fujisawa, and M. Kojima, "Implementation and evaluation of SDPA 6.0 (semidefinite programming algorithm 6.0)," *Optimization Methods and Software* **18**, 491 (2003).

[116] "SDPA (semidefinite programming algorithm)," http://sdpa.sourceforge.net (2015), (accessed May 3, 2015).

[117] J. F. Sturm, "Using SeDuMi 1.02, a matlab toolbox for optimization over symmetric cones," *Optimization Methods and Software* **11**, 625–653 (1999).

[118] B. Borchers, "CSDp, a C library for semidefinite programming," *Optimization Methods and Software* **11**, 613–623 (1999).

[119] S. Sra, *Optimization for machine learning* (MIT Press, Cambridge, Mass, 2012).

[120] S. Boyd, L. El Ghaoui, E. Feron, and V. Balakrishnan, *Linear Matrix Inequalities in System and Control Theory* (Society for Industrial and Applied Mathematics, 1994).

[121] F. Alizadeh, "Interior point methods in semidefinite programming with applications to combinatorial optimization," *SIAM Journal on Optimization* **5**, 13–51 (1995).

[122] P. M. Bentler and J. A. Woodward, "Inequalities among lower bounds to reliability: With applications to test construction and factor analysis," *Psychometrika* **45**, 249–267 (1980).

[123] D. P. Bertsekas, *Constrained Optimization and Lagrange Multiplier Methods* (Athena Scientific, 1996).

[124] D. Klein, "Lagrange multipliers without permanent scarring," (2002).

[125] Y. Nesterov and A. Nemirovski, *Interior Point Polynomial Algorithms in Convex Programming*, Studies in Applied and Numerical Mathematics, Vol. 13 (SIAM, Philadelphia, 1994).

[126] Y. Nesterov and A. Nemirovski, "Self-concordant functions and polynomial time methods in convex programming," *Tech. report for USSR Acad. Sci. Centr. Econ. & Math. Inst., Moscow* (1990).

[127] W. Press, *Numerical recipes : the art of scientific computing* (Cambridge University Press, Cambridge, UK New York, 2007).

[128] J. R. Shewchuk, "An introduction to the conjugate gradient method without the agonizing pain," (1994).

[129] J. Povh, F. Rendl, and A. Wiegele, "A Boundary Point Method to Solve Semidefinite Programs," *Computing* **78**, 277 (2006).

[130] J. Malick, J. Povh, F. Rendl, and A. Wiegele, "Regularization Methods for Semidefinite Programming," *SIAM Journal on Optimization* **20**, 336 (2009).

[131] Z. Wen, D. Goldfarb, and W. Yin, "Alternating direction augmented lagrangian methods for semidefinite programming," *Math. Prog. Comp.* **2**, 203–230 (2010).

[132] W. Karush, *Minima of Functions of Several Variables with Inequalities as Side Constraints*, Master's thesis, Dept. of Mathematics, Univ. of Chicago, Chicago, Illinois (1939).

[133] H. W. Kuhn and A. W. Tucker, in *Proceedings of the Second Berkeley Symposium on Mathematical Statistics and Probability* (University of California Press, Berkeley, Calif., 1951) pp. 481–492.

[134] I. Talmi, *Simple models of complex nuclei : the shell model and interacting boson model* (Harwood Academic Publishers, Chur, Switzerland Langhorne, Pa., U.S.A, 1993).

[135] G. N. Lewis, "The atom and the molecule," *Journal of the American Chemical Society* **38**, 762 (1916).

[136] A. C. Hurley, J. Lennard-Jones, and J. A. Pople, "The molecular orbital theory of chemical valency. XVI. a theory of paired-electrons in polyatomic molecules," *Proceedings of the Royal Society of London A: Mathematical, Physical and Engineering Sciences* **220**, 446 (1953).

[137] P. Surján, in *Correlation and Localization*, Topics in Current Chemistry, Vol. 203, edited by P. Surján, R. Bartlett, F. Bogár, D. Cooper, B. Kirtman, W. Klopper, W. Kutzelnigg, N. March, P. Mezey, H. Müller, J. Noga, J. Paldus, J. Pipek, M. Raimondi, I. Røeggen, J. Sun, P. Surján, C. Valdemoro, and S. Vogtner (Springer Berlin Heidelberg, 1999) pp. 63–88.

[138] A. J. Coleman, "Structure of fermion density matrices. II. antisymmetrized geminal powers," *Journal of Mathematical Physics* **6**, 1425 (1965).

[139] J. M. Blatt, "Electron pairs in the theory of superconductivity," *Progress of Theoretical Physics* **23**, 447 (1960).

[140] R. McWeeny and B. T. Sutcliffe, "The density matrix in many-electron quantum mechanics. III. generalized product functions for beryllium and four-electron ions," *Proceedings of the Royal Society of London A: Mathematical, Physical and Engineering Sciences* **273**, 103 (1963).

[141] F. Weinhold and E. Wilson, "Reduced density matrices of atoms and molecules. II. on the N-representability problem," *Journal of Chemical Physics* **47**, 2298 (1967).

[142] S. Shaik and P. Hiberty, *A Chemist's Guide to Valence Bond Theory* (Wiley, 2007).

[143] J. H. van Lenthe and G. G. Balint-Kurti, "The valence-bond self-consistent field method (VB-SCF): Theory and test calculations," *Journal of Chemical Physics* **78**, 5699 (1983).

[144] H. Schaefer, *Methods of Electronic Structure Theory*, Modern Theoretical Chemistry (Springer US, 2013).

[145] P. A. Limacher, P. W. Ayers, P. A. Johnson, S. De Baerdemacker, D. Van Neck, and P. Bultinck, "A new mean-field method suitable for strongly correlated electrons: Computationally facile antisymmetric products of nonorthogonal geminals," *Journal of Chemical Theory and Computation* **9**, 1394 (2013).

[146] L. Bytautas, T. M. Henderson, C. A. Jiménez-Hoyos, J. K. Ellis, and G. E. Scuseria, "Seniority and orbital symmetry as tools for establishing a full configuration interaction hierarchy," *Journal of Chemical Physics* **135**, 044119 (2011).

[147] M. Van Raemdonck, D. R. Alcoba, W. Poelmans, S. De Baerdemacker, A. Torre, L. Lain, G. E. Massaccesi, D. Van Neck, and P. Bultinck, "Polynomial scaling approximations and dynamic correlation corrections to doubly occupied configuration interaction wave functions," *The Journal of Chemical Physics* **143**, 104106 (2015), 10.1063/1.4930260.

[148] K. Boguslawski, P. Tecmer, P. W. Ayers, P. Bultinck, S. De Baerdemacker, and D. Van Neck, "Efficient description of strongly correlated electrons with mean-field cost," *Physical Review B* **89**, 201106 (2014).

[149] P. A. Johnson, P. W. Ayers, P. A. Limacher, S. De Baerdemacker, D. Van Neck, and P. Bultinck, "A size-consistent approach to strongly correlated systems using a generalized antisymmetrized product of nonorthogonal geminals," *Computational and Theoretical Chemistry* **1003**, 101 (2013).

[150] T. Stein, T. M. Henderson, and G. E. Scuseria, "Seniority zero pair coupled cluster doubles theory," *Journal of Chemical Physics* **140**, 214113 (2014).

[151] T. M. Henderson, I. W. Bulik, T. Stein, and G. E. Scuseria, "Seniority-based coupled cluster theory," *Journal of Chemical Physics* **141**, 244104 (2014).

[152] P. A. Limacher, T. D. Kim, P. W. Ayers, P. A. Johnson, S. De Baerdemacker, D. Van Neck, and P. Bultinck, "The influence of orbital rotation on the energy of closed-shell wavefunctions," *Molecular Physics* **112**, 853 (2014).

[153] S. Kirkpatrick, C. D. Gelatt, and M. P. Vecchi, "Optimization by simulated annealing," *Science* **220**, 671 (1983).

[154] V. Černý, "Thermodynamical approach to the traveling salesman problem: An efficient simulation algorithm," *Journal of Optimization Theory and Applications* **45**, 41 (1985).

[155] T. Lee and G. Scuseria, in *Quantum Mechanical Electronic Structure Calculations with Chemical Accuracy*, Understanding Chemical Reactivity, Vol. 13, edited by S. Langhoff (Springer Netherlands, 1995) pp. 47–108.

[156] W. Poelmans, M. Van Raemdonck, B. Verstichel, S. De Baerdemacker, A. Torre, L. Lain, G. E. Massaccesi, D. R. Alcoba, P. Bultinck, and D. Van Neck, "Variational optimization of the second order density matrix corresponding to a seniority-zero configuration interaction wave function," *Journal of Chemical Theory and Computation* **11**, 4064 (2015).

[157] K. A. Brueckner and W. Wada, "Nuclear saturation and two-body forces: Self-consistent solutions and the effects of the exclusion principle," *Physical Review* **103**, 1008 (1956).

[158] R. K. Nesbet, "Brueckner's theory and the method of superposition of configurations," *Physical Review* **109**, 1632 (1958).

[159] W. J. Hehre, R. F. Stewart, and J. A. Pople, "Self-consistent molecular-orbital methods. i. use of gaussian expansions of slater-type atomic orbitals," *Journal of Chemical Physics* **51**, 2657 (1969).

[160] S. Wouters, P. A. Limacher, D. Van Neck, and P. W. Ayers, "Longitudinal static optical properties of hydrogen chains: Finite field extrapolations of matrix product state calculations," *Journal of Chemical Physics* **136**, 134110 (2012).

[161] R. Horn and C. Johnson, *Topics in Matrix Analysis* (Cambridge University Press, 1994).

[162] P. Siegbahn, A. Heiberg, B. Roos, and B. Levy, "A Comparison of the Super-CI and the Newton-Raphson Scheme in the Complete Active Space SCF Method," *Physica Scripta* **21**, 323 (1980).

[163] R. Raffenetti, K. Ruedenberg, C. Janssen, and H. Schaefer, "Efficient use of jacobi rotations for orbital optimization and localization," *Theoretica chimica acta* **86**, 149 (1993).

[164] G. H. Golub and C. F. Van Loan, *Matrix Computations* (The Johns Hopkins University Press, Baltimore, 1989).

[165] F. Murnaghan, *The unitary and rotation groups*, Lectures on applied mathematics (Spartan Books, 1962).

[166] D. K. Hoffman, R. C. Raffenetti, and K. Ruedenberg, "Generalization of euler angles to N-dimensional orthogonal matrices," *Journal of Mathematical Physics* **13**, 528 (1972).

[167] R. C. Raffenetti and K. Ruedenberg, "Parametrization of an orthogonal matrix in terms of generalized eulerian angles," *International Journal of Quantum Chemistry* **4**, 625 (1969).

[168] J. Ivanic and K. Ruedenberg, "A MCSCF method for ground and excited states based on full optimizations of successive jacobi rotations," *Journal of Computational Chemistry* **24**, 1250 (2003).

[169] G. Gidofalvi and D. A. Mazziotti, "Active-space two-electron reduced-density-matrix method: Complete active-space calculations without diagonalization of the n-electron hamiltonian," *Journal of Chemical Physics* **129**, 134108 (2008).

[170] K. C. Mundim and C. Tsallis, "Geometry optimization and conformational analysis through generalized simulated annealing," *International Journal of Quantum Chemistry* **58**, 373 (1996).

[171] L. A. C. Malbouisson, A. M. d. C. Sobrinho, M. A. C. Nascimento, and M. D. d. Andrade, "Optimization of geometry at hartree-fock level using the generalized simulated annealing," *Applied Mathematics* **03**, 1526–1531 (2012).

[172] M. Dias De Andrade, M. Nascimento, K. Mundim, and L. Malbouisson, "GSA algorithm applied to electronic structure II: UHF-GSA method," *International Journal of Quantum Chemistry* **106**, 2700–2705 (2006).

[173] M. D. De Andrade, M. A. C. Nascimento, K. C. Mundim, A. M. C. Sobrinho, and L. A. C. Malbouisson, "Atomic basis sets optimization using the generalized simulated annealing approach: New basis sets for the first row elements," *International Journal of Quantum Chemistry* **108**, 2486–2498 (2008).

[174] M. Moret, P. Bisch, K. Mundim, and P. Pascutti, "New stochastic strategy to analyze helix folding," *Biophysical Journal* **82**, 1123–1132 (2002).

[175] M. A. Moret, P. G. Pascutti, P. M. Bisch, and K. C. Mundim, "Stochastic molecular optimization using generalized simulated annealing," *Journal of Computational Chemistry* **19**, 647–657 (1998).

[176] W. Gropp, E. Lusk, and A. Skjellum, *Using MPI: Portable Parallel Programming with the Message Passing Interface*, 2nd ed. (The MIT Press, 1999).

[177] M. Snir, S. W. Otto, S. Huss-Lederman, D. W. Walker, and J. Dongarra, *MPI: The Complete Reference*, 2nd ed., Vol. 1 (The MIT Press, 1998).

[178] J. M. Turney, A. C. Simmonett, R. M. Parrish, E. G. Hohenstein, F. A. Evangelista, J. T. Fermann, B. J. Mintz, L. A. Burns, J. J. Wilke, M. L.

Abrams, N. J. Russ, M. L. Leininger, C. L. Janssen, E. T. Seidl, W. D. Allen, H. F. Schaefer, R. A. King, E. F. Valeev, C. D. Sherrill, and T. D. Crawford, "Psi4: an open-source ab initio electronic structure program," *Wiley Interdisciplinary Reviews: Computational Molecular Science* **2**, 556 (2012).

[179] P.-O. Löwdin, "On the non-orthogonality problem connected with the use of atomic wave functions in the theory of molecules and crystals," *Journal of Chemical Physics* **18**, 365 (1950).

[180] B. C. Carlson and J. M. Keller, "Orthogonalization procedures and the localization of wannier functions," *Physical Review* **105**, 102 (1957).

[181] I. Mayer, "On löwdin's method of symmetric orthogonalization," *International Journal of Quantum Chemistry* **90**, 63–65 (2002).

[182] D. R. Hartree, "The wave mechanics of an atom with a non-coulomb central field. part I. theory and methods," *Mathematical Proceedings of the Cambridge Philosophical Society* **24**, 89 (1928).

[183] "GNU general public license," http://www.gnu.org/licenses/gpl.html (2007), (accessed May 3, 2015).

[184] W. Poelmans, "FullDOCI solver," https://github.com/wpoely86/DOCI-Exact (2015), (accessed May 3, 2015).

[185] D. C. Sorensen, "Implicit application of polynomial filters in a k-step arnoldi method," *SIAM Journal on Matrix Analysis and Applications* **13**, 357 (1992).

[186] Y. Saad, *Numerical Methods for Large Nonsymmetric Eigenvalue Problems (Algorithms & Architectures for Advanced Scientific Computing)* (Manchester University Press, 1995).

[187] S. Wouters, W. Poelmans, P. W. Ayers, and D. V. Neck, "CheMPS2: A free open-source spin-adapted implementation of the density matrix renormalization group for ab initio quantum chemistry," *Computer Physics Communications* **185**, 1501 (2014).

[188] S. Wouters, W. Poelmans, S. D. Baerdemacker, P. W. Ayers, and D. V. Neck, "CheMPS2: Improved DMRG-SCF routine and correlation functions," *Computer Physics Communications* **191**, 235 (2015).

[189] S. Wouters and D. Van Neck, "The density matrix renormalization group for ab initio quantum chemistry," *The European Physical Journal D* **68**, 272 (2014), 10.1140/epjd/e2014-50500-1.

[190] S. Wouters, T. Bogaerts, P. Van Der Voort, V. Van Speybroeck, and D. Van Neck, "Communication: DMRG-SCF study of the singlet, triplet, and quintet states of oxo-mn(salen)," *Journal of Chemical Physics* **140**, 241103 (2014).

[191] S. R. White, "Density matrix formulation for quantum renormalization groups," *Physical Review Letters* **69**, 2863 (1992).

[192] S. R. White and R. L. Martin, "Ab initio quantum chemistry using the density matrix renormalization group," *Journal of Chemical Physics* **110**, 4127 (1999).

[193] G. K.-L. Chan and M. Head-Gordon, "Highly correlated calculations with a polynomial cost algorithm: A study of the density matrix renormalization group," *Journal of Chemical Physics* **116**, 4462 (2002).

[194] U. Schollwöck, "The density-matrix renormalization group in the age of matrix product states," *Annals of Physics* **326**, 96 (2011), january 2011 Special Issue.

[195] S. Rommer and S. Östlund, "Class of ansatz wave functions for one-dimensional spin systems and their relation to the density matrix renormalization group," *Physical Review B* **55**, 2164 (1997).

[196] P.-O. Löwdin, "Quantum theory of many-particle systems. III. extension of the hartree-fock scheme to include degenerate systems and correlation effects," *Physical Review* **97**, 1509 (1955).

[197] W. A. Goddard, "Improved quantum theory of many-electron systems. III. the gf method," *Journal of Chemical Physics* **48**, 450 (1968).

[198] I. Mayer, in *The Spin-Projected Extended Hartree-Fock Method*, Advances in Quantum Chemistry, Vol. 12, edited by P.-O. Löwdin (Academic Press, 1980) pp. 189 – 262.

[199] P. Lykos and G. W. Pratt, "Discussion on the hartree-fock approximation," *Reviews of Modern Physics* **35**, 496 (1963).

[200] H. Fukutome, "Unrestricted hartree-fock theory and its applications to molecules and chemical reactions," *International Journal of Quantum Chemistry* **20**, 955 (1981).

[201] J. L. Stuber and J. Paldus, "Symmetry breaking in the independent particle model," (Kluwer Academic, Dordrecht, The Nederlands, 2003) Chap. 4, pp. 67–139.

[202] C. A. Jiménez-Hoyos, T. M. Henderson, and G. E. Scuseria, "Generalized hartree–fock description of molecular dissociation," *Journal of Chemical Theory and Computation* **7**, 2667 (2011).

[203] C. A. Jiménez-Hoyos, T. M. Henderson, T. Tsuchimochi, and G. E. Scuseria, "Projected hartree–fock theory," *Journal of Chemical Physics* **136**, 164109 (2012).

[204] "Jmol: an open-source java viewer for chemical structures in 3D," http://www.jmol.org (2015), (accessed May 3, 2015).

[205] A. Herrez, *How to Use Jmol to Study and Present Molecular Structures*, Vol. I (Lulu.com, 2008).

[206] A. Bondi, "van der waals volumes and radii," *Journal of Physical Chemistry* **68**, 441–451 (1964).

[207] J. Paldus, P. Piecuch, L. Pylypow, and B. Jeziorski, "Application of Hilbert-space coupled-cluster theory to simple $(H_2)_2$ model systems: Planar models," *Physical Review A* **47**, 2738 (1993).

[208] J. P. Finley, R. K. Chaudhuri, and K. F. Freed, "Applications of multireference perturbation theory to potential energy surfaces by optimal partitioning of H: Intruder states avoidance and convergence enhancement," *Journal of Chemical Physics* **103**, 4990 (1995).

[209] T. V. Voorhis and M. Head-Gordon, "Benchmark variational coupled cluster doubles results," *Journal of Chemical Physics* **113**, 8873 (2000).

[210] K. Kowalski and K. Jankowski, "Full solution to the coupled-cluster equations: the H_4 model," *Chemical Physics Letters* **290**, 180 (1998).

[211] K. Kowalski and K. Jankowski, "Towards Complete Solutions to Systems of Nonlinear Equations of Many-Electron Theories," *Physical Review Letters* **81**, 1195 (1998).

[212] D. Kats and F. R. Manby, "Communication: The distinguishable cluster approximation," *Journal of Chemical Physics* **139**, 021102 (2013).

[213] C. Edmiston and K. Ruedenberg, "Localized atomic and molecular orbitals," *Reviews of Modern Physics* **35**, 457 (1963).

[214] P.-D. Fan and P. Piecuch, "Intriguing accuracies of the exponential wave function expansions exploiting finite two-body correlation operators in calculations for many-electron systems," *Journal of Molecular*

Structure: THEOCHEM Coupled-cluster Methods: Theory and Applications. A Collection of Invited Papers in Honor of Debashis Mukherjee on the Occasion of his 60th Birthday, **768**, 3 (2006).

[215] I. Hubač, P. Mach, and S. Wilson, "Multireference Brillouin-Wigner coupled cluster (MR-BWCC) theory applied to the H_8 model: Comparison with CCSD(T) theory," *International Journal of Quantum Chemistry* **104**, 387 (2005).

[216] J. Hachmann, W. Cardoen, and G. K.-L. Chan, "Multireference correlation in long molecules with the quadratic scaling density matrix renormalization group," *Journal of Chemical Physics* **125**, 144101 (2006).

[217] P. Piecuch and L. Adamowicz, "State-selective multireference coupled-cluster theory employing the single-reference formalism: Implementation and application to the H_8 model system," *Journal of Chemical Physics* **100**, 5792 (1994).

[218] D. Zgid and M. Nooijen, "The density matrix renormalization group self-consistent field method: Orbital optimization with the density matrix renormalization group method in the active space," *Journal of Chemical Physics* **128**, 144116 (2008).

[219] R. E. Peierls, *Quantum Theory of Solids* (Clarendon Press, 1996).

[220] X. Li and J. Paldus, "Reduced multireference coupled cluster method: Ro-vibrational spectra of N_2," *Journal of Chemical Physics* **113**, 9966 (2000).

[221] M. Couty and M. B. Hall, "Generalized molecular orbital theory II," *Journal of Physical Chemistry A* **101**, 6936 (1997).

[222] G. K.-L. Chan, M. Kállay, and J. Gauss, "State-of-the-art density matrix renormalization group and coupled cluster theory studies of the nitrogen binding curve," *Journal of Chemical Physics* **121**, 6110 (2004).

[223] A. D. Becke, "A new mixing of hartree–fock and local density-functional theories," *Journal of Chemical Physics* **98**, 1372 (1993).

[224] C. Lee, W. Yang, and R. G. Parr, "Development of the colle-salvetti correlation-energy formula into a functional of the electron density," *Physical Review B* **37**, 785 (1988).

[225] P. A. Limacher, P. W. Ayers, P. A. Johnson, S. De Baerdemacker, D. V. Neck, and P. Bultinck, "Simple and inexpensive perturbative correction schemes for antisymmetric products of nonorthogonal geminals," *Physical Chemistry Chemical Physics* **16**, 5061 (2014).

[226] J. P. Perdew, R. G. Parr, M. Levy, and J. L. Balduz, "Density-functional theory for fractional particle number: Derivative discontinuities of the energy," *Physical Review Letters* **49**, 1691 (1982).

[227] W. Yang, Y. Zhang, and P. W. Ayers, "Degenerate ground states and a fractional number of electrons in density and reduced density matrix functional theory," *Physical Review Letters* **84**, 5172 (2000).

[228] A. J. Cohen, P. Mori-Sanchez, and W. Yang, "Insights into current limitations of density functional theory," *Science* **321**, 792–794 (2008).

[229] R. S. Mulliken, "Electronic population analysis on LCAO-MO molecular wave functions. I," *The Journal of Chemical Physics* **23**, 1833 (1955).

[230] J. Hubbard, "Electron correlations in narrow energy bands," *Proceedings of the Royal Society of London A: Mathematical, Physical and Engineering Sciences* **276**, 238 (1963).

[231] S. R. White, D. J. Scalapino, R. L. Sugar, E. Y. Loh, J. E. Gubernatis, and R. T. Scalettar, "Numerical study of the two-dimensional hubbard model," *Physical Review B* **40**, 506 (1989).

[232] E. H. Lieb and F. Y. Wu, "Absence of mott transition in an exact solution of the short-range, one-band model in one dimension," *Physical Review Letters* **20**, 1445 (1968).

[233] E. H. Lieb and F. Wu, "The one-dimensional hubbard model: a reminiscence," *Physica A: Statistical Mechanics and its Applications* **321**, 1 (2003).

[234] F. H. L. Essler, H. Frahm, F. Göhmann, A. Klümper, and V. E. Korepin, *The One-Dimensional Hubbard Model* (Cambridge University Press, 2010).

[235] C. L. Cleveland, "Obtaining a heisenberg hamiltonian from the hubbard model," *American Journal of Physics* **44**, 44 (1976).

[236] D. J. Wales and J. P. K. Doye, "Global optimization by basin-hopping and the lowest energy structures of lennard-jones clusters containing up to 110 Atoms," *The Journal of Physical Chemistry A* **101**, 5111–5116 (1997).

[237] W. H. Dickhoff and D. Van Neck, *Many-Body Theory Exposed!* (World Scientific, 2008).

[238] D. M. Brink and G. R. Satchler, *Angular momentum* (Oxford university press, 1993).

[239] W. Poelmans, "v2DM-DOCI solver," https://github.com/wpoely86/doci_sdp-atom (2015), (accessed May 3, 2015).